

UNIVERSITY OF SOUTHAMPTON

**THE INFLUENCE OF BIOLOGICAL, SEDIMENTOLOGICAL AND
PHYSICAL FACTORS ON SEDIMENT STABILITY IN
INTERTIDAL WATERS**

By
MAX RUDOLF MUSKANANFOLA

Thesis submitted to The University of Southampton in fulfilment of the
requirements for the degree of Doctor of Philosophy

**DEPARTMENT OF OCEANOGRAPHY
FACULTY OF SCIENCE
DECEMBER 1994**

UNIVERSITY OF SOUTHAMPTON

ABSTRACT

FACULTY OF SCIENCE OCEANOGRAPHY

Doctor of Philosophy

THE INFLUENCE OF BIOLOGICAL, SEDIMENTOLOGICAL AND PHYSICAL FACTORS ON SEDIMENT STABILITY IN INTERTIDAL WATERS

by Max Rudolf Muskananfola

In situ studies on sediment stability and macrobenthic organisms are described; these were undertaken over a 28 month period at Solent Breezes, Southampton Water. The study consisted of the monthly collection of field data, including the shear strength of the surficial sediment and the tube density of *Lanice conchilega*. Sediment cores were collected also for the analysis of macrobenthic organisms and other parameters. The data obtained are analysed statistically, to establish correlation between the parameters under investigation.

Solent Breezes is a relatively stable environment, with no distinct accretional or erosional patterns. The majority of the velocity profiles measured in the overlying waters, during a spring tidal cycle, are logarithmic in character. Critical friction velocities range from 0.25 cm s^{-1} to 5.71 cm s^{-1} ; these correspond to critical bed shear stresses of 0.01 N m^{-2} and 3.36 N m^{-2} . Roughness lengths range from 0.02 cm to 14.30 cm .

Biological investigations have revealed the presence of 29 species of benthic macrofauna. The total number of species and individuals varies seasonally. *Lanice* tube densities range from $3.13 \text{ per } 100 \text{ cm}^2$ (July 1993) to $8.80 \text{ per } 100 \text{ cm}^2$ (November 1991). Tube density is affected by failure of larval recruitment, mortality, species interactions and predation. Principal components analysis reveals that the factors responsible for the existing pattern are: (i) bioavailability of organic matter (protein, bacterial protein, organic matter and grain size characteristics); (ii) sediment strength; and (iii) physical controls (temperature, salinity and moisture content).

Sedimentological investigations reveal that the area is covered with fine-grained sediments with mean grain size ranging from 3.18Φ (August 1992) to 2.84Φ (July 1991). Organic matter content ranged from 0.91% (June 1991) to 2.01% (July 1992). The silt/clay content ranged from 0.1% (July 1991) to 0.73% (September 1991).

The mean shear strength of the surficial sediments ranged from 2.11 KPa (January 1992) to 4.08 Kpa (November 1991). Statistical analysis reveals that the shear strength is affected negatively by pore-water temperature and grain size; it is affected positively by tube density. Using winter data only, the model reveals a positive effect of pore-water temperature on shear strength. It can be inferred that (at least, to a certain extent) the tube density of *Lanice conchilega* influences sediment stability. Tube density itself is influenced by recruitment, mortality, and species interactions.

LIST OF CONTENTS

	Page
TITLE	
ABSTRACT	
LIST OF CONTENTS	i
LIST OF FIGURES	vii
LIST OF PLATES	xiii
LIST OF TABLES	xiv
LIST OF SYMBOLS	xvii
ACKNOWLEDGEMENTS	xix
CHAPTER I	
INTRODUCTION	1
1.1. Background to the Study	1
1.2. Identification of the Problem	3
1.3. Aims of the Study	6
CHAPTER 2	
LITERATURE REVIEW	7
2.1. Introduction	7
2.2. Sediment Stability	7
2.2.1. Shear Strength	9
2.2.2. Erodibility	11
2.2.3. Forces Acting on a Particle in the Bed	11
2.2.4. Initiation of Sediment Movement	16
2.3. <i>Lanice conhilega</i>	17
2.3.1. Distribution	17

2.3.2. Larval Development	18
2.3.3. Tube Building	20
2.4. Biological Parameters	23
2.4.1. Algae	23
2.4.2. Microbenthos	25
2.4.3. Meiobenthos	25
2.4.4. Macrobenthos	25
2.4.5. Benthic Communities	28
2.5. Sedimentological Parameters	31
2.5.1. Moisture Content	31
2.5.2. Organic Matter Content	32
2.5.3. Grain Size	32
2.5.4. Sediment Density	33
2.5.5. Atterberg Limits	33
2.6. Physical Parameters	34
2.6.1. Pore-Water Temperature	34
2.6.2. Pore-Water Salinity	34
2.6.3. Subaerial Exposure Time	34

CHAPTER 3	
EXPERIMENTAL SITE	36
3.1. Introduction	36
3.2. Location	36
3.2.1. The Study Area	36
3.2.2. Regional Geology	39
3.3. Biological Setting	40
3.3.1. Benthos	40
3.3.2. Phytoplankton	40
3.4. Sedimentological Setting	41
3.4.1. Topography and Bathymetry	41

3.4.2. Distribution of Sediments	44
3.4.3. Sediment Transport Patterns	44
3.4.4. Rates of Sedimentation	46
3.5. Physical Setting	47
3.5.1. Water Temperature	47
3.5.2. Salinity of the Waters	48
3.5.3. Tidal Features	49
3.5.4. Tidal Currents	51
3.5.5. Waves	51
CHAPTER 4	
INSTRUMENTATION AND METHODS	52
4.1. Introduction	52
4.2. Field and Laboratory Instrumentation	52
4.2.1. Shear Vane	52
4.2.2. Supporting Field Equipment	53
4.2.3. Accretion/Erosion Measurements	55
4.2.4. Velocity Gradient Rig	55
4.2.5. X-Ray System	55
4.2.6. Particle Size Analysis	56
4.3. Field Measurements	58
4.3.1. Biological Methods	58
4.3.2. Sedimentological Methods	58
4.3.3. Velocity Profile Measurements	59
4.4. Laboratory Procedures	60
4.4.1. Biological Methods	60
4.4.2. Sedimentological Methods	60
4.4.3. Physical Measurements	62
4.5. Statistical Analysis	63
4.5.1. Regional Setting Data	63

4.5.2. Data from the Biological Investigations	63
4.5.3. Data from Sedimentological Investigations	65
CHAPTER 5	
RESULTS: REGIONAL CONDITIONS	67
5.1. Introduction	67
5.2. Bathymetry	67
5.3. Accretion and Erosion	68
5.4. Sediment Structure and Density	70
5.4.1. Sediment Structure	70
5.4.2. Sediment Density	82
5.5. Velocity Profiles	97
5.5.1. Introduction	97
5.5.2. Friction Velocities over the Study Area	99
5.5.3. Bed Roughness Length	100
CHAPTER 6	
RESULTS: BIOLOGICAL INVESTIGATIONS	104
6.1. Introduction	104
6.2. <i>Lanice conchilega</i> (Pallas 1766)	104
6.3. Total Species of Benthic Macrofauna	108
6.4. Total Individuals of Benthic Macrofauna	108
6.5. Total Protein	110
6.6. Bacterial Protein	110
6.7. Bacterial Abundance	113
6.8. Phytoplankton Abundance	113
6.9. Diatom Relative Abundance	114
6.10. Community Structures	114
6.10.1. Dominant Species	115

6.10.2. Seasonal Grouping	126
6.10.3. Diversity	128
 CHAPTER 7	
RESULTS: SEDIMENTOLOGICAL INVESTIGATIONS	137
7.1. Introduction	137
7.2. Shear Strength	137
7.3. Pore-Water Temperature	140
7.4. Pore-Water Salinity	140
7.5. Grain Size Analyses	141
7.5.1. Frequency Distributions - Histograms	141
7.5.2. Statistical Parameters of Grain Size	141
7.5.3. Scatter Plots of the Textural Parameters	164
7.6. Moisture Content	166
7.7. Low Water Height	169
7.8. Organic Matter Content	169
7.9. Silt/Clay Content	170
7.10. Tube Density	170
7.11. Meteorological Data	170
7.12. Laboratory Experiment	176
 CHAPTER 8	
DISCUSSION	179
8.1. Introduction	179
8.2. Shear Stress and Strength	179
8.3. The Effects of Temperature on Shear Strength	184
8.4. Statistical Model	185
8.4.1. Data Matrix	188

8.4.2. Correlation Matrix	188
8.4.3. Cluster Analysis	194
8.4.4. Principal Components Analysis (PCA)	195
8.4.5. Multiple Linear Regression	202
8.5. Comparison with Previous Studies	205
8.5.1. The Shields' Diagram	205
8.5.2. Intertidal Sediment Stability	210
 CHAPTER 9	
CONCLUSIONS AND FUTURE RESEARCH	216
9.1. Introduction	216
9.2. Regional Setting	216
9.3. Biological Investigations	217
9.4. Sedimentological Investigations	219
9.5. Future Research	221
 REFERENCES	
APPENDICES	222
	244

LIST OF FIGURES

	Page
Figure 1.1. A schematic representation of the parameters under investigation	5
Figure 2.1. (A) Forces acting on a grain resting on a bed of similar grains, (B) Analysis of moments acting on a grain at the beginning of grain movement (from Middleton and Southard, 1984)	13
Figure 2.2. Life cycle (larval development) of <i>Lanice conchilega</i> . Key: 1 = Fertilised Egg; 2 = Trochophora Larva (2 days old); 3 = Aulophora Larva (dorsal view); 4 = Juvenile <i>Lanice</i> (side view); 5A = Spawning Female <i>Lanice</i> in an aquarium; and 5B = Male <i>Lanice</i> in an aquarium (from Kessler, 1963)	19
Figure 3.1. The Solent Estuarine System (after Tubbs, 1980)	37
Figure 3.2. Site for the field experimental studies	38
Figure 3.3. Circulation pattern of sediment in the Solent. E = Areas of Cliff Erosion (from Dyer, 1980)	42
Figure 3.4. Generalised bathymetric chart of the Solent Region (based upon British Geological Survey, 1988): contours in metres	43
Figure 3.5. Distribution of surface sediment types in the Solent. M = Mud, S = Sand, G = Gravel (from Dyer, 1980)	45
Figure 4.1. Principal components of the Shear Vane Apparatus (after Serota and Jangle, 1972)	54
Figure 4.2. The Malvern Laser Diffraction Particle Sizer System (from Malvern Instruments Particle Sizer Reference Manual, 1987)	57

Figure 5.1. Bathymetry of the Solent Breezes sampling site, expressed in terms of 0.05 m contour with arbitrary height reference. Circled numbers represent relative location of the 16 Core sediment samples taken for X-Ray photography and density measurements	69
Figure 5.2. Accretion and erosion observed at Solent Breezes, during January 1992 to July 1992	70
Figure 5.3(a). Sediment density of Cores 1 and 2	84
Figure 5.3(b). Sediment density of Cores 3 and 4	85
Figure 5.3(c). Sediment density of Cores 5 and 6	86
Figure 5.3(d). Sediment density of Cores 7 and 8	87
Figure 5.3(e). Sediment density of Cores 9 and 10	88
Figure 5.3(f). Sediment density of Cores 11 and 12	89
Figure 5.3(g). Sediment density of Cores 13 and 14	90
Figure 5.3(h). Sediment density of Cores 15 and 16	91
Figure 5.4. Mean density of the upper 5 cm of the surficial sediment samples, collected at Solent Breezes in October 1993 (for relative location of cores, see Figure 5.1)(X error bars represent standard errors)	96
Figure 5.5. Friction velocity, roughness length, determination coefficient and water depth during a spring tidal cycle at Solent Breezes in September 1992	102
Figure 6.1. Long-term variation in mean tube density of <i>Lanice conchilega</i> , mean total species and mean total individuals of benthic macrofauna (Y error bars represent standard errors)	107
Figure 6.2. Correlations between mean total species and mean tube density, mean total individuals and mean tube density, mean total species and mean total individuals	109

Figure 6.3.	Long-term variation in total protein, bacterial protein and bacterial abundance. Dotted lines with hollow circles represent data from Mattin (1992)	112
Figure 6.4.	Annual variation in phytoplankton abundance and diatom as percentage of total phytoplankton (data from Kifle, 1992)	116
Figure 6.5.	Long-term (seasonal) variability of <i>Euclymene oerstedii</i> , <i>Exogone hebes</i> , <i>Aracidea minuta</i> and <i>Pygospio elegans</i>	121
Figure 6.6.	Long-Term (Seasonal) Variability of <i>Scoloplos armiger</i> , <i>Nepthys hombergii</i> , <i>Tanaissus lilljeborgi</i> and <i>Syllis sp</i>	122
Figure 6.7.	Dendrogram showing classification of monthly data of benthic macrofauna from Solent Breezes, Southampton Water. Abundance data are root-root transformed prior to the Bray-Curtis measure	127
Figure 6.8.	Long-term variation in diversity (Shannon and Weaver, 1963), richness (Margalef, 1958) and evenness (Pielou, 1966) of benthic macrofauna from Solent Breezes, Southampton Water	130
Figure 7.1.	Long-term measurements of mean shear strength, pore-water temperature and pore-water salinity (Y error bars represent standard errors)	139
Figure 7.2(a).	Grain size distributions of surficial sediment samples, as histograms, June 1991 and July 1991 (Y error bars represent standard errors)	145
Figure 7.2(b).	Grain size distributions of surficial sediment samples, as histograms, August 1991 and September 1991 (Y error bars represent standard errors)	146
Figure 7.2(c).	Grain size distributions of surficial sediment samples, as histograms, October 1991 and November 1991 (Y error bars represent standard errors)	147

Figure 7.2(d). Grain size distributions of surficial sediment samples, as histograms, December 1991 and January 1992 (Y error bars represent standard errors)	148
Figure 7.2(e). Grain size distributions of surficial sediment samples, as histograms, February 1992 and March 1992 (Y error bars represent standard errors)	149
Figure 7.2(f). Grain size distributions of surficial sediment samples, as histograms, April 1992 and May 1992 (Y error bars represent standard errors)	150
Figure 7.2(g). Grain size distributions of surficial sediment samples, as histograms, June 1992 and July 1992 (Y error bars represent standard errors)	151
Figure 7.2(h). Grain size distributions of surficial sediment samples, as histograms, August 1992 and September 1992 (Y error bars represent standard errors)	152
Figure 7.2(i). Grain size distributions of surficial sediment samples, as histograms, October 1992 and November 1992 (Y error bars represent standard errors)	153
Figure 7.2(j). Grain size distributions of surficial sediment samples, as histograms, December 1992 and January 1993 (Y error bars represent standard errors)	154
Figure 7.2(k). Grain size distributions of surficial sediment samples, as histograms, February 1993 and March 1993 (Y error bars represent standard errors)	155
Figure 7.2(l). Grain size distributions of surficial sediment samples, as histograms, April 1993 and May 1993 (Y error bars represent standard errors)	156
Figure 7.2(m). Grain size distribution of surficial sediment samples, as histograms, June 1993 and July 1993 (Y error bars represent standard errors)	157

Figure 7.2(n). Grain size distributions of surficial sediment samples, as histograms, August 1993 and September 1993 (Y error bars represent standard errors)	158
Figure 7.3. Long-term measurements of mean grain size, mean sorting and mean skewness of surficial sediment samples (Y error bars represent standard errors)	162
Figure 7.4. Relationships between mean sorting and mean grain size (A), and mean skewness and mean grain size (B)	165
Figure 7.5. Long-term measurements of mean moisture content, low water height (for explanation, see text) and mean organic matter content (Y error bars represent standard errors)	168
Figure 7.6. Long-term variation in mean silt/clay content and mean tube density (Y error bars represent standard errors)	172
Figure 7.7. Long-term variation in mean daily air temperature, mean daily wind speed, mean daily rainfall and mean daily sunshine (Y error bars represent standard errors)	175
Figure 7.8. Correlations between shear strength and temperature (A), and shear strength and straw density, at different temperatures (B)	178
Figure 8.1. Relationship between shear stress and shear strength (derived from Dunn, 1959)	181
Figure 8.2. Long-term variation in critical shear stresses and friction velocities: based upon <i>in situ</i> shear strength (a and b); and based upon mean grain size (c and d)	183
Figure 8.3. (a) <i>In situ</i> shear strength measurements at a tube density of 10 per 100 cm ² , (b) Predicted shear strength from <i>in situ</i> (pore) water temperature measurements	187
Figure 8.4. Dendrogram showing classification of parameters, using Hierarchical Cluster Analysis	196
Figure 8.5(a). Factor loadings of Factors 1, 2 and 3	200
Figure 8.5(b). Factor loadings of Factors 4 and 5	201

Figure 8.6. The Shields' Curve, with the addition of data from previous studies and the present investigation	209
Figure 8.7. Relationship between shear strength and flow velocity required to erode <i>in situ</i> sediment samples in a flume (data from Burke, 1989)	214

LIST OF PLATES

	Page
Plate 5.1(a). X-Ray photographs of Cores 1 and 2 (for relative location of cores, see Figure 5.1)	72
Plate 5.1(b). X-Ray photographs of Cores 3 and 4 (for relative location of cores, see Figure 5.1)	73
Plate 5.1(c). X-Ray photographs of Cores 5 and 6 (for relative location of cores, see Figure 5.1)	74
Plate 5.1(d). X-Ray photographs of Cores 7 and 8 (for relative location of cores, see Figure 5.1)	75
Plate 5.1(e). X-Ray photographs of Cores 9 and 10 (for relative location of cores, see Figure 5.1)	76
Plate 5.1(f). X-Ray photographs of Cores 11 and 12 (for relative location of cores, see Figure 5.1)	77
Plate 5.1(g). X-Ray photographs of Cores 13 and 14 (for relative location of cores, see Figure 5.1)	78
Plate 5.1(h). X-Ray photographs of Cores 15 and 16 (for relative location of cores, see Figure 5.1)	79

LIST OF TABLES

	Page
Table 5.1. Accretion and erosion (in cm) at Solent Breezes from January 1992 to July 1992	68
Table 5.2. Sediment density (in g cm ⁻³) within the upper 5 cm of the surficial sediments from Solent Breezes (October, 1993)	95
Table 5.2. Continued (see above)	95
Table 5.3. All Pairwise Multiple Comparisons Test on the sediment density of the upper 5 cm, using Student-Newman-Keuls Method (at 5 % level of significance)	97
Table 5.4. Friction velocity, bed roughness length, shear stress and coefficient of determination	101
Table 6.1. Mean tube density of <i>Lanice conchilega</i> , mean total species and mean total individuals of benthic macrofauna	106
Table 6.2. Total protein, bacterial protein and bacterial abundance	111
Table 6.3. Phytoplankton and diatom relative abundance (data from Kifle, 1992)	115
Table 6.4. Species abundance of benthic macrofauna at Solent Breezes per 100 cm ² from October 1991 to March 1992	117
Table 6.4. Continued, from April 1992 to September 1992	118
Table 6.4. Continued, from October 1992 to March 1993	119
Table 6.4. Continued, from April 1993 to September 1993	120

Table 6.5.	Diversity (Shannon and Weaver, 1963), richness (Margalef, 1958) and evenness (Pielou, 1966) of macrobenthic organisms from October 1991 to September 1993	129
Table 6.6.	Percent variance of each Principal Components (Components accounting for 92 % of variance)	132
Table 6.7.	Values of p for the correlations between the abundance of benthic macrofauna and other parameters (p < 0.05 is significant)	133
Table 6.8.	Spearman Rank Correlation Coefficient (rho) with a confidence level 5 percent	134
Table 7.1.	Mean shear strength, pore-water temperature and pore-water salinity	138
Table 7.2.	Grain size distribution of surficial sediment Samples for size range from 0.00 Φ to 3.00 Φ from June 1991 to September 1993	142
Table 7.2.	Continued, for size range from 3.50 Φ to 6.50 Φ from June 1991 to September 1993	143
Table 7.2.	Continued, for size range from 7.00 Φ to 10.00 Φ from June 1991 to September 1993	144
Table 7.3.	Parameters and descriptive terms applied to various ranges of grain size parameters (from Folk and Ward, 1957)	160
Table 7.4.	Textural parameters (in Φ) of statistical sediment samples from Solent Breezes	161
Table 7.5.	Mean moisture content, low water height and mean organic matter content	167
Table 7.6.	Mean silt/clay content and mean tube density	171
Table 7.7.	Mean daily air temperature, mean daily wind speed, mean daily rainfall and mean daily sunshine	174
Table 7.8.	Water temperature and shear strength of sediment	177
Table 7.9.	Straw density, temperature at 4°C and 17°C	177

Table 8.1.	Derived critical shear stresses and friction velocities (1 - represents <i>in situ</i> measurements; 2 - represents measurements based on grain size)	182
Table 8.2.	<i>In situ</i> shear strength measurement at tube density of 10 per 100 c ² and shear strength predicted based on <i>in situ</i> temperature	186
Table 8.3.	Data matrix for the present investigation	189
Table 8.3.	(Continued)	190
Table 8.3.	(Continued)	191
Table 8.4.	Correlation matrix between the various (normalised) parameters measured as part of the present investigation	192
Table 8.5.	Percentage variance represented by each of the Principal Components	198
Table 8.6.	Factor loadings of the five Factors explaining the majority of the variation in the data set	199
Table 8.7.	Shields' Entrainment Function and Grain Reynolds Number for the data obtained during the present investigation	208

LIST OF SYMBOLS

τ	=	shear strength or stress
C	=	cohesion
σ	=	effective pressure
θ	=	angle of internal friction or Shields entrainment function
N	=	normal load
μ	=	pore-water pressure
Q_u	=	unconfined compressive strength
F	=	failure load
O	=	original cross-sectional area of sample
α	=	angle between the plane of failure and the plane on which the major principal stress is applied
γ	=	submerged specific weight
D _n	=	nominal diameter
F _G	=	total gravity force
u	=	velocity
A	=	cross-sectional area of the sphere (grain)
H'	=	diversity
J	=	evenness
n_i	=	number of individuals of the i th species
N	=	total number of individuals or revolution per second
L _w	=	liquid limit
P _w	=	plastic limit
I _w	=	plasticity index
P	=	pulse count
T	=	time
W	=	water (moisture) content
M ₁	=	pre-weighed crucible
M ₂	=	weight of crucible and sediment
M ₃	=	weight of crucible and dry sediment

O	=	organic matter content
A	=	weight of sample and crucible
B	=	weight of crucible and samples after all organic material burned off
C	=	pre-weighed crucible
u_z	=	velocity at height z
u_*	=	shear (friction) velocity
u_c	=	critical friction velocity
τ_c	=	critical shear stress
ρ	=	fluid density or Spearman rank correlation
k	=	von Karman constant
z_0	=	roughness length
h	=	average vertical extent or effective obstacle height
s	=	cross-sectional area seen by the flow
BP	=	bacterial protein
TP	=	total protein
BA	=	bacterial abundance
β	=	regression coefficient
y	=	dependent variable
x	=	independent variable
WT	=	pore-water temperature
GT	=	grain size
TD	=	tube density
ρ_s	=	density of sediment
δ	=	thickness of viscous sublayer
Re.	=	Reynolds number
θ_t	=	Shields criterion
ν	=	kinematic fluid viscosity
D	=	grain diameter

ACKNOWLEDGEMENTS

I would like to thank both my supervisors: Prof. M.B. Collins and Dr. M. Shearer, for their advice, supervision, encouragement and criticisms during the period of the study. Mr. G.A. Rowe and Mr. J.D. Brooks, are thanked also for their continuous assistance provided during the field sampling and laboratory work; likewise Mr. X. Ke, for his assistance in the measurement of velocity profiles.

Mr. D. Anderson, technician from the Department of Geography, is acknowledged for providing the Shear Vane equipment used for measuring shear strength; similarly Mr. W.J.B. Gibbs, technician from the Department of Oceanography, for constructing equipment capable of measuring erosion and deposition. I am indebted also to: Mr. D.M. Crowfoot, Mr. K. Padley, Mr. D. Hutchison, Mr. J.W. Davis and Dr. F. Ding, for their assistance during the fieldwork; Mrs. K. Davis, for drawing some of the figures; Dr. I.W. Croudace, Mr. B.A. Marsh and Mr. J. Lewis, of the Department of Geology, University of Southampton, for use of the Faxitron X-Ray System, to obtain x-ray photographs of sediment cores; Dr. G.C. Sills and Mr. C. Waddup, of the Department of Engineering Science, University of Oxford, for the provision of the Metal Ceramic X-Ray tube for measuring sediment density; Dr. R.I.L. Powys, of the Department of Earth Science, University of Cambridge, for use of the (Malvern) Particle Sizer to measure grain size characteristics. Thanks are due also to: Mr. J.S. Cross and Mr. H. Powell, for their assistance in the measurement of the bathymetry (topography) of the study area; Ms. C. Hobson, for drawing the initial graph of bathymetry contours; and Dr. S. Gao, for his comments on Chapters 7 and 8.

Lastly, but most deeply, I thank my dearest friend and wife Leni, for her companionship and support during the last stage of writing up my thesis.

This study was supported by the Overseas Development Administration (ODA), through The British Council.

CHAPTER 1

INTRODUCTION

1.1. Background to the Study

Sediment stability at the intertidal sea-bed is one of the basic parameters affecting sediment dynamics in coastal waters. The degree of tidal resuspension of fine-grained and organic rich sediment into the water column is controlled by bottom stability. Seafloor stability changes temporally (Rhoads *et al.*, 1978) and the processes that control these changes are complex (Yingst and Rhoads, 1978). Stability of marine sediments may be influenced by biological processes, such as stabilisation and destabilisation (bioturbation). These animal-sediment relationships may involve the activities of microfauna, meiofauna and macrofauna in the marine environment. In laboratory experiments, it has been shown that microfaunal organisms and dense aggregation of tube-building polychaetes stabilise the sediment surface (Rhoads *et al.*, 1978). In contrast, bioturbation by macrofauna reduces the stability of the surface (Rhoads and Young, 1970; Young and Southard, 1975, 1978). Most of the experiments described elsewhere were carried out in the laboratory; only a few were undertaken in the field, especially those related to *in situ* shear strength measurements (cf Amos *et al.*, 1988).

In intertidal waters, most soft-bottom sediment deposition is dominated often by the presence of biogenous structures. These structures exist in a variety of forms, for example: mounds and pits, produced by feeding activities of benthic infauna (Rhoads and Young, 1970; Rhoads, 1974; Hylleberg, 1975; Cadee, 1976); patterns introduced by sea grasses, which are abundant in shallow coastal waters (Scoffin, 1970; Fonseca, 1989); and animal tubes constructed by benthic organisms, which protrude above the bottom substratum (Fager, 1964; Mills, 1967; Bailey-Brock, 1979; Jumars, 1975).

Protruding biogenous structures in marine habitats can influence sea-bed stability and the ecology of benthic communities. For instance, several studies

have revealed the association of animal tubes and sea grasses with "stable" beds (Fager, 1964; Mills, 1967; Neumann *et al.*, 1970; Young and Rhoads, 1971; Fonseca and Fisher, 1986). The presence of animal tubes may also lead to: changes in the abundance and richness of species (Sanders *et al.*, 1962; Bailey-Brock, 1979; Wilson, 1979); and an increase in flow velocities and energy required to move sediment grains (Muskananfola, 1990); increase in the shear strength of sediment (Meadows and Tait, 1989; Meadows and Hariri, 1991) . Also, potentially important stabilisation activities include binding with mucus and other extracellular products of micro-organisms (Frankel and Mead, 1973; Holland *et al.*, 1974; Paterson, 1989; Paterson *et al.*, 1990). The process responsible directly for these species interactions remain, however, unexplained thoroughly.

Evidence is increasing that the laboratory measurement of sediment erodibility, which is an important factor in conceptual or numerical sediment modelling, bears little relationship to the behaviour of sediments in the field (Luckenbach, 1986; Amos *et al.*, 1988). Such differences occur because it has been assumed that the behaviour of sediment samples in the flume is representative of that within their natural marine environments. Many of the physical properties of the sediments deposited naturally are not, however, reproducible in the laboratory. Changes in the physical properties affecting sediment stability may have important effects on the results of the laboratory experiments on sediment dynamics. For instance, the results of freshwater flume experiments may not be applicable to the studies representative of the natural marine environments, as salt water flocculation influences strongly the behaviour of sediments during deposition and erosion. Also, benthic organisms may affect the erosion and stabilisation of sediments, which is difficult to imitate in flume experiments.

Estuaries and intertidal waters are amongst the most productive of all the aquatic ecosystems which support fisheries of commercial and recreational value (Ryther, 1969; Sutcliffe, 1973; Stockner *et al.*, 1979 and Bruno *et al.*, 1980). Consequently, the understanding of processes controlling sediment stability in these waters is of paramount importance to their ecological, economic, aesthetic

and scientific development. Likewise, a knowledge of sediment stability/erodibility is a factor of considerable significance to coastal engineering (Paterson and Daborn, 1991), amenity, marine culture and fisheries developments.

On the basis of the above considerations, a field (*in situ*) study was undertaken at Solent Breezes, Southampton Water. Solent Breezes was selected as the area for investigation because: (1) it is densely populated with animal tubes of *Lanice conchilega*; (2) it is relatively easily accessible (from the Department of Oceanography); and (3) it is somewhat protected from human activities and, hence, there is little disturbance to the natural habitat. The main research themes being investigated are as follows:

- (1) the effect of *Lanice conchilega* tubes on intertidal flat sediment stability (shear strength) which, in turn, affects sediment transport and turbidity through resuspension of bottom sediment (reducing light penetration);
- (2) the influence of *Lanice conchilega* on the distribution of macrobenthic organisms; and
- (3) the influence of other biological, sedimentological and physical factors on sediment stability and the structure of macrobenthic communities.

1.2. Identification of the Problem

Shear strength has been identified elsewhere as influencing sediment stability. Such strength can be expressed in terms of shear stress (Dunn, 1959; Graf, 1971), which is normally used by scientists and engineers in the study of sediment dynamics. On the other hand, shear strength itself is influenced by a variety of interrelated biological, sedimentological and physical controls. The present study, therefore, is concerned mainly with coastal sediment stabilisation through the use of shear strength as the dependent variable and other parameters (biological, sedimentological and physical) as the independent variables. This investigation concentrates upon a number of important parameters, such as: temperature and salinity of the pore-water; organic matter content, moisture

content of the sediment deposits; grain size and silt/clay content of the sediments; bottom topography of the intertidal flats; sediment structure and density; exposure of the flats to the sunshine; erosional/depositional patterns; tube density of *Lanice conchilega*; and the number of species and abundance of macrobenthic organisms. A null hypothesis is proposed in the analyses, such that there is no relationship between the dependent and independent variables; this is compared against an alternative hypothesis, that there is a relationship between dependent and independent variables. A schematic representation of the parameters under investigation is delineated on the flow chart shown as Figure 1.1. The Figure shows the hypothetical influence of biological, sedimentological and physical parameters on shear strength; this, in turn, influences sediment stability/erodibility. Such conditions influence the local and regional sediment dynamics. Also, there is a feedback between the biological and sedimentological parameters whilst, at the same time there may be interaction between certain types of parameters i.e. tube density may affect species/individual abundance (biological); and organic matter content may affect moisture content (sedimentological).

In order to establish the dynamic balance between the parameters outlined on Figure 1.1 and to obtain a reliable set of results, the area selected for the study has four important features: moderate tidal current speeds, with minimal interference from wave action; only limited variation in the type of sediment deposit and their supply; a relatively flat bottom topography; and high densities of *Lanice* tubes. The study was undertaken in such a way that long-term field observations were obtained on the parameters under investigation, with particular reference to seasonal variability. The field measurements extended over 28 months, in order to obtain an extensive and representative data set. The field study was complemented with laboratory experiments, under controlled conditions, to support the *in situ* observations.

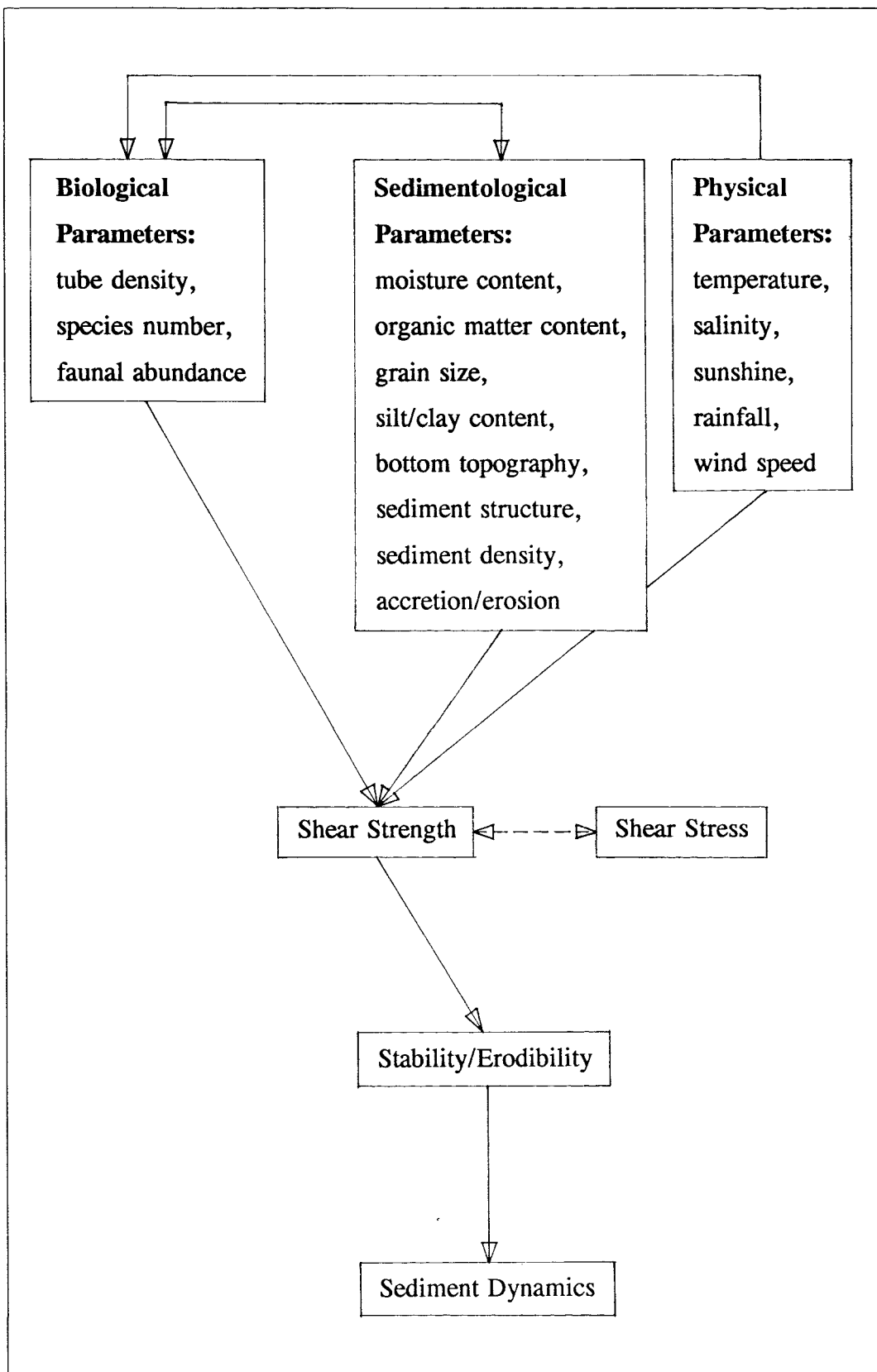


Figure 1.1. A schematic representation of the parameters under investigation

1.3. Aims of the Study

This series of experiments has been designed to study animal-sediment interactions, on the basis of the biological, sedimentological and physical considerations outlined below.

- (1) A long-term study to establish the effects of *Lanice conchilega* tubes, biological parameters (number of species and abundance of macrobenthic organisms), sedimentological parameters (moisture content, organic matter content, grain size, silt/clay content, accretion/erosion, bottom topography, sediment structure and density), and physical parameters (temperature, salinity, sunshine, rainfall, wind speed) on sediment stability in intertidal waters. Likewise, to consider the consequences of such interactions on sediment transport and coastal waters productivity.
- (2) To utilise the data obtained on shear strength to predict further seasonal stability of localised sediment deposits, through the derivation of shear stress from measurements of shear strength. In this way, to establish a model for predicting shear strength and shear stress in intertidal flat water.
- (3) A long-term study on the effects of *Lanice conchilega* tubes on macrobenthic organism distributions, to establish any interactive relationship. Likewise, to examine the control of any of the parameters under study, on the distribution of *Lanice conchilega* and macrobenthic organisms.

CHAPTER 2

LITERATURE REVIEW

2.1. Introduction

This Chapter reviews and describes previous *in situ* or laboratory studies relevant to this area of research. Such investigations can be grouped into five main areas of interest: sediment stability; the ecology of *Lanice conchilega*; and biological, sedimentological, and physical parameters controlling sediment stability. Each of these variables is discussed below, within the context of the present investigation, in order to identify and establish the most important factors contributing to intertidal flat sediment stabilisation.

2.2. Sediment Stability

The resistance of fine-grained sediment to erosion is associated directly with water content, viscosity, bulk density and the Atterberg limits of sediments (Zeman, 1983); these influence the strength of the sediments. Likewise, the shear strength of subtidal, fine-grained sediment has been found to be influenced by gravity forces and the consolidation of individual grains (Kirby and Parker, 1983). At the same time, shear strength is related to the threshold of sediment movement and the erosion rate; therefore, the main factor responsible for the stabilisation of sediment in subtidal areas is gravitational (Mehta, 1986).

These assumptions are not sufficient to explain the stability of intertidal flat sediments, however, which can sometimes be some 80 times more difficult to erode (Amos and Mosher, 1985). Sediment stability in intertidal waters can be explained only partly by dewatering (Anderson and Howell, 1984), or alteration of the packing of the sediment particles resulting in an increase in the inter-particle attractive forces which are important with regard to erosion threshold

(Postma, 1967). On the basis of *in situ* studies undertaken elsewhere, it has been predicted that the stability of surficial cohesive sediments increases generally in a shoreward direction (Amos *et al.*, 1988). The strength varied, however, in accordance with the length of the (tidal) emersion period; thus, the elevation on the shoreline and the prevailing environmental conditions. An immediate response of the surface shear strength of cohesive sediment, to the changes in environmental conditions, is exemplified by a sudden decrease in sediment stability following rainfall (Paterson *et al.*, 1990).

In the latter study referred to above, sediment stability at low-shore stations did not increase after several hours of exposure to the atmosphere. This condition may be due to the proximity of the water table or simply that a longer exposure period was needed to change the stability under the relevant climatic conditions (Paterson *et al.*, op. cit.). Similarly, sediment stability at high-shore stations did not increase immediately after emersion. Nonetheless, an increase in stability occurred after several hours of exposure. This phenomenon supports the theory that, under certain environmental conditions, a minimum period is required before sediment stability begins to increase.

Elsewhere, it has been shown that temporal changes in the bulk properties of intertidal sediment and their shear strengths are caused by atmospheric effects, during exposure (Anderson and Howell, 1984; Kraeuter and Wetzel, 1986). At the same time, summer atmospheric conditions have been interpreted as having a greater influence on shear strength (and, subsequently, the erodibility of surface, intertidal (mid-latitude) mudflat sediments), than changes controlled by prevailing oceanographic or biological conditions (Amos *et al.*, 1988).

In summary, it can be deduced that sediment stability in intertidal waters is controlled by gravity, geotechnical properties of the grains, and the exposure time to summer atmospheric conditions. To some extent, however, it is revealed also that biological factors may influence the stability of intertidal flats; in order to comprehend thoroughly the problem of sediment stability, these latter factors are studied in the present investigation.

2.2.1. Shear Strength

One of the most fundamental parameters controlling soil strength is the resistance of a soil (or sediment) to deformation in shear; this is defined as shear strength. Shear strength itself is a function of cohesion and internal friction, together with the effective load directed normal to the plane of the shear failure. Non-cohesive materials, such as sands and coarse silts, derive their shear strength from high levels of internal friction between grains. In contrast, cohesive materials such as silts and clays normally have lower friction values; therefore, their shear strength depends upon much higher values of cohesion (Pestrong, 1969).

Interstitial pore-waters exert a considerable influence on the results of shear strength measurements. In sediment deposits which do not lose pore-waters, the imposed load is borne largely by the pore-water; therefore, the shear strength is essentially equal to the cohesion of the sediment. In sediments associated with drainage of pore-water, leading to increased grain-to-grain contact, the shear strength is a function of the cohesion and friction angle of the sediment; as well as the imposed load. These relationships can be represented by:

$$\tau = C + \sigma' \tan \theta \quad (2.1)$$

where τ is the shear strength, C is the cohesion, σ' is the effective pressure and θ is the angle of internal friction.

The effective pressure is expressed as $\sigma' = (N - \mu)$, where N is the normal load and μ is the pore-water pressure. Under fully drained conditions, however, $\mu = 0$ and $\sigma' = N$; hence,

$$\tau = C + N \tan \theta \quad (2.2)$$

In a fully undrained condition, $\mu = N$ and $\sigma' = 0$; therefore,

$$\tau = C \quad (2.3)$$

In non-cohesive sediment, such as clean sands and coarse silts, equation (2.2) becomes

$$\tau = N \tan \theta \quad (2.4)$$

For cohesive sediments, the shear strength may be determined through the use of triaxial testing or an unconfined compressive strength testing apparatus. Here, the shear strength of clays and other materials (behaving like clays) is equal to one half of the unconfined compressive strength (Q_u) of the sample:

$$\tau = \frac{1}{2} Q_u \quad (2.5)$$

The unit load which results in the destruction of the sample in this apparatus is its unconfined compressive strength, which is determined by the following relationship:

$$Q_u = \frac{F}{O} \quad (2.6)$$

where F = failure load, O = original cross-sectional area of sample.

It can be shown also that the angle between the plane of failure and the plane on which the major principal stress is applied (α) is equal to

$$\alpha = 45^\circ + \frac{\theta}{2} \quad (2.7)$$

This angle (α) can be measured directly from the geometry of the sheared sample. For a quick-undrained unconfined compression test, where failure occurs before pore-waters have a chance to drain, it may be assumed that the pore-water bears the normal load. Under such conditions, θ is assumed to be 0 and equation 2.3 applies, therefore

$$Q_u = 2C = 2\tau \quad (2.8)$$

If the samples do not shear cleanly and deform by bulging, then the unit load that causes a decrease in the height of the sample by 20% is assumed to be unconfined compressive strength.

The above approach for measuring the shear strength of soil (or sediment deposits) in the laboratory uses the 'triaxial apparatus' (Terzaghi and Peck, 1967). Another most versatile piece of equipment is the 'vane-shear apparatus', which can be used in both laboratory and *in situ* investigations. The latter

apparatus is used in the present investigation, the detailed characteristics and how it operates are described in Section 4.2.1.

2.2.2. Erodibility

The erodibility of fine-grained abyssal sediments depends upon various forces, acting on surface sediment particles exposed to bottom current activity (Southard, 1974). These forces are related to the dynamics of the turbulent boundary-layer flow, the physical and chemical nature of the sediment particles and the past history of the sediments, including the effects of flocculation and the activity of benthic organisms. Time scale also determines, at least in part, the problem of erodibility.

In general, various aspects of erodibility require investigation: (1) the lowest velocity at which movement occurs, termed the critical velocity or threshold velocity; (2) the rates of erosion at particular velocities greater than the threshold velocity; (3) the size, nature, and location of particles (or larger solid units) removed from the sediment surface; and (4) the form or geometry of the eroded surface. Of these characteristics, the attention of the most scientists has been directed towards threshold velocities. However, there is some disadvantage in using such a velocity to characterise the strength of the current acting on a sediment surface, in that the time-average velocity must increase away from the sediment-fluid interface (from zero to a maximum value). Hence, the free-stream value (well away from sediment surface) and the nature of the velocity distribution depend upon both the strength of the flow and the detailed geometry of the sediment surface.

2.2.3. Forces Acting on a Particle in the Bed

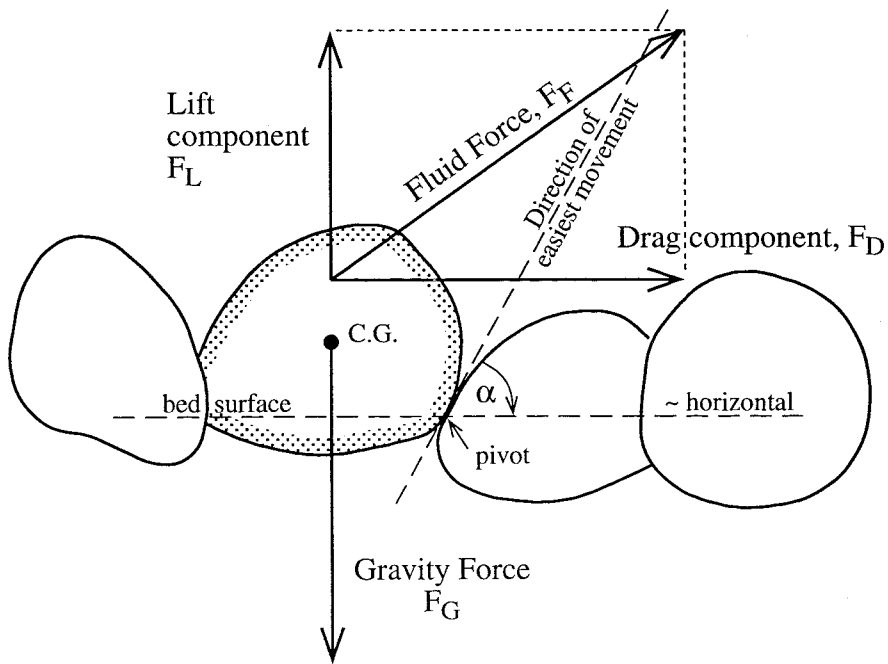
Assuming that a sediment is cohesionless in character, there are two opposing forces acting on the sediment grains: those tending to retain the grain in place (the submerged weight of the grain); and those tending to lift, roll, or slide the grain from its position in the bed (forces of fluid lift and drag) (Middleton

and Southard, 1984). The combination of different fluid forces (lift and drag) produces a resultant, acting downstream and at some angle to the bed. Such a resultant force can move the grain in a number of ways: (1) lifting the grain from the grains beneath it; (2) sliding the grain along some path of "easiest movement", over the grains such as those downstream of it; or (3) rotating the grain about some "pivot" formed by one or two of the grains in the bed (Figure 2.1). In the first case outlined above, the grain must be raised up rather steeply from the bed; therefore, the lift forces must be at least as important as the drag forces. In the second case, the balance is between the component of the fluid force (acting upwards in the direction of easiest movement) and the component of the gravity and the frictional forces (acting in the opposite direction). In the third case, the balance is between the moments of fluid forces tending to rotate the grain in the downflow direction, and the moment of gravity force tending to hold the grain in place in the bed. It is considered generally that the third case is the most realistic one. However, analysis of the other two cases leads to approximately similar conclusions, except for the different coefficients involved.

The gravity force acts through the centre of gravity, but the position of the pivot and the direction of the easiest movement vary greatly from grain to grain. Such variation is due to differences in the size and shape of the grains, together with their local packing. The fluid force does not necessarily act through the centre of gravity of the grain; it may be expected to act through some point above the centre of gravity, because the upper part of the grain is more exposed to fluid forces than the lower part. In addition, the fluid forces vary from grain to grain; they are strongest for the most exposed grains. The forces fluctuate also with time because of turbulent motions, even within the viscous sublayer of the flow with a steady time-average-velocity. This summary indicates, therefore, that any criterion established by researches for the initiation of sediment movement will not be completely deterministic; rather it will be stochastic (statistical) in character. Further details on the forces involved in the movement are presented below.

Forces Acting on a Grain

A



Analysis of Moments (for Drag component)

B

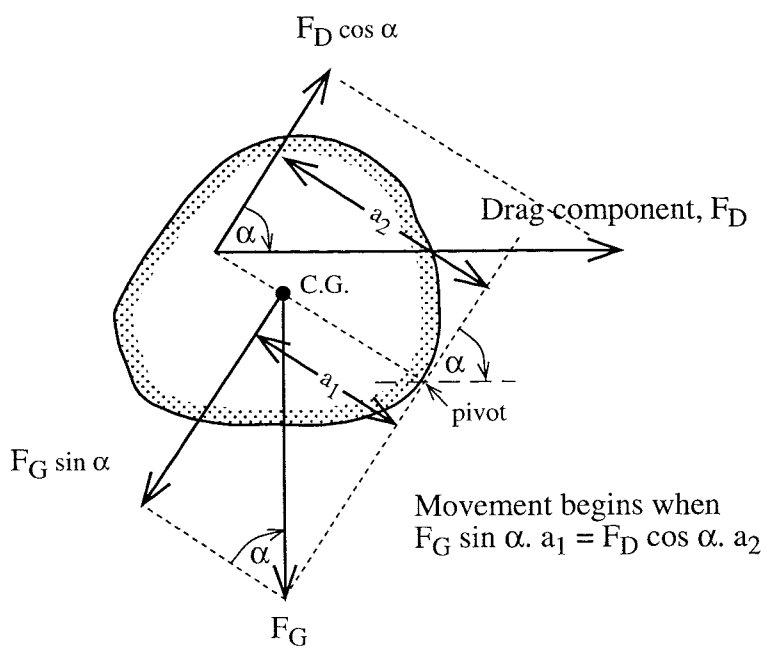


Figure 2.1. (A) Forces acting on a grain resting on a bed of similar grains, (B) Analysis of moments acting on a grain at the beginning of grain movement (from Middleton and Southard, 1984)

(a) Gravity Force

The total gravity force acting on a grain is the product of its volume multiplied by the submerged specific weight ($\gamma_s - \gamma$). If D_n is the nominal diameter and the volume is represented by $(\pi/6)D_n^3$, then the total gravity force F_G is

$$F_G = \left(\frac{\pi}{6}\right) D_n^3 (\gamma_s - \gamma) \quad (2.9)$$

The component of this force that opposes sliding of the grain, in the direction of easiest movement, is $F_G \sin \alpha$ (where α is the angle that the direction of easiest movement makes with the horizontal (Figure 2.1))

(b) Frictional Forces

The friction between grains is not considered explicitly in most published theoretical analysis of grain motion; however, its effect is considered to be accounted for by the value chosen for α . The problem is analogous to that of the angle of repose of sands (Statham, 1977) i.e. the surface slope of a sand deposit can be established only to a certain limiting angle, which is called the angle of initial yield. Beyond this angle, the downslope component of gravity forces acting on a surface layer of sand exceeds the resistance offered by a combination of frictional forces and upslope components of gravity (resulting from interaction between the weight and geometry of the grains).

It has been assumed elsewhere that the angle α is similar to that of the initial yield of a sand slope immersed in water; this, for a typical sand, is about 35° (Carrigy, 1970). Nonetheless, the angle of repose for a single grain of a fixed bed composed of other grains is not necessarily the same as the mass angle of repose assumed by a pile of grains (Miller and Byrne, 1966). The angle for a single grain on a fixed bed of similar grains is larger, within the range from 45° to 70° . The actual angle depends upon the grain sphericity and roundness (with smaller values for more spherical and more rounded grains) and on the sorting of the deposit (with smaller values for better sorted grains). For grains smaller than

the average size in the (fixed) bed the angle is larger, and for grains larger than those in the bed the angle is smaller. The low value for grains larger than the average for the bed suggests the possibility that larger-than-average grains may actually be the easiest to move.

(c) Fluid Forces

There are two kinds of fluid forces acting on a grain resting on the bed: (1) those due to viscous drag, acting mainly on the upper exposed surface of the grain; and (2) those due to the unequal distribution of dynamic pressure on the grain surface. Viscous forces are likely to be important at low boundary Reynolds numbers, $u.D/\nu < 5$. Overall, it is convenient to distinguish the two components of the fluid force regardless of its origin: drag acting parallel to the flow and therefore parallel to the bed; and lift acting normal to the bed. The drag force can be represented by the following equation:

$$F_D = C_D \left(\frac{\rho U^2}{2} \right) A \quad (2.10)$$

where C_D is the drag coefficient, ρ is the fluid density, U is the velocity, and A is the cross-sectional area of the sphere (or grain).

The lift force arises because of the asymmetry of the flow around a grain resting on the bed. As higher fluid velocities are developed over the top of the grain, rather than underneath it, an asymmetrical pressure distribution occurs. Higher pressures act upward on the lower surface on the grain, than on the upper surface of the grain acting downward. This difference results in a net upward lift force. Lift forces, cannot be expected to act on grains that are freely suspended in a fluid, therefore, because flow around such particles is symmetrical about the line of flow. Consequently, the lift force component decreases very rapidly as a grain rises up above the sediment/water interface (Chepil, 1961; Willetts and Murray, 1981). The lift force for a given spherical grain is given by the following equation:

$$F_L = C_L \left(\frac{\rho U^2}{2} \right) A \quad (2.11)$$

where, in the case of a unit length of a cylinder, $A = D$; in the case of a sphere, $A = \pi D^2/4$. The resultant force on a grain is obtained by adding F_D and F_L , vectorially.

2.2.4. Initiation of Sediment Movement

Grains begin to move on the bed when the combined lift and drag forces produced by the fluid, become large enough to counteract the gravity and frictional forces that hold the grain in place. The initiation of movement may be (Figure 2.1) represented by the equation:

$$a_1 (F_G \sin \alpha) = a_2 (F_D \cos \alpha) \quad (2.12)$$

The left hand side of this equation represents the total moment due to gravity, tending to: rotate the grain upstream about the pivot; or to hold it in place against the moment due to fluid drag forces, tending to rotate the grain downstream. The right hand side of this equation represents this fluid drag moment, in a purely conventional way.

Such physical controls on sediment movement are modified, as will be demonstrated by the results of the present investigation, by biological activity. The presence of organisms can either stabilise or destabilise sediments, resulting in less or more easily erodible surfaces than their abiotic counterparts (Jumars and Nowell, 1984). For example, arrays of animal tubes are likely to stabilise the bed by shielding it from the overlying faster flow (Rhoads *et al.*, 1978; Eckman, 1983). In contrast, organisms which produce surficial traces as they crawl across a sediment surface may enhance the erodibility (i.e. destabilise) the sediments (Nowell *et al.*, 1981).

2.3. *Lanice conchilega*

Lanice conchilega is a terebellid polychaete which is rather large, strongly cephalised and tubicolous. The anterior end is equipped with a series of very extensible tentacles, whilst the lips are heavily muscular and pliable. *Lanice* feed on detritus, including diatoms, other unicellular algae, and various small invertebrates and larvae (Sanders *et al.*, 1962; Ronan, 1977). The tentacles of the polychaete are usually held so that in cross-section they present a shallow inverted U or V-shaped form to the bed. The cells along the edges of the V are mucus-producing, whilst the median cells are ciliated. During the feeding process, smaller particles are transported in a mucus string along the median strip of the V, down to the proximal end of the tentacles. The proximal part of the tentacles are smooth and rounded; hence, the mucus string is transferred to the mouth by muscular lips. Large particles are pulled in close to the body by muscular contraction of the tentacles and, in most cases, several tentacles will collaborate to pull in large particles (Watson, 1916).

The tubes of *Lanice conchilega* are topped by a fan-shaped branching structure which has been suggested to have several functions, such as: snares for food; support for filter-feeding tentacles; closure of tubes at low tide; and protective mimicry (Watson, 1890). The fans of *Lanice conchilega* are orientated at right angles to the current, allowing transported material to deposit within the quiet areas behind the fans (Ziegelmeier, 1952 and 1969). It is supposed that most tubes of terebellids are blind-ended; however, in coarse sediments, terebellid tubes are open at both ends (Seilacher, 1953). Such headward irrigation indicates that the tube must be open at the lower end. Also, the tubes of some terebellid species have been described as U-shaped (Rhoads, 1967), and this is thought to be associated with a low flux of food materials (Ziegelmeier, 1952). However, U-shaped tubes are not usual in adult *Lanice*.

2.3.1. Distribution

Several studies have described species-associations dominated by *Lanice*

conchilega (Ollivier, 1969; Eagle, 1975; Buhr, 1979). It is recorded from the shallow sand association of various Scottish beaches (Watkin, 1942; McIntyre and Eleftheriou, 1968; Eleftheriou and Nicholson, 1975); and as widely distributed in European waters. In Europe, the distribution is as follows: Denmark (Blegvad, 1914); Scotland (McIntyre, 1958; Perkins, 1974); England (Spooner and Moore, 1940; Howells, 1964; Eagle, 1975); France (Ruillier, 1959; Ollivier, 1969); Germany (Ziegelmeier, 1952 and 1963; Reineck et al., 1968; Stripp, 1969; Buhr, 1976 and 1979); and the Netherlands (Beukema, 1976).

Lanice conchilega has several typical features: a distinctive vertical tube (Ziegelmeier, 1952); an aggregated habit (Ziegelmeier, 1952; Beukema, 1976; Buhr, 1979); a preference to exist in well-sorted sands and strong currents (Ziegelmeier, 1952; Howells, 1964; Ollivier, 1969; Buhr and Winter, 1977); a distribution which extends from low water to 50 m water depth (Spooner and Moore, 1940; Reineck et al., 1968; Perkins, 1974; Buhr and Winter, 1977); and a tube diameter 1 - 7 mm, tube length 1 - 50 cm, with a body tissue biomass of 1 - 35 mg dry weight (Buhr and Winter, 1977).

2.3.2. Larval Development

The sexes of *Lanice conchilega* are separate and the sexually mature organisms are readily distinguished. The males and females become mature from April to the end of June in Sylt (in German Bight) (Kessler, 1963). The developing gametes are carried in the coelomic fluid. Male gametes are visible through the thin wall body as a milky-white mass and the female gametes as red-brown globules. The ripe gametes are released directly into the water, where fertilisation occurs. The fertilised egg develops into a free-living trochophore larva and metamorphoses rapidly into a worm-like aulophore larva (Figure 2.2), some 6 - 10 days after fertilisation. During the metamorphosis process, the larva begins to build a simple tube; this consists of mucus and detritus, which will develop into a typical mucus tube when the metamorphosis is complete. The tube is secreted by an exclusively larval structure, the dorsal gland. This secretion is

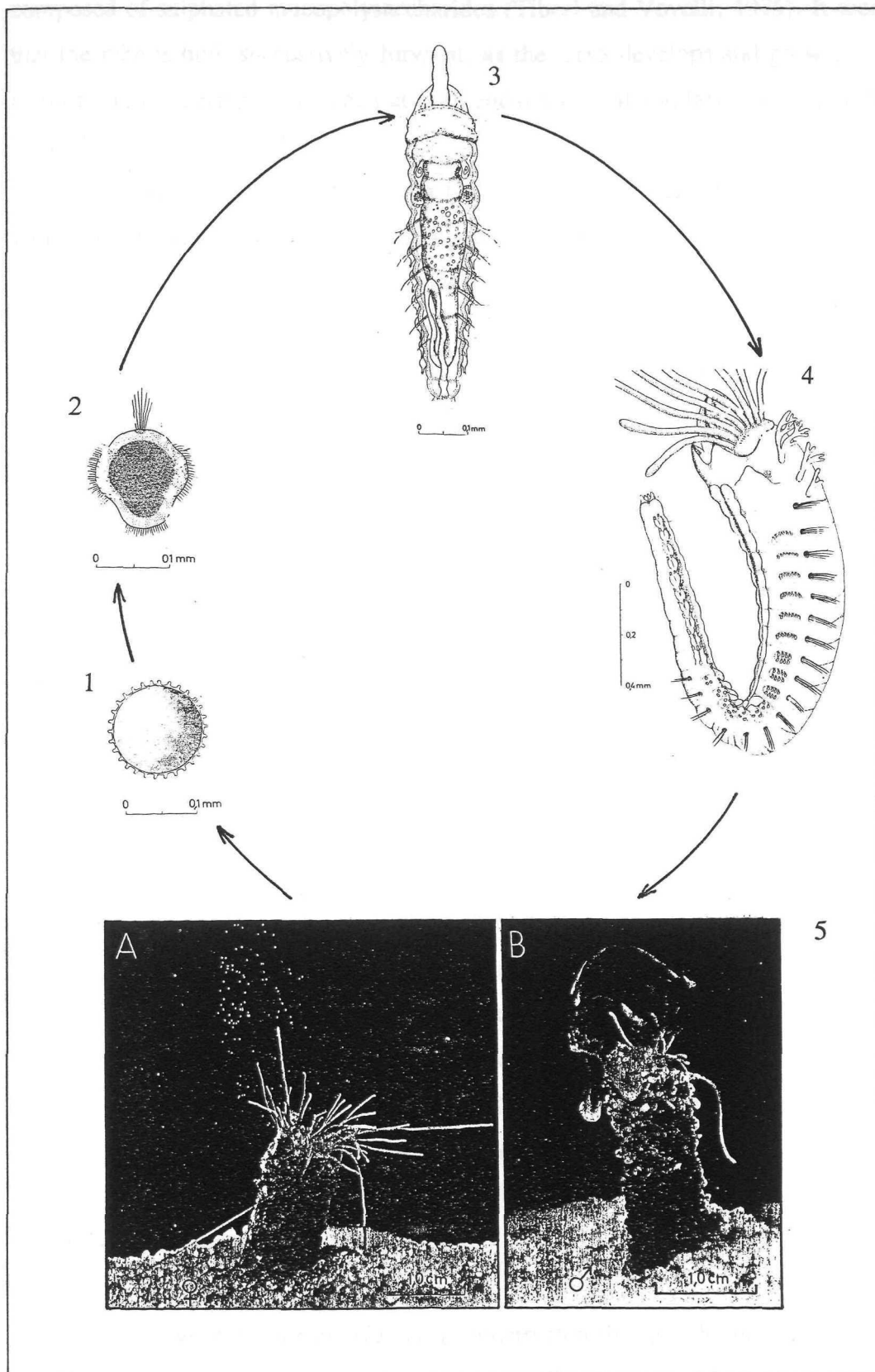


Figure 2.2. Life cycle (larval development) of *Lanice conchilega*. Key: 1 = Fertilised Egg; 2 = Trophophora Larva (2 days old); 3 = Aulophora Larva (dorsal view); 4 = Juvenile *Lanice* (side view); 5A = Spawning Female *Lanice* in an aquarium; and 5B = Male *Lanice* in an aquarium (from Kessler, 1963)

composed of sulphated mucopolysaccharides (Tiberi and Vovelli, 1975). It seems that the tube is built successively forward, as the larva develops and grows, resulting in a tapering form (open at both ends) with oblique layers visible in the wall of the tubes.

The aulophore larva moves constantly within the clear tube. It remains within the plankton and is transported by currents. As *Lanice conchilega* has a prolonged larval life, this planktonic stage may last up to 2 - 3 months (Thorson, 1946). This long period results in large-scale dispersal of the larvae. This type of dispersal is advantageous, where success in survival and reproduction varies independently from place to place (Strathmann, 1974).

The rudimentary organs of the aulophore larva develop into gills, setae, setal hooks, mouth, lips and prostomial tentacles during the period of planktonic life and prior to settlement. The exact timing and mechanisms by which settlement occurs, however, is not known. At the time of settlement the extensile, prostomial tentacles are usually well-developed and capable of the same coordination as in the adult.

When settlement is complete the juvenile worm burrows into the sediment, in exactly the same manner as adult individuals removed from their tubes. The larval tubes (mucus secreted by the body surface in adult) serves as a surface for exerting hydrostatic pressure, through peristaltic waves of the body (Seilacher, 1951). The propulsive force of the hydrostatic waves are directed vertically downward into the sediment, whilst the prostomial tentacles assist in pushing and moulding the sediment particles into a mucus-lined tube. The initial tube is U-shaped as the young worms burrow for 1 - 3 cm, then turns back up towards the surface. The tube is then extended above the sediment surface (substratum) and decorated with a tiny fringe, like the adult tubes.

2.3.3. Tube Building

The tube of *Lanice conchilega* is constructed through the mucoidal binding of shell fragments and mineral grains (Ziegelmeier, 1952 and 1969). Selection of particles does not occur beneath the sediment surface; rather the

burrow is lined with muco-polysaccharide layers, binding the sediments particularly to the burrow wall (Bielakoff *et al.*, 1975). Above the sediment surface, the tube is built of selected grains and shell fragments which are carefully attached with muco-polysaccharides (Wunderlich, 1970). *Lanice conchilega* selects generally large grains and shell fragments to construct the projecting tube; small grains and narrow fragments are used to build prolonged filaments that comprise a fan-shaped fringe. The fringe extends from the aperture, having its borders prolonged into several small branches formed of the same fragments, and which serve to lodge the tentacles (Cuvier, 1836). The precise nature of the tube varies according to the available material. However, the general form consists of two semicircular plates extended above the circular opening of the tubes (which has 4 - 5 mm outside diameter). The plates and the cylindrical tube end in irregular branching filaments, which are 1 - 5 times as long as the tube diameter. The filaments diameter is dependent upon the available particle size. However, if a wide range of sizes is available, it has been found that the worm generally selects particles of 0.5 - 1 mm (in their narrowest dimension); these are attached lengthwise, to build the fringe elements.

There have been some conflicting findings between various studies as to the function of the fringe. Such interpretations may be summarised as follows: (a) the fringe is oriented perpendicular to the prevailing currents, acting like a fish trap placed across ebbing tidal channels (Seilacher, 1951); (b) the fringe functions as a snare (Ziegelmeier, 1952), with filter feeding tentacles (Ziegelmeier, 1952; Watson, 1890); (c) with the fringe functioning as baffles, slowing the current and allowing sedimentation of fine-grained particles between the tubes (Ziegelmeier, 1969). Several studies have been undertaken of feeding in of *Lanice conchilega*. The following mechanisms have been suggested: detritus feeding (Ziegelmeier, 1969); filter feeding (Buhr, 1979); facultative suspension feeding (Buhr, 1976); all utilising a sieving effect, whereby large food particles are caught in the fringe and collected by the tentacles (Buhr, 1979).

There has been no specific study on the mineral composition of *Lanice conchilega* tubes. Studies of other species of polychaetes, however, have revealed that the tubes were composed almost entirely (95 % or more) of tabular-shaped,

heavy mineral grains; these are mostly (80 - 85%) of green hornblende, ranging in size from 62 - 80 μm . Particle counting carried out on these tubes indicated that the worms must have handled about 25,000 sand grains per centimetre of tube, constructed with an outside diameter of 0.6 mm (Fager, 1964). However, mineral composition of tubes is likely to be species specific and locally dependent.

In *Lanice* the process of tube-forming involves a great deal of manipulation by a special 'Lippenorgan' (Watson, 1901). During this process, the sand grains are either accepted or rejected. The diameter and the length of the tube is increased by adding onto the upper rim. The particles are attached by their lower portion so that the tube is imbricated upwards. Hence, when the worm twists the tube in the sand, the vertical movement is mostly downward and the worm can compensate for the increased tube length (Watson, op.cit.). During rough weather conditions, wave surge was seen to stir up the sand and move the suspension past/through the brachial crown. On days when there was little or no wave surge, the worms were seen to bend the tube over and pick up particles from the adjacent sand (Fager, 1964). Tubes can reach 12 - 13 cm in length and 4 - 5 mm in outside diameter.

The sand particles forming the tubes are attached together by a thin organic layer of a quick-setting proteinaceous material (Fager, 1964). The living worm is able to protect the organic layer against bacterial attack. However, empty tubes start to decompose within a week or less, in aerated seawater in the laboratory. This observation suggests that the concentration of heavy minerals formed by the worms would not persist long after their death, if the tubes were in a sand layer subjected to stirring by waves. In contrast, long tubes which sometimes reach this layer (and either the death of mature worms or gradual attrition of juvenile tubes) could result in a high concentration of heavy minerals within the sand.

The presence of the adult tube may influence the settlement behaviour of juvenile *Lanice conchilega*, either hydrodynamically (through the entrainment process occurring in local areas of disturbed flow) or chemically (through some attractant in the tube or secreted by adult individuals) (Kessler, 1963). These

possibilities have not been studied specifically, but observations on the flow disturbance of single and paired tubes in unidirectional flow appear to show that the settling larvae worms find the adult tubes an attractive substratum; small tubes are commonly clustered around larger and older tubes. Insufficient evidence is available to suggest that the activities of the adult deposit-feeding organisms prevent juvenile worms from settling successfully, within the radius of their tentacles. The size of the fully-developed aulophore tube (1.6 mm long and 0.15 in diameter) prevents the adult from ingesting juvenile worms. The successful recruitment of large numbers of juvenile worms into an established population of older worms (Buhr and Winter, 1977; Buhr, 1979) may be responsible for the 'patchiness' observed in marine environment.

When the juvenile individuals of *Lanice conchilega* grow, the initial narrow U-shaped tubes are abundant. The process of tube renewal, as growth occurs, seems to continue throughout the life of the worm (Ziegelmeier, 1952; Schäfer, 1972). It is possible that during this process some spacing may occur, from the initial cluster about the adult tubes. Single and mixture size classes of adult tubes have been observed rarely to be in contact along their length. Likewise, the tops of the tubes are spread relatively evenly at densities above 2000 m⁻². However, an apparently regular distribution may be a random filling of the available space, with cylinders that cannot overlap (Simberloff, 1979).

Reproduction of *Lanice conchilega* occurs over an extended period, as larvae are observed from April - October (Wolff, 1973). Large numbers of planktonic larvae are released (Kühl, 1972); these settle on a variety of substrata, but appear to prefer aggregating near established adult organisms (see also Section 2.3.2).

2.4. Biological Parameters

2.4.1. Algae

Only a few field and laboratory studies have revealed that extracellular

mucus secreted by benthic microalgae can stabilize the sea bed and, hence, inhibit the motion of sediment grains (Neumann *et al.*, 1970; Coles, 1979; de Boer, 1981; Paterson, 1989). Such stabilization is defined as the binding of sediment particles with polysaccharide materials (Vos *et al.*, 1988; Grant and Gust, 1987). Similarly, little is known about the mechanisms by which benthic organisms modify the stability of bottom sediments. Microbial binding of surfaces of natural sediment has been identified (Neumann *et al.*, 1970; Frankel and Mead, 1973), but it has been revealed that bacteria and diatoms adhere to surfaces using extracellular materials (Robert and Gouleau, 1977; Costerton *et al.*, 1978). Finally, more research is required into how exopolymers extend between grains and which organisms are important in binding particles.

The microbial binding of marine sediments may produce a uniform 'carpet' on a flat surface. Rough flow and active sediment transport will affect the distribution of microalgae. Burrowing activities of benthic organisms may also disrupt the mucus binding of sediments (Neumann *et al.*, 1970). Elsewhere, the horizontal distribution of chlorophyll-a and ATP (Adenosine TriPhosphate) in marine sediments has been investigated (Skjoldal, 1982), whilst Fazio *et al.*, (1982) have analysed polysaccharides from various mucus sources, but not in relation to sediment stabilisation.

In terms of field measurements, the greatest increase in sediment stability has been recorded at stations high on the shoreline: here a high density of matrix diatoms were found to develop on the surface of sediment deposits (Paterson *et al.*, 1990). The accumulation of mucilage at the surface depends upon several factors including the species of diatom (Holland *et al.*, 1974), the density of the population, and the surface residence time. The latter is not equal to the emersion period, since diatoms may stay at the surface of sediment for only part of the total emersion period (Admiraal, 1984).

The effect of a diatom matrix (assemblages) cannot be separated easily from the effect of subaerial exposure, although it seems that dense populations influence sediment stability. The mechanisms through which epipelagic (motile) diatoms stabilise sediments (see Paterson, 1988), are related to the physical characteristics of the mucilage produced for locomotion (Edgar and Pickett-

Heaps, 1984). Providing that the mucopolysaccharide matrix at the surface becomes dehydrated, the sediment will become more tightly bound in the thickening matrix. Dewatering of the sediment and dehydration of the matrix, therefore, may act together to increase sediment stability (Paterson *et al.*, op. cit.).

2.4.2. Microbenthos

The populations of microorganisms in marine sediments are associated mainly with particle surfaces; this has important biological implications for the sedimentary environment (Anderson and Meadows, 1978). Bacterial films can have significant effects on the properties of sediment, particularly through increasing adhesion between particles and altering the granulometry (Webb, 1969). Extracellular and autolytic products of microorganisms living on the grains, and within the interstices, can also foster sediment stability through the accumulation of mucilaginous materials (Frankel and Mead, 1973).

2.4.3. Meiobenthos

The dominant meiofauna present in marine sediments are nematodes. The population abundance of this taxon in fine-grained shelf sediments can be of the order of 8 to 9×10^5 individuals m^{-2} , but may reach 4 times this density (Juario, 1975). Meiobfaunal nematodes can establish rapidly a closely-spaced network of thread-like intergranular burrows within the surface layer of the sediment, utilising mucus secretion for strengthening these structures (Cullen, 1973). Evidence that nematodes can stimulate bacterial production in sediments (Gerlach, 1978), increasing the microbial activity on detritus (Finley and Tenore, 1982), suggests that they may be doubly effective in binding sediment.

2.4.4. Macrobenthos

Animal tubes may stabilize marine sediments, by altering the character of

the flow near the sea-bed. At a certain tube density, the interaction of flow perturbations caused by individual tubes may produce a 'skimming' flow (Morris, 1955); this effectively protects the bed from erosion. Within such a flow, the maximum turbulent kinetic energy and shear stress occur far away from the sea-bed. Studies performed to predict the tube density at which more or less kinetic energy impinges upon the sea-bed have not been well quantified. The results show some lack of agreement between experimenters (Nowell and Church, 1979). Such lack of agreement may be the result of a number of factors, such as the problem of dynamic and geometric scaling or the effect of mucus secreted by sediment- associated organisms.

Burrowing cerianthid anemones, which are commonly present in heavily bioturbated sediment, can markedly influence the shear strength of sediments (Rowe, 1974). This increase may be due to mucus production, which leads to particle-to-particle adhesion. In contrast, biogenic reworking can decrease the critical erosion velocity of mud (Young and Southard, 1978) and sands (Grant *et al.*, 1982).

Studies on the impact of roughness elements on flow have been undertaken widely (Wooding, 1973). Only a few experiments have been carried out, however, on the effects of animal tubes or other biogenous roughness elements on substratum stability (Rhoads *et al.*, 1978; Yingst and Rhoads, 1978; Eckman *et al.*, 1981).

Sediment stability and grain size have an important influence on the distribution of marine benthos in a soft-bottom substratum. Numerous studies support this assumption, for example: high correlation between specific faunal assemblages and grain size (Sanders, 1958; Wieser, 1959); a change in the community structure, in accordance with the degree of sediment stability (Rhoads and Young, 1970); the ability of some species to select substrates, on the basis of particle size (Meadows, 1964; Gray, 1971); and optimal foraging models, predicting that particle size is an important control on energy intake by surface deposit feeders (Taghon *et al.*, 1978).

Since the classical work of Petersen (1913), benthic macrofaunal communities have been related to habitat type (Jones, 1950). For example, Gray

(1974) has shown that sediment type is an important factor in determining species composition in a community. At the same time, temporal and spatial differences may occur within a particular habitat type, due to biological interactions (Rhoads, 1974). The basic differences between the composition of benthic communities of different habitats are determined mainly, however, by physical factors i.e. biological factors are of minor importance (Jones, 1950). Tidal currents and wave-induced currents determine the nature of the habitat, the stability of sediments, the pattern of food supply for benthic organisms; in extreme cases, they may even cause severe physical stresses on organisms (Wildish, 1977). The above studies concentrate mainly upon physical and biological interactions; only a few are available, however, on the relationship between tube density and the abundance and richness of species (Sanders *et al.*, 1962; Bailey-Brock, 1979; Wilson, 1979).

Most investigations into marine benthic ecology have been directed towards the short-term sampling of a particular marine environments, in an attempt to delimit macrobenthic species or assemblages (Whitlatch, 1977). The results obtained reveal that generally, given species assemblages are affected greatly by sedimentary parameters such as grain size. These assemblages are not tightly functioning units, but tend to be composed of individualistically distributed species; these, in turn, respond to a complex set of environmental and biological parameters. Such findings enable the prediction of the occurrence of certain faunal assemblages, on the basis of a particular set of sedimentary parameters. For longer periods of time, however, the predictive capability for determining the distribution of a given species is reduced greatly. Generally, any naturally-occurring community of organisms is not only distributed spatially but also temporally. In order to understand fully the patterns of community organisation of macrobenthic organisms, therefore, more long-term studies are necessary to provide basic knowledge concerning temporal community structure and factors affecting the compositional change of species.

Although temporal changes in community structure and species composition in subtidal environments have been investigated (Sanders, 1960; Pearson, 1971; Tenore, 1972; Watling, 1975), there are fewer studies concerned

with time-related community changes in intertidal environments (Johnson, 1970; Bloom *et al.*, 1972; Holland and Polgar, 1976). These latter environments are suitable habitats to study the effects of seasonal change, or the associated physical parameters fluctuate with greater amplitude than in adjacent subtidal habitats. Such fluctuations subject the inhabitant organisms to greater stress.

2.4.5. Benthic Communities

(a) *Species Diversity*

The organisation of a benthic community can be simply represented by the number of species and the number of individuals within each species, which is defined as diversity (Gray, 1981). A number of methods are available to measure diversity; however, the most widely used is that of Shannon-Wiener method (Shannon and Weaver, 1963):

$$H' = - \sum_{i=1}^s p_i \log_2 p_i \quad (2.13)$$

where $p_i = n_i/N$ (n_i is the number of individuals of the i th species and N is the total number of individuals) and S is the total number of species.

In general, the diversity index increases with an increase in the number of species. However, the diversity index will also increase as the proportion of individuals within each species becomes more constant.

The diversity index measures both species richness and evenness. The latter can be obtained by dividing the observed diversity value, by the maximum possible value. Evenness (J) (Pielou, 1966) can be defined, therefore, as:

$$J = \frac{H'}{H'_{\max}} \quad (2.14)$$

where H' is the diversity and $H'_{\max} = \log_2 S$. Unfortunately, the diversity index value is often reported merely as H' and the evenness component is not included. Consequently, in some cases, it cannot be determined whether any change in diversity is due to an increased number of species, or to a more even distribution

of individuals between each species.

For typical benthic communities, by plotting diversity (H') against $\log_2 S$ and diversity against evenness (J), it can be established whether the diversity index is more responsive to an increase in the number of species ($\log_2 S$) or to an increasing evenness in the distribution of individuals among species (Gray, 1981). Diversity as measured by the Shannon Wiener index is usually poorly correlated with $\log_2 S$, but has a better correlation with J . The addition of a rare species to the community has little effect, therefore, on diversity; a change in dominance has a larger effect. These patterns can be derived for most subtidal macrobenthos and meiobenthos. However, not all communities show such trends. For instance, bird communities have a higher correlation of H' with $\log_2 S$, indicating that the addition of a rare species is relatively more important than a change in the dominance pattern. This relationship may be due to the fact that bird species are largely territorial; consequently, the dominance pattern remains fairly constant.

The other method which has been used widely to measure the diversity of marine benthic organisms is the 'rarefaction method' (Sanders, 1968). This approach is a graphical method of expressing diversity: high diversity is represented by steep curves, with low diversity by shallow ones.

The deep-sea diversity is much higher than that of shallower water areas. Such a trend can be explained on the basis of the Stability-Time Hypothesis (Sanders, 1968). Near an environmental extreme such as the high intertidal zone, for example, the fauna is subjected to environmental factors which fluctuate in an unpredictable manner. As many species are unable to tolerate such unpredictable fluctuations, the species number is low. In contrast, the deep-sea is an extremely constant environment, with no light and almost no change in temperature, salinity or oxygen for relatively short periods (of months and years) or even very long periods (such as thousands of years). This constancy has enabled the species to adapt to each other rather than needing to adapt to the rigours of the environment; this contrasts with intertidal areas. Finally, since the quantity of food reaching the bottom of the deep-sea from the surface is small, then the densities of animals per square metre are low.

The Stability-Time Hypothesis, however, is not entirely consistent when considering Non-equilibrium Theory (Intermediate Disturbance Theory) (Connel, 1978; Huston, 1979). This theory is based upon the concept that competition leads always to a reduction in diversity, due to competitive exclusion forcing species out of community. This situation is commonly mediated in practice because random disturbance prevents competitive exclusion from taking place and, hence, raises the diversity level. However, if the disturbance exceeds a certain level then the disturbance itself will eliminate species from the community, reducing diversity. Disturbance is the primary structuring force in non-equilibrium theory and such diversity has a non-linear relationship with disturbance. Therefore, pollution could increase, decrease, or cause diversity to become constant. Some field evidence has been presented to support the non-equilibrium theory, including pollution studies, whereby intermediate pollution levels have raised diversity (Pearson *et al.*, 1983; Lambshead, 1986; and Moore and Pearson, 1986).

(b) Community Structure

A relationship between benthic communities and environmental factors can be expressed in terms of that between feeding type and the silt-clay content of the sediment deposits (Sanders, 1958). The highest densities of suspension feeders occur in sandy sediments. Sediments with a grain size of around 0.18 mm are the easiest to transport; therefore, their occurrence indicates the minimal wave and currents action (Gray, 1981). This property may be exploited by suspension feeders, creating the highest densities at this particular grain size. In contrast, deposit feeders reach their highest densities in muddy sediments; this is due to the high organic matter content.

The absence of suspension feeders within silt-clay deposits can be explained by the 'trophic-group amensalism hypothesis' (Rhoads and Young, 1970). Within this context, amensalism means that one population (suspension-feeders) is inhibited whereas another (deposit-feeders) is not. The explanation suggested for this hypothesis was that the unstable silt-clay cannot be colonised

by larvae of suspension-feeders, because their gill structures would be rapidly clogged by resuspended materials. Suspension-feeders, therefore, tend to favour more sandy substrate with firm sediment, enabling their larvae to attach. This latter substrate is not suitable for deposit feeders, as there is not sufficient food to support them and locomotion is difficult on coarse-grained particles. Also, suspension-feeders could destroy the larvae of potentially recolonising deposit feeders. The hypothesis applies only to communities of the continental shelf, however, where primary productivity is high and food is not limited to suspension-feeders.

In a later study, it was found that suspension feeders increased along a gradient of increasing silt-clay content (Young and Rhoads, 1971); this is in direct contradiction with the aforementioned hypothesis. In this case, it was argued that the tubes of a polychaete stabilised the sediment, allowing suspension-feeders to colonise in large numbers. On the basis of these examples, it may be deduced that sediment stabilisation by polychaete tubes is important in structuring benthic communities.

2.5. Sedimentological Parameters

2.5.1. Moisture Content

The porosity or moisture content of sediment affects the packing of particles and alters the erosion characteristics of intertidal flat deposits. Natural dewatering will decrease, therefore, sediment erodibility (Anderson, 1983). Moisture content affects the cohesive strength of fine-grained sediments and, likewise, the threshold erosion velocity of fine-grained sediments (Southard, 1974); this is because inter-particle bonding decreases with increasing moisture content. For example, a decrease in moisture content in an estuarine mud by 5 % or less, has resulted in an increase in the threshold erosion velocity by a factor of 1.5 to 2.0 (Young, 1977). Elsewhere, it has been also shown that decreasing the moisture content increases the critical shear strength of cohesive channel deposits

(Parthenaides and Paaswell, 1970).

2.5.2. Organic Matter Content

The presence of organic matter content can increase the cohesiveness of sediments and, hence, their resistance to erosion (Young, 1977; Niedoroda *et al.*, 1981). For example, the organic carbon content in the Windsor mudflat (in Minas Basin, Bay of Fundy) increases with decreasing grain size (Turk *et al.*, 1980); this is because the finer-grained sediment has a greater surface area, which can support the growth of microorganisms. Offshore, it has been identified that the presence of organic matter, with high moisture content and deformability may be responsible for the ductile behaviour displayed by most slope sediments (Busch and Keller, 1983). In this particular example, gravitational forces alone were not sufficient to cause sediment failure at any of the slope locations.

2.5.3. Grain Size

The size of particles is an important parameter controlling sediment stability; as the grain size decreases, the cohesiveness of the sediment increases. Clay particles (with diameters of less than 0.002 mm) are cohesive in character; therefore, they stabilize larger grains through electrostatic forces between adjacent grain surfaces. These forces are defined as inter-particle bonding. In contrast, silt (diameter 0.002 - 0.063 mm) and sand particles (diameter 0.063 - 2.000 mm) have the properties of non-cohesive sediments. In this case, the primary stabilising force is gravity (Niedoroda *et al.*, 1981).

A relationship exists between the critical shear stress required to suspend sediments and their grain size (Smerdon and Beasley, 1959). Interestingly, an increased current velocity is required to entrain very small grains (Hjulström, 1939). To erode cohesive sediments, inter-particle bonds on the clay particles must be broken down (Ariathurai and Arulanandan (1978). Subsequently, the erodibility of cohesive sediment becomes a function of grain size. Decreases in grain size will lead to an increase in the surface area between grains, which will

result in stronger inter-particle bonds. Therefore, the critical shear stress needed to erode a sediment increases with clay content. This assumption is valid, however, only under certain conditions; beyond these, the critical shear stress needed to initiate movement remains constant (Ariathurai and Arulanandan, 1978; Thorn and Parsons, 1980).

2.5.4. Sediment Density

Laboratory flume experiments have demonstrated that denser muds are more resistant to erosion than less dense material (Thorn and Parsons, 1980; Owen, 1977; and Allersma, 1982). Such experiments have shown that a bed of sediment exhibits an increasing resistance to erosion, as the surface layers are eroded away; this will cease, if the shear stress remains constant. By increasing the applied shear stress, the erosion pattern will resume until a new equilibrium is attained. These phenomena are associated with the density of the bed density. On the basis of *in situ* studies, no relationship was established between differences in erosion rates and changes in the bulk density of intertidal flat sediments (Amos and Mosher, 1985).

2.5.5. Atterberg Limits

The Atterberg Limits describe the consistency of soils (or sediments), related to the liquid limit, plastic limit and plasticity index of the soils (Terzaghi and Peck, 1967). The *liquid limit* (L_w) is defined as the water content (expressed as a percentage of the dry weight) at which two sections of a pat of soil barely touch each other, but do not flow together, when subjected in a cup to the impact of the sharp blows from below (BS 1377, 1975). The *plastic limit* (P_w) or lower limit of the plastic state, is the water content at which the soil begins to crumble when rolled out into thin threads. The numerical difference between the liquid limit and the plastic limit is the *plasticity index* (I_w). It has been shown, on the basis of laboratory experiments, that greater critical shear stresses are required for erosion at higher plasticity indices (Smerdon and Beasley (1959). Likewise,

field measurements have shown that the clay content had a direct effect on the plasticity of the sediments (Amos and Mosher, 1985).

2.6. Physical Parameters

2.6.1. Pore-Water Temperature

The temperature of water contained within deposits affects the strength of cohesive sediments. As the temperature increases, the strength of the cohesive sediment decreases; this is because the strength of inter-particle bonding decreases due to the increase in temperature (Kelly and Gularte, 1981; Ariathurai and Arulanandan, 1978). As a generalisation, therefore, warmer sediments may be more easily eroded than those at lower temperatures.

2.6.2. Pore-Water Salinity

The strength of cohesive sediments decreases with increasing pore-water content and decreasing fluid salinity. The rate of erosion, at any given shear strength, decreases as the pore-water salinity increases (Owen, 1977). In other cases, leaching salt from a clay has been found to reduce the strength of the clay by between 0.01 to 0.001 of its original value (Martin, 1962). Similarly, the number of inter-particle bonds per unit area increases with increasing salinity and decreasing water content (Kelly and Gularte, 1981). Elsewhere, it has been shown that the rate of erosion of sediments in fresh water is some 1.6 - 2 times greater than for saline marine waters (Mehta *et al.*, 1982).

2.6.3. Subaerial Exposure Time

The strength of sediments has been shown to increase as the subaerial exposure time increases. Hence, the amount of solar heating can affect the stability of cohesive sediment (Dunn, 1959; Kamphius and Hall, 1983). Overconsolidated fine-grained sediment on mudflats have been identified as

(probably) being affected by compaction, resulting from solar heating and negative pore pressure due to falling water levels (Amos and Mosher, 1985). Furthermore, Amos *et al.*, (1988) showed that atmospheric conditions during summer have a greater effect on the shear strength of intertidal flat deposits than other biological/oceanographical controls (although this conclusion must be modified on the basis of more recent studies (Amos, pers. comm.)).

CHAPTER 3

EXPERIMENTAL SITE

3.1. Introduction

This Chapter reviews and describes previous scientific (oceanographical) information concerning the area under investigation. The aim of the review was to obtain as much information as possible related to biological (benthos, phytoplankton), sedimentological (topography and bathymetry, distribution of sediments, sediment transport patterns, rates of sedimentation) and physical aspects (water temperature, water salinity, tidal characteristics, tidal currents and waves) relating to the study area. These data will be considered also within the context of the interpretation and discussion of the results of the present investigation.

3.2. Location

3.2.1. The Study Area

The study was undertaken at Solent Breezes, Southampton Water. Solent Breezes is an intertidal sandy mudflat situated between Southampton and Portsmouth (Figure 3.1); it is located at 50° 49.48' N and 1° 16.42' W (Figure 3.2). The site consists of sandy mudflats, approximately 200 m in width at low water. The low tide area is covered by coarse-grained shingle, whilst the mid low tide area (where the study was undertaken), consists of fine-grained sand overlying silty clay deposits. Human activities, such as bait digging and dredging, do not occur to any significant extent. Consequently, the area may be regarded as 'natural'. Solent Breezes is protected, by the Isle of Wight, against storms approaching from the English Channel; it is, therefore, relatively

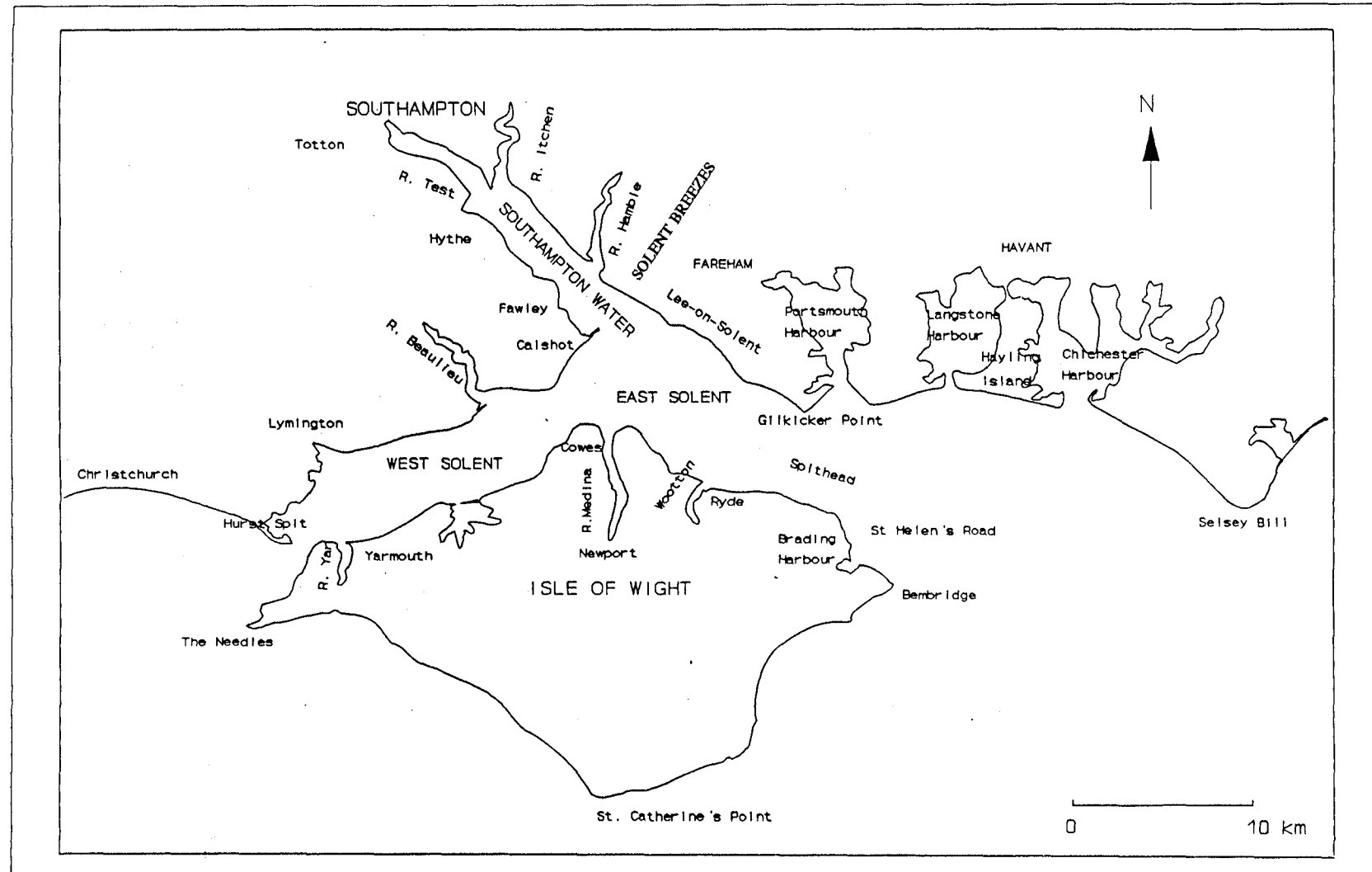


Figure 3.1. The Solent Estuarine System (after Tubbs, 1980)

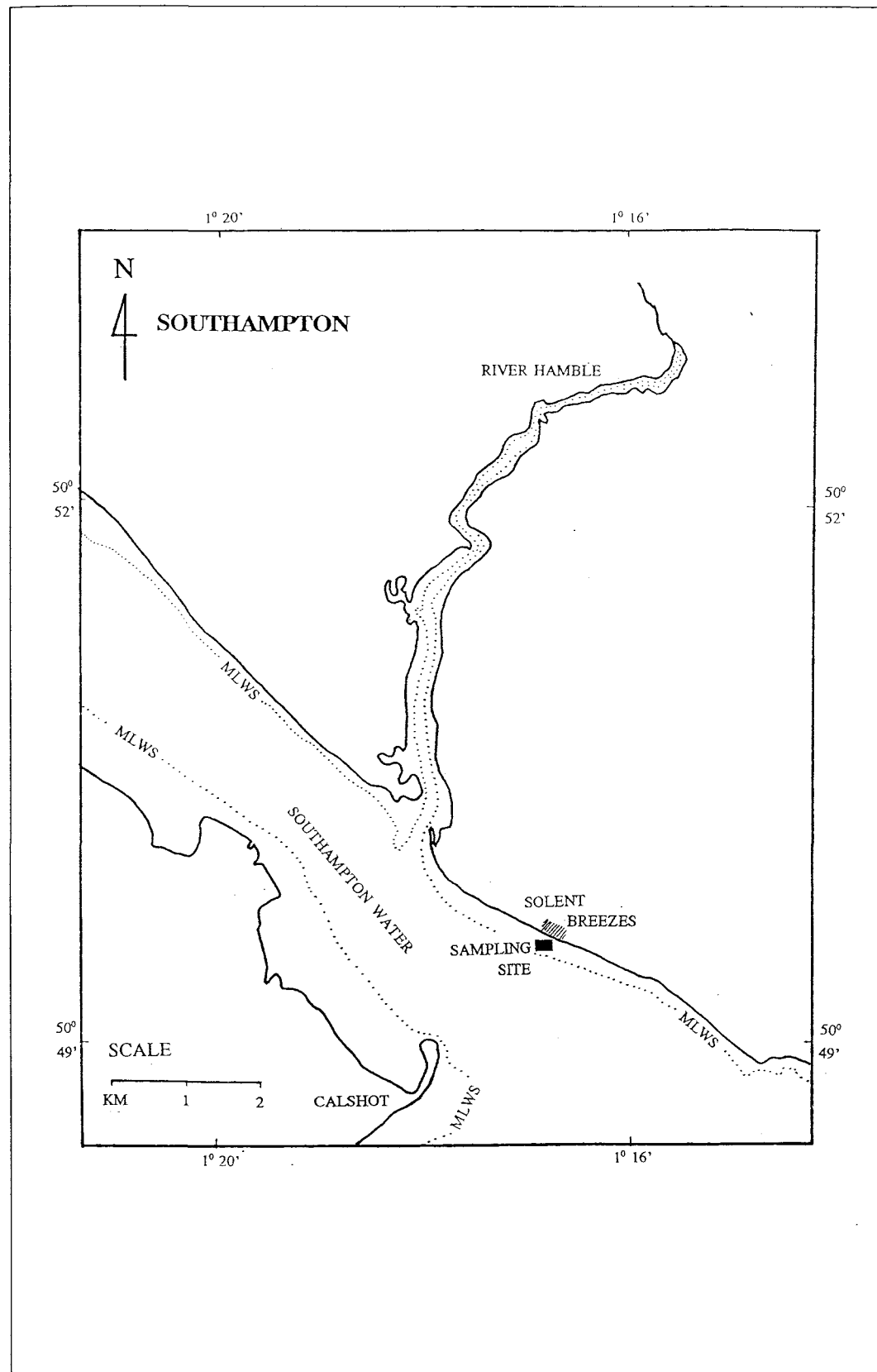


Figure 3.2. Site for the field experimental studies

sheltered and stable. The dominant biomass is the polychaete worm, *Lanice conchilega*; this is densely distributed around the area, with its presence causing the bed to be raised slightly above the surrounding sediment. The tidal range over the area, referred to Chart Datum is as follows:

MHWS - MLWS : 4.5 m - 0.8 m

MHWN - MLWN : 3.7 m - 2.0 m

Three major rivers discharge into Southampton Water, above Solent Breezes: River Test, River Itchen and River Hamble. The area is associated with high tidal current speeds (for example, 2.2 cm s^{-1} to 43.5 cm s^{-1} recorded near bed and at the surface, during spring tide at the present investigation) and a double high water, which is characteristics of the region (see also Section 3.5).

3.2.2. Regional Geology

The estuaries of Southampton Water and the Solent (including Portsmouth, Langstone and Chichester Harbours) lie at the centre of the Hampshire Basin (West, 1980). These are the latest of a series of shallow-water bodies, which have existed since the relatively deep Chalk sea-floor was uplifted about 65 million years ago. During the Palaeogene (Eocene and Oligocene), a wide variety of sediments (which frequently contain abundant plant and animal remains), accumulated in the shallow seas, estuaries, lakes and lagoons. These deposits now exist beneath and around the modern estuaries. After deposition, a long phase of folding, uplift and erosion occurred during the Neogene (Miocene and Pliocene). Then, during glacial phases of the Pleistocene, the valleys of the local rivers were excavated to well below the present sea-level before being finally flooded during the Flandrian Transgression; this created the modern estuaries of the region.

3.3. Biological Setting

3.3.1. Benthos

The Solent has, until recently, lacked any established marine laboratories. Consequently, there is little published information available on the benthos, compared with other areas like the Clyde and Plymouth (Thorp, 1980). Detailed studies at particular locations and of species have been undertaken, however, by the University of Southampton and other related establishments around the adjacent regions. Some species have been found to be more abundant in the Eastern Solent, whilst others occurred more frequently in the West (Fischer-Piette, 1936). This distribution pattern may be due to the fact that on the basis of temperature, salinity and substrate distribution, the Solent can be divided into East and West basins (Crisp and Southward, 1958). On the basis of available published data, faunistic studies would appear to have been limited, for example, to littoral studies on Langstone Harbour (Juniper, 1963; Alexander, 1969; Bone, 1973; Thorpe, 1977), Southampton Water (Raymont, 1964; Holmes, 1971; Esser, 1972; Barnes, 1973) and the Solent (Barnes *et al.*, 1973).

3.3.2. Phytoplankton

Unlike the adjacent areas, such as Portsmouth and Langstone Harbour, photosynthetic processes in Southampton Water are dominated by planktonic rather than benthic algae (Williams, 1980). In contrast to the adjacent coastal waters which have spring and autumn bloom, the seasonal cycle of phytoplankton in the estuary is characterised by a single summer bloom. Blooms have been observed to occur between May and July; they take either the form of a single intensive bloom or a more protracted event (Raymont and Carrie, 1964; de Souza Lima and Williams, 1978; Bryan, 1980). Concentrations of chlorophyll *a* vary from about 1 - 2 $\mu\text{g l}^{-1}$ during the winter months and 10 - 20 $\mu\text{g l}^{-1}$ during the summer; this may exceed 40 $\mu\text{g l}^{-1}$ at the peak of the bloom. There is a decrease

in the maximum concentrations of chlorophyll *a*, from mid-estuary towards the sea.

3.4. Sedimentological Setting

3.4.1. Topography and Bathymetry

Within the Solent area, longshore sediment movement is common due to the available coastal features (Dyer, 1980). Most of the estuaries and inlets have well-developed spits, which have been derived mostly from material from local cliff erosion (Figure 3.3); some small inlets have been sealed off completely. Tidal deltas have formed at the entrances to Langstone and Chichester Harbours whilst, in other places, the currents across the mouths of the inlets are too strong for such deltas to be formed. Bars are present, however, across some of the smaller inlets; this leads to a low volume of the associated tidal prism. There are three main sub-tidal banks within the Solent system, which may have considerable influence on the water circulation and sedimentation patterns; the Solent Bank, in the West Solent; the Brambles Bank, centrally located at the junction of the East and West Solent and Southampton Water; and the Ryde Middle Bank, located in the deep channel to the south of the Brambles Bank (Figure 3.4).

The localised bottom topography is important in the control of the sediment transport ways and in determining the direction of transport (Dyer, 1980). In the West Solent, gravel waves or dunes occur extensively and are typically 1 - 2 m in height and 10 - 20 m in wavelength (Dyer, 1971). In several places, the asymmetry of the dunes shows that they are moving in opposite directions on opposite sides of the channel. Similarly, they often change rapidly in the direction of movements, over short distances.

Sandwaves of up to 7 m in height and 120 m in wavelength occur on the Prince Consort Shoal (in Cowes), whilst at the entrance to Portsmouth Harbour, there are small trains of asymmetrical sand and gravel waves (Dyer, 1980). The

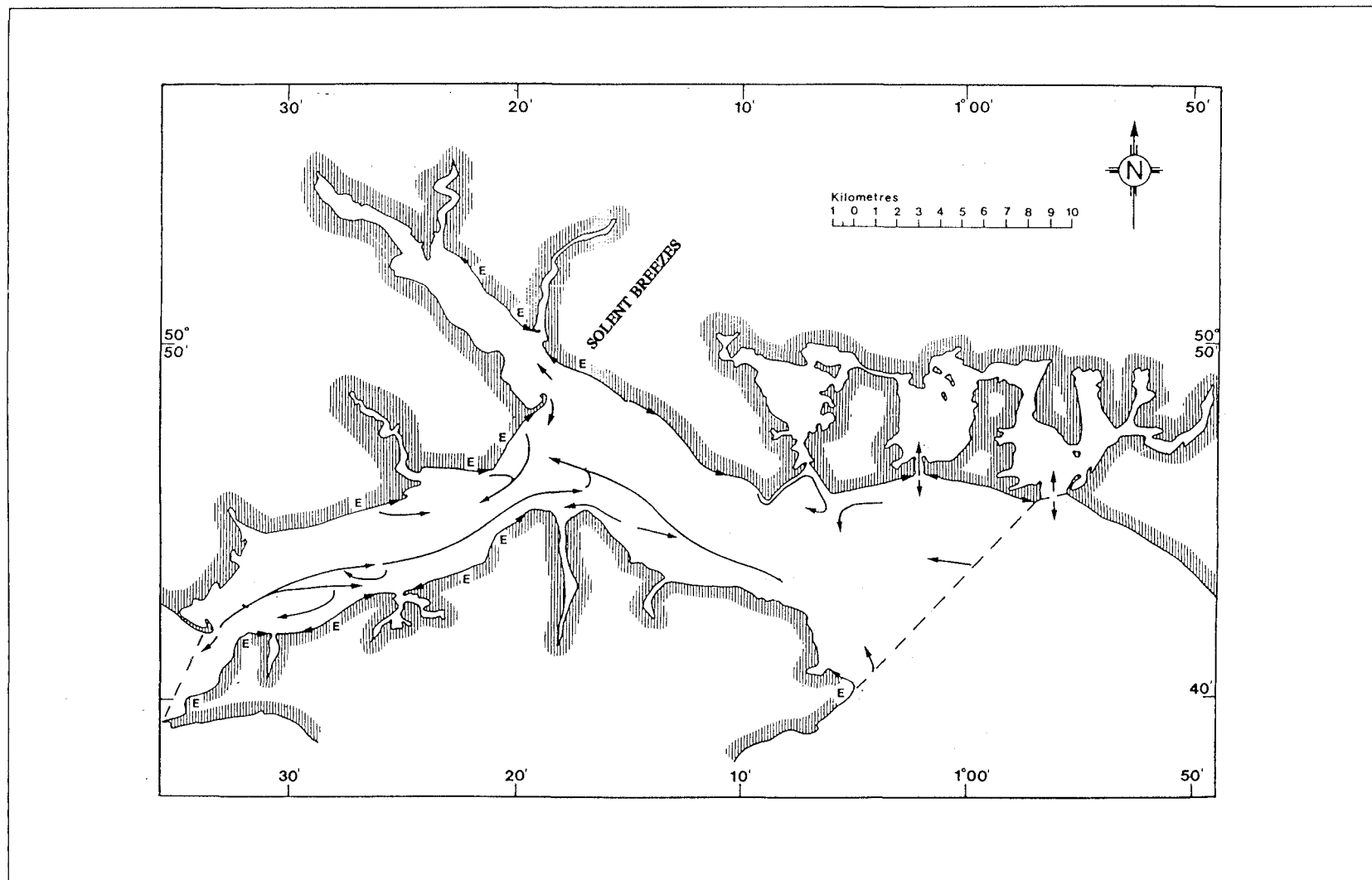


Figure 3.3. Circulation pattern of sediment in the Solent. E = Areas of Cliff Erosion (from Dyer, 1980)

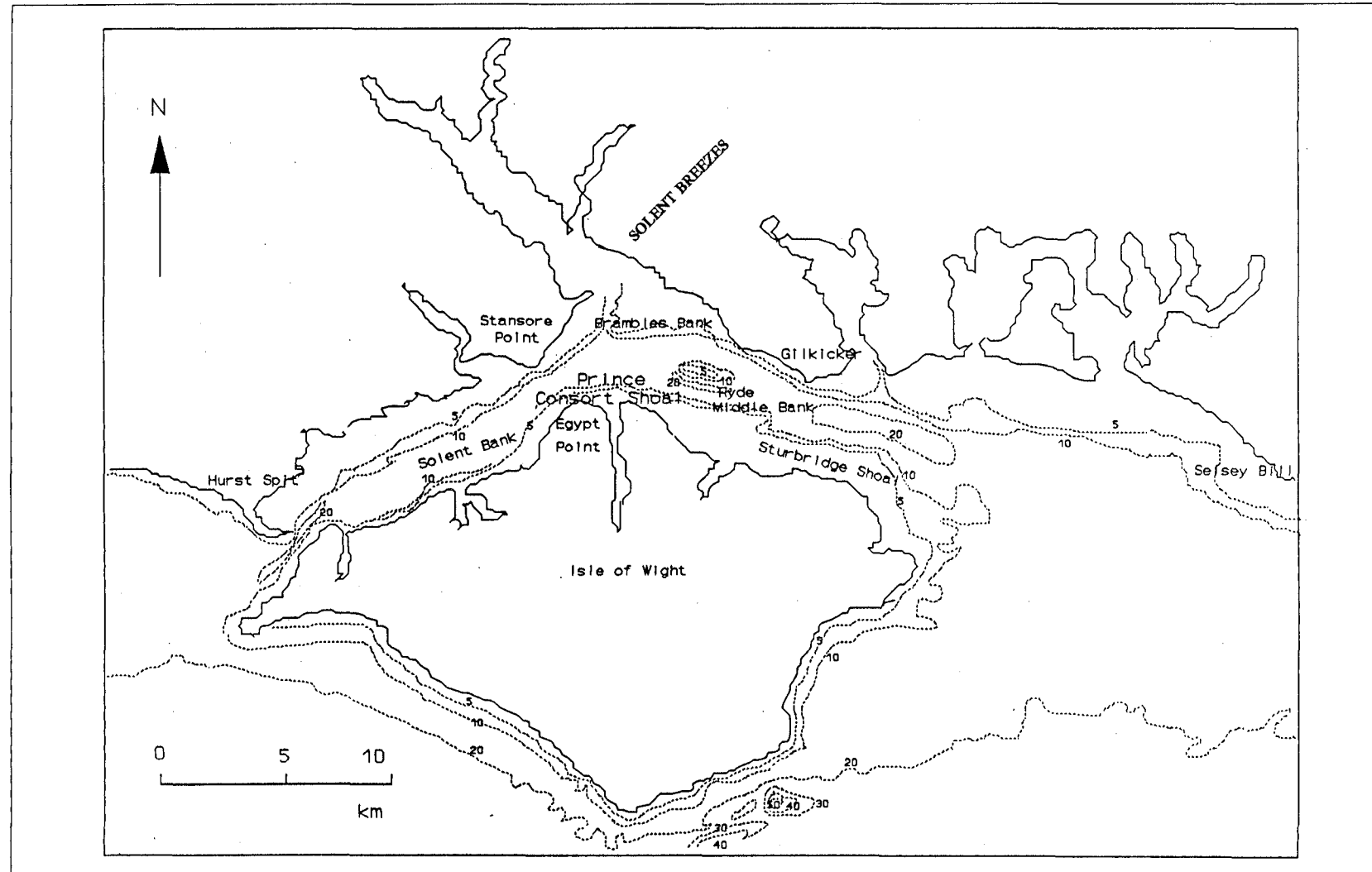


Figure 3.4. Generalised bathymetric chart of the Solent Region (based upon British Geological Survey, 1988): contours in metres

sedimentary topography of the East Solent consists of small irregular and hummocky dunes, with narrow trains of sandwaves on the edges of the Banks (Lonsdale, 1970). In Southampton Water, cohesive sediment (muds) furrows were identified resulting from short periods of erosion followed by long periods of deposition (Flood, 1981).

3.4.2. Distribution of Sediments

Four modes of sediments have been identified in the Solent: a gravel mode at 16 mm (-4 Φ); a coarse sand mode at 0.35 mm (1.5 Φ); a medium sand mode at 0.17 mm (2.6 Φ); and a clay which in a flocculated state has a fall velocity equivalent to a grain size of 0.02 mm (5.7 Φ) (Dyer, 1980). Particle size characteristics of different parts of the area are shown on Figure 3.5. The West Solent is covered mainly by gravel containing various proportions of coarse sand (Dyer, 1971), with the areas of symmetrical gravel waves containing higher proportions of sand than those of asymmetrical waves. In shallow waters of the northern part of the West Solent, the proportion of mud is high and extensive tidal mudflats are present in the littoral zones. Within the inlets, therefore, mud deposits are exclusively present.

The majority of the East Solent and the whole of Southampton Water are covered with mud or sandy mud (Dyer, 1980). Although some of the muds which infill the inlets may be derived from the rivers, the greatest proportion probably originates from the sea and enters into the estuarine circulation. The extent of the sandy gravel deposits appear to be a significant influence on depositional processes in the Solent (Lonsdale, 1970; Dyer, 1971 and 1972a). There is also a fairly clear relationship between mean grain size and the maximum shear stress exerted by the tidal currents (Dyer, 1972b), with the smaller sized material found under conditions of lower ambient currents.

3.4.3. Sediment Transport Patterns

Studies on the general circulation patterns of sediment in the Solent are

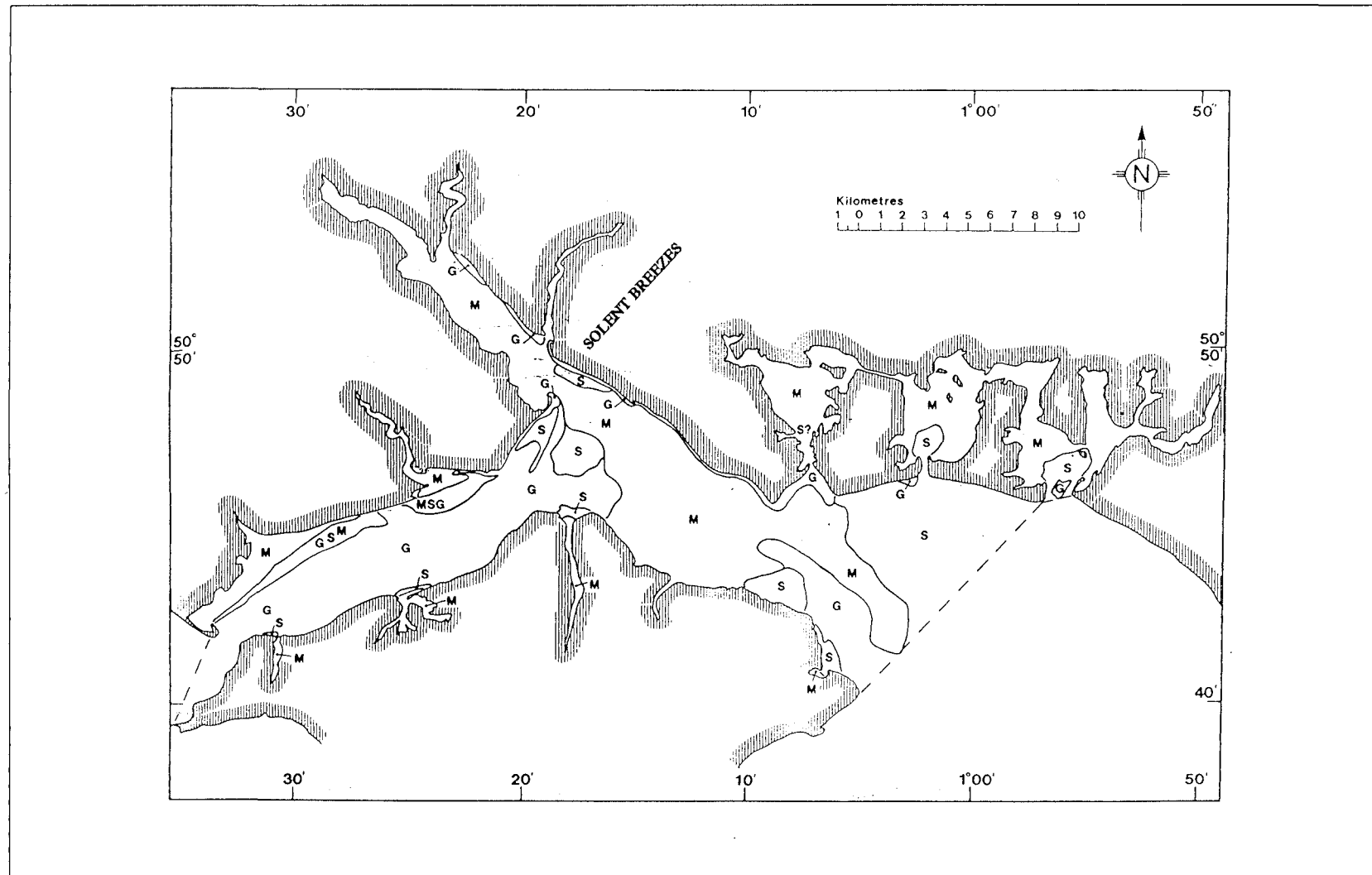


Figure 3.5. Distribution of surface sediment types in the Solent. M = Mud, S = Sand, G = Gravel (from Dyer, 1980)

based mainly on the transport pathways, asymmetry of the bedforms and other sedimentary characteristics (Lonsdale, 1969; Dyer, 1971 and 1972a). In the deeper water regions, there appears to be general movement of material into the Solent from either end. Sands and gravels are transported eastward from Christchurch Bay (in the west), by recirculating eddies into the deeper waters from the beaches of Hurst Spit. The Solent Bank has probably been formed by one of these eddies, forming a temporary resting place for sediment passing towards the east. Gravel transport terminates off Cowes whilst coarse sand appears to accumulate on the Prince Consort Shoal (Figure 3.4). The medium-grained sand, however, moves in an anticlockwise direction, and accumulates on the Brambles Bank (Dyer, 1969). Sand and mud enter also from the eastern end of the region. Much of the sand appears to pass northwards into Hayling Bay, with the majority of the remainder accumulating on the Ryde Sand. It seems that the mud is deposited in the East Solent (i.e. offshore of Solent Breezes), it is then carried into estuaries on the normal estuarine circulation and deposited during the long high water stand. This process is probably enhanced by the phase lag between the currents in the Solent and those in the inlets (Dyer, *op. cit.*).

In the littoral regions and on the beaches, exposure to wave attack is of paramount importance (Dyer, 1980). Gravel or bedrock are present on the exposed coasts, whilst mud and sand occur on the rest. The configuration of the inlets mouths may have been adjusted, such that longshore transport is towards the inlet on both sides. Thus, the coarser sediment is swept outwards along the entrance channel; in some cases, it may recirculate onto the beach. In the West Solent and on the northern side of the East Solent, the predominant longshore transport direction is towards the east, resulting in some of this material reaching deeper waters (Figure 3.2).

3.4.4. Rates of Sedimentation

Only limited documented data on rates of erosion are available. However, additional information could be obtained by studying the available charts and Ordnance Survey maps. Such an analysis has revealed that the cliffs at Barton in

Christchurch Bay have been receding at 1 m y^{-1} since 1895, which would constitute a volume of material in the range of $10^5 \text{ m}^3 \text{ y}^{-1}$ entering the Solent/Christchurch area (May, 1964).

Based upon divers observations averaged over several days, it was recorded that bedload transport of sea features off Stansore Point (Figure 3.4) achieved rates of $8 \times 10^{-5} \text{ g cm}^{-1} \text{ s}^{-1}$ with a mean value of $8 \times 10^{-7} \text{ g cm}^{-1} \text{ s}^{-1}$. However, cross channel transport rates may be much lower, because these values may represent only small variations in a larger pattern of movement. Transport rates recorded from the movement of sand waves in Prince Consort Shoal were $1 - 4 \times 10^{-5} \text{ g cm}^{-1} \text{ s}^{-1}$ (Dyer, 1969).

In terms of suspended sediment movement, surface and mid-depth concentrations ranged from $2 - 50 \text{ mg l}^{-1}$ in Southampton Water (at high tide over an 18 month period) (Head, 1969). Highest values occurred at mid-depth at the mouth of the estuary, whilst the lowest concentrations were measured during the summer. A turbidity maximum is probably present in Southampton Water; this may occur also in other inlets with a sufficiently intense estuarine circulation.

Deposition rates of $2 - 6 \text{ mm y}^{-1}$ have been calculated semi-empirically for Southampton Water (Dyer, op. cit.).

3.5. Physical Setting

3.5.1. Water Temperature

Water temperature variations throughout the Solent and Southampton Water are controlled by various processes, including: solar heating and evaporative cooling of the sea water brought in by tidal currents; the mixing of sea water with river water at a different temperature; the thermal effects induced by the periodic contact of sea water with intertidal mudflats; and the warming produced by discharges from industrial outfalls (Carr *et al.*, 1980). In the Solent, distinctive temperature contributions are provided by river and outfall discharges and intertidal mudflats. In Southampton Water, the combined river flow from the

Rivers Test and Itchen reaches a maximum of about $28 \text{ m}^3 \text{ s}^{-1}$ in late winter, declining to a minimum of $14 \text{ m}^3 \text{ s}^{-1}$ in summer; the flow of River Hamble is negligible. These river flows, however, are much smaller compared with the tidal flow into the estuary, which reaches a maximum of about $7500 \text{ m}^3 \text{ s}^{-1}$ on spring tides. The river water is cooler than the sea water in winter and warmer in summer; its annual mean temperature ($10.9 \text{ }^{\circ}\text{C}$) is significantly lower than the Solent waters ($12.0 \text{ }^{\circ}\text{C}$). Salinity measurements show that in the upper reaches of Southampton Water, the river water is mixed with about 10 times as much sea water. Such mixing produces a natural local seaward increase in temperature, which has an annual mean value of about $0.1 \text{ }^{\circ}\text{C}$ (Jarman and de Turville, 1974). Larger differences occur as a result of seasonal and daily variations in weather conditions, tidal range and river flow.

The adjacent intertidal mudflat may influence the temperature of Southampton Water. It has been indicated elsewhere that, at the mouth of the River Beaulieu, an increase in the intertidal mud temperature (of $7 \text{ }^{\circ}\text{C}$ at 1 cm depth and $1.6 \text{ }^{\circ}\text{C}$ at 10 cm, over a 3 day period in June with diminishing cloud cover and more direct insolation), resulted in river water temperatures increasing by $3 \text{ }^{\circ}\text{C}$ close to the shallow water areas around high water slack. Thermal discharge from industrial waste heat may also increase the water temperature in Southampton Water and the West Solent. In a theoretical study of this effect, it was estimated that approximately 60 % of the heat discharged is dissipated by evaporation within Southampton Water: the remaining is conveyed into the Solent by tidal action (Jarman and de Turville, 1974).

3.5.2. Salinity of the Waters

Salinity is an important physical parameter controlled by the hydraulic conditions within an estuary and the freshwater inflow (Webber, 1980). Spatial and seasonal variations of salinity can be used as the basis for the calculations of turbulence exchange and estuarine circulation; these are relevant to the dispersion of contaminants or heated waters (Jarman and de Turville, op. cit.). Southampton Water is a partially mixed estuary; however, its salinity structure depends very

much on the tidal state and, to a lesser degree, the seasonal cycle in freshwater flow. Minimal stratification occurs at high water and the surface salinity normally exceeds 30 ‰ at Dock Head, during summer and autumn.

Consequently, the surface salinity at low water at Calshot may fall below 30 ‰ in the wetter months and: at such times, stratification is increased considerably. The vertical difference in salinity at the seaward end of the system ranges typically from 0.5 to 2 - 3 ‰

3.5.3. Tidal Features

The tidal features which occur in the Solent area are some of the most complex in the world. The tidal characteristics of the English Channel are the controlling factor with respect to the Solent. High water in the eastern region occurs at about the same time as low water at Penzance, whilst the range is at a minimum half-way along the Channel in the vicinity of Poole Bay. This pattern indicates a degree of resonance with the semi-diurnal oceanic tide, with the natural oscillation period of the English Channel being about 10 hours. Although the tidal range to the west of Isle of Wight is relatively small, there is considerable water movement with maximum currents of 2.5 knots (1.29 m s^{-1}) or more. In regions in the vicinity of a nodal (tidal) point, where the amplitude of the semi-diurnal (M2) constituent is weak, combination with a powerful shallow-water constituent (M4) is liable to result. Subject to favourable phase differences, this interaction may result in double high or double low waters.

There is an east to west gradient in this water surface, commencing at about two hours before high water at Portsmouth, such that the ebb is running fast whilst water levels within the system are still rising. A reversal to a west-east gradient occurs at a corresponding, but shorter, time before low water at Portsmouth. Surface tidal streams in the West Solent are much higher (up to 4 knots) (2.06 m s^{-1}) than in the East Solent (up to 2.5 knots) (1.29 m s^{-1}) and the open waters of Spithead and beyond; this is due to the closer proximity to a tidal node and the smaller cross-sectional area of the channel (Hydrographer of the Navy, 1974). Several studies have been undertaken on flow conditions in the

West Solent (Dyer and King, 1975; Blain, 1980). Maximum ebb and flood flows at Hurst Narrows during a typical spring tide were found to be 59,000 and 36,000 $\text{m}^3 \text{ s}^{-1}$, respectively. The mean flow was estimated at 1400 $\text{m}^3 \text{ s}^{-1}$, from east to west, depending on meteorological influences (which sometimes reverse the flow direction).

Generally, in the Solent region, there is a long period of 'still stand' around high water; this extends to about 3 hours. Consequently, the ebb period is shortened to around 4 hours, instead of the customary 6 hours. The flood is of normal duration, but there is an intermediate stand of about an hour, commencing approximately 2 hours after low water. In consequence, contrary to normal estuarine behaviour, the ebb currents are more rapid than those on the flood. This mechanism provides, therefore, a beneficial flushing of silts and contaminants towards the sea. As with tidal flow elsewhere, the location of the dominant ebb and flood currents may vary due to the influence of the bottom configuration. In the case of the tidal curve for Southampton, these characteristics have been accentuated and the double high water is pronounced. A harmonic analysis of this curve shows that it is composed of many shallow-water constituents, whilst the sixth diurnal (M6) rather than the quarter diurnal (M4) component is an important factor in controlling the second high water (Doodson and Warburg, 1941). This phenomenon may be due, in part, to some resonance effects within Southampton Water itself. The unique shape of the Southampton Water tidal curve demonstrates how the combination of various influencing factors makes the Solent tidal regime one of the most complex and difficult to explain in the world.

The tidal prisms for the Solent (Hurst Narrows to Ryde-Gylkicker)(Figure 3.4) have been estimated at 540×10^6 and $270 \times 10^6 \text{ m}^3$ for a typical spring and neap tide, respectively (Blain, 1980). Of these total volumes, Southampton Water contributes about 20 %. The volume of water entering and leaving the West Solent (at Hurst Castle) is estimated at $900 \times 10^6 \text{ m}^3$ for a typical spring tide, and $550 \times 10^6 \text{ m}^3$ for a typical neap tide. Corresponding volumes for the eastern entrance (Ryde-Gylkicker) are $650 \times 10^6 \text{ m}^3$ and $430 \times 10^6 \text{ m}^3$ respectively.

3.5.4. Tidal Currents

The tidal conditions within the Solent and Southampton Water are known to be complicated, with a tidal range that can reach 5 m at Southampton (Dyer, 1980). The currents which occur within the Solent are dominated by the differing tidal amplitudes and phases at either end. The currents change direction before high or low water, even though they are following a smooth tidal curve. Generally, there is only a short period of slack water during the tidal cycle and the currents are almost symmetrical. In contrast, slack water within Southampton Water and the other inlets coincides with high or low tides, together with complicated effects due to a double peak on the flood tide and a double high water at spring tides (see above). These factors produce a fast ebb flow of short duration and a slower extended flood flow: there is a long period of slack water at high tide. The maximum speed of surface currents exceeds 2 m s⁻¹ in the West Solent and 1.5 m s⁻¹ in the mouths of the inlets, such as Portsmouth Harbour.

3.5.5. Waves

The coastlines are exposed to wave action which is generally from a SW or SE quarter due to the sheltering effect of the Isle of Wight. The Solent consists of comparatively sheltered waters, although there are considerable variations in wave conditions depending upon the geographical setting (Webber, 1980). For instance, the regions exposed to waves from the English Channel (such as in the western entrance in the vicinity of the Needles or at the eastern end of the Spithead), can, on some occasions, receive extreme waves according to the wind direction. The maximum wave height registered in Poole Bay, during a 4 year period, was 8.8 m (Henderson and Webber, 1977). At Lee-on-Solent (Figure 3.1), a maximum significant wave height of over 1.2 m has been observed on a number of occasions during the autumn or winter months (Russell, 1974). Here, there is a high likelihood of significant waves with a height of up to 0.6 m occurring at any time of the year.

CHAPTER 4

INSTRUMENTATION AND METHODS

4.1. Introduction

This Chapter describes the instrumentation and methods used in the present investigations, during both the field (sampling) and laboratory experiments. The instrumentation used in the field consisted of: a shear vane, for measuring shear strength of surficial sediment deposits; supporting field equipment, for monthly collection of biological and sedimentological samples; an accretion/erosion gauge, for measuring monthly accretion and erosion; and a velocity gradient rig, together with an inflatable rubber boat, for measuring velocity profiles over the intertidal flats. Equipment used in the laboratory consisted of: an X-Ray System, for obtaining X-Ray photographs of sediment composition; metal ceramic X-ray tubes, for measuring sediment density; and a (Malvern) Particle Sizer, for measuring grain size diameters and their distribution. In addition, glass containers were used for laboratory experiments on the shear strength of the sediments.

4.2. Field and Laboratory Instrumentation

4.2.1. Shear Vane

Since 1918, the shear vane has been used for determining the *in situ* shear strength of saturated clay; however, it was accepted generally as an alternative to the triaxial tests (see Section 2.2.1) on undisturbed samples from boreholes and pits (Serota and Jangle, 1972). In 1966, initially for the sole purpose of assessing the shear strength of cohesive soils, the same investigators devised a pocket-size vane for rapid readings. This early instrument had two limitations: firstly, the

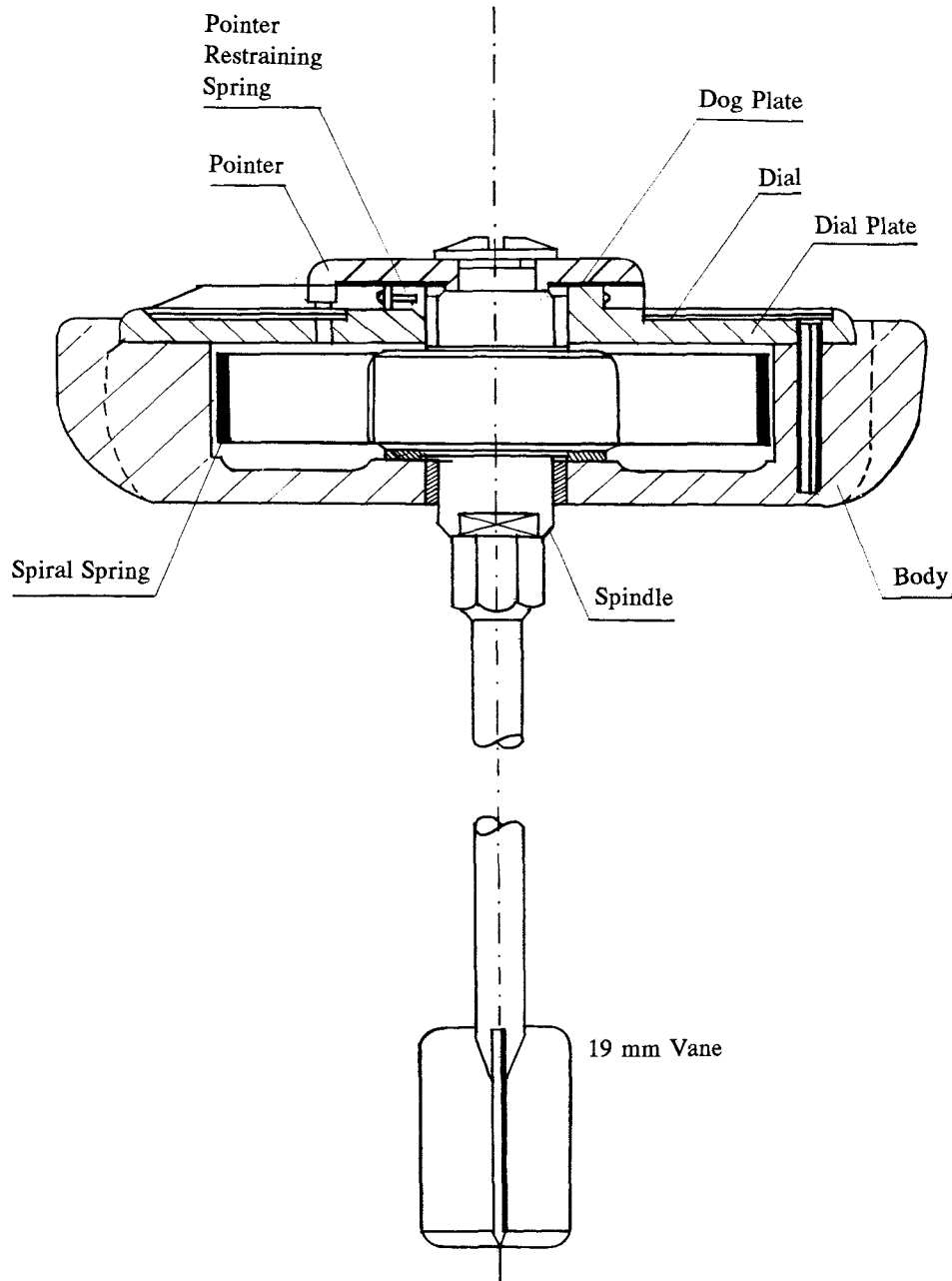
right-angled corners of the vane tended to round off; and, secondly, the instrument readings were in angular measures, which had to be converted into shear strength using a calibration chart.

Inspired by the fact that the instrument was providing more consistent results than the laboratory triaxial test, a thorough investigation and development programme was undertaken; this was to determine how accurately the vane could be rated and to improve its scope and precision, either as a field or laboratory instrument (Serota and Jangle op. cit.). In the study, special attention was given to: the torque-deflection characteristics; the effect of the rate of application of torque; the reproducibility of the results; the optimum number and size of vanes, to provide the most useful working range for a single torsion head; calibration of each vane against remoulded clays of known strength; testing the performance using undisturbed samples; and eliminating the need for a calibration chart. As a result, a well-developed shear vane was created (Figure 4.1), which is used now extensively in soil mechanics and oceanographic investigations. In the system devised, the inner end of a steel helical spring is held in a central spindle carrying the vane rod; the outer end is attached to the aluminium casing.

In operation, the vane is pushed into the soil/sediment and the torsion head is rotated at a constant speed. The torque is registered by the movement of a 'maximum' pointer, from a factory set zero; this has been shown to be virtually proportional to the applied shear stress for each vane size. Reproducibility tests showed that the vane produced deviation of less than one per cent, in two readings out of three (in practice the average of three readings is acceptable unless one of the readings shows a significant deviation). The shear strength readings obtained are expressed in KPa (Kilo Pascal).

4.2.2. Supporting Field Equipment

Equipment required for monthly sampling, in addition to the shear vane, consists of: (a) a plexiglass core, of 6 cm inside diameter and 20 cm long for collecting benthic macrofauna samples from the intertidal flats; (b) a sieve, with inside diameter of 19.5 cm and mesh size of 500 μm , for determining individuals



NOT TO SCALE

Figure 4.1. Principal components of the Shear Vane Apparatus (after Serota and Jangle, 1972)

samples randomly (by throwing the sieve and collecting the samples from where it fell); and (c) plastic bags, for carrying the sediment/faunal samples to the laboratory.

4.2.3. Accretion/Erosion Measurements

The instrument devised was constructed from a small PVC pipe (60 cm in length) with 1 cm scale interval; this was fixed firmly to a flat PVC board (20 cm x 30 cm). The system was buried some 30 cm into the sediments. The level of surface sediments was recorded monthly (by measuring the level of the surface sediment against the scaled-pipe), at the time of sampling, in order to establish accretion and erosion rates. The instrument did not cause any significant localised scour.

4.2.4. Velocity Gradient Rig

Velocity profile measurements were undertaken using a velocity gradient rig, and a direct reading current meter deployed from inflatable rubber boat. The currents were measured using the "Braystoke" BFM 001 Meter (supplied by Valeport Marine Scientific Ltd, Devon). The meter has been designed for use in fresh, salt or effluent waters. The horizontally-mounted rotor can be used with wading rods, hand suspended or with a cableway system. It is designed to measure accurately water velocity in open channels, with flows varying from 0.03 metres/second to in excess of 5 metres/second. Calibration of the meter has been established by Hydraulics Research Limited (UK) to British Standard BS3680 (Part 8A) (1973). The group calibration used is +/- 1.5 % of measured velocity; this has been confirmed by other research institutes, in tow tank tests.

4.2.5. X-Ray System

A dual cabinet Faxitron X-Ray System was used to obtain radiographs of the sediment cores. The model (Hewlett-Packard Model 43855B); is a self-

contained, radiation-shielded cabinet X-ray system; this is designed to give high resolution of small to medium size objects of all types. This is a facility shared between the Departments of Oceanography and Geology, at the University of Southampton.

4.2.6. Particle Size Analysis

In order to establish the grain size distribution of the sediment samples, the Malvern Laser Diffraction Particle Sizer was used (at the Department of Earth Sciences, University of Cambridge). The Malvern Sizers provide a complete range of measurement systems, for the analysis of particle size distributions within the range of 1 - 1800 microns. Depending upon the instrument type and appropriate sample handling, the instrument can measure the size distribution by volume (weight) of: solids in liquids; solids in gases; gases in liquids (bubble sizing); liquids in liquids (i.e. immiscible liquids, emulsions etc.). The layout of the instrument is shown on Figure 4.2. The accuracy of the measurements are +/- 4 % on volume median diameter measured by an approved technique using a Diffraction Reference Reticule.

The instrument utilises the principle of the diffraction of (laser) light from the particles. A low power visible laser transmitter produces a parallel, monochromatic beam of light; this illuminates the particles, through the use of an appropriate sample cell or other measurement technique. The incident light is diffracted by the illuminated particles to provide a stationary diffraction pattern, regardless of particle movement. As the particles enter and leave the illuminated area, the diffraction pattern evolves (always reflecting the instantaneous size distribution in this area). Thus, by integration over a suitable period and using a continuous flux of particles through the illuminated area, a representative bulk sample of the particles contributes to the final measured diffraction pattern.

A Fourier transform lens focuses the diffraction pattern onto a multi-element photo-electric detector, which produces an analogue signal proportional to the incident light intensity. This detector is interfaced directly to a computer, which reads the diffraction pattern and performs digitally the necessary

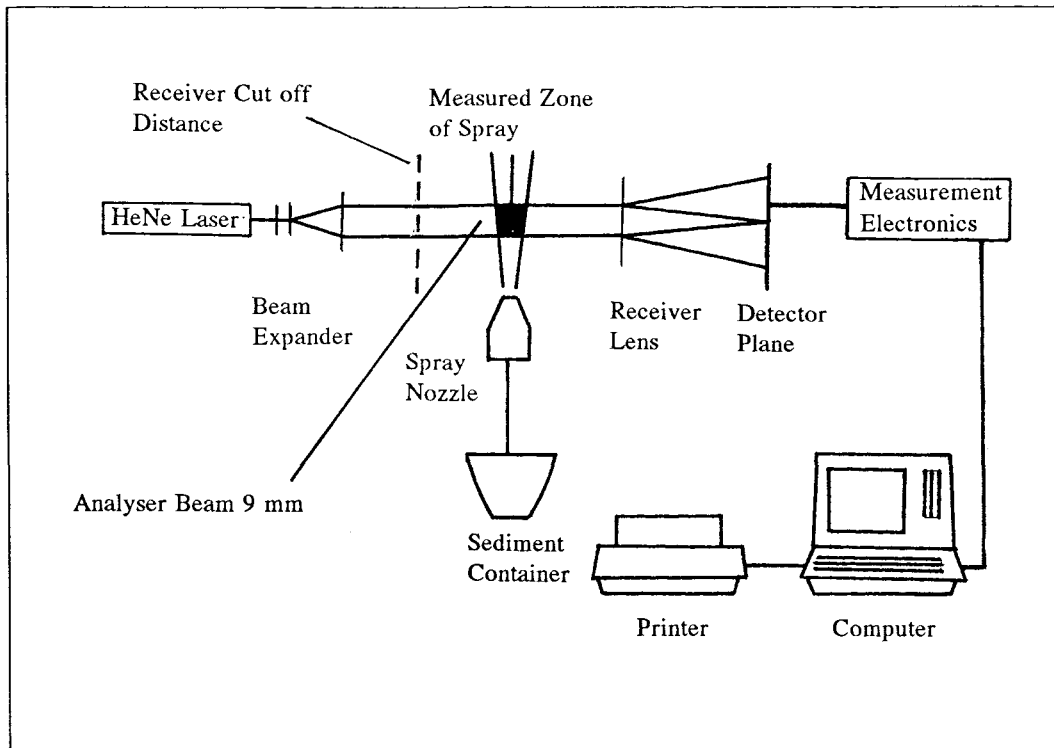


Figure 4.2. The Malvern Laser Diffraction Particle Sizer System
 (from Malvern Instruments Particle Sizer Reference Manual, 1987)

integrations. Having measured a diffraction pattern, the computer software applies a non-linear 'least squares' analysis, to establish the size distribution to provide the most closely fitting diffraction pattern. The form of analysis used most regularly is the "Model Independent" size analysis, which is able to measure multimoded particle sizes with high resolution. Additional options are available, however, to analyse the size distribution as a two parameter analytical function; these are the Rosin-Rammler, the Log-Normal and Normal functions. Such analytical approaches are generally used only in measurement situations where the resolution of size information is sacrificed, to result tolerance under highly variable measurement conditions (such as may arise in unattended process control).

4.3. Field Measurements

4.3.1. Biological Methods

The biological field sampling approaches included (see also Section 4.3.2 (below)): (1) determination of the area to be sampled randomly, using a sieve of inside diameter 19.5 cm; (2) establishing the *Lanice* tube density within that area; and (3) the collection of sediment samples, to a depth of 10 cm (using a plexiglass core of diameter 6 cm), for the analysis of macrofauna in the laboratory. The sediment samples were placed in labelled plastic bags. On each sampling occasion, at least 10 to 30 sample cores were collected from the intertidal flat; this was to establish an average value for each particular sampling occasion. Samples were collected on a monthly basis, during low tide, over a period of 28 months. Each (biological) field sampling exercise required some three hours of field work.

4.3.2. Sedimentological Methods

The sedimentological field sampling approaches which were utilised included: (1) determining the area to be sampled, using a sieve of inside diameter 19.5 cm (as above); (2) counting the *Lanice* tube density within that area (see Section 4.3.1); (3) taking 3 *in situ* measurements of bed shear strength (at each location), using the shear vane apparatus; (4) collecting sediment samples from the top few millimetres of the deposits (placed in labelled plastic bags, for the analysis of mean grain size, sample composition, moisture content, and organic matter content in the laboratory). Only the upper few millimetres are being sampled, because the resistance to erosion is controlled mainly at the sediment-water interface. To measure the shear strength, the shear vane probe was inserted into the sediment deposits up to a depth of 5 cm; it was then rotated until shear occurred. Measurements were recorded directly from readings taken from the shear vane, in KPa (Kilo Pascal). At least 10 sediment samples were collected during each sampling occasion, for the analysis of physical properties. Surface

pore-water temperature and salinity were measured *in situ*. The temperature was measured using a mercury thermometer; the salinity was measured using a refractometer.

For the measurement of erosion and deposition, a small PVC pipe (60 cm in length) was fixed firmly to a flat PVC board (20 cm × 30 cm); this instrument was buried some 30 cm into sediments. The level of the surface sediments was recorded monthly, at the time of sampling, in order to establish erosion and deposition rates. Finally, during each of the sampling occasions, visual observations were obtained of the ripple wavelength and the presence of any algae on the sediment deposits.

4.3.3. Velocity Profile Measurements

Velocity profile measurements were obtained using the velocity gradient rig and direct reading current meter deployed from an inflatable rubber boat (see Section 4.2.4). The rig was fixed vertically to the sea bed, using three guy ropes which were tied to steel poles. The poles were inserted some 50 cm into the sediment. The rig was then connected to a digital meter on the boat. The five sensors of the rig were positioned (logarithmically) at 9 cm, 23 cm, 43 cm, 83.5 cm and 153.5 cm, respectively, above the sea bed. The corresponding ln (natural logarithm) of these values are: 2.2 cm, 3.1 cm, 3.8 cm, 4.4 cm and 5.0 cm respectively. With the control unit linked to the flow meters, via the cable supplied, the current speed was recorded every 15 minutes over 300 seconds. To establish the flow velocity, from the time and pulse counts measured by the control unit, a value of N (revolution per seconds) must be derived:

$$N = \frac{P}{T} \quad (4.1)$$

where P = pulse count and T = time (in seconds).

The velocity, in metres per second, was obtained then from a calibration chart supplied by the manufacturers. Surface water waves were observed every 15 minutes, using a vertically-scaled rod and a stop watch. The directions of the

waves and winds which prevailed during the survey were mostly towards the coast i.e. from SE to NW. The latter were obtained visually using a compass.

4.4. Laboratory Procedures

4.4.1. Biological Methods

The samples collected were sieved through a sieve of 500 μm diameter. Organisms retained by the sieve were fixed with a 40 % formalin solution and stained with phloxine B (C.I. No. 45410), within plastic bags. The samples were then washed into a white tray, so that the stained organisms could be easily removed. These organisms were stored initially in 70 % alcohol; they were then identified to species level (if possible), counted and stored again in 70 % alcohol.

4.4.2. Sedimentological Methods

(a) *Moisture Content*

The moisture content of a sediment is referred to as the amount of water contained within a porous sediment. To determine the moisture content, the sediment is placed in a pre-weighed crucible (M_1) and the weight of the crucible and the sediment is recorded (M_2). The sample is then placed in the oven, for 24 hours at 70° C. After the sample is completely dry, the weight of the crucible and the dry sediment is recorded (M_3). The moisture content expressed as a percentage of the dry soil mass (BS 1377, 1975) is calculated from:

$$W = \frac{(M_2 - M_3)}{(M_3 - M_1)} \times 100\% \quad (4.2)$$

(b) Organic Matter Content

About 3 - 4 g of dry samples were placed into a small pre-weighed crucible (C). The weight of the sample and the crucible were then recorded (A). The sample was placed in a muffle furnace, at 550⁰ C, for 24 hours; this was to ensure that all the organic material was burned off completely. The crucibles were placed then in a desiccator, until cool enough to weigh (B). The total organic matter content was calculated as follows:

$$O = \frac{(A - B)}{(A - C)} \times 100\% \quad (4.3)$$

(c) Overall Sample Composition

To determine the composition of the sediment samples, they were first dried completely i.e. for 24 hours in the oven, at 70⁰ C. The dried samples were divided using a splitter (majority of the samples were used for composition analysis and 100 g were kept for grain size analysis). This was done because the grain size analysis could not be undertaken immediately. The samples were then sieved through a series of sieves (2000 μ m, 1000 μ m, 500 μ m, 250 μ m, 125 μ m, and 63 μ m) in order to determine the percentages of silt/clay, sand, and gravel.

(d) Grain Size Distribution

The grain size analysis was performed using The Malvern Laser Diffraction Particle Sizer (see Section 4.2.6). About 2 g of sediment taken from the sub samples (described in Section 4.4.2.c above) was placed into the container of a stirrer, which was filled with water up to 75 % of its capacity. The container was connected to the Sizer and a computer, then the measurement was undertaken using 600 mm lens. Each sample required about 75 seconds to complete. The results were then analysed using a specially-developed computer programme, in order to obtain the mean, sorting and skewness of the samples.

(e) Sedimentary Structure

The structure of the sediments was obtained by obtaining X-Ray radiographs of the 16 cores samples (Section 4.2.5). In order to determine the correct film exposure, initial trials were undertaken with different exposure times and voltages. As the cores were not of a similar thickness in cross-section (between the edges and the centre), even exposure was achieved by placing the core in a carton box filled with white fine sands, prior to exposure. Each sample was placed on the bottom shelf of the system (122 cm from the X-Ray source; it was exposed for 15 minutes, at a voltage of 86 kv. The film was processed following normal photographic procedure, with contact prints obtained.

(f) Sediment Density

Sediment density throughout the length of the cores was measured using the MCN 160 and MCN 161 Metal Ceramic X-Ray tubes (at the Soil Mechanics Laboratory, Department of Engineering Science, University of Oxford). The sediment core samples were exposed for 4 minutes at 160 kv. The top of the cores were filled with sea water, as a reference level for the density measurements.

4.4.3. Physical Measurements

The effect of ambient temperature on shear strength was studied by collecting and taking sediment samples back to the laboratory, for a specific investigation. Shear strengths were derived for different (plastic) straw densities, at different air temperatures. Nine glass containers (with inside dimensions of 18 cm in length, 12 cm in width and 12 cm in height) were filled with dry sediments obtained from the study area, then filled with sea water. Plastic straws were then inserted into the sediments, in eight containers at different densities. The remaining container was left without straws, to act as a control. The containers were left at various locations in the Department, of different

temperatures, for 24 hours. Shear strengths were measured then using a shear vane. Three measurements were taken from each container, with the average values being taken.

4.5. Statistical Analysis

The biological, sedimentological and physical data obtained were plotted and analysed statistically (using Sigma Plot, Sigmastat and Unistat softwares). Linear and multiple regressions, together with multivariate analysis, were performed to test the various proposed hypotheses. These approaches are parametric statistical methods, which assume that the residuals of the data (the difference between the predicted and observed values) are normally-distributed with constant variance. The data were tested firstly for their normality, using the Kolmogorov-Smirnov Test (Glantz, 1992). If the results showed that the data were normally-distributed, parametric tests were used; otherwise, nonparametric tests were applied.

4.5.1. Regional Setting Data

Of these data sets, sediment density is the only parameter needed to be analysed statistically, to establish if there is any significant difference in the sediment density within the upper 5 cm throughout the study area. As the sediment density varies spatially and with increased depth, the density at each cm of top 5 cm was taken. These measurements were combined, in order to obtain a mean density for each of the sampling sites. The Kruskal-Wallis One Way ANOVA (Glantz, op. cit.) was then applied to the mean data, to test for any significant difference between the various sites.

4.5.2. Data from the Biological Investigations

In addition to the numerical fluctuations in the individual species, with

time, monthly data on macrofauna composition were compared using the Bray-Curtis similarity classification. This approach was adopted because the Bray-Curtis similarity coefficients most closely resembled the predicted similarities for benthic faunal abundance data (Burd *et al.*, 1990). The above analysis produced a dendrogram illustrating the similarities between monthly samples, derived from the number of individuals of each of the species occurring. In order to reduce the bias caused by certain dominant species, the raw data were transformed using 'double square root transform' (root(root X)), before applying the ordination. The root-root transformation has the effect not only of reducing the weighting of the abundant species, but also has the advantage that when similarity is assessed (by the Bray-Curtis measure), the coefficient is invariant to a scale change (Field *et al.*, 1982).

The data on macrofauna were collected over 24 months; thus, it was necessary to determine the initial factors (using 'principal components analysis') before progressing to any further analyses. Principal components analysis is one of the several methodological steps in factor analysis. Factor analysis itself is a multivariable method intended to explain relationships among several difficult-to-interpret, correlated variables in terms of a few conceptually meaningful, relatively independent factors (Kleinbaum *et al.* 1988). The Principal components analysis is used to explain as much of the total variation in the data as possible, with as few factors or principal components as possible (Kleinbaum *et al.*, op. cit.). The total variation is defined mathematically to be the sum of the sample variances of the k variables. Conceptually, the total variation is a measure of the uncertainty associated with the observations on all p variables. Uncertainty refers to the proportion of the observations on the units of study which differ from one another.

The first principal component (PC(1)) is the weighted linear combination of the variables which accounts for the largest amount of the total variation in the data. Thus, PC(1) is the linear combination of the X 's variables,

$$PC(1) = w_{(1)1} X_1 + w_{(1)2} X_2 + \dots + w_{(1)p} X_p \quad (4.4)$$

where $w(1)1, w(1)2, \dots, w(1)p$ represent the weights chosen to maximise the

quantity variance of PC(1), divided by total variation. Total variation is the sum of all the sample variances. Therefore, no linear combination of the X's will have as large a variance as PC(1).

The second principal component (PC(2)) is the weighted linear combination of the variables which are uncorrelated with PC(1), that accounts for the maximum amount of the remaining total variation not already accounted for by PC(1). In other words:

$$PC(2) = w_{(2)1} X_1 + w_{(2)2} X_2 + \dots + w_{(2)p} X_p \quad (4.5)$$

Hence, this component is the linear combination of the X's that has the largest variance of all the linear combinations, which are uncorrelated with PC(1).

In general, the i th principal component $PC(i)$ is the linear combination of:

$$PC(i) = w_{(i)1} X_1 + w_{(i)2} X_2 + \dots + w_{(i)p} X_p \quad (4.6)$$

This expression has the largest variance of all linear combinations, which are uncorrelated with all of the previous $i - 1$ principal components. Actually, it is possible to derive as many principal components as there are original variables. In most practical applications, however, most of the total variation in the data is usually accounted for by the first few components. In addition, these components are selected to be mutually uncorrelated. Thus, the analytical objective of parsimony and independence are quite often achieved by this method.

The principal components scores were associated then with other parameters using the 'Spearman rank correlation coefficient' (Glantz, 1992). Use of the coefficient identified the potential factors responsible for the present community structure of the macrobenthic organisms.

4.5.3. Data from Sedimentological Investigations

For these particular data sets, multivariate analysis was also used. Firstly, the correlation matrix of all the parameters under study was established. Such results provide an initial indication of any interrelationship between parameters. This procedure was followed then by cluster analysis to provide the distance of

similarity between the variables; and the principal components analysis to identify the most important variables causing major variation in the data. Finally, multiple regression analysis was performed, in order to establish a model for the prediction of shear strength of deposits overlain by intertidal waters.

Note: Detailed explanations on some of these statistical methods (i.e. Cluster Analysis and Multiple Linear Regression) are described in Sections 8.4.3 and 8.4.5, respectively.

CHAPTER 5

RESULTS: REGIONAL CONDITIONS

5.1. Introduction

This Chapter describes the results of the experiments undertaken on regional conditions of the study area, together with their interpretation and discussion. The aim of this particular investigation is to provide recent information on oceanographical conditions (physical and sedimentological) which occur in the area under investigation. The intended parameters consist of: bathymetry, accretion and erosion, sediment structure and density, and velocity profiles. The obtained data function as an aid to establish the most important parameters responsible for the existing patterns of biological and sedimentological conditions at Solent Breezes, Southampton Water.

5.2. Bathymetry

A general description of the bathymetry (seabed depth and form) of the Solent, as depicted on Admiralty Charts, shows there to be a maximum depth of 60 m in the scour hole at the Hurst Narrows. Elsewhere, depths range from about 15 to 25 m. In the West Solent, gravels with admixtures of coarse sand cover the channel, with sands and muds on the margins and within the estuaries. Gravel waves or dunes of low amplitude with 1 - 2 m high and 10 - 20 m long, are observed commonly associated with the channel gravels. In the East Solent and Southampton Water, the extensive occurrence of sandy muds or muds (with patches of sand at the mouths of some estuaries or on some banks) are common. Occasionally, these seabed sediment structures adopt a number of interesting forms. For example, there are sandwaves up to 7 m high and 120 m long and megaripples in the sand patches; elsewhere, the sedimentary topography consists

of small, irregular and hummocky dunes. In Southampton Water, linear erosional furrows occur; these are aligned with the current flow.

A localised description of the bathymetry of the study site, based upon field survey data, reveals that average water depth is 4.5 m at MHWS. The bed consists of fine-grained sands within the upper 5 to 10 cm; below this, there is a layer of mud. Along the coastline, at the high water mark, gravels and shingles occur extensively. The study site consists of a comparatively very flat area, with transverse slope tangent of 0.005 ($\alpha = 0^\circ 17' 11''$) (Figure 5.1); it is covered with relatively high density of *Lanice conchilega* tubes. Intensive monthly sampling activities occurred at an area of around 70 m \times 70 m, represented by the square (outer dashed lines) on Figure 5.1.

5.3. Accretion and Erosion

Measurements on accretion and erosion were undertaken for only 7 months of the study period; this was due to the disappearance of the equipment buried into the sediment (which might have been removed by digging activities). The results of this phase of the investigation are presented in Table 5.1 and shown on Figure 5.2. From these data, the area appears to be relatively stable. There are no distinct patterns of accretion and erosion during the period of measurements. The graph is stable over the first four months; it then fluctuates within the range of 0.1 - 0.2 cm during the last three months.

Table 5.1. Accretion and erosion (in cm) at Solent Breezes from January 1992 to July 1992

January 1992	February 1992	March 1992	April 1992	May 1992	June 1992	July 1992
0.0	-0.1	-0.1	-0.1	-0.2	0.0	-0.2

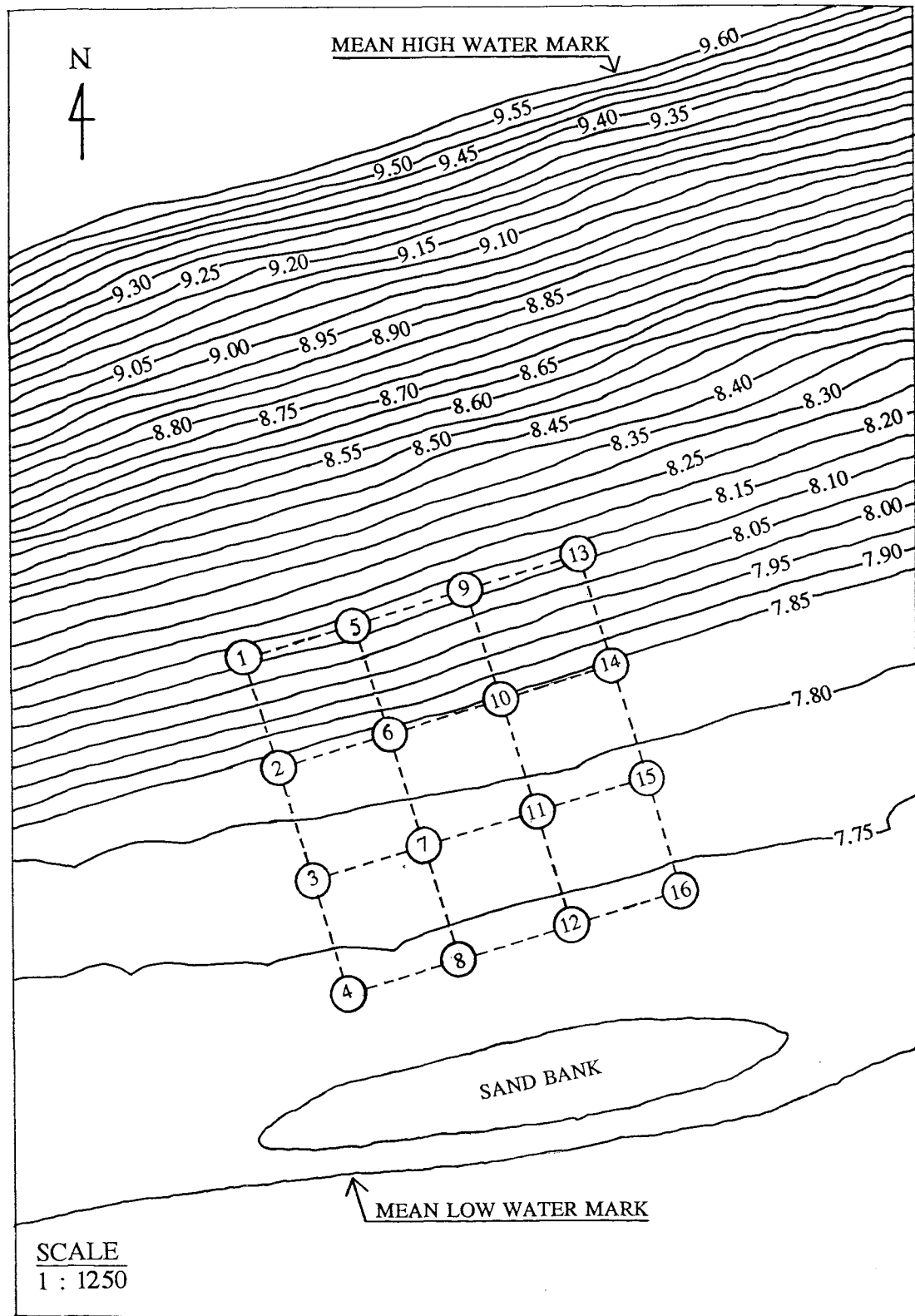


Figure 5.1. Bathymetry of the Solent Breezes sampling site, expressed in terms of 0.05 m contours with arbitrary height reference. Circled numbers represent relative location of the 16 Core sediment samples taken for X-Ray photography and density measurements

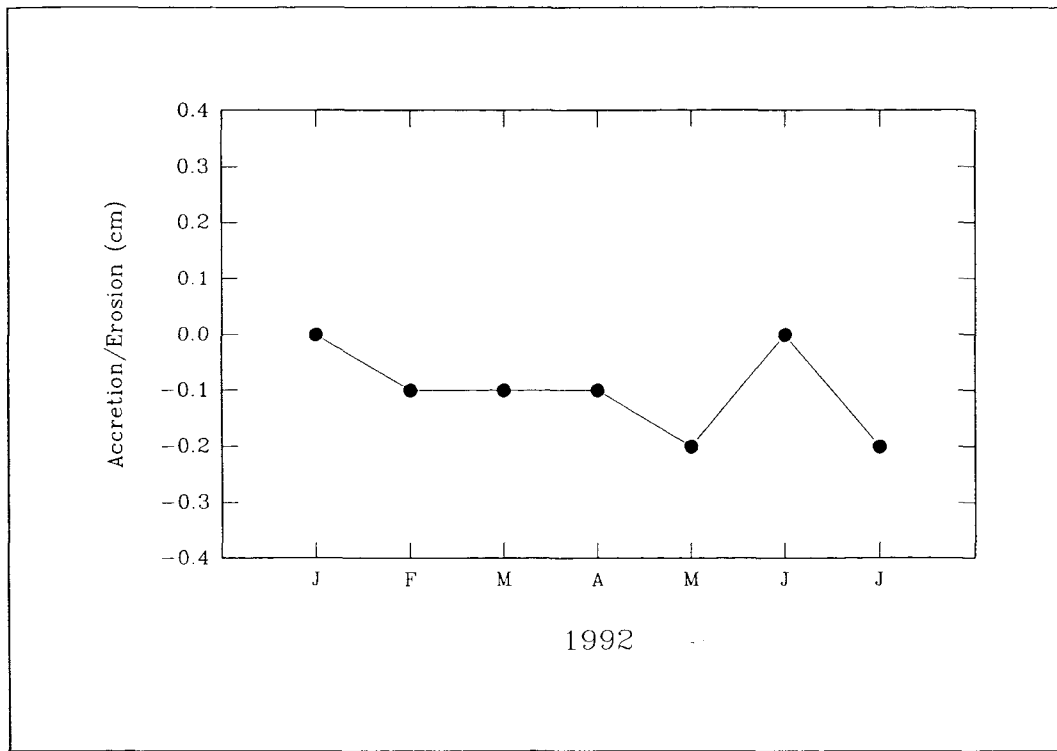


Figure 5.2. Accretion and erosion observed at Solent Breezes, during January 1992 to July 1992

5.4. Sediment Structure and Density

In order to investigate the structure of the sediment deposits and their density, 16 core samples (of 6 cm inside diameter) were collected from Solent Breezes in late October 1993. The relative locations of each of the cores, within the study site, are shown on Figure 5.1. The area is represented by the square (outer dashed lines) of around 70 m × 70 m with numbers 1 to 16 (in circles) represent number of core samples.

5.4.1. Sediment Structure

Sediment structure was studied by obtaining X-Ray Photographs of 16 cores from the study area. The objective of this exercise was to identify any extensive bioturbation within the upper 5 cm of the sediment, where the shear

strength was measured (Section 7.2). The results of X-Ray photographs are shown on Plates 5.1(a to h). In all the X-Ray photographs presented, white or lighter sections represent sandy material, whilst the black or darker sections represent muds (silt/clay).

(a) Cores 1 and 2 (Plate 5.1(a))

Core 1 consists of three layers: sand within the upper 8 cm, followed by mud in the middle and sand at the bottom. Some dead shells of the gastropod *Littorina littorea* are distributed randomly within the upper 5 cm, including a large shell located within the surface sediments. There is a single tube of *Lanice conchilega* in the middle of the core, located at a depth of 15 - 20 cm from the surface. There is no evidence of bioturbation of the sediment deposits within this core.

The proportion of sand in core 2 is less than in core 1; only about 5 cm of the second core consists of sand. The middle section of the core contains mud, whilst the lower part is dominated by sand. Four *Littorina littorea* shells can be identified in this core; one at 1 cm depth, with the remainder found at a depth of 18 cm from the surface. There is also a large shell of a mollusc at the surface and a tube of *Lanice conchilega* at a depth of 5 cm from the surface. The middle part of the core consists of different sediment layers, which may represent different depositional conditions. Once again, there is no obvious evidence of sediment bioturbation within this core.



(b) Cores 3 and 4 (Plate 5.1(b))

Core 3 can be differentiated into two parts; the upper 5 cm is dominated by sand, whilst the remainder is mud. A single shell of *Littorina littorea* is present at 2 cm depth, whilst there are another two shells below 25 cm depth. The distribution of the sediment is uniform throughout the core, with no evidence of bioturbation.

Core 4 consists of two distinctive parts: the upper part (up to 9 cm depth)

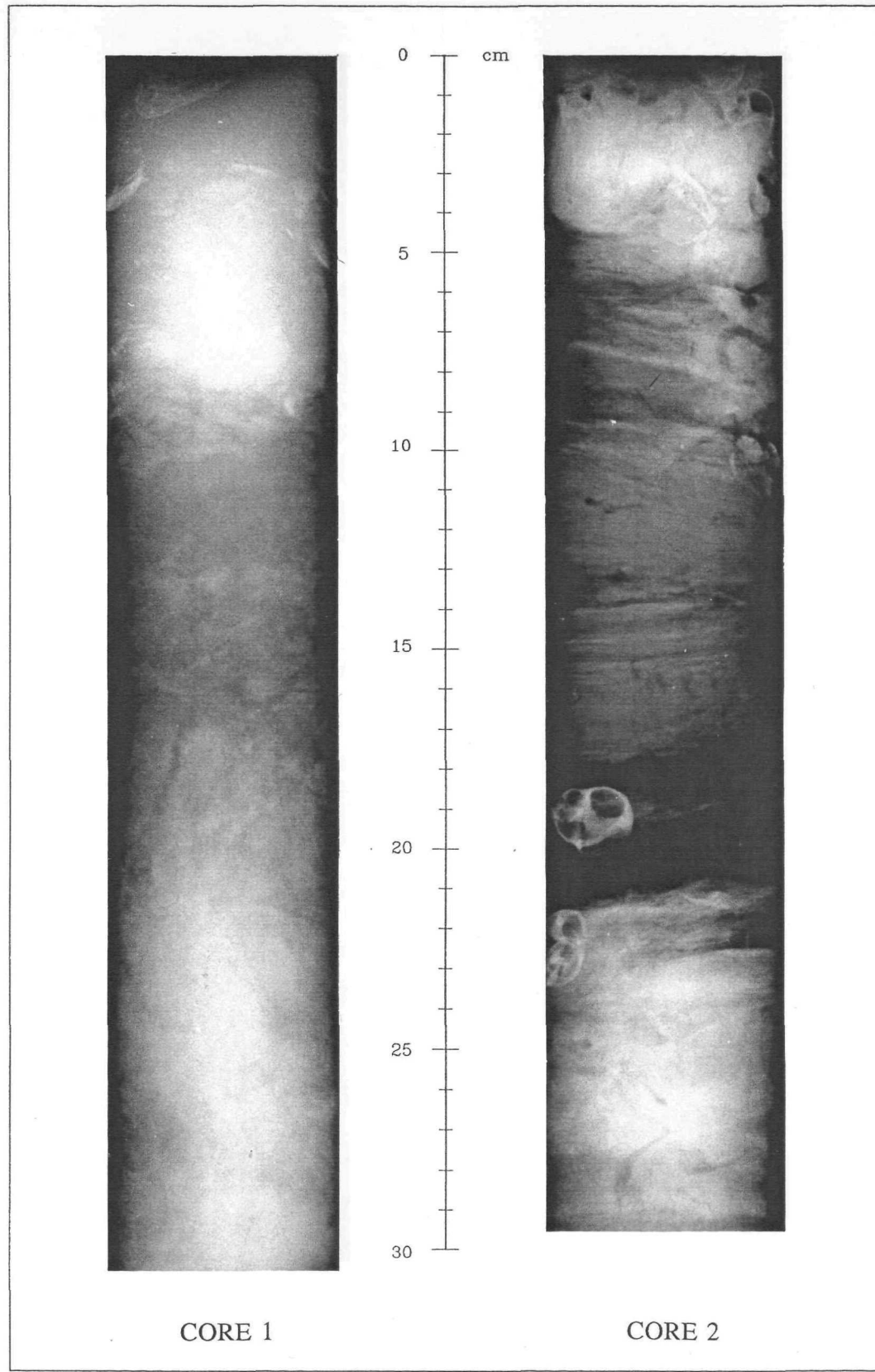


Plate 5.1(a). X-Ray photographs of Cores 1 and 2 (for relative location of cores, see Figure 5.1)

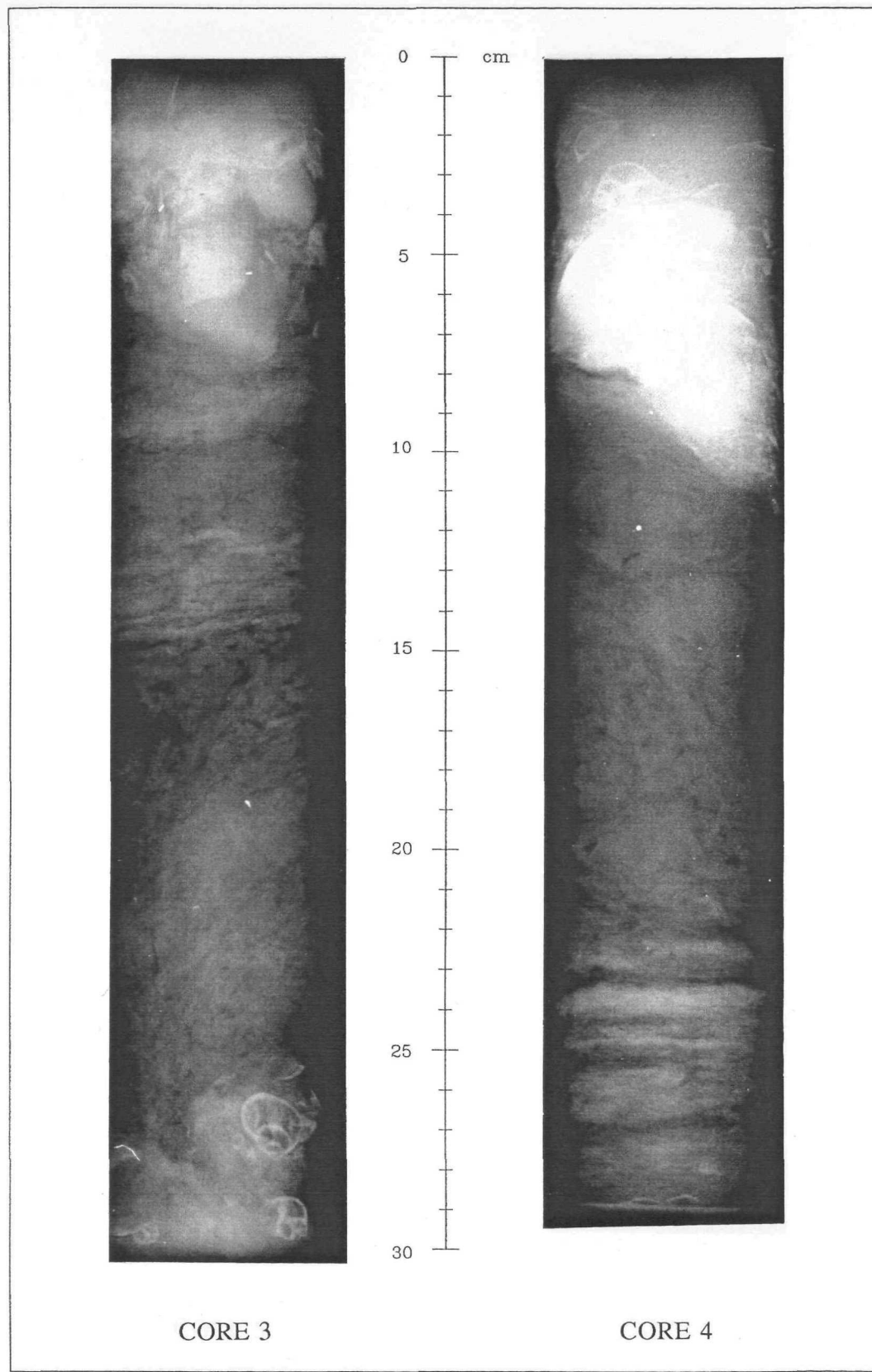


Plate 5.1(b). X-Ray photographs of Cores 3 and 4 (for relative location of cores, see Figure 5.1)

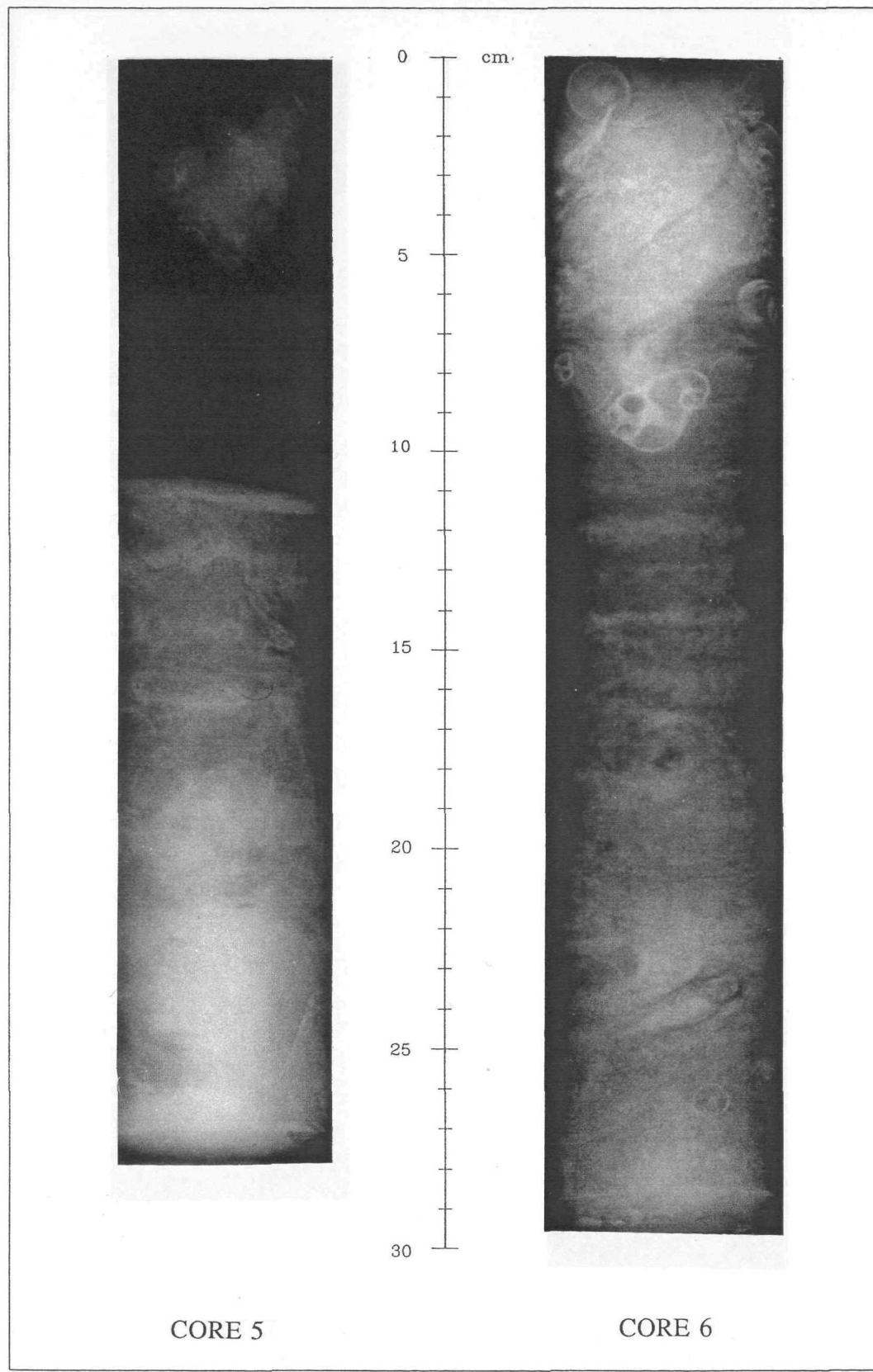


Plate 5.1(c). X-Ray photographs of Cores 5 and 6 (for relative location of cores, see Figure 5.1)

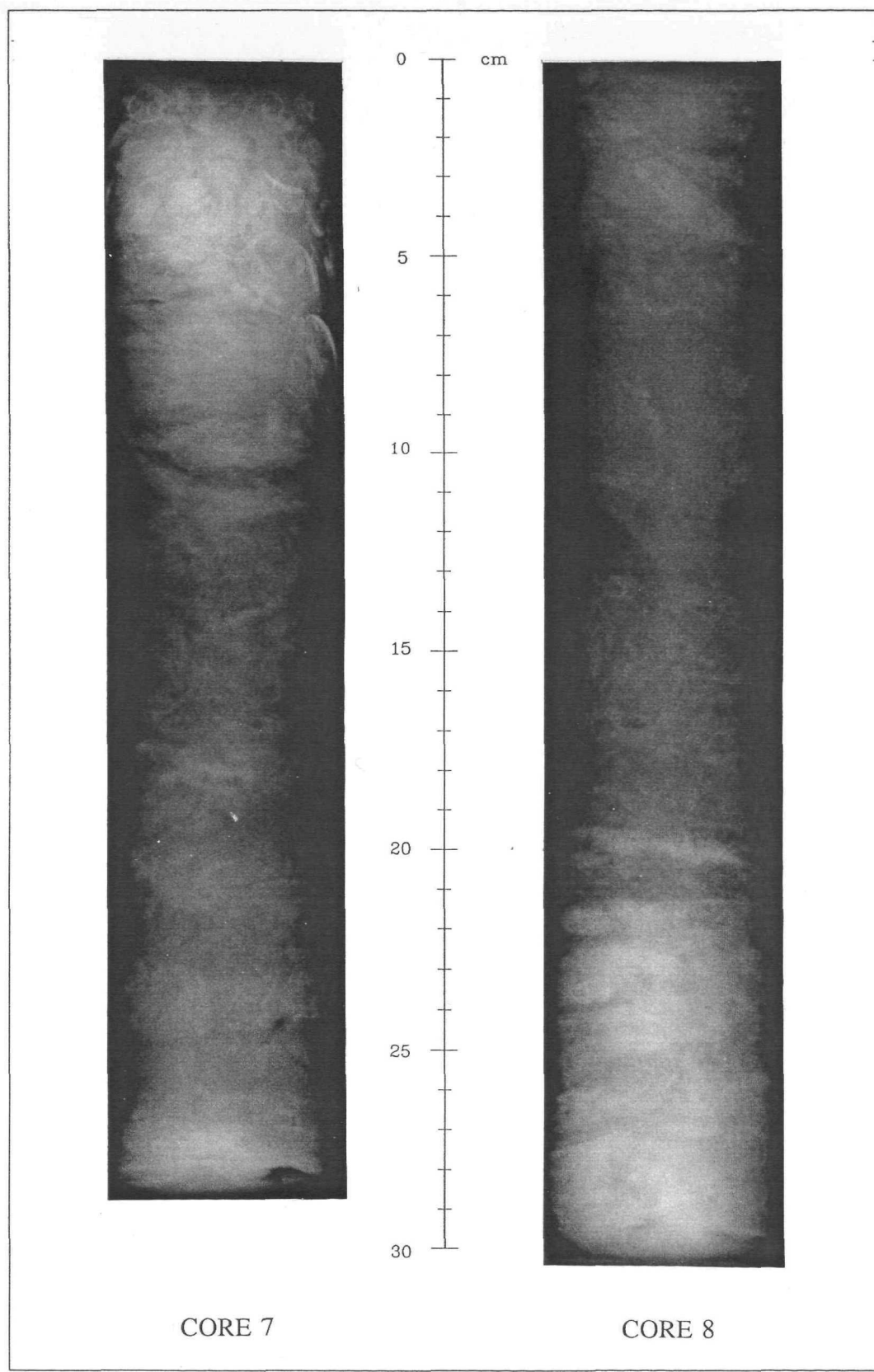


Plate 5.1(d). X-Ray photographs of Cores 7 and 8 (for relative location of cores, see Figure 5.1)

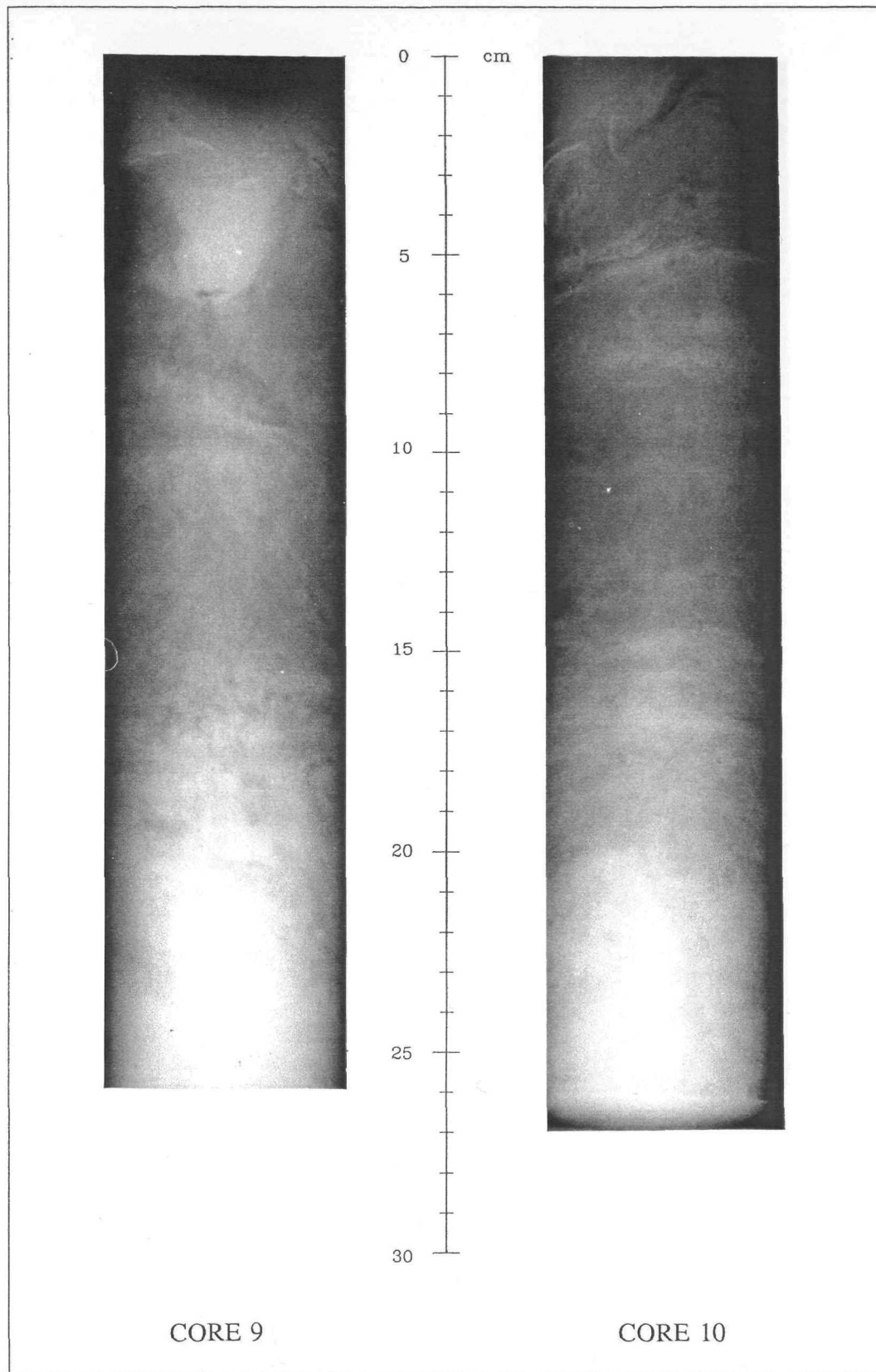
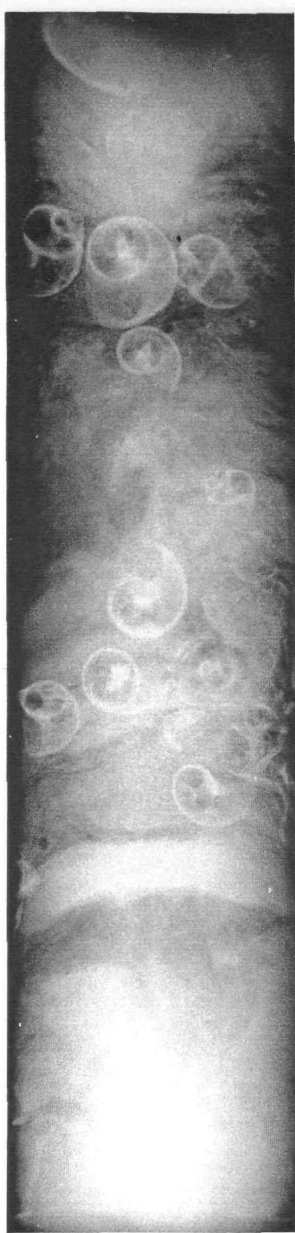


Plate 5.1(e). X-Ray photographs of Cores 9 and 10 (for relative location of cores, see Figure 5.1)



CORE 11



CORE 12

Plate 5.1(f). X-Ray photographs of Cores 11 and 12 (for relative location of cores, see Figure 5.1)



CORE 13



CORE 14

Plate 5.1(g). X-Ray photographs of Cores 13 and 14 (for relative location of cores, See Figure 5.1)

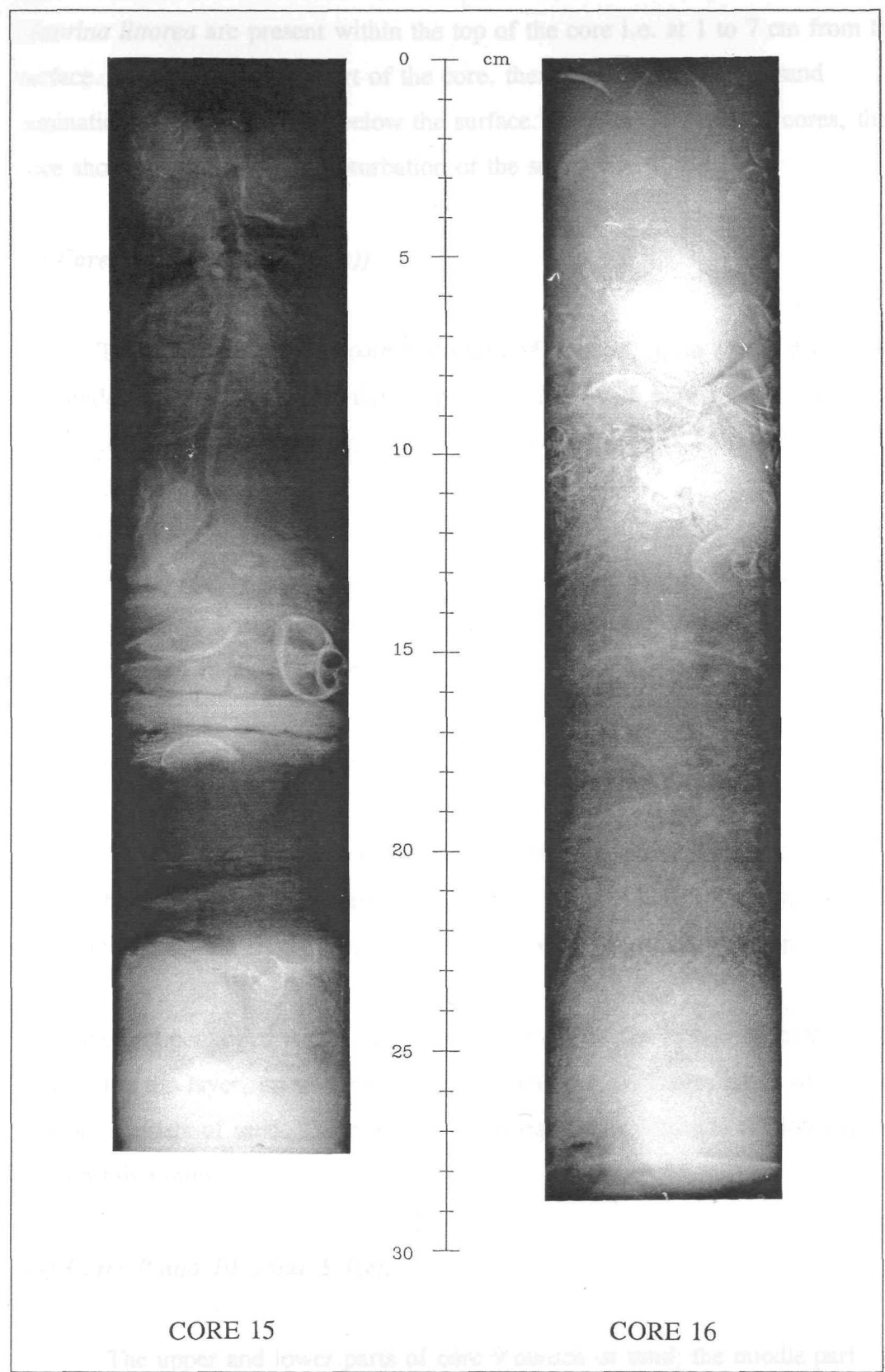


Plate 5.1(h). X-Ray photographs of Cores 15 and 16 (for relative location of cores, see Figure 5.1)

consists of sand, whilst the remainder of the sample is mud. Some shells of *Littorina littorea* are present within the top of the core i.e. at 1 to 7 cm from the surface. Within the bottom part of the core, there are some mud and sand laminations located at 22 cm below the surface. As with the previous cores, this core shows no evidence of bioturbation of the sediments.

(c) Cores 5 and 6 (Plate 5.1(c))

The upper part of this core is dominated by mud, up to 15 cm deep; the remainder is sand. Generally, this core lacks shells, with only a small shell (organism) within the top 1 cm. There is also no evidence of bioturbation within this particular core.

The composition of core 6 differs to that of core 5. The core consists of sand at the surface and up to a depth of 8 cm; the rest is dominated by muddy sediments. There are some shells of *Littorina littorea* within the top layer and a single shell at a depth of 26 cm. Bioturbation is not evident within this core.

(d) Cores 7 and 8 (Plate 5.1(d))

The upper layer, up to 6 cm, is dominated by sand; the remainder is mud. Small shells of *Littorina littorea* are distributed within the top layer, to the depth of 9 cm. There is a single tube of *Lanice conchilega* in the upper 1 cm of the core.

The material contained within this core appears to be distributed uniformly: sand covers the top layer, up to 4 cm deep; the middle part contains mud, whilst the bottom consists of sand. There are no shells present or evidence of bioturbation within this sample.

(e) Cores 9 and 10 (Plate 5.1(e))

The upper and lower parts of core 9 consist of sand; the middle part consists of mud. There are some small shells of *Littorina littorea* present at the

top sandy layer. Overall, the sample reveals no sign of bioturbation of the sediment.

Most parts of core 10 contain mud up to 20 cm deep: the rest contains sand. A tube of *Lanice conchilega* appears at 2 cm, with some small shells at a depth of about 5 cm. This sample, as with many of the others (see above) shows no evidence of bioturbation.

(f) Cores 11 and 12 (Plate 5.1(f))

The top and bottom layers of core 11 consist of sand; the middle layer, between 5 cm - 17 cm, consists of mud with a large number of *Littorina littorea* shells. There is, in addition, a large shell (mollusc) and a tube of *Lanice conchilega* contained within the top layer (2 cm from the surface).

The upper layer of core 12, up to 14 cm, contains sand; the bottom consists of mud. There are also numerous small shells spread throughout this sample, from the top to the bottom. No bioturbation is evident within this sample.

(g) Cores 13 and 14 (Plate 5.1(g))

The upper 5 cm of core 13 contains sand, followed by mud up to 20 cm deep; the bottom part is covered with sand. From the surface up to a depth of 23 cm, the core contains shells of *Littorina littorea*, a large shell appears within the surface sediments. There is no evidence of bioturbation of the sediments within this sample.

Core 14 consists of sand in the upper part, mud in the middle and sand at the bottom. Two tubes of *Lanice conchilega* together with some small shells (gastropods) appear within the upper 6 cm. Shells are also found at a depth of 7 cm - 11 cm. There is, as elsewhere, no evidence of bioturbation in this sample.

(h) Cores 15 and 16 (Plate 5.1(h))

There are several distinct variations in the sediments contained within

core 15. The deposits, from the surface to the bottom, are as follows: sand, mud, sand, mud and sand. An adult and a long tube of *Lanice conchilega* protrudes from a depth of 13 cm. One shell of *Littorina littorea* is located at 15 cm, whilst another is at a depth of 23 cm. There is no sign of bioturbation throughout the sample.

The sedimentary structure of core 16 can be divided into three parts: sandy top, muddy middle and sandy bottom. Some small shells of *Littorina littorea* appear within the upper 14 cm. It seems also that bioturbation did not occur in this sample.

From the results presented above, there is no evidence of extensive bioturbation of the surficial sediments. Hence, either the surface sediments have been relatively stable or the benthic organisms become relatively less abundant in response to the low temperatures. The cores were collected in late October 1993, when the water temperature dropped 11° C. The presence of tubes of *Lanice conchilega* in some of the cores, to depths of 13 cm, may represent the level of identifiable disturbance on the sediments of this area. The movement, feeding processes, burrow construction and maintenance of polychaetes have major effects on the physical and chemical properties of such sediments (Yingst and Rhoads, 1978; Meadows and Tufail, 1986; Meadows and Tait, 1989; Meadows and Hariri, 1991). Benthic organisms, in general, and polychaetes, in particular, can alter significantly the properties of surface sediment over a very small area. Where only limited bioturbation is present within a surface sediment layer, as in this study, it may be attributed to the varying nature of the spatial distribution of benthic organisms in an intertidal mudflat environment (cf Meadows and Tufail, 1986).

5.4.2. Sediment Density

Sediment density was measured using the MCN 160 and MCN 161 Metal Ceramic X-Ray tubes, as described in Section 4.4.2.f. The purpose of the study was to investigate any possible major variation in sediment density, especially

within the upper 5 cm. Emphasis was placed upon interpretation of this section of the samples, to compare with the location of the shear strength measurements and the X-radiography (see above). The results of the density measurements are shown on Figures 5.3(a to h). The general trends shown by the density profiles on the Figures reveals that the densities tend to be higher at the top than at the bottom (with the exception of cores 5, 9, 10, 11 and 15). High sediment densities represent sandy material, whilst the low sediment densities represent muds (silty clay). Variation between the high and low densities represents, therefore, the structural variation between the sands and muds in the samples (cf Plate 5.1((a) to (h))).

(a) Cores 1 and 2 (Figure 5.3(a))

The high density within core 1 occurs in the upper 9 cm; this then decreases considerably, fluctuates and finally increases gradually towards the bottom of the sample.

The high density section of core sample 2 takes up less than 5 cm, out of the whole core length. This region is followed by a steep and fluctuating decrease, to the lowest density at a depth 20 cm. This change is superseded by a steep increase in the gradient, then a gradual one.

(b) Cores 3 and 4 (Figure 5.3(b))

Visually, the pattern of sediment density in core 4 is significantly different from the previous two profiles. It seems that a thickness of less than 5 cm of the surficial sediments has a high density. The density decreases then gradually along the middle of the core, increasing towards the bottom. The density of this core 4 varies considerably. The upper layer represents low density sediments. This association is followed by a density increase up to 6 cm, then a gradual decrease to a depth of 12 cm; it is then distributed uniformly up to 24 cm. Beneath this depth, the density fluctuates and decreases towards the bottom of the core.

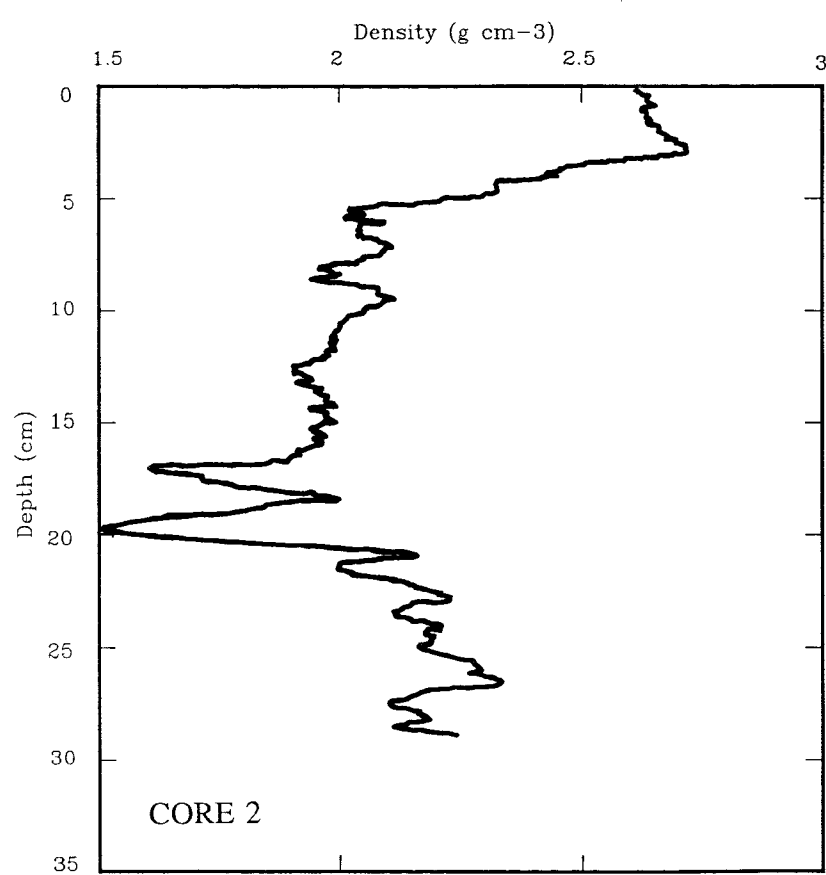
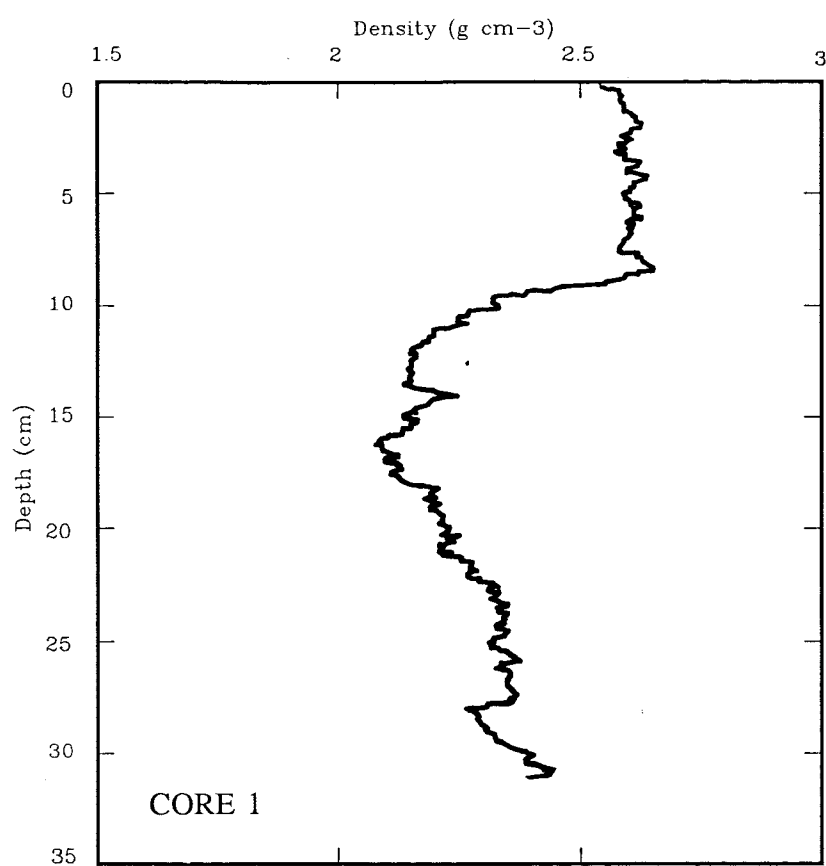


Figure 5.3(a). Sediment density of Cores 1 and 2

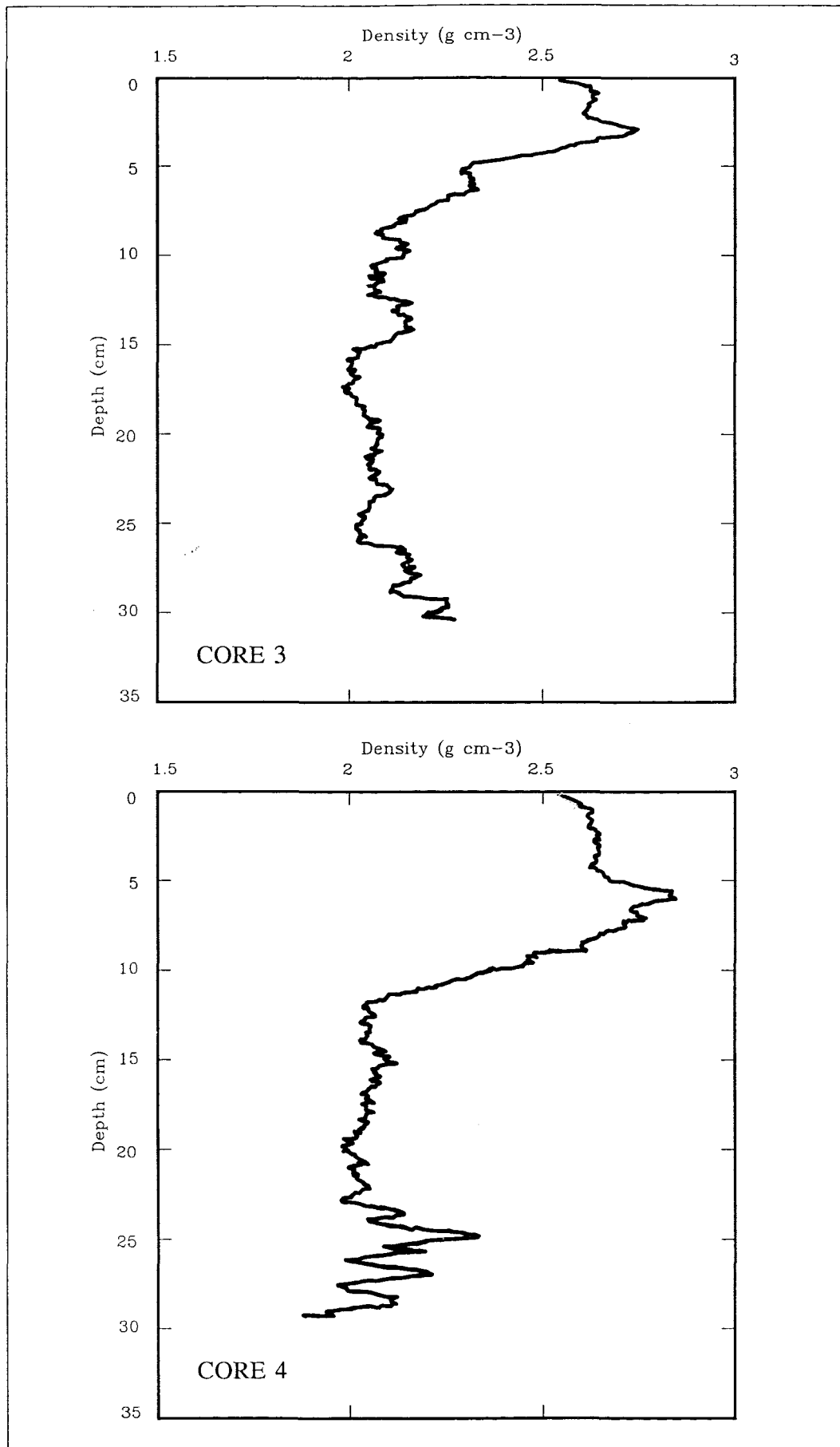
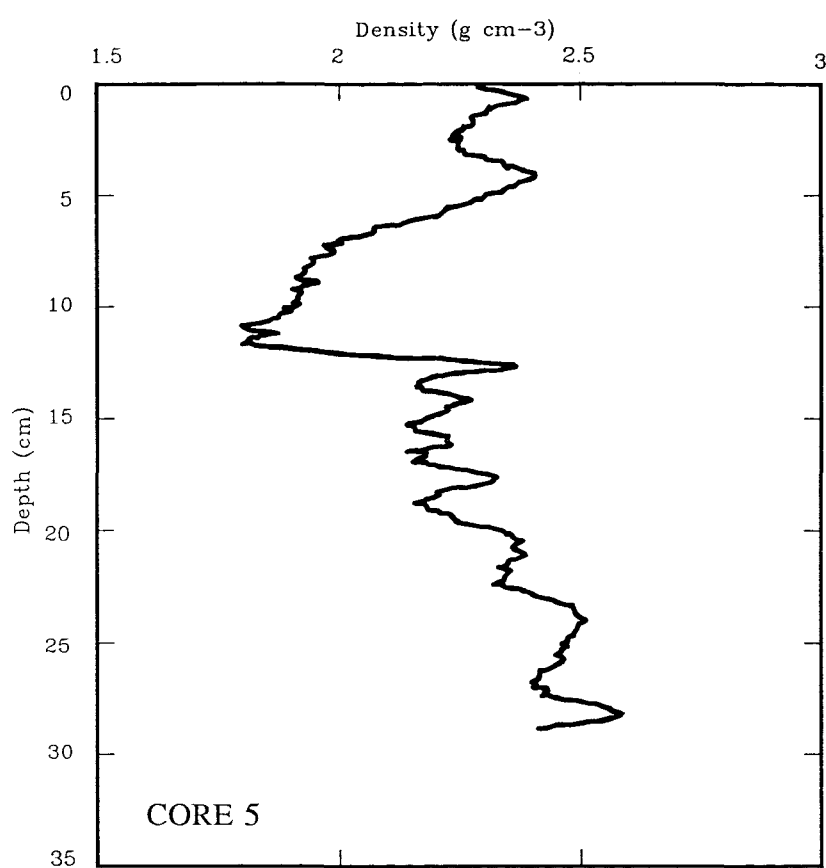
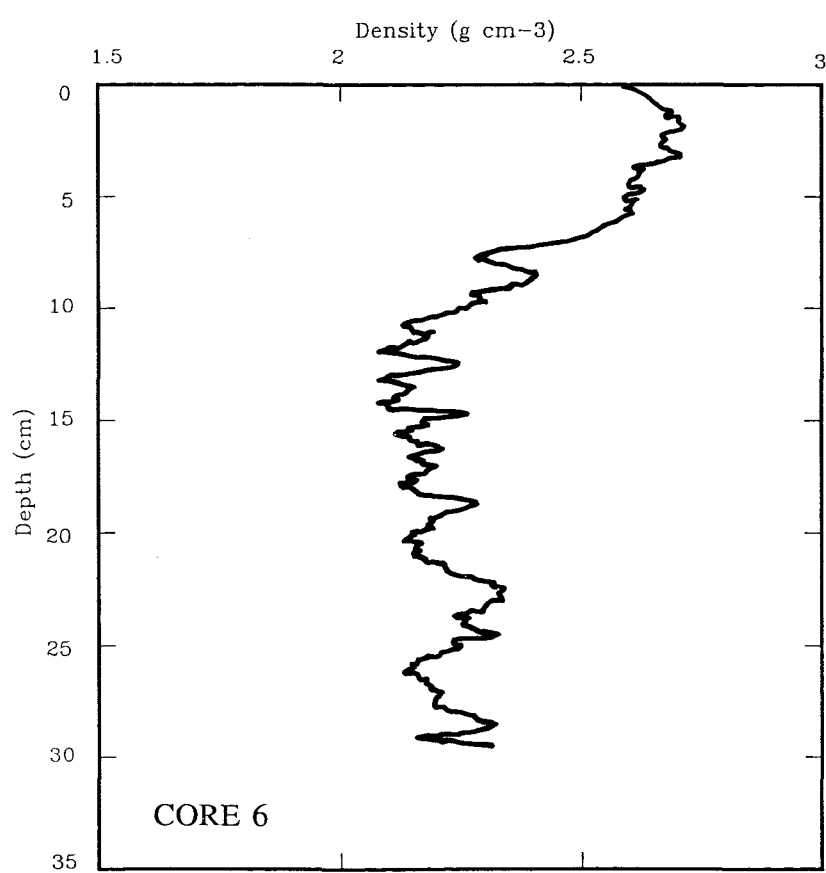


Figure 5.3(b). Sediment density of Cores 3 and 4



CORE 5



CORE 6

Figure 5.3(c). Sediment density of Cores 5 and 6

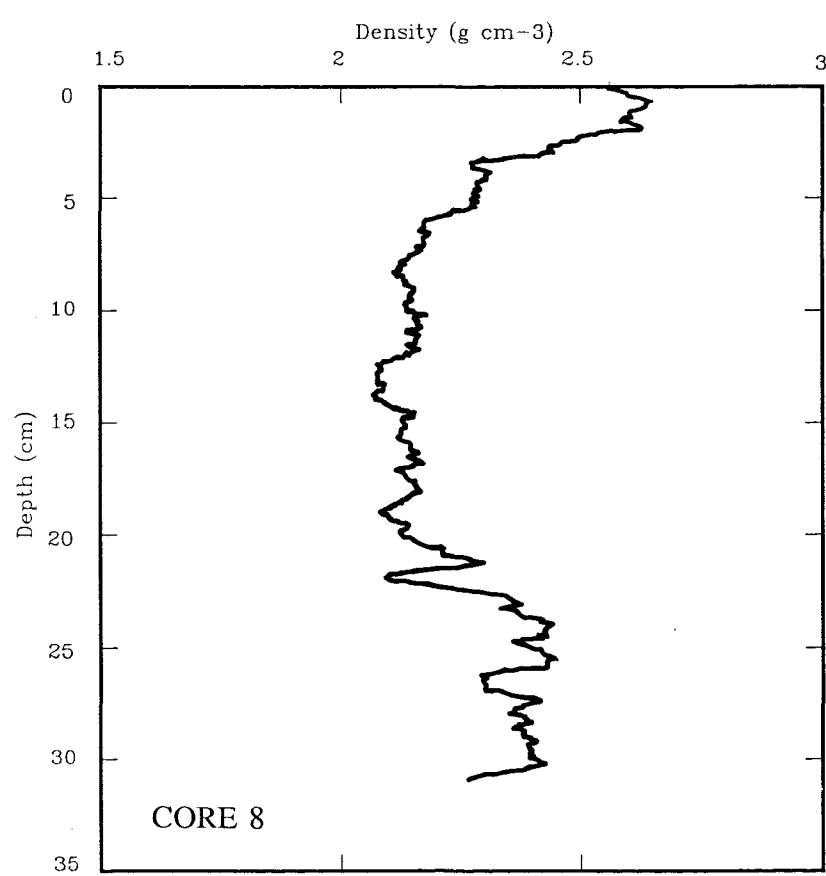
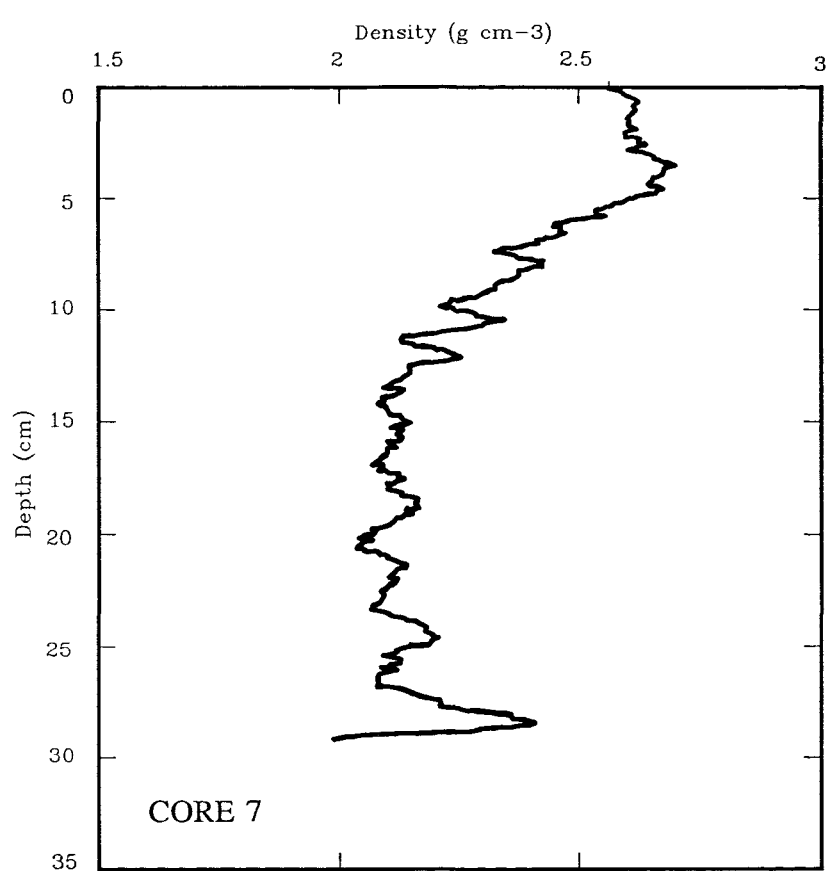


Figure 5.3(d). Sediment density of Cores 7 and 8

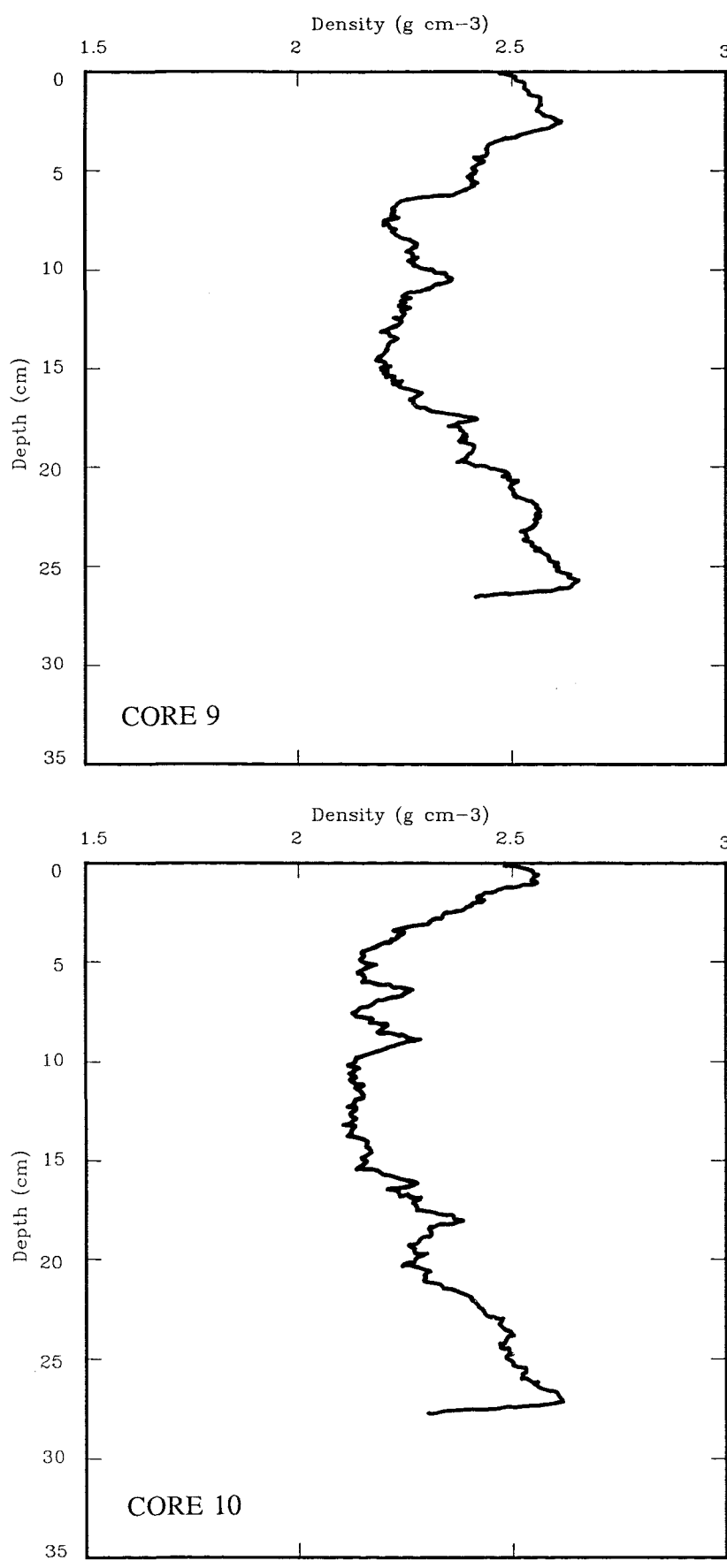


Figure 5.3(e). Sediment density of Cores 9 and 10

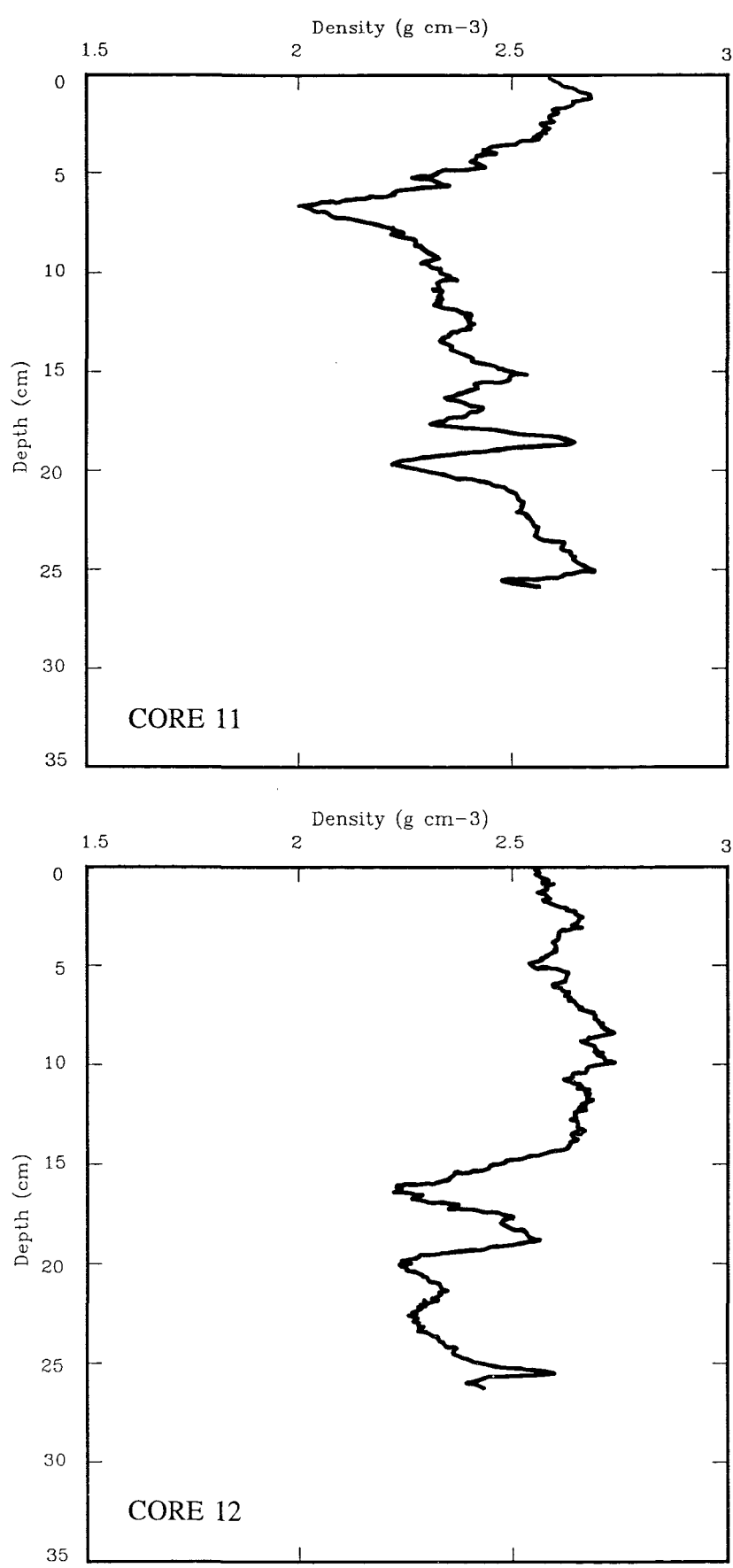


Figure 5.3(f). Sediment density of Cores 11 and 12

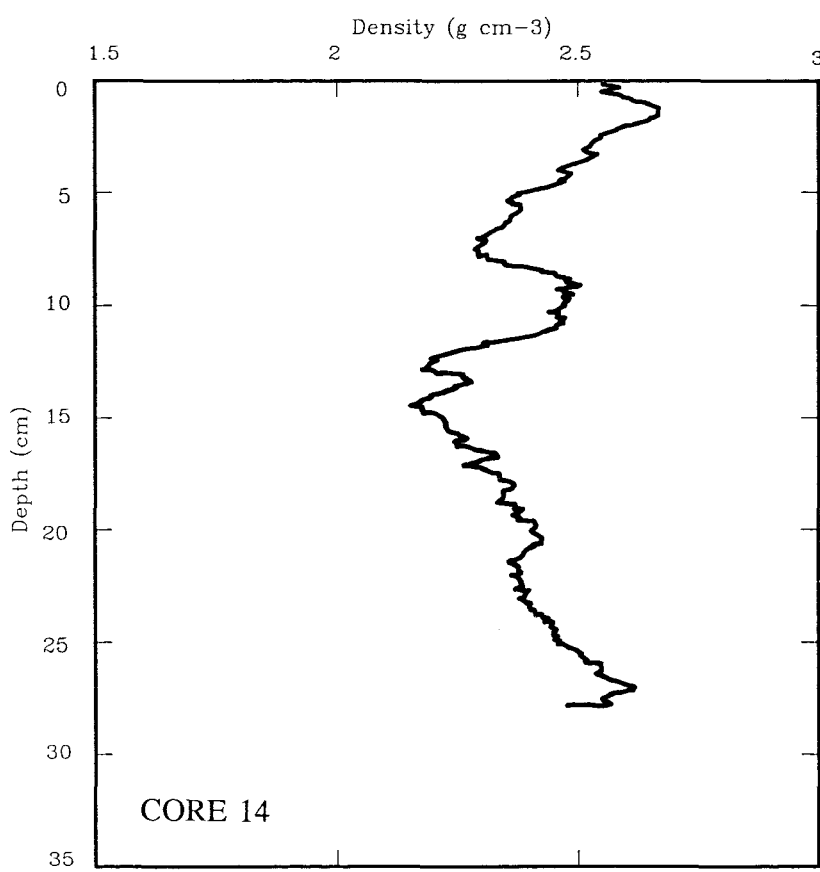
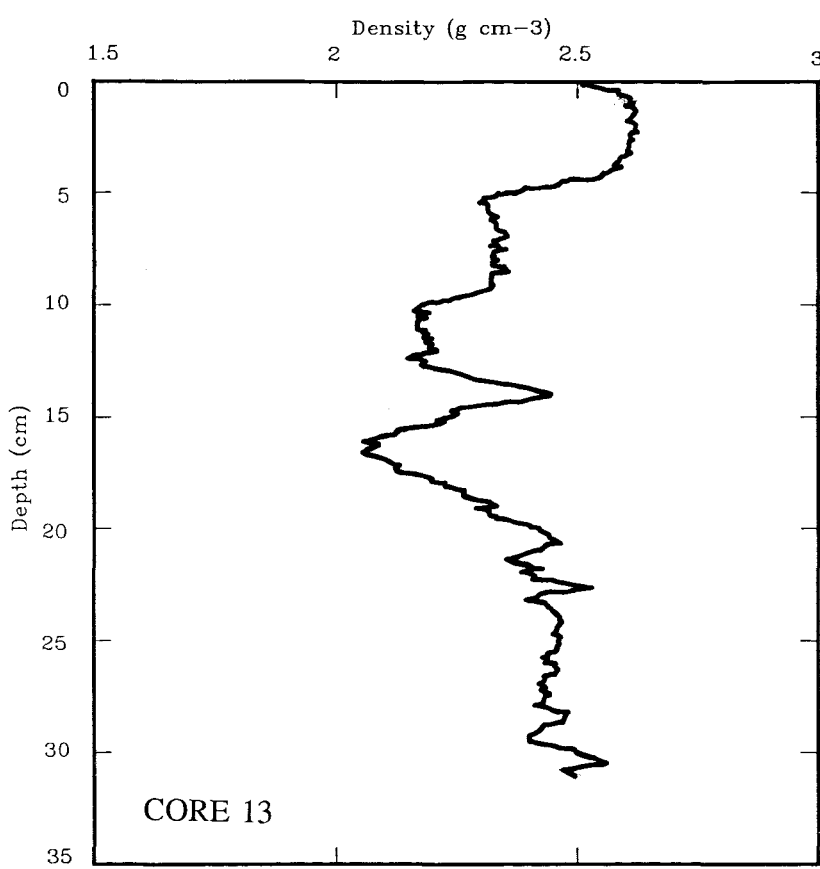


Figure 5.3(g). Sediment density of Cores 13 and 14

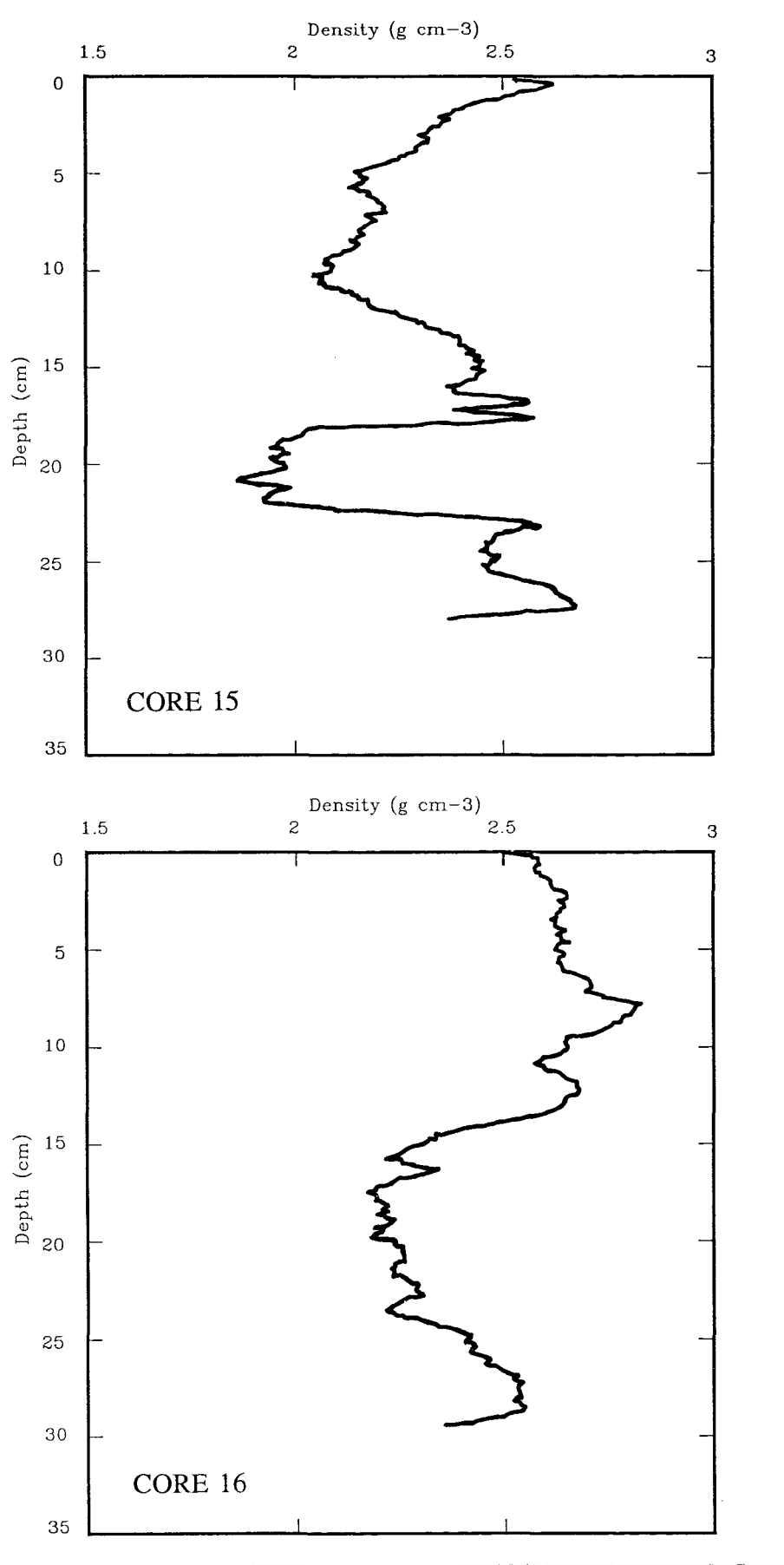


Figure 5.3(h). Sediment density of Cores 15 and 16

(c) Core 5 and 6 (Figure 5.3(c))

Within the upper 5 cm of core 5, the density fluctuates; this is followed by a gradual decrease to a depth of 12 cm. The density then increases greatly, and fluctuates gradually towards the bottom of the core.

Sediments at the surface of core 6 are associated with a high density. A gradual decrease occurs up to a depth of 12 cm. The density then fluctuates and increases slightly towards the bottom of the core.

(d) Cores 7 and 8 (Figure 5.3(d))

From the surface sediments, the density in core 7 increases up to 4 cm; it then decreases gradually up to 14 cm, fluctuates and is distributed with insignificant variation to the bottom. At the very (bottom) end of the sample, the density increases steeply at 29 cm.

The high density in core 8 occurs only within the upper 3 cm; it then decreases gradually, followed by a relatively uniform and static density up to 20 cm. The density gradient then fluctuates, increasing again towards the bottom of the core.

(e) Cores 9 and 10 (Figure 5.3(e))

The density in core 9 increases from the top of the surface sediment, up to 3 cm; it then decreases and fluctuates up to 16 cm. This pattern is followed by a gradual increase up until the end of the sample. A steep increase occurs at the very end of the core.

The upper 1 cm of core 10 is associated with a high density, which later declines gradually up until 5 cm; it fluctuates then slightly to 16 cm, followed by gradual and considerable increases towards the bottom end of core. At the very end of the core sample, the density falls remarkably.

(f) Cores 11 and 12 (Figure 5.3(f))

Only the upper 2 cm of this core 11 has a high density. The density then decreases markedly up to 6 cm; this is followed by a sharp increase. This increase is followed by fluctuating and gradual increases in density to the end of the core. The density varies significantly at depths of between 15 and 20 cm. The upper 14 cm of core 12 has a high density; this then decreases rapidly up to 16 cm, fluctuating considerably to the end of the sample.

(g) Cores 13 and 14 (Figure 5.3(g))

High densities occur within the upper 4 cm of core 13; these are followed by a sharp and fluctuating decrease, up to 16 cm. This pattern is followed by a steep increase in gradient, then a gradual and slight increase at the bottom of the core.

Only top 2 cm of core 14 has a high density, which decreases sharply up to 7 cm. The density then increases sharply, followed by a sharp decrease to 15 cm. The density increases subsequently towards the end of the core.

(h) Cores 15 and 16 (Figure 5.3(h))

Only the upper 1 cm of core 15 consists of high density sediments. The remainder is associated with a steep and fluctuating decrease, occurring up to 11 cm. The density then increases sharply, reaching a peak at a depth of 18 cm. A rapid decrease occurs again, fluctuating at depths of 19 to 22 cm; this is followed by a sharp increase, reaching a peak at 23 cm deep, then fluctuating to the end of core.

The high density in core 16 covers the upper 13 cm; it has its peak at 8 cm. The density decreases steeply then up to 15 cm; it fluctuates and increases gradually, then decreases rapidly before the end of the core.

Based upon the results described above, the density of the sediment deposits within the upper 5 cm of each of the cores varies only slightly and insignificantly. To obtain a representative (average) density, the upper layers of all samples were divided into 5 sections, 1 cm in length. The mean density of each core sample is derived on the basis of these 6 data points. The results of this synthesis are presented in Table 5.2 and on Figure 5.4.

The density data presented in Table 5.2 has been analysed statistically, in order to establish any significant variation within the upper 5 cm of the sediment deposits. As the assumptions for a parametric test were violated, the Kruskal-Wallis One Way ANOVA on Ranks (non-parametric) test was adopted. The results obtained show (Table 5.3) that the differences in the median values among the core samples are greater than would be expected by chance; therefore, there is a statistically significant difference ($P < 0.001$). To isolate which samples differ from the others, a multiple comparison test was adopted. The test used was the Student-Newman-Keuls (SNK) method, as the present data of equal size which fulfil the requirements for this method.

The difference between each individual sample, against all the other 15 samples, ranged from 33.33 % to 100 % (at 5 % level of significance) (Table 5.3). Only two (cores 8 and 9), differ (by 100 %) from all the other samples. These cores were collected from the edge of the study area (Figure 5.1), where the main sampling activity was restricted during the period of study i.e. around the centre of the outer dashed lines. It can be assumed, therefore, that the extreme effects of these density variations did not influence the shear strength measurements.

Interrelationships between sediment density, the x-ray photographs and the relative locations of the core samples (Figure 5.1, Plate 5.1(a) to (h), and Figure 5.4) reveal that Cores 5, 10 and 15 contain sediments of low density. This observation indicates that the upper part (5 cm) of these cores were composed mainly of mud (silt/clay materials). The remaining cores contain sediment of relatively high density (sand materials).

Table 5.2. Sediment density (in g cm⁻³) within the upper 5 cm of the surficial sediments from Solent Breezes (October, 1993)

	Core 1	Core 2	Core 3	Core 4	Core 5	Core 6	Core 7	Core 8
Top	2.54	2.61	2.54	2.54	2.29	2.58	2.56	2.56
1 cm	2.60	2.64	2.63	2.51	2.33	2.68	2.58	2.59
2 cm	2.60	2.69	2.60	2.63	2.28	2.70	2.60	2.50
3 cm	2.60	2.58	2.71	2.63	2.28	2.70	2.65	2.36
4 cm	2.63	2.38	2.53	2.63	2.43	2.63	2.66	2.26
5 cm	2.61	2.20	2.28	2.75	2.29	2.61	2.61	2.25
Mean	2.60	2.52	2.55	2.62	2.32	2.65	2.61	2.42
Median	2.60	2.60	2.57	2.63	2.29	2.66	2.61	2.43
Std.Err	0.01	0.08	0.06	0.03	0.02	0.02	0.02	0.06

Table 5.2. Continued (see above)

	Core 9	Core 10	Core 11	Core 12	Core 13	Core 14	Core 15	Core 16
Top	2.47	2.48	2.58	2.55	2.50	2.55	2.51	2.50
1 cm	2.53	2.50	2.68	2.59	2.59	2.64	2.48	2.59
2 cm	2.56	2.40	2.59	2.63	2.59	2.59	2.35	2.65
3 cm	2.53	2.28	2.56	2.65	2.58	2.50	2.29	2.65
4 cm	2.44	2.19	2.45	2.60	2.53	2.48	2.25	2.65
5 cm	2.41	2.18	2.31	2.63	2.31	2.38	2.13	2.65
Mean	2.49	2.34	2.53	2.61	2.52	2.52	2.34	2.62
Median	2.50	2.34	2.57	2.62	2.56	2.53	2.32	2.65
Std.Err	0.02	0.06	0.05	0.02	0.04	0.04	0.06	0.03

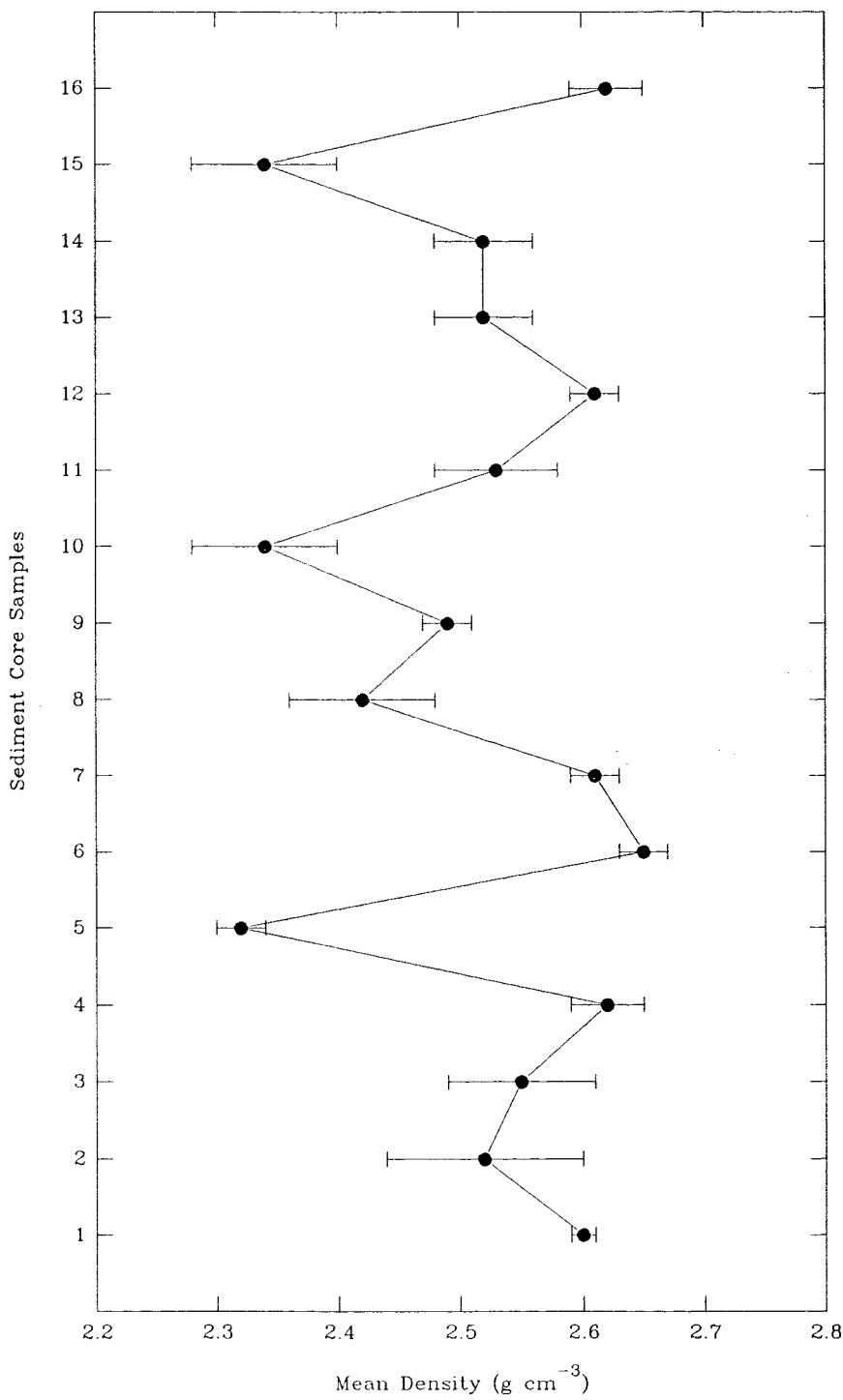


Figure 5.4. Mean density of the upper 5 cm of the surficial sediment samples, collected at Solent Breezes in October 1993 (for relative location of cores, see Figure 5.1)(X error bars represent standard errors)

Table 5.3. All Pairwise Multiple Comparisons Test on the sediment density of the upper 5 cm, using Student-Newman-Keuls Method (at 5 % level of significance)

No	1	2	3	4	5	6	7	8	9	10	11	12	13	14	15	16
1	nd	nd	nd	nd	d	nd	nd	d	d	d	nd	nd	nd	nd	d	nd
2	nd	nd	nd	nd	d	d	nd	d	d	d	nd	nd	nd	nd	d	nd
3	nd	nd	nd	nd	d	d	nd	d	d	d	nd	nd	nd	nd	d	nd
4	nd	nd	nd	nd	d	nd	nd	d	d	d	nd	nd	nd	nd	d	nd
5	d	d	d	d	nd	d	d	d	d	nd	d	d	d	d	nd	d
6	nd	d	d	nd	d	nd	nd	d	d	d	d	nd	d	d	d	nd
7	nd	nd	nd	nd	d	nd	nd	d	d	d	nd	nd	nd	nd	d	nd
8	d	d	d	d	d	d	d	nd	d	d	d	d	d	d	d	d
9	d	d	d	d	d	d	d	d	nd	d	d	d	d	d	d	d
10	d	d	d	d	nd	d	d	d	d	nd	d	d	d	d	nd	d
11	nd	nd	nd	nd	d	d	nd	d	d	d	nd	nd	nd	nd	d	nd
12	nd	nd	nd	nd	d	nd	nd	d	d	d	nd	nd	nd	nd	d	nd
13	nd	nd	nd	nd	d	d	nd	d	d	d	nd	nd	nd	nd	d	nd
14	nd	nd	nd	nd	d	d	nd	d	d	d	nd	nd	nd	nd	d	nd
15	d	d	d	d	nd	d	d	d	d	nd	d	d	d	d	nd	d
16	nd	nd	nd	nd	d	nd	nd	d	d	d	nd	nd	nd	nd	d	nd

Key: nd - not different; d - different

5.5. Velocity Profiles

5.5.1. Introduction

Various studies have been undertaken elsewhere on the vertical structure of velocities (i.e. profiles) near the sea bed (Charnock, 1959; Sternberg, 1966;

Dyer, 1970 and 1980; Channon and Hamilton, 1971). The results have verified that under neutral stability and steady flow conditions, the velocity profile close to a hydraulically rough bed can be represented by the von Karman-Prandtl equation. This equation enables the calculation of bed shear stress, which is an important parameter in the studies of sediment dynamics. For a sea bed which is occupied by numerous bedforms, considerable difficulty emerges because the total stress measured will be the sum of the skin friction and the form drag (Dyer, 1980). Form drag refers to the integral of the horizontal component of the normal pressure distribution over the bedform length. Hence, it is only the skin friction which causes sediment movement. The presence of any bedforms creates an internal boundary layer within the flow, causing acceleration over the crest and deceleration near the trough. This effect decreases with a height of up to about two or three times the (ripple) wave height above the crest, where the flow becomes uniform (Krugermeier *et al.*, 1978). The flow near the bed is comparatively steady, even though it is not uniform. Logarithmic velocity profiles may occur if the bedforms are large; these vary over the bedforms and can be used as a measure of the skin friction (Dyer, 1970). Also, a logarithmic profile can be measured above the internal boundary layer; however, the measured drag will represent here the total drag on the bed surface.

Several studies have investigated the effect of bedforms on the structure of the associated velocity profiles: (i) establishing the relationship between the bedforms and the profiles, by averaging profiles over the complete wave-length of the bedforms (Smith and McLean, 1977); and investigating the effect of ripples on velocity profiles, using numerical models (Smith, 1969; Taylor *et al.*, 1976). The first of these studies was undertaken by analysing the development of the internal boundary layers downstream of a topographic change and their effect on the velocity profiles; this led to the calculation of form drag and skin friction, separately. A problem arises in such analyses, however, if the lowermost internal boundary layer is located below the lowest current meter. This approach does not then enable an accurate determination of the bed shear stress. The second study showed that, for sinusoidal waveforms within the bed sediments typically 25 - 33 % of the total drag consists of form drag. The use of these models requires,

however, accurate representation of the bed shape and surface roughness on the bed form. This requirement arises because the form drag contribution is sensitive to the asymmetry of the bedforms and the occurrence of flow separation.

The velocity profile close to a hydraulically rough bed can be represented by the von Karman-Prandtl equation:

$$\frac{u_z}{u_*} = \frac{1}{k} \ln \left(\frac{z}{z_0} \right) \quad (5.1)$$

where u_z is the velocity at height z (above the bed), k is the von Karman constant (taken as = 0.4), z_0 is the roughness height (representing the height at which long-term average velocity equals zero). From equation (5.1), for measurements made within the log-layer, a plot of $\ln z$ versus u_z produces a straight line; the slope of this is equal to k/u_* , whilst the intercept on the $\ln z$ axis gives $\ln z_0$. The data obtained on velocity profiles for the present investigation were analysed using the regression form of the above equation, as follows:

$$\ln z = a + b u_z \quad (5.2)$$

This expression was used to calculate the slope of the relationship between height above the bed to horizontal velocity. On the basis of a knowledge of slopes, shear velocities (u_*) and stresses (τ) could be obtained using the following relationship,

$$u_* = \left(\frac{\tau}{\rho} \right)^{\frac{1}{2}} \quad (5.3)$$

where ρ is the fluid density (here taken as 1.03 g cm⁻³).

From equation (5.3) boundary shear stress may be obtained as,

$$\tau = u_*^2 \rho \quad (5.4)$$

5.5.2. Friction Velocities over the Study Area

Velocity profile measurements were expressed using equation 5.2: a typical plot of 5 min u_* values (friction velocity), shear stress, bed roughness

length and coefficient of determination are shown in Table 5.4 and Figure 5.5. The velocity profile is regarded as logarithmic in character if the value of r^2 is greater than 0.8 (Inman, 1963). Using this criterion, the results obtained show that, over a tidal cycle, some 70 % of the velocity profiles are significantly logarithmic; in contrast 30 % of the measurements are not significantly logarithmic at the 95 % level of confidence. For the logarithmic profiles, u_* increases with an increase in water depth. U_* reaches a maximum (5.71 cm s⁻¹) at the beginning of the peak of the first high water; it then decreases, followed by a gradual increase towards the end of the low water period. Critical friction velocities range from 0.25 cm s⁻¹ to 5.71 cm s⁻¹; these correspond to critical bed shear stress of 0.01 N m⁻² to 3.36 N m⁻².

Logarithmically insignificant profiles appear to occur, on occasions, throughout the whole of the tidal cycle. Generally, however, 13 % occur during the onset of high water; likewise 10 % occur during full high water, whilst 7 % occur during low water. This interpretation appears to be in agreement with studies undertaken elsewhere, whereby the frequency of occurrence of the logarithmic profile was found to be higher on the flood than on the ebb phase of the tide. Such a pattern was more pronounced over the upper part, rather than the lower part, of the intertidal zone (van Smirren, 1982). Since the majority of the profiles observed at Solent Breezes are logarithmic, this implies that the velocity profiles on the intertidal flats of the study area follow generally the von Karman-Prandtl equation. The higher frequency of logarithmic profiles recorded on the (Solent) intertidal flats may be related to the accretion and propagation of the intertidal zone. Any lower frequency of occurrence of logarithmic profiles, in an offshore direction, may represent erosion or scour of sediments over the intertidal flats.

5.5.3. Bed Roughness Length

Bed roughness lengths differ according to bed type. At the same time, the presence of ripples and *Lanice conchilega* tubes will affect the bed roughness length. For an hydraulically smooth bed, the bed roughness length $z_0 = \nu/9u_*$,

Table 5.4. Friction velocity, bed roughness length, shear stress and coefficient of determination

Time (hour)	Water Depth (m)	Friction Velocity (cm s ⁻¹)	Critical S. Stress (N m ⁻²)	Roughness Length (cm)	Coeff. of Determination, r ²
09.00	0.40	5.00	2.58	8.33	0.71
09.15	0.60	0.29	0.01	0.02	0.84
09.30	0.70	0.25	0.01	0.10	0.86
09.45	0.70	4.00	1.65	27.66	0.01
10.15	0.80	1.00	1.03	3.60	0.90
10.30	0.80	1.11	0.13	3.00	0.46
10.45	0.85	1.21	0.15	1.38	0.83
11.00	1.05	1.38	0.20	0.51	0.80
11.15	1.25	2.11	0.46	0.57	0.99
11.30	1.50	5.00	2.58	6.36	0.93
11.45	1.60	5.71	3.36	10.80	0.73
12.00	2.05	5.71	3.36	8.76	0.87
12.15	2.30	5.71	3.36	8.08	0.92
12.30	2.60	5.71	3.36	9.68	0.92
12.45	3.00	4.00	1.65	14.30	0.88
13.00	3.60	3.64	1.36	20.09	0.56
13.30	3.60	1.38	0.20	14.44	0.67
13.45	3.50	1.90	0.37	6.96	0.91
14.00	3.40	1.67	0.29	12.43	0.88
14.30	3.55	0.95	0.09	2.83	0.16
14.45	3.55	1.29	0.17	3.56	0.93
15.00	3.40	1.48	0.23	4.85	0.94
15.15	3.20	1.21	0.15	7.32	0.94
15.30	3.00	3.08	0.98	18.73	0.31
16.15	2.90	0.89	0.08	0.72	0.90
16.30	2.60	2.11	0.46	2.01	0.99
16.45	2.35	2.86	0.84	1.39	0.98
17.00	2.00	2.86	0.84	0.63	0.84
17.15	1.40	5.71	3.36	5.93	0.85
17.30	1.20	6.67	4.58	8.85	0.46

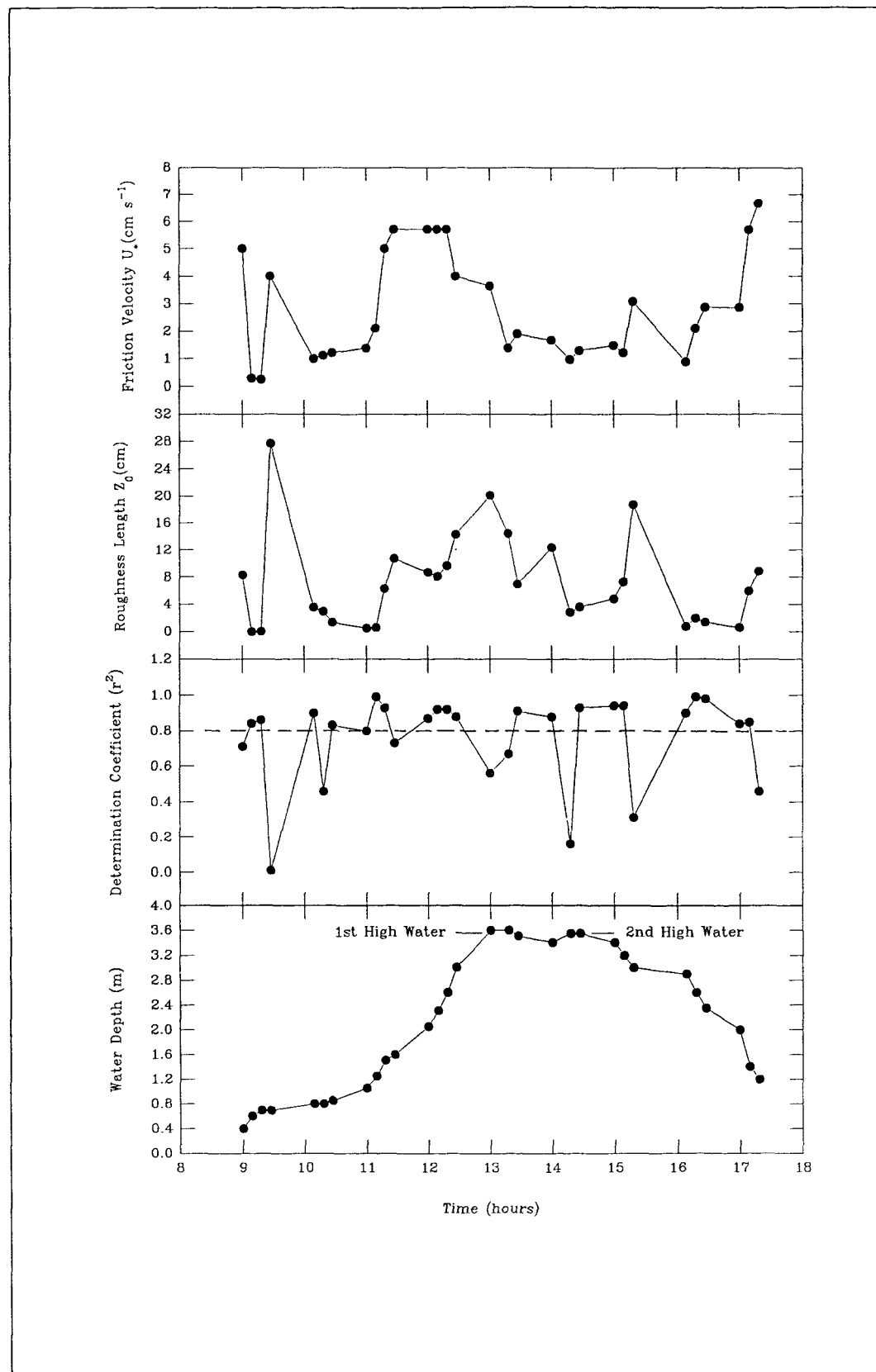


Figure 5.5. Friction velocity, roughness length, determination coefficient and water depth during a spring tidal cycle at Solent Breezes in September 1992

where ν is the kinematic viscosity (obtained by dividing the molecular viscosity by water density). For an hydraulically rough bed of uniform grain size of diameter D , the bed roughness length $z_0 = D/30$. The first method of calculating z_0 derives z_0 values of the order of 10^{-3} , with z_0 decreasing with an increase in u_* . The latter relates also to z_0 values of around 10^{-3} cm, but the relationship is independent of bed shear stress. For a bed with large roughness elements, it has been proposed by Lettau (1969) that the bed roughness length is given by $z_0 = 0.5 h/S$; here h is the average vertical extent or effective obstacle height (cm), and S is the cross sectional area seen by the flow (per horizontal area S).

The results obtained during the present investigation indicate that the bed roughness length follows a pattern similar to that exhibited by the friction velocity (see Table 5.4 and Figure 5.5). Of the 'significant' logarithmic profiles observed, z_0 increases in accordance with an increase in water depth; it reaches a maximum of 14.30 cm at the beginning of the full high water peak, fluctuating then decreasing towards low water. Z_0 increases again at the end of low water. Z_0 ranges from 0.02 cm to 14.30 cm. Most of the ripple crestlines observed on the sandflat under investigation lie parallel to the coast line. Hence, the flood currents arrive at the intertidal zone from a direction of $300^\circ - 40^\circ$, crossing the ripples (cf Evans and Collins, 1975). The influence of the bedforms on the velocity profiles during flood tide, therefore, will be higher in sandflat. Current speeds recorded on the intertidal flat varied from 2.2 cm s^{-1} to 43.5 cm s^{-1} , near-bed and at the surface, respectively. Bedforms were observed during low water, on every sampling occasion. At such times, ripples were distributed generally in regular patterns; they had an average wavelength of about 5 cm and height of around 2 cm. This observation indicates that the area under study is basically stable, tidally dominated and protected from waves.

CHAPTER 6

RESULTS: BIOLOGICAL INVESTIGATIONS

6.1. Introduction

This chapter describes the results of biological investigations together with their interpretation and discussion. These include a consideration of interactions between the tube density of *Lanice conchilega* and total species, total individuals, total protein, bacterial protein, bacterial abundance, phytoplankton abundance, diatom abundance, community structure, dominant species, diversity and correlations between principal components of the abundance of benthic macrofauna with parameters under investigation. Seasonal variabilities are described using mean values of monthly data. Since the data obtained include numerous parameters, a multivariate method of analysis, Principal Components Analysis, was adopted. The initial components of the benthic macrofauna data were obtained using the Principal Components Analysis (PCA) as described in Section 4.5.2. The principal components obtained were then correlated to other variables, both physical and sedimentological, in order to explain the existing pattern of *Lanice conchilega* and benthic macrofauna at Solent Breezes, Southampton Water. Also, to establish those environmental factors which are most likely to be responsible for the observed distribution of macrofauna in the area under investigation.

6.2. *Lanice conchilega* (Pallas, 1766)

Lanice conchilega is a polychaete worm, widely distributed in northwestern Europe and around Britain (Fish and Fish, 1989). This species has a delicate body, up to 300 mm in length, which contains up to 300 segments. The tube is made of mud, sand and shell fragments. The anterior end, flattened

and extended into finger-like projections covered with sand and shell fragments, often extends well above the surface of the sediment. At Solent Breezes, on average, the tubes extend 1 to 2 cm above the sediment surface and have a mean diameter of around 5 mm. The species is found in fine-sand and silty-sand habitats on the lower shore and below, often in very large numbers. They feed on organic detritus picked up from the surface of the sediment by long tentacles on the head. The anterior projections of the tube are set at right angles to the predominant current flow and cause suspended organic matter to be deposited behind them, where the water is relatively still. The polychaete is also able to feed on suspended particles trapped by mucus on the tentacles. The sexes are separate and breeding occurs during spring and summer. Gametes are discharged into the sea where fertilisation occurs. The larva have a long pelagic life of about two months.

The mean tube density of *Lanice conchilega* is shown in Table 6.1 and in Figure 6.1. Tube density decreased gradually from October 1991 to September 1993 and with no apparent seasonality. The population of *Lanice* in the first year of the study was therefore generally higher than in the second year. This trend may result from recruitment failure or from species interactions. During this period several dominant species of benthic macrofauna increased in abundance, e.g. *Euclymene oerstedii*, *Pygospio elegans*, *Nephtys hombergii* and *Syllis sp* (Figures 6.5 and 6.6). The population increase of these dominant species coincides with the decrease in the abundance of *Lanice* tubes. These four species may possibly have consumed the larvae of *Lanice*. This suggestion seems to be logical and acceptable because it has been found that these species, especially carnivorous species such as *Nephtys hombergii* feeds on molluscs, crustacean and other polychaetes (Fish and Fish, 1989); *Syllis sp* feeds on hydroids, bryozoan and other colonial invertebrates (Fauchald and Jumars, 1979). The lowest density of *Lanice* tubes occurred in July 1993 and the highest density occurs in November 1991. Plotting tube density against macrofauna abundance (species or individuals), it seems that there are weak negative correlations between tube density and total numbers of species or individuals as shown on Figure 6.2. High density of *Lanice* tubes tends to coincide with low density of macrofauna. This

Table 6.1. Mean tube density of *Lanice conchilega*, mean total species and mean total individuals of benthic macrofauna

Month (Year)	Tube Density (100 cm ⁻²)	Total Species (100 cm ⁻²)	Total Individuals (100 cm ⁻²)
October (1991)	7.40	9.60	17.70
November	8.80	9.50	13.57
December	7.33	8.67	12.67
January (1992)	5.80	3.67	4.67
February	7.83	6.17	7.57
March	6.37	7.10	9.20
April	6.53	10.53	13.57
May	6.87	9.37	15.23
June	6.50	10.07	15.37
July	7.52	11.83	17.48
August	5.87	12.20	21.50
September	4.27	10.03	17.33
October	5.00	9.77	16.77
November	4.76	8.48	11.29
December	4.65	9.35	14.53
January (1993)	4.00	9.00	12.00
February	4.90	8.81	14.43
March	4.06	15.06	32.31
April	5.03	17.73	28.67
May	4.72	13.40	18.48
June	4.33	11.53	19.47
July	3.13	12.80	19.20
August	4.73	10.73	16.50
September	4.85	10.90	15.30

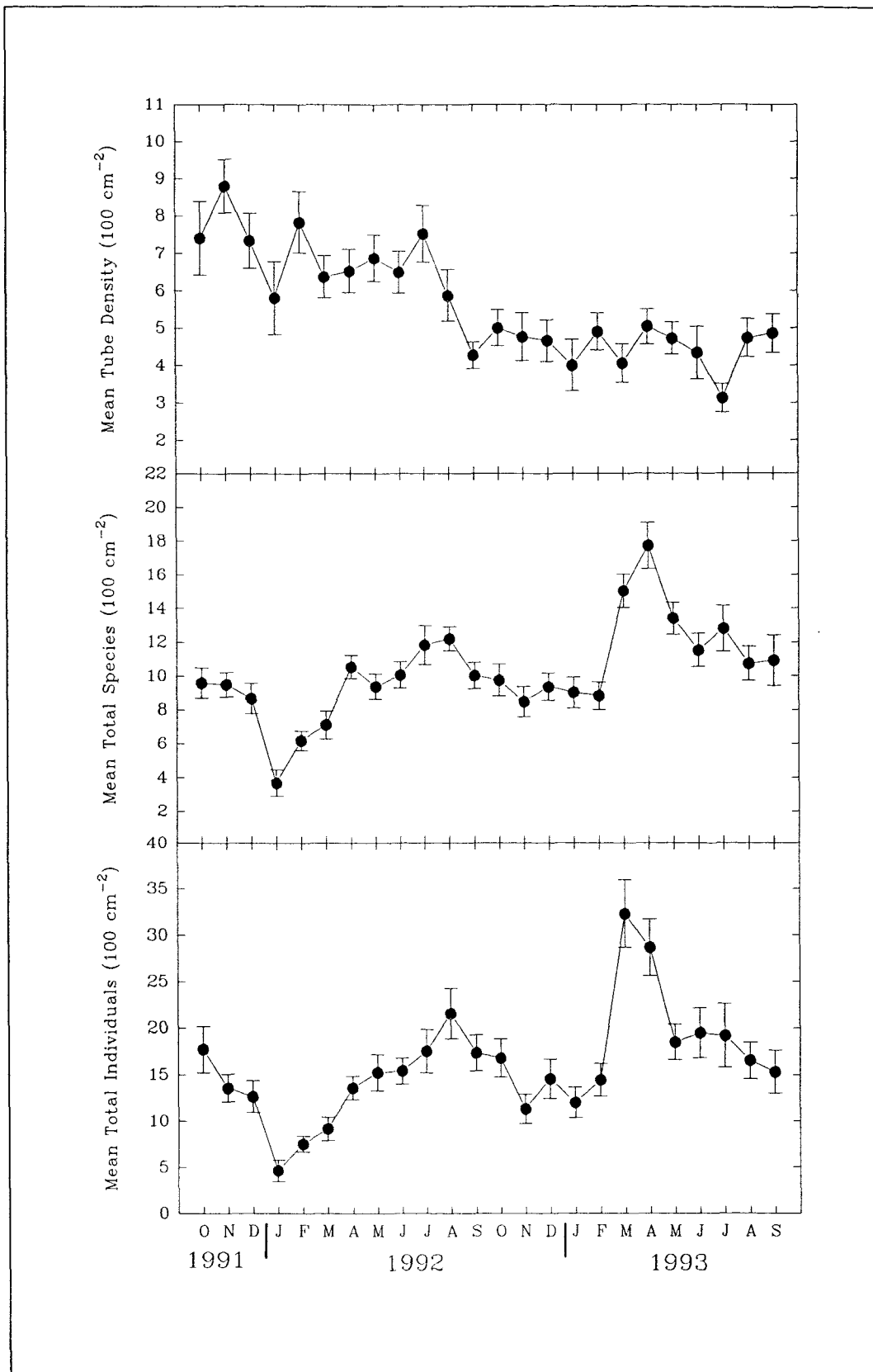


Figure 6.1. Long-term variation in mean tube density of *Lanice conchilega*, mean total species and mean total individuals of benthic macrofauna (Y error bars represent standard errors)

may be the results of several factors: limited space available between tubes for macrofauna, predation of macrofauna by *Lanice*, high mortality rate of macrofauna during post spawning period, and failure in recruitment or settlement of macrofauna larvae due to changed localised hydrodynamic conditions.

6.3. Total Species of Benthic Macrofauna

Twenty nine species of macrobenthic organism were identified during the period of this study. The total species numbers per 100 cm² of macrofauna recorded during the experiment are shown in Table 6.1 and on Figure 6.1. The number of species fluctuates seasonally, high numbers occurred in summer and low numbers occurred in winter, and increased from the first year to the second year. The lowest number of species was recorded in January 1992 and the highest one was recorded in April 1993. The total species shows a pattern of seasonality, though with year to year variation in the seasonal pattern.

6.4. Total Individuals of Benthic Macrofauna

The total numbers of individuals of benthic macrofauna per 100 cm² are shown in Table 6.1 and on Figure 6.1. This follows a similar pattern to that for total species; numbers fluctuate seasonally, then increase towards the end of the study. It seems also to show a pattern of seasonality. Comparing the abundance trend of total species and total individuals, it appears that changes in number of individuals and species are related. By establishing the Least Square regression to both parameters, the results show a strong significant correlation (at 5 % level of significance) with $r = 0.93$ as shown on Figure 6.2. The possible argument behind this trend is that benthic fauna reproduce in early spring; this will lead to high abundance in summer. In contrast, during winter mortality tends to be high which will lead to low abundance. Summer reproduction causes rare species to become more abundant, therefore, increases the number of species sampled.

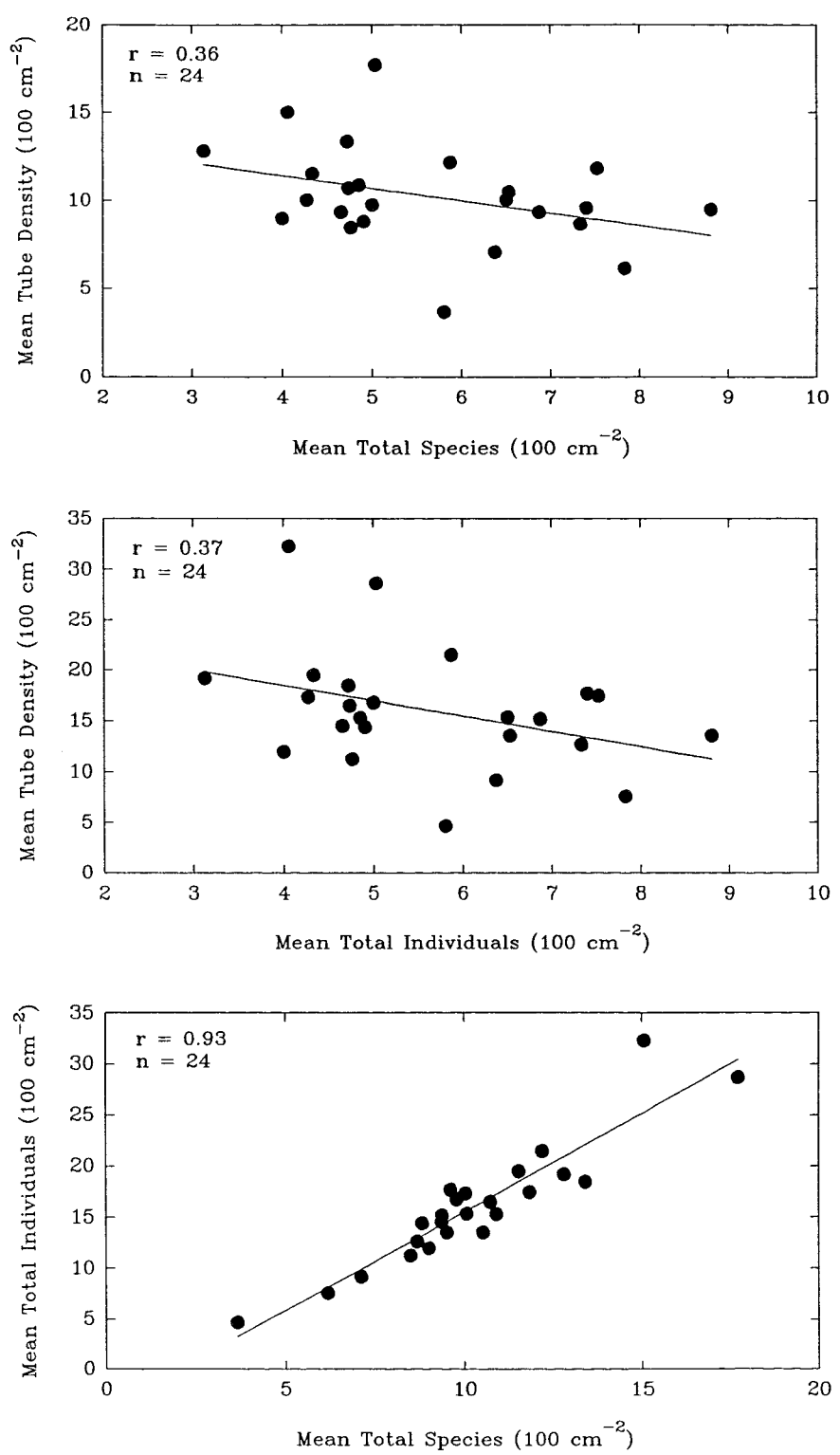


Figure 6.2. Correlations between mean total species and mean tube density, mean total individuals and mean tube density, mean total species and mean total individuals

6.5. Total Protein

Mattin (1992) carried out a study on total protein content of surface sediments samples from Solent Breezes, Southampton Water, utilising the method developed by Mayer *et al.* (1986), to measure the enzymatically available protein content of sediments. It was shown that there is a relationship between total protein and total organic content, where total protein contributes a certain percentage to the total organic content. In order to obtain total protein of the sediment samples in the present study, Mattin's data (the percentage contribution of protein to organic matter) were used to calculate the total protein since the primary data on total organic content of the present study are not available. The calculated total protein of surficial sediment are shown in Table 6.2 and in Figure 6.3. It appears that the total protein shows a seasonal pattern, where low concentrations occur during winter months and high concentrations occur during summer months. The lowest concentration was calculated as 0.78 mg per g dry sediment in November 1991 and the highest concentration as 2.42 mg per g dry sediment in July 1992. This seems logical as the protein concentration is affected by the content of organic matter. During summer months, organic matter content is generally higher than in winter months. This phenomenon is due to the blooming of phytoplankton or the relatively calm weather during summer months leading to the deposition of fine materials including organic matter. The increase of benthic primary production in summer months may lead also to this finding. The other possibility may be due to greater flux of organic matter from surface productive waters.

6.6. Bacterial Protein

It was also shown by Mattin (1992) that bacterial protein contributes (certain percentage) to the total amount of available protein. Mattin's data (the percentages of bacterial protein) are used to calculate bacterial protein of the present data as follows,

Table 6.2. Total protein, bacterial protein and bacterial abundance

Month (Year)	Total Protein (mg g ⁻¹ ds)	Bacterial Protein × 10 ⁴ (mg g ⁻¹ ds)	Bacterial Abundance × 10 ⁹ (g ⁻¹ ds)
June (1991)	1.27	29.51	0.84
July	1.31	29.53	0.84
August	1.61	29.27	0.84
September	1.27	15.60	0.45
October	0.98	11.51	0.33
November	0.78	6.72	0.19
December	1.08	14.28	0.41
January (1992)	1.02	5.31	0.15
February	1.24	9.28	0.27
March	1.30	14.40	0.41
April	1.22	23.92	0.68
May	2.10	29.42	0.84
June	1.99	46.38	1.33
July	2.42	54.45	1.56
August	1.97	35.83	1.02
September	1.02	12.53	0.36
October	1.06	12.50	0.36
November	0.86	7.43	0.21
December	1.57	20.67	0.59
January (1993)	0.93	4.84	0.14
February	0.83	6.24	0.18
March	0.95	10.58	0.30
April	1.10	21.53	0.62
May	2.31	32.32	0.92
June	1.70	39.57	1.13
July	1.97	44.43	1.27
August	1.98	36.11	1.03
September	1.85	22.81	0.65

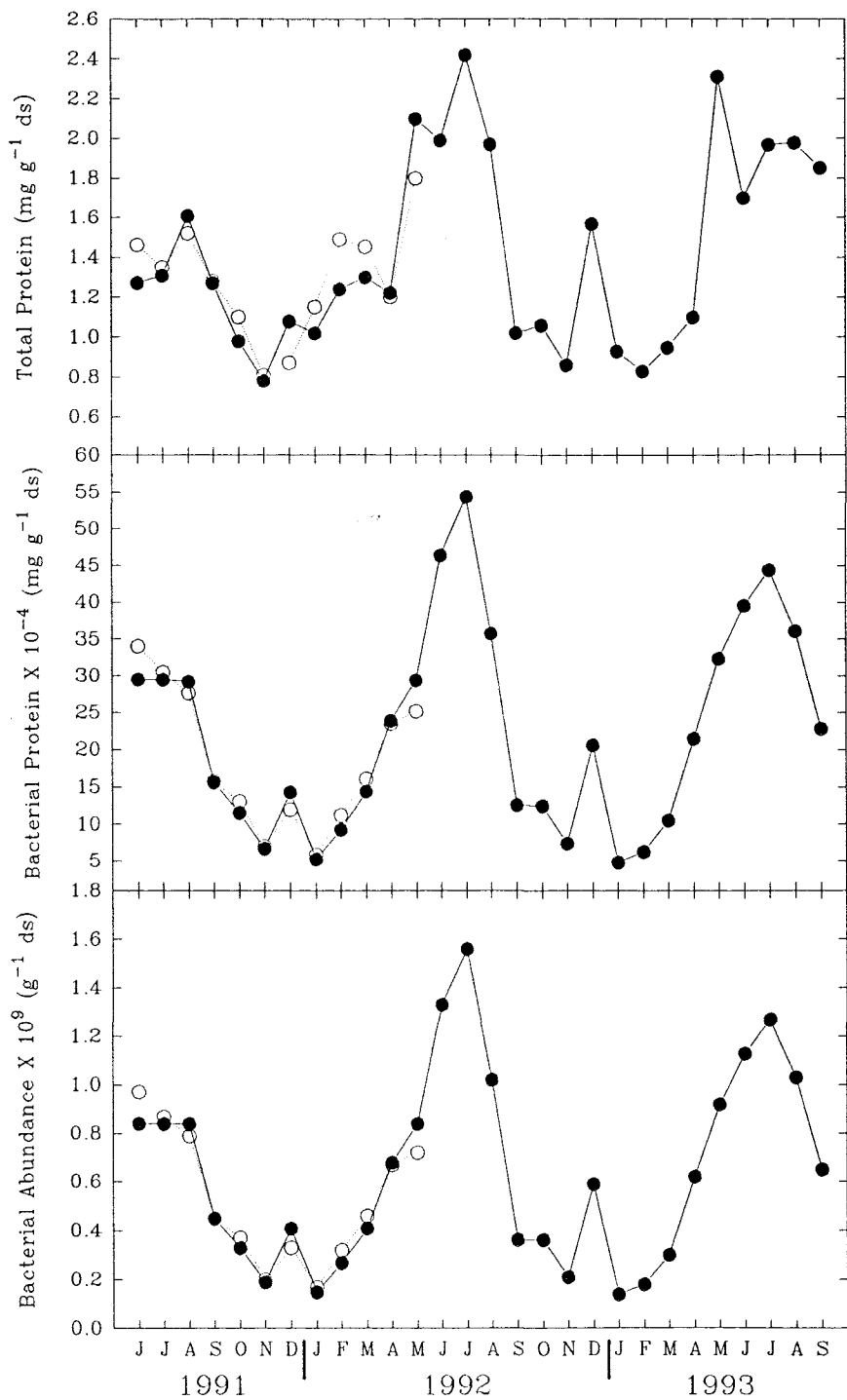


Figure 6.3. Long-term variation in total protein, bacterial protein and bacterial abundance. Dotted lines with hollow circles represent data from Mattin (1992)

$$BP = \frac{PBP}{100} \times TP \quad (6.1)$$

where BP is bacterial protein (mg g^{-1} dry sediment), PBP is percentage bacterial protein, and TP is total protein (mg g^{-1} dry sediment). The calculated bacterial protein of the present study is shown in Table 6.2 and in Figure 6.3. From this Figure, it appears that bacterial protein shows a similar seasonal pattern as total protein. This can be understood because bacterial protein is estimated from total protein and is a constituent of total protein.

6.7. Bacterial Abundance

Assuming that bacteria contain 1.4×10^{-14} g carbon per cell (Mayer *et al*, 1986) with a carbon to nitrogen ratio of 4 : 1 and all nitrogen is assumed to be protein, the bacterial abundance can consequently be estimated as follows,

$$BA = \frac{\frac{BP}{1000}}{0.25 \times 1.4 \times 10^{-14}} \quad (6.2)$$

where BA is bacterial abundance (g^{-1} dry sediment) and BP is bacterial protein (mg g^{-1} dry sediment). The estimated bacterial abundance of the present study is shown in Table 6.2 and on Figure 6.3. This Figure discloses also that bacterial abundance reveals a relatively similar pattern as those exhibited by total protein and bacterial protein.

6.8. Phytoplankton Abundance

Since phytoplankton abundance was not investigated in the present study, secondary data are used. This was obtained from a study performed by Kifle (1992) on phytoplankton abundance at Calshot, Southampton Water, during 1988, which is close to Solent Breezes. The data can, therefore, be used as a representative illustration of phytoplankton abundance from the area of the

present study. For the illustration of seasonal phytoplankton abundance, data from Kifle (1992) are used in accordance with the needs of the present study. The estimated phytoplankton abundance is shown in Table 6.3 and on Figure 6.4. Low phytoplankton abundance occurs in January and February, followed by an increase in March and reaches its peak (blooming) in April. Abundance then decreases gradually towards the end of the year. The lowest numbers of phytoplankton occur in January ($165 \text{ cells ml}^{-1}$) and the highest in April ($1636 \text{ cells ml}^{-1}$). This suggests that at Solent Breezes, there is only one main bloom period during the year. The winter period is characterised by a sparse population of phytoplankton.

6.9. Diatom Relative Abundance

For data on diatom abundance, the present study also uses data from Kifle (1992). The estimated percentage diatoms abundance against the total phytoplankton are shown in Table 6.3 and on Figure 6.4. Diatom abundance shows similar patterns to the abundance of total phytoplankton. The abundance of diatoms is relatively high during winter months, increases to a peak in April, then decreases gradually to the end of the year. The highest percentage of diatoms was recorded in April with 65.84 % and the lowest percentage was recorded in October with 0.61 % of total phytoplankton.

6.10. Community Structures

The total number of individuals of benthic macrofauna from Solent Breezes monthly sampling are presented in Table 6.4. It seems from Table 6.4 that benthic macrofauna at Solent Breezes are composed of a few dominant species that existed in relatively large numbers throughout the period of investigation, fluctuating seasonally, with some rarer species occurring sporadically. Twenty-nine species were identified during the period of study. The

Table 6.3. Phytoplankton and diatom abundance (data from Kifle, 1992)

Month	Phytoplankton (cell ml ⁻¹)	Diatoms (%)*
January 1988	165	50.35
February 1988	210	48.76
March 1988	413	49.68
April 1988	1636	65.84
May 1988	1018	34.58
June 1988	914	20.33
July 1988	628	14.89
August 1988	656	7.65
September 1988	604	4.22
October 1988	480	0.61
November 1988	616	8.05
December 1988	597	3.61

* Diatoms as percentage of total phytoplankton

existing species were dominated by *Euclymene oerstedii*, *Exogone hebes*, *Aricidea minuta*, *Pygospio elegans*, *Scoloplos armiger*, *Nephrys hombergii*, *Tanaissus lilljelborgi*, and *Syllis sp.*

6.10.1. Dominant Species

The seasonal variability of the eight most dominant species are displayed diagrammatically in Figures 6.5 and 6.6, in descending order of percentage contribution to the total macrofaunal abundance. In this study, those species that contribute more than 3 % to the total individuals of macrobenthic organisms are referred to as dominant species.

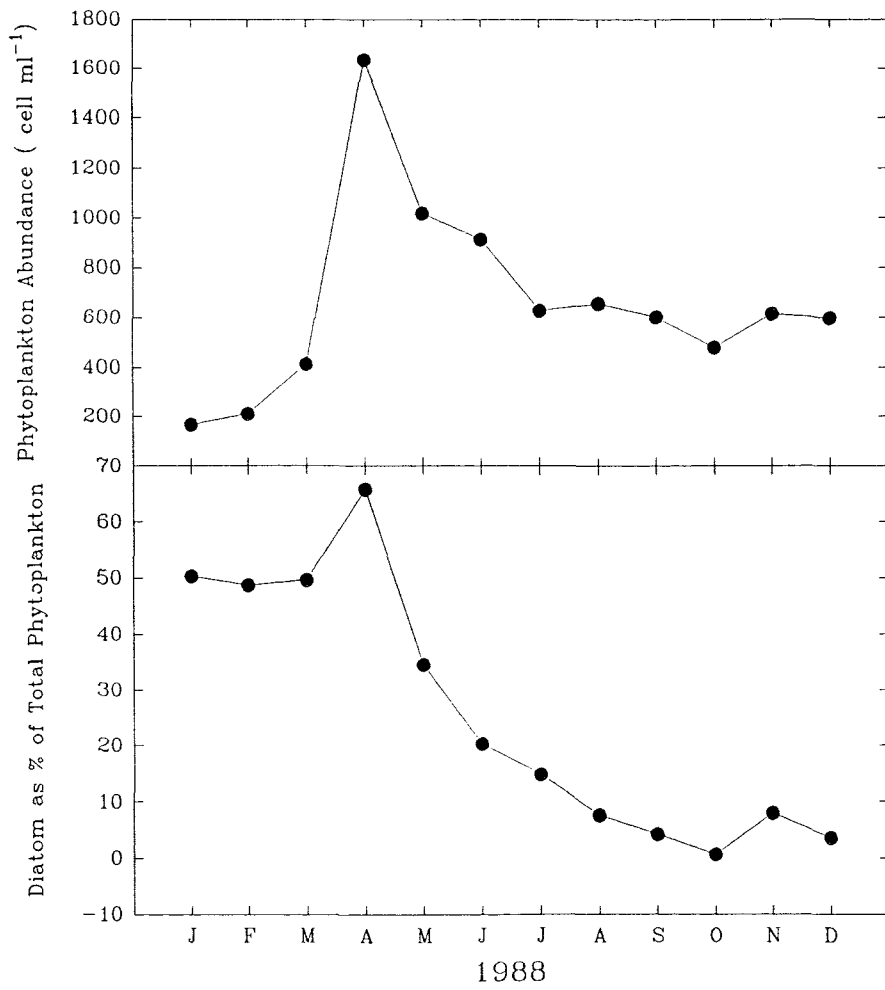


Figure 6.4. Annual variation in phytoplankton abundance and diatom as percentage of total phytoplankton (data from Kifle, 1992)

Table 6.4. Species abundance of benthic macrofauna at Solent Breezes per 100 cm² from October 1991 to March 1992

Species	Oct 1991	Nov 1991	Dec 1991	Jan 1992	Feb 1992	March 1992
<i>Anaitides maculata</i>	1.77	0.59			0.12	0.12
<i>Eumida sp.</i>						
<i>Syllis sp.</i>		0.12				
<i>Exogone hebes</i>	3.42	1.30	0.12		0.35	2.24
<i>Nereis juvenile</i>			0.47			
<i>Nephtys hombergii</i>	0.59	1.77	1.06	0.94	1.89	0.59
<i>Scoloplos armiger</i>	0.71	0.94	5.07	0.71	0.24	1.06
<i>Pygospio elegans</i>						
<i>Euclymene oerstedi</i>	3.30	2.95	1.89	2.36	2.95	2.24
<i>Pomatocerus triqueter</i>					0.24	0.12
<i>Aricidea minuta</i>	3.07	3.89	2.12		0.47	0.83
<i>Oligochaeta</i>	1.30	0.12	0.24		0.24	0.12
<i>Ampelisca brevicornis</i>	0.83	0.35	0.12		0.24	
<i>Atylus swammerdami</i>	0.24					
<i>Gammarus locusta</i>				0.24		0.12
<i>Harpacticoid (meiofauna)</i>						
<i>Microprotopus maculatus</i>						
<i>Pontocrates altamarinus</i>						
<i>Glycera tridactyla</i>			0.12			
<i>Dexamine spinosa</i>						0.12
<i>Megalopa larva (crab)</i>						
<i>Urothoe poseidonis</i>		1.12	0.12		0.12	
<i>Bathyporeia sarsi</i>			0.12		0.12	0.35
<i>Microdeutopus sp.</i>	2.12	0.83	0.35			
<i>Corophium arenarium</i>					0.35	0.47
<i>Tanaissus lilljeborgi</i>			0.59			0.71
<i>Bodotria pulchella</i>				0.24		
<i>Crangon crangon</i>	0.12		0.12			
<i>Carcinus maenas</i>		0.24	0.12			

Table 6.4. Continued, from April 1992 to September 1992

Species	April 1992	May 1992	June 1992	July 1992	August 1992	Sept 1992
<i>Anaitides maculata</i>	0.35	0.12			0.13	0.25
<i>Eumida sp.</i>						
<i>Syllis sp.</i>				0.15		
<i>Exogone hebes</i>	1.65	4.48	1.77	5.23	5.81	6.82
<i>Nereis juvenile</i>	0.24			0.15		0.13
<i>Nephtys hombergii</i>	1.30	0.94	1.06	0.92	0.88	0.51
<i>Scoloplos armiger</i>	0.71	0.35	5.07	1.08	1.01	0.38
<i>Pygospio elegans</i>				0.15		
<i>Euclymene oerstedi</i>	3.89	3.66	2.83	3.85	4.43	5.31
<i>Pomatocerus triquester</i>						
<i>Aricidea minuta</i>	0.94	1.89	1.18	2.15	2.15	2.40
<i>Oligochaeta</i>	0.47				3.03	1.39
<i>Ampelisca brevicornis</i>					0.13	
<i>Atylus swammerdami</i>				0.31		
<i>Gammarus locusta</i>	0.24		0.47		0.13	
<i>Harpacticoid (meiofauna)</i>	0.71	0.12				
<i>Microprotopus maculatus</i>		0.12	1.06	1.85	0.51	
<i>Pontocrates altamarinus</i>						
<i>Glycera tridactyla</i>						
<i>Dexamine spinosa</i>						
Megalopa larva (crab)						
<i>Urothoe poseidonis</i>	0.24		0.12			
<i>Bathyporeia sarsi</i>	0.94	0.24	0.24	0.15		
<i>Microdeutopus sp.</i>					1.90	0.13
<i>Corophium arenarium</i>	0.35					0.38
<i>Tanaissus lilljeborgi</i>	1.06	3.19	1.53	0.62	0.63	
<i>Bodotria pulchella</i>	0.24				0.13	0.13
<i>Crangon crangon</i>				0.46		
<i>Carcinus maenas</i>	0.12			0.31	0.13	

Table 6.4. Continued, from October 1992 to March 1993

Species	Oct 1992	Nov 1992	Dec 1992	Jan 1993	Feb 1993	March 1993
<i>Anaitides maculata</i>		0.18				
<i>Eumida sp.</i>						
<i>Syllis sp.</i>		0.72	2.90	0.38	0.54	3.32
<i>Exogone hebes</i>	6.32	2.17	2.68	1.90	2.71	6.16
<i>Nereis juvenile</i>	0.51					0.95
<i>Nephtys hombergii</i>	1.14	0.54	0.45	2.65	0.90	1.18
<i>Scoloplos armiger</i>	0.51	1.44	0.89	0.38	0.36	0.47
<i>Pygospio elegans</i>					2.17	8.29
<i>Euclymene oerstedi</i>	4.67	4.15	4.01	6.44	5.23	5.69
<i>Pomatocerus triqueter</i>						
<i>Aricidea minuta</i>	1.26	0.90	2.45	1.14	0.54	3.32
<i>Oligochaeta</i>			0.22			
<i>Ampelisca brevicornis</i>						
<i>Atylus swammerdami</i>	0.38				0.36	0.47
<i>Gammarus locusta</i>		0.18		0.38		
<i>Harpacticoid (meiofauna)</i>						
<i>Microprotopus maculatus</i>	1.39					
<i>Pontocrates altamarinus</i>						0.24
<i>Glycera tridactyla</i>						
<i>Dexamine spinosa</i>						
Megalopa larva (crab)						
<i>Urothoe poseidonis</i>					0.36	
<i>Bathyporeia sarsi</i>					0.36	
<i>Microdeutopus sp.</i>						
<i>Corophium arenarium</i>						0.24
<i>Tanaissus lilljeborgi</i>	0.13	0.54				1.90
<i>Bodotria pulchella</i>	0.25	0.36	0.22		0.90	
<i>Crangon crangon</i>						
<i>Carcinus maenas</i>	0.13		0.22			

Table 6.4. Continued, from April 1993 to September 1993

Species	April 1993	May 1993	June 1993	July 1993	August 1993	Sept 1993
<i>Anaitides maculata</i>	0.13			0.51		0.19
<i>Eumida</i> sp.	0.38		0.25			0.38
<i>Syllis</i> sp.	2.91	1.21				
<i>Exogone hebes</i>	5.18	2.88	1.77	3.28	3.10	2.65
<i>Nereis</i> juvenile		1.36	1.01		0.17	
<i>Nephtys hombergii</i>	1.26	0.61	0.25	0.76	0.86	
<i>Scoloplos armiger</i>	0.63	0.76	0.51	2.53	1.38	0.57
<i>Pygospio elegans</i>	6.19	3.34	4.55	2.53	2.41	2.84
<i>Euclymene oerstedii</i>	4.30	4.40	6.32	5.05	4.13	4.17
<i>Pomatocerus triquester</i>						
<i>Aricidea minuta</i>	2.78	2.27	3.28	1.26	1.21	1.52
<i>Oligochaeta</i>			0.25		0.17	
<i>Ampelisca brevicornis</i>						
<i>Atylus swammerdami</i>	0.13	0.30		0.76	0.86	0.38
<i>Gammarus locusta</i>				1.26	0.52	
<i>Harpacticoid</i> (meiofauna)	0.25	0.30				
<i>Microprotopus maculatus</i>						1.52
<i>Pontocrates altamarinus</i>				0.25		
<i>Glycera tridactyla</i>			0.25			
<i>Dexamine spinosa</i>						
<i>Megalopa</i> larva (crab)			0.25			
<i>Urothoe poseidonis</i>		0.15	0.25			
<i>Bathyporeia sarsi</i>	0.38	0.45	0.51		0.17	
<i>Microdeutopus</i> sp.						
<i>Corophium arenarium</i>				0.51	1.21	0.57
<i>Tanaissus lilljeborgi</i>	2.53	0.30	0.25			
<i>Bodotria pulchella</i>	1.39					
<i>Crangon crangon</i>				0.25	0.17	
<i>Carcinus maenas</i>				0.25		

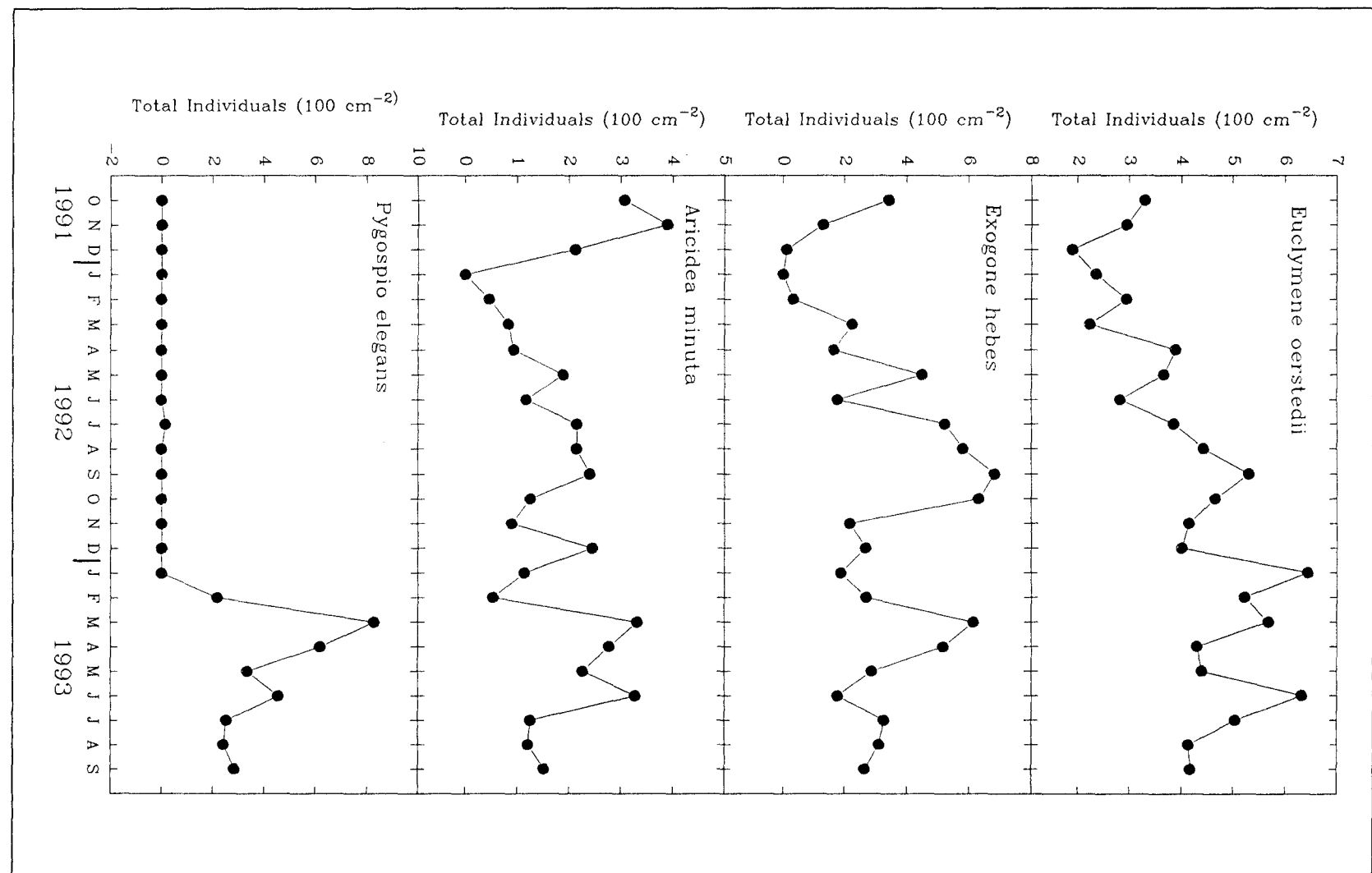


Figure 6.5. Long-term (seasonal) variability of *Euchymene oerstedii*, *Exogone hebes*, *Aricidea minuta* and *Pygospio elegans*

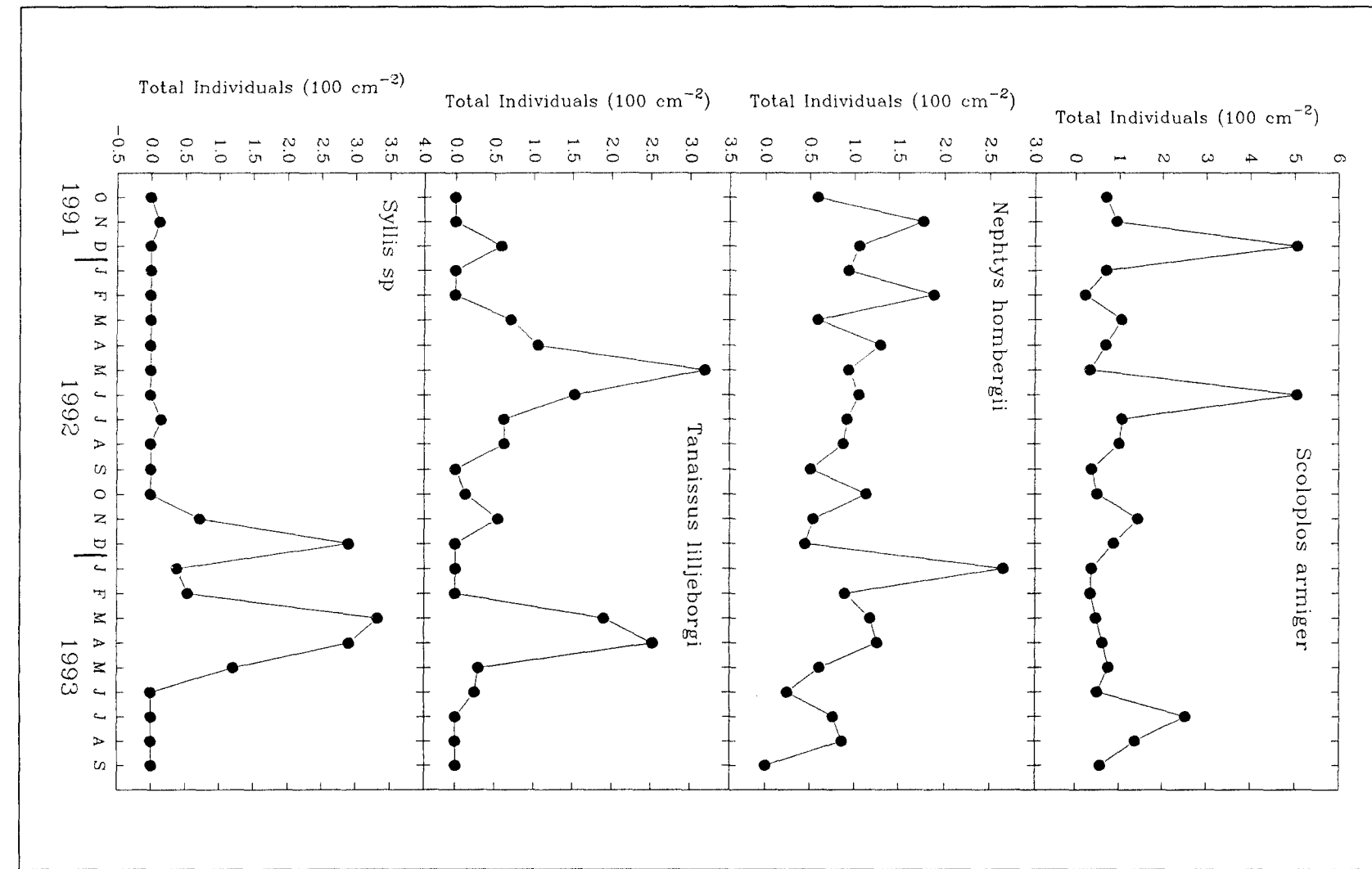


Figure 6.6. Long-term (seasonal) variability of *Scoloplos armiger*, *Nephtys hombergii*, *Tanaissus lilljeborgii* and *Syllis sp*

(a) *Euclymene oerstedii* (Claparede, 1863)

Euclymene oerstedii contributes 25.6 % to the total individuals of macrobenthic organisms over the sampling period. The total number of individuals of this species decreased from October 1991 to December 1991. This is followed by an increase towards the summer with some fluctuations, reaching its peak in September 1992. The population then decreased towards spring and increased again, attaining its peak in July 1993, then decreasing towards the end of the sampling period.

(b) *Exogone hebes* (Webster and Benedict, 1884)

Exogone hebes contributes 19.3 % to the total individuals of macrobenthic organisms. Figure 6.1 shows that the total individuals of this species decreased towards January 1992, increased in summer 1992, followed by a decrease in Winter 1992/93, increases in May, then decreases towards summer.

(c) *Aricidea minuta* Southward, 1956

Aricidea minuta contributes 11.2 % to the total individuals of macrobenthic organisms. The population of this species is high in October and November 1991, decreased in January 1992, followed by a gradual increase towards summer with some fluctuations.

(d) *Pygospio elegans* Claparede, 1863

Pygospio elegans contributes 8.5 % to the total individuals of macrobenthic organisms. It is the most versatile spionid studied to date (Fauchald and Jumars, 1979). Spionids are usually tubicolous worms found in high frequency and in abundance on all substrates in shallow water. They can leave their tubes and build new tubes when necessary; they can filter by building a mucus net within their tubes, can feed either on plankton with the help of their

palps, or on surface deposits. In principle, it is a surface deposit-feeder with good discriminatory powers to select particles both on size and on content. They are discretely motile; and therefore, they can move around as adults but do not do so while feeding.

The population of this species shows different patterns; it was absent during the first year of study. The population started to recruit in January 1993, followed by a sudden increase to a peak in March 1993, then decreased gradually towards summer.

(e) *Scoloplos armiger* (O.F. Müller, 1776)

Scoloplos armiger contributes 7.2 % to the total individuals of macrobenthic organisms. The individuals of this species can grow up to 120 mm in length with up to 200 or more segments. They are widely distributed in north-west Europe and around Britain on the lower shore and in the sublittoral, burrowing in muddy sand (Fish and Fish, 1989). They are able to tolerate reduced salinity and are found in the lower reaches of estuaries where they feed on organic detritus. The sexes are separate and when ripe, males are whitish in colour and the females are brownish. On the south coast of England, breeding occurs in early spring. There is no pelagic state and the larvae are benthic. They first breed after two years old and live for about four years.

This species showed a relatively stable population during the two year sampling period, except for December 1991, July 1992 and July 1993, when higher number of individuals were recorded.

(f) *Nephtys hombergii* (Savigny, 1818)

Nephtys hombergii contributes 6.0 % to the total individuals of macrobenthic organisms. Body length and segment number vary, often reaching about 200 mm in length and up to 200 segments. This species is widely distributed in north-west Europe and is found burrowing in sand, muddy-sand, mud and gravel in intertidal and sublittoral waters (Fish and Fish, 1989). It is

carnivorous, feeding on molluscs, crustaceans and other polychaetes. The sexes are separate and individuals breed several times over a number of years. It first matures at two or three years of age and breeds during April and May. The worms remain in the sediment during spawning, with eggs and sperm released onto the surface of the sediment during low tide. Fertilisation occurs when the gametes are mixed by the incoming tides. The larvae are pelagic and the adult can live up to six years.

The population of this species shows a stable pattern like *Scoloplos armiger*, however, it has higher abundance. Higher densities were recorded during November 1991, February 1992 and January 1993. The general trend is a declining population density from October 1991 towards the end of the investigation.

(g) *Tanaissus lilljelborgi* Stebbing, 1891

Tanaissus lilljelborgi contributes 3.6 % to the total individuals of macrobenthic organisms. This species was absent during the first year of study, recruited in May 1992, increased and reached a peak in May, then decreased subsequently towards winter 1993. The species occurred again in March 1993 and reached its highest density in April 1993, followed by a decline.

(h) *Syllis sp* Savigny, 1818

Syllis sp contributes 3.2 % to the total individuals of macrobenthic organisms. They are carnivores feeding on hydroids, bryozoans and other invertebrates (Fauchald and Jumars, 1979). Some species may be tubicolous but most are free living and non-tubicolous. Certain species are highly selective deposit-feeders, feeding on the surface of the mud. The species which inhabit muddy bottom, usually feed on diatoms.

This species shows a similar pattern to *Pygospio elegans*. It was absent during the first year of study with recruitment starting in October 1992 and reaching its highest density in December 1992. The population then declined in

January and February 1993, increased in March and April 1993, followed by a steep decrease and disappears in June 1993.

6.10.2. Seasonal Grouping

In addition to comparing the seasonal variability of individual species, the entire species assemblages can be compared on a monthly basis. For this purpose, the Bray-Curtis similarity classification is used as described in Section 4.5.2. The results are shown in the form of a dendrogram as Figure 6.7.

The dendrogram appears to divide the monthly samples into 5 main clusters (at around 63 % similarities) with the characteristics outlined below.

Cluster 1

This cluster consist of only one sample containing the dominant species *Euclymene oerstedii*; this was collected in January 1992. The mean tube density of *Lanice conchilega* was 5.80 per 100 cm². The mean total species number was 3.67 per 100 cm²; whilst that of the mean total individuals was 4.67 per 100 cm². The mean Shannon-Wiener diversity index of the macrofauna was 1.27.

Cluster 2

This cluster consists of 8 samples which were collected from October 1991 to December 1991, February 1992 to April 1992, in August 1992 and September 1992. The dominant species in cluster 2 are *Scoloplos armiger*, *Euclymene oerstedii*, *Aricidea minuta* and *Exogone hebes*. The mean tube density of *Lanice conchilega* was 6.80 per 100 cm². The mean total species number was 9.23 per 100 cm², whilst that for the mean total individuals was 14.14 per 100 cm². The mean Shannon-Wiener diversity index for the macrofauna was 2.01.

Cluster 3

This cluster consists of 7 samples which were collected from May 1992 to July 1992, from October 1992 to January 1993. The dominant species in Cluster 3 consist of *Exogone hebes*, *Scoloplos armiger*, *Euclymene oerstedii*, and *Aricidea*

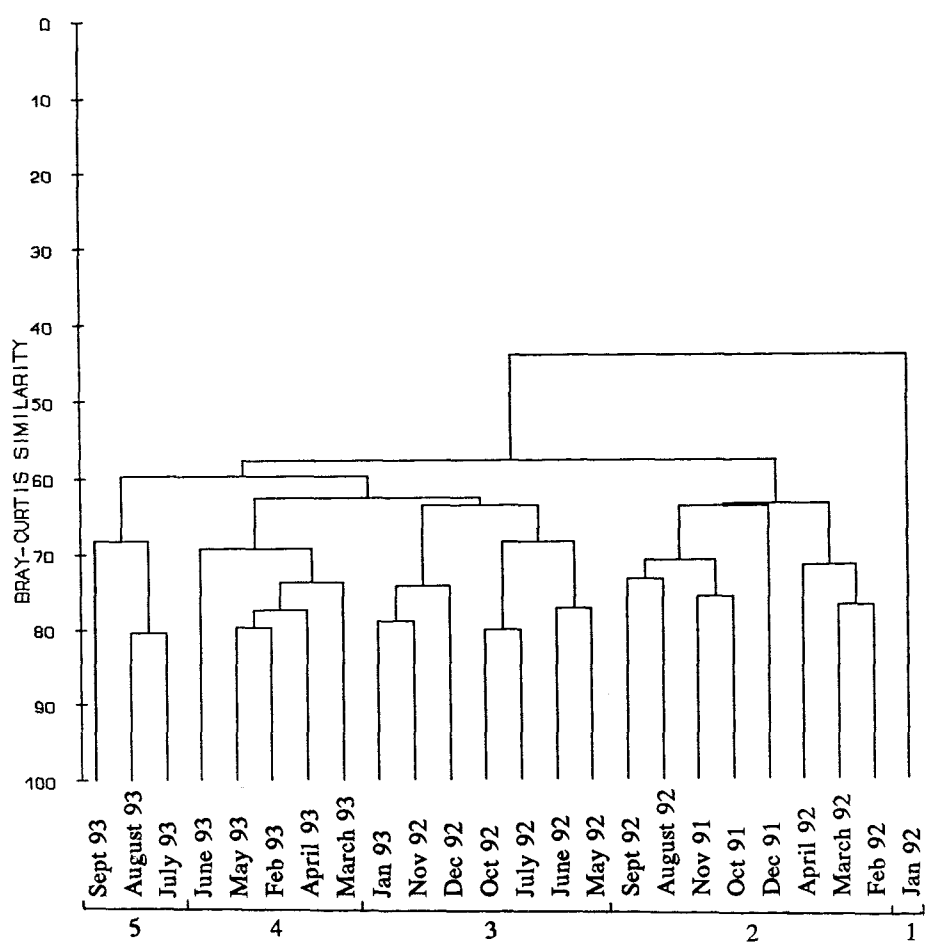


Figure 6.7. Dendrogram showing classification of monthly data of benthic macrofauna from Solent Breezes, Southampton Water. Abundance data are root-root transformed prior to the Bray-Curtis measure

minuta. The mean tube density of *Lanice conchilega* was 5.61 per 100 cm². The mean total species number was 9.70 per 100 cm², whilst that of the mean total individuals was 14.67 per 100 cm². The mean Shannon-Wiener diversity index for the macrofauna was 1.80.

Cluster 4

This cluster consists of 5 samples which were collected from February 1993 to June 1993. The dominant species in Cluster 4 were *Pygospio elegans*, *Exogone hebes*, *Euclymene oerstedi*, *Aricidea minuta*, *Syllis sp*, and *Tanaissus lilljeborgi*. The average tube density of *Lanice conchilega* was 4.61 per 100 cm². The mean total species number was 13.31 per 100 cm², whilst that for the mean total individuals was 22.67 per 100 cm². The mean Shannon-Wiener diversity index for the macrofauna was 2.05.

Cluster 5

This cluster consists of 3 samples which were collected in July 1993 to September 1993. The dominant species in Cluster 5 were *Euclymene oerstedi*, *Exogone hebes*, *Pygospio elegans*, and *Scoloplos armiger*. The mean tube density of *Lanice conchilega* was 4.24 per 100 cm². The mean total species number was 11.48 per 100 cm², whilst that of the mean total individuals was 17.00 per 100 cm². The mean Shannon-Wiener diversity index of the macrofauna was 2.09.

6.10.3. Diversity

The diversity of macrobenthic organisms is shown in Table 6.5 and on Figure 6.8. This Figure shows that diversity index remained relatively stable during the period of investigation with slight increase during the second year. Diversity varies throughout the study; the lowest diversity is 1.27 which occurs in January 1992 and the highest one is 2.38 which occurs in April 1992. It seems that diversity shows a slight seasonal pattern, being slightly lower in winter months than in summer months. The diversity index is higher from March to October, suggesting that conditions are more stable during these months. The

6.5. Diversity (Shannon and Weaver, 1963), richness (Margalef, 1958) and evenness (Pielou, 1966) of macrobenthic organisms from October 1991 to September 1993

Month (Year)	Diversity	Richness	Evenness
October (1991)	2.10	3.50	0.88
November	2.08	4.14	0.84
December	1.91	5.52	0.71
January (1992)	1.27	2.66	0.79
February	1.83	5.52	0.74
March	2.10	5.44	0.82
April	2.38	5.75	0.86
May	1.73	3.31	0.75
June	1.93	3.30	0.84
July	2.04	4.55	0.77
August	2.05	4.27	0.78
September	1.63	3.47	0.68
October	1.75	3.55	0.73
November	1.87	3.73	0.81
December	1.79	3.03	0.81
January (1993)	1.47	2.32	0.75
February	1.93	3.75	0.80
March	2.03	3.17	0.82
April	2.18	3.88	0.83
May	2.15	4.13	0.84
June	1.95	4.36	0.74
July	2.16	4.06	0.84
August	2.15	4.29	0.84
September	1.95	3.34	0.85

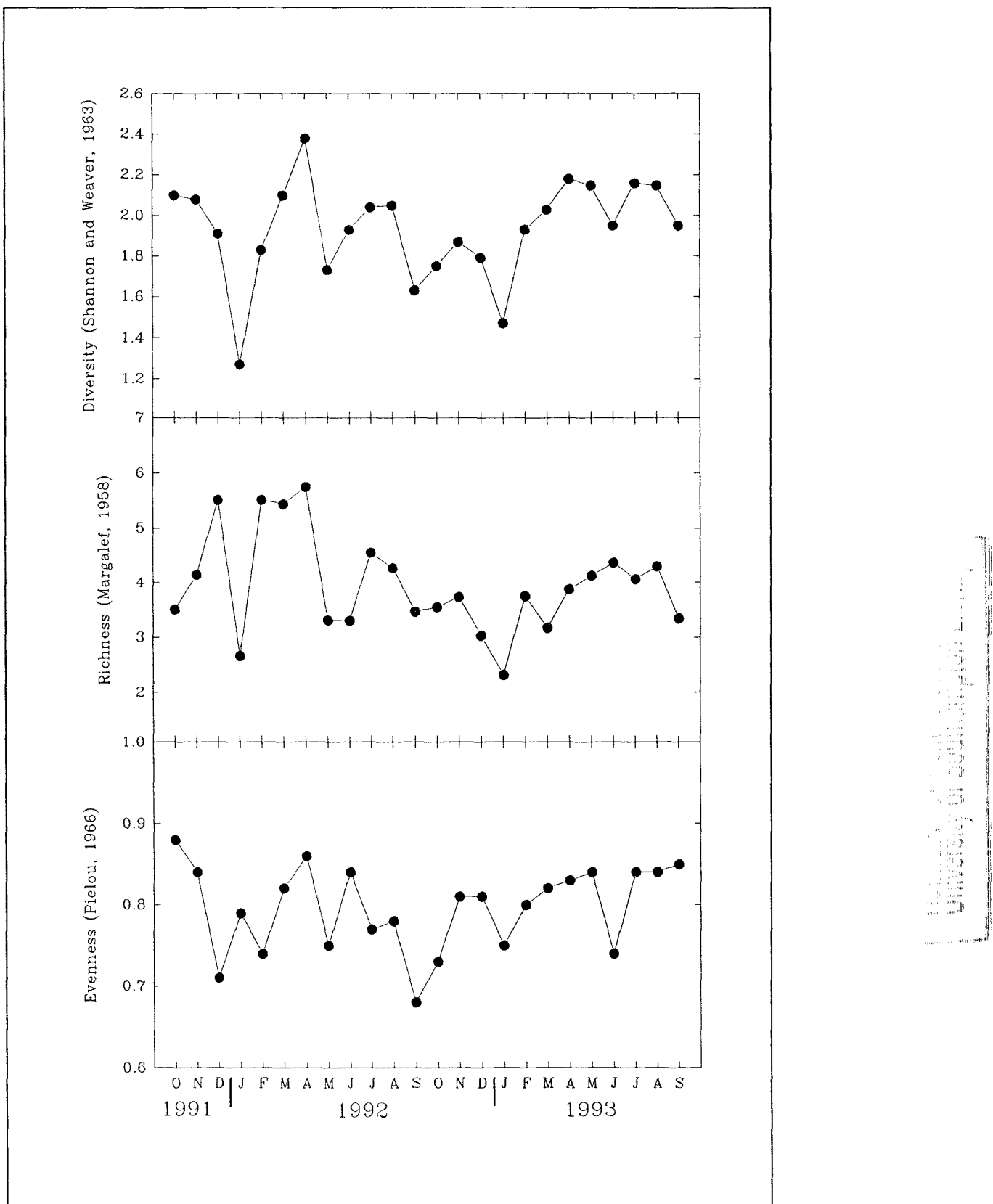


Figure 6.8. Long-term variation in diversity (Shannon and Weaver, 1963), richness (Margalef, 1958) and evenness (Pielou, 1966) of benthic macrofauna from Solent Breezes, Southampton Water

variability observed in the diversity index may be due to variability in the environmental parameters, as it was suggested by Sanders (1968) that diversity in intertidal shallower areas are much lower than the deep sea. This is because in intertidal waters, the fauna is subjected to environmental factors that fluctuate in an unpredictable manner. Many species, therefore, are not able to tolerate this fluctuation. Figure 6.8 shows also species richness and species evenness, which are components of the diversity index. In general, increase in the number of species will lead to an increase in diversity index. However, the diversity index will also increase as the proportion of individuals per species becomes more constant (Gray, 1981). Species richness fluctuated considerably and is slightly higher in the first than in the second year of the study. In consequence, the number of species identified in the second year is more constant than in the first year. It appears also that species evenness varied considerably in the first year which suggests that the proportion of individuals per species is less constant than in the second year. It can, therefore, be suggested that less disturbances occur in the second year than in the first year. Perhaps the most factors influencing these indices is the seasonal pattern of recruitment and mortality plus disturbance.

In order to identify the environmental parameters which may be responsible for community structure, the data on macrobenthic organisms were analysed using the Principal Components Analysis, as described in Section 4.5.2. The percentage variances of each Principal Component are presented in Table 6.6. From this table it seems that the first eight components account for 77.71 % of the variance. The principal components are then correlated with physical and sedimentological parameters under study using Spearman's Rank Correlation analysis. The values of p obtained from this correlation are presented in Table 6.7 and the Spearman's Rank Correlation Coefficient (ρ) in Table 6.8.

The parameters that correlate significantly as highlighted in Tables 6.7 and 6.8 are those that may have determined the existing patterns of macrobenthic organisms as described by the Principal Components Analysis.

There are six parameters revealing negative significant correlations with Principal Component 1: sediment sorting, organic matter content, protein, bacterial protein, bacterial abundance and silt/clay content. These parameters

Table 6.6. Percentage variance of each Principal Components
(Components accounting for 92 % of variance)

Component	Percent Variance	Cumulative Percent Variance
1	21.93	21.93
2	12.44	34.37
3	10.65	45.02
4	9.08	54.10
5	6.80	60.90
6	6.29	67.20
7	5.49	72.68
8	5.03	77.71
9	4.50	82.22
10	3.80	86.02
11	3.43	89.45
12	2.29	91.74

may be linked partially with each other; for instance, sediment sorting to some degree may link with organic matter content. The finer the sediment the more the total particle surface area which in turns leads to more surface for adsorbed organic and bacteria. The amount of organic matter content may link with protein content which subsequently may link with bacterial protein and bacterial abundance. The amount of organic matter content may also link with silt/clay content, where high content of silt/clay may automatically allow more organic matter to be buried. It can be inferred, therefore, that component 1 relates to the bioavailability of organic matter within the sediment, affecting structure of benthic

Table 6.7. Values of p for the correlations between the abundance of benthic macrofauna and other parameters (p < 0.05 is significant)

Parameters	Principal Components							
	1	2	3	4	5	6	7	8
Shear Strength	0.44	0.01	0.31	0.02	0.21	0.33	0.01	0.11
Shear Stress	0.44	0.01	0.31	0.02	0.21	0.33	0.01	0.11
Temperature	0.23	0.49	0.06	0.07	0.15	0.11	0.14	0.29
Salinity	0.40	0.22	0.01	0.02	0.33	0.28	0.10	0.23
Grain Size	0.14	0.12	0.29	0.29	0.16	0.18	0.34	0.31
Sediment Sorting	0.01	0.06	0.40	0.39	0.33	0.15	0.34	0.33
Sediment Skewness	0.32	0.29	0.02	0.25	0.20	0.34	0.24	0.15
Moisture Content	0.31	0.26	0.02	0.07	0.49	0.02	0.21	0.47
Low Water Height	0.34	0.17	0.23	0.11	0.38	0.08	0.41	0.03
Organic Content	0.04	0.26	0.27	0.12	0.47	0.21	0.23	0.47
Protein	0.01	0.46	0.46	0.12	0.38	0.06	0.09	0.36
Bacterial Protein	0.01	0.41	0.19	0.07	0.41	0.06	0.14	0.23
Bacterial Abund.	0.01	0.41	0.19	0.07	0.41	0.06	0.14	0.23
Silt/Clay Content	0.04	0.43	0.26	0.24	0.20	0.13	0.07	0.49
Tube Density	0.10	0.01	0.32	0.09	0.22	0.22	0.31	0.11
Air Temperature	0.11	0.42	0.08	0.01	0.16	0.19	0.10	0.21
Wind Speed	0.23	0.10	0.29	0.23	0.34	0.14	0.21	0.46
Rainfall	0.42	0.33	0.08	0.47	0.20	0.17	0.40	0.26

Table 6.8. Spearman Rank Correlation Coefficient (rho) with confidence level of 95 percent

Parameters	Principal Components							
	1	2	3	4	5	6	7	8
Shear Strength	0.03	-0.45	0.11	-0.43	-0.18	0.09	0.50	-0.26
Shear Stress	0.03	-0.45	0.10	-0.43	-0.18	0.09	.50	-0.26
Temperature	-0.16	0.01	-0.33	-0.30	0.22	0.26	0.23	0.18
Salinity	0.05	-0.16	-0.55	-0.42	-0.10	0.12	0.27	-0.16
Grain Size	-0.23	0.25	0.16	-0.12	0.21	0.20	-0.09	0.11
Sediment Sorting	-0.53	0.33	0.06	-0.06	-0.10	0.22	0.09	0.10
Sediment Skewness	0.10	-0.12	-0.41	0.15	-0.18	0.09	-0.15	-0.22
Moisture Content	-0.11	0.14	0.43	-0.31	0.01	-0.41	0.17	-0.02
Low Water Height	-0.09	-0.20	-0.16	-0.26	-0.06	0.29	0.05	0.40
Organic Matter Content	-0.35	0.13	0.13	-0.25	0.02	0.18	0.16	-0.02
Protein	-0.47	-0.02	-0.02	-0.25	0.07	0.33	0.28	0.08
Bacterial Protein	-0.53	-0.05	-0.19	-0.31	0.05	0.33	0.23	0.16
Bacterial Abund.	-0.53	-0.05	-0.19	-0.31	0.05	0.33	0.23	0.16
Silt/Clay Content	-0.37	0.04	-0.14	-0.15	0.18	0.24	0.31	-0.01
Tube Density	0.27	-0.57	-0.10	-0.28	0.17	0.16	0.11	-0.26
Air Temperature	-0.26	0.04	-0.30	-0.52	0.21	0.19	0.28	0.17
Wind Speed	-0.16	-0.27	0.12	-0.16	0.09	-0.23	0.17	0.02
Rainfall	-0.04	-0.10	-0.29	0.01	0.18	-0.20	-0.05	0.14

community.

There are three parameters which have negative correlations with Principal Component 2: shear strength, shear stress and tube density. Shear strength is closely associated with shear stress since in this study shear stress is estimated from shear strength. Shear strength may also be considered to be related with tube density, as increase in tube density leads to the increase of shear strength. Based on these considerations, it can be inferred that component 2 relates negatively to factors controlling sediment strength and compaction.

Three parameters correlate with Principal Component 3: salinity and sediment skewness correlate negatively and moisture content correlate positively. The most important parameters in this case are salinity and moisture content which may affect distribution of benthic macrofauna. Component 3 relates to seasonal variation in physical factors (salinity and moisture content).

Four parameters correlate negatively with Principal Component 4: shear strength, shear stress, salinity and air temperature. Again, shear strength and shear stress are linked with each other and may indirectly affect macrobenthic organisms. Temperature affects shear strength and stress. As temperature and salinity change seasonally, component 4 may relate to seasonal changes in macrofaunal community.

There is no parameter that seems to correlate with Principal Component 5, whilst there is only one parameter (moisture content) correlating negatively with Principal Component 6. Two parameters correlate positively with Principal Component 7: shear strength and shear stress, which are considered to indirectly affect the distribution of benthic macrofauna. For Principal Component 8, only one parameter (low water height) that demonstrates a positive correlation, which is quite unexpected in this study. This suggests that to a certain extent, low water level may determine the distribution of macrobenthic organisms as the increase in water height leads to the increase in the individuals abundance, suggesting a vertical (upward/downward) migration by elements of the fauna.

In accordance with the objectives of the Principal Components Analysis, where the first Principal Component accounts for the largest amount of the total variation in the data followed by the next Principal Components, the variables

represented by the first few Principal Components are responsible for the existing pattern of benthic macrofauna identified at Solent Breezes (at least, during the period of the investigation). Based upon the correlations established between the various principal components and parameters under study, the main parameters which affect the distribution of benthic macrofauna may be summarised as: (i) bioavailability of organic matter (protein, bacterial protein, organic matter, grain size characteristics); (ii) factors influencing sediment strength (shear strength of the sediment, tube density of *Lanice conchilega*); and (iii) seasonally varying physical factors (temperature, salinity and moisture content). The bioavailability of organic matter might be expected to determine the trophic structure of benthic communities. Total organic matter relates to the grain size of the surficial sediments. Tube density may affect benthic organisms by/through the following mechanisms: providing protection from predators; altering hydrodynamic conditions near the boundary layer, which may increase and/or reduce the success of recruitment; serving as a food source for the organisms, by trapping and depositing organic matter around their tubes; and adults *Lanice* may predate upon newly-settled larvae of benthic macrofauna.

CHAPTER 7

RESULTS: SEDIMENTOLOGICAL INVESTIGATIONS

7.1. Introduction

This Chapter describes, interprets and discusses the results obtained concerning the sedimentological, together with other related, investigations i.e. shear strength, (pore-water) temperature, (pore-water) salinity, grain size characteristics, moisture content, low water height, organic matter content, silt/clay content, and the tube densities. In addition to the measurements obtained *in situ*, secondary data sets have been obtained from the Meteorological Office (Bracknell); these include daily climatological observations of air temperature, wind speed, rainfall and (hours of) sunshine. Laboratory experiments are also described; these were undertaken on the effect of temperature on the shear strength of the sediments, using varying (ambient) temperatures and straw densities.

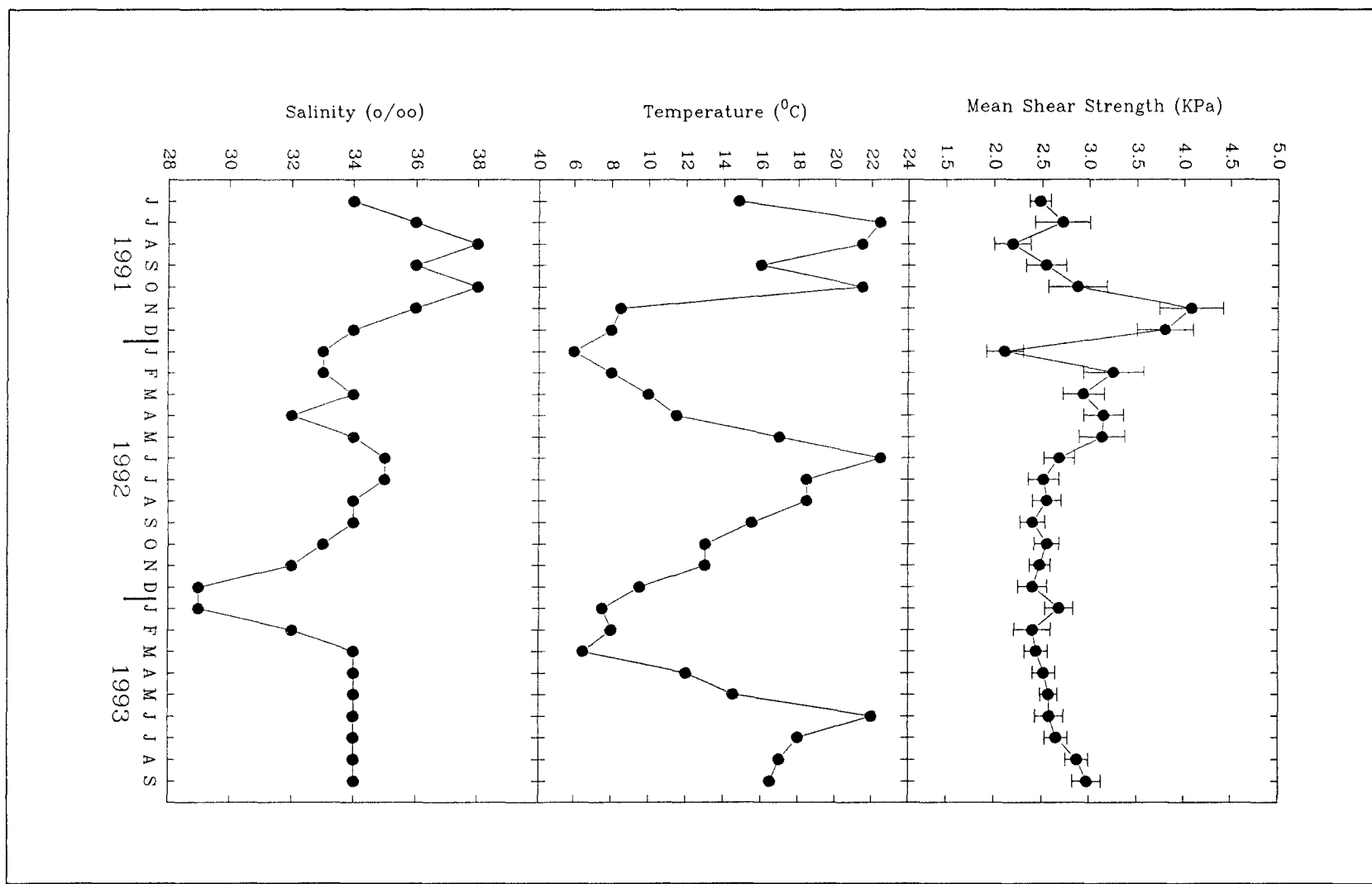
7.2. Shear Strength

The long-term results of the shear strength measurements are shown in Table 7.1 and on Figure 7.1, together with some of the accompanying environmental variables. Shear strength may be seen to fluctuate considerably, particularly, during the first part of the study period. Measured strengths are slightly higher in the first year of the investigation, particularly from the October to May, than in the second year. From the beginning of the second year, the shear strength remains relatively stable; this is followed by a slight increase in August and September 1993. The lowest shear strength (2.11 KPa) occurred in January 1992, whilst the highest (4.08 KPa) was in November 1991. These values coincide with low and high densities of *Lanice* tubes, respectively

Table 7.1 Mean shear strength, pore-water temperature and pore-water salinity

Month (Year)	Shear Strength (KPa)	Temperature (°C)	Salinity (‰)
June (1991)	2.48	14.8	34.0
July	2.72	22.5	36.0
August	2.19	21.5	38.0
September	2.54	16.0	36.0
October	2.87	21.5	38.0
November	4.08	8.5	36.0
December	3.80	8.0	34.0
January (1992)	2.11	6.0	33.0
February	3.25	8.0	33.0
March	2.94	10.0	34.0
April	3.15	11.5	32.0
May	3.13	17.0	34.0
June	2.68	22.5	35.0
July	2.52	18.5	35.0
August	2.55	18.5	34.0
September	2.40	15.5	34.0
October	2.55	13.0	33.0
November	2.48	13.0	32.0
December	2.40	9.5	29.0
January (1993)	2.68	7.5	29.0
February	2.40	8.0	32.0
March	2.44	6.5	34.0
April	2.52	12.0	34.0
May	2.57	14.5	34.0
June	2.58	22.0	34.0
July	2.65	18.0	34.0
August	2.87	17.0	34.0
September	2.97	16.5	34.0

Figure 7.1. Long-term measurements of mean shear strength, pore-water temperature and pore-water salinity (Y error bars represent standard errors)



recorded during those months (see Section 6.2); this suggests that tube densities may be responsible for the changes in shear strength. Such an interpretation is in agreement with that revealed by previous studies, which have demonstrated that stable beds are associated with the presence of animal tubes and sea grasses (Fager, 1964; Mills, 1967; Neuman *et al.*, 1970; Young and Rhoads, 1971; Fonseca and Fisher, 1986).

7.3. Pore-Water Temperature

Pore-water temperatures measured during the period of study are shown in Table 7.1 and on Figure 7.1. The measurements show a seasonal pattern, with high temperatures during the summer months and low temperatures during winter. This pattern is identical to those shown by mean daily air temperature and mean daily sunshine (see later, Figure 7.7). This relationship suggests that pore-water temperature is affected mainly by (daily) air temperature and the amount of sunshine. The lowest pore-water temperature (6°C) was recorded in January 1992, whilst the highest (22.5°C) was recorded in July 1991 and June 1992.

7.4. Pore-Water Salinity

The results of pore-water salinity measurements are shown, once again, in Table 7.1 and on Figure 7.1. The data reveal that salinity does not follow the same seasonal patterns as shown by temperature. Thus *in situ* (pore-water) salinity does not depend only on ambient temperatures, but may depend upon other factors such as rainfall and/or freshwater input and localised wind conditions. The lowest recorded salinity (29‰) occurred in December 1992 and January 1993, whilst the highest (38‰) was in August 1991 and October 1991. The salinities recorded in August and October 1991 appear to be particularly high for estuarine waters such as Southampton Water. These extremes may be

due to the combined effect of extended periods of sunshine and high wind speeds during the days of the sampling.

7.5. Grain Size Analyses

7.5.1. Frequency Distributions - Histograms

The grain size data are presented initially in terms of histograms (cf McManus, 1988). The number of columns selected for display depends generally upon the number of scales selected during the grain size determination and on the grain size spread of the sample (Buller and MacManus, 1979). In this study, the grain size classes adopted were at 0.5 Φ intervals, from 0 Φ to 10 Φ . The results are presented in Table 7.2 and on Figures 7.2(a) to 7.2(n). All the samples show a unimodal distribution within the very fine-grained sand size range. The highest weight frequency within all of the samples occur at 2.5 Φ . Such a consistency in the grain size patterns throughout all the samples may reflect: (i) percentage contained the continuity of supply of fine-grained materials; and/or (ii) relatively stable hydrodynamic conditions at Solent Breezes.

7.5.2. Statistical Parameters of Grain Size

Since the data presented previously in graphical form are limited in terms of intercomparisons, simple statistical techniques are used now to characterise the grain size distributions (McManus, 1988). The two principal forms of analysis used normally are: (a) graphical methods, where values derived directly from the plotted cumulative frequency curves are entered into established formulae; and (b) moment methods, where the characteristics of sample grains are used in the computation. The results obtained define the position of the size distribution plot,

Table 7.2 Grain size distribution of surficial sediment samples for size range from 0.00 Φ to 3.00 Φ from June 1991 to September 1993

Month (Year)	Φ						
	0.00	0.50	1.00	1.50	2.00	2.50	3.00
June (1991)	0.05	0.11	0.72	4.15	20.56	43.47	23.59
July	0.03	0.07	0.65	3.79	20.39	44.86	23.74
August	0.02	0.04	0.67	4.10	20.73	42.13	22.05
September	0.01	0.02	0.56	3.42	18.24	39.97	24.58
October	0.01	0.03	0.60	3.65	19.79	43.07	25.74
November	0.03	0.06	0.72	4.28	21.35	44.86	22.95
December	0.02	0.05	0.59	3.53	19.20	45.17	25.79
January (1992)	0.01	0.03	0.44	2.68	14.64	38.39	30.74
February	0.07	0.16	0.81	4.50	19.46	39.23	26.53
March	0.01	0.03	0.37	2.19	12.39	39.05	34.07
April	0.03	0.06	0.65	3.84	16.87	38.36	28.24
May	0.02	0.03	0.45	2.68	14.95	40.01	31.33
June	0.01	0.02	0.42	2.59	13.63	38.66	31.54
July	0.02	0.04	0.48	2.87	14.76	38.23	30.65
August	0.02	0.04	0.41	2.42	12.79	35.96	33.35
September	0.01	0.03	0.37	2.23	12.87	37.49	34.38
October	0.01	0.02	0.35	2.10	12.65	37.98	32.84
November	0.01	0.03	0.40	2.43	13.23	37.58	33.18
December	0.02	0.03	0.42	2.52	14.96	40.00	31.75
January (1993)	0.02	0.05	0.56	3.35	17.24	40.64	28.15
February	0.03	0.06	0.47	2.73	14.42	38.55	32.10
March	0.01	0.03	0.50	3.01	15.76	41.29	29.66
April	0.02	0.04	0.46	2.72	15.33	41.48	30.54
May	0.02	0.04	0.36	2.15	15.09	44.36	26.96
June	0.02	0.04	0.46	2.79	15.91	41.80	28.65
July	0.01	0.03	0.44	2.67	14.65	39.76	30.97
August	0.01	0.03	0.40	2.43	14.37	38.58	29.80
September	0.01	0.02	0.72	4.44	23.73	42.73	19.36

Table 7.2. Continued, for size range from 3.50 Φ to 6.50 Φ from June 1991 to September 1993

Month	Φ						
	3.50	4.00	4.50	5.00	5.50	6.00	6.50
June (1991)	3.37	1.38	1.13	0.02	0.02	0.04	0.51
July	3.39	1.66	0.12	0.03	0.04	0.03	0.28
August	4.17	2.06	0.16	0.16	0.21	0.14	0.85
September	5.20	1.80	0.14	0.31	0.36	0.29	1.55
October	3.88	1.31	0.09	0.01	0.01	0.02	0.32
November	2.73	0.95	0.09	0.01	0.01	0.03	0.40
December	2.49	0.90	0.11	0.02	0.02	0.04	0.44
January (1992)	7.03	1.98	0.18	0.07	0.11	0.16	0.90
February	6.24	1.61	0.13	0.05	0.16	0.03	0.26
March	7.16	1.99	0.17	0.03	0.04	0.06	0.56
April	7.07	1.99	0.13	0.03	0.03	0.06	0.60
May	6.12	1.64	0.15	0.03	0.03	0.06	0.57
June	6.82	2.05	0.20	0.07	0.12	0.17	0.95
July	7.70	2.29	0.30	0.15	0.13	0.10	0.59
August	7.99	2.81	0.38	0.10	0.14	0.13	0.85
September	7.71	2.37	0.25	0.04	0.05	0.05	0.49
October	7.83	2.21	0.25	0.08	0.13	0.16	0.87
November	7.92	2.17	0.15	0.02	0.03	0.06	0.63
December	6.06	1.61	0.13	0.02	0.03	0.05	0.54
January (1993)	6.10	1.65	0.11	0.02	0.02	0.04	0.46
February	7.08	2.11	0.23	0.04	0.06	0.07	0.50
March	5.16	1.60	0.15	0.02	0.02	0.05	0.60
April	4.82	1.58	0.19	0.02	0.02	0.06	0.60
May	3.84	1.79	0.26	0.22	0.33	0.29	1.37
June	5.22	1.90	0.15	0.02	0.03	0.08	0.69
July	5.95	1.95	0.30	0.07	0.09	0.12	0.75
August	7.32	2.73	0.25	0.07	0.10	0.16	0.96
September	4.17	1.00	0.03	0.04	0.04	0.10	0.85

Table 7.2. Continued, for size range from 7.00 Φ to 10.00 Φ from June 1991 to September 1993

Month	Φ						
	7.00	7.50	8.00	8.50	9.00	9.50	10.00
June (1991)	0.62	0.44	0.31	0.22	0.16	0.11	0.08
July	0.31	0.22	0.16	0.11	0.08	0.06	0.04
August	0.82	0.58	0.41	0.29	0.21	0.14	0.10
September	1.16	0.82	0.58	0.41	0.29	0.20	0.15
October	0.48	0.34	0.24	0.17	0.12	0.09	0.06
November	0.50	0.36	0.25	0.18	0.13	0.09	0.06
December	0.54	0.39	0.27	0.19	0.14	0.10	0.07
January (1992)	0.86	0.61	0.43	0.30	0.22	0.16	0.11
February	0.30	0.21	0.15	0.11	0.07	0.06	0.04
March	0.62	0.44	0.31	0.22	0.15	0.11	0.08
April	0.67	0.48	0.34	0.24	0.17	0.12	0.09
May	0.63	0.45	0.32	0.23	0.16	0.11	0.08
June	0.89	0.63	0.45	0.32	0.23	0.16	0.11
July	0.56	0.40	0.28	0.20	0.14	0.10	0.07
August	0.85	0.60	0.42	0.30	0.22	0.15	0.11
September	0.54	0.38	0.27	0.19	0.14	0.10	0.07
October	0.82	0.58	0.41	0.29	0.21	0.15	0.10
November	0.71	0.50	0.35	0.25	0.18	0.13	0.09
December	0.62	0.44	0.31	0.22	0.16	0.11	0.08
January (1993)	0.52	0.37	0.26	0.18	0.13	0.10	0.07
February	0.51	0.36	0.25	0.18	0.13	0.09	0.07
March	0.70	0.49	0.35	0.25	0.17	0.13	0.09
April	0.70	0.50	0.35	0.25	0.18	0.12	0.09
May	0.95	0.67	0.48	0.34	0.24	0.17	0.12
June	0.74	0.52	0.37	0.26	0.19	0.13	0.09
July	0.73	0.52	0.36	0.26	0.18	0.13	0.09
August	0.92	0.65	0.46	0.33	0.23	0.16	0.11
September	0.90	0.64	0.45	0.32	0.22	0.16	0.11

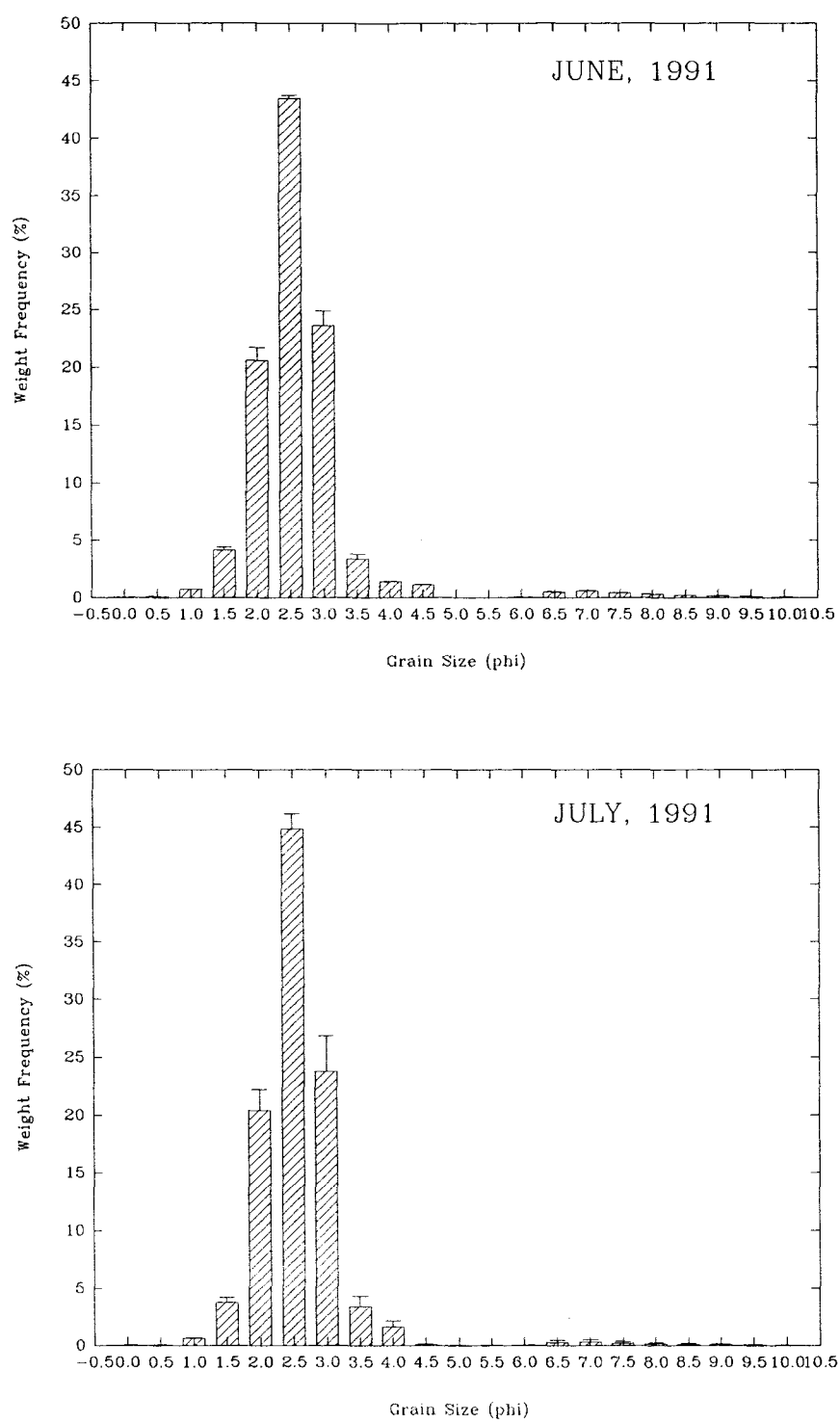


Figure 7.2(a). Grain size distributions of surficial sediment samples, as histograms, June 1991 and July 1991 (Y error bars represent standard errors)

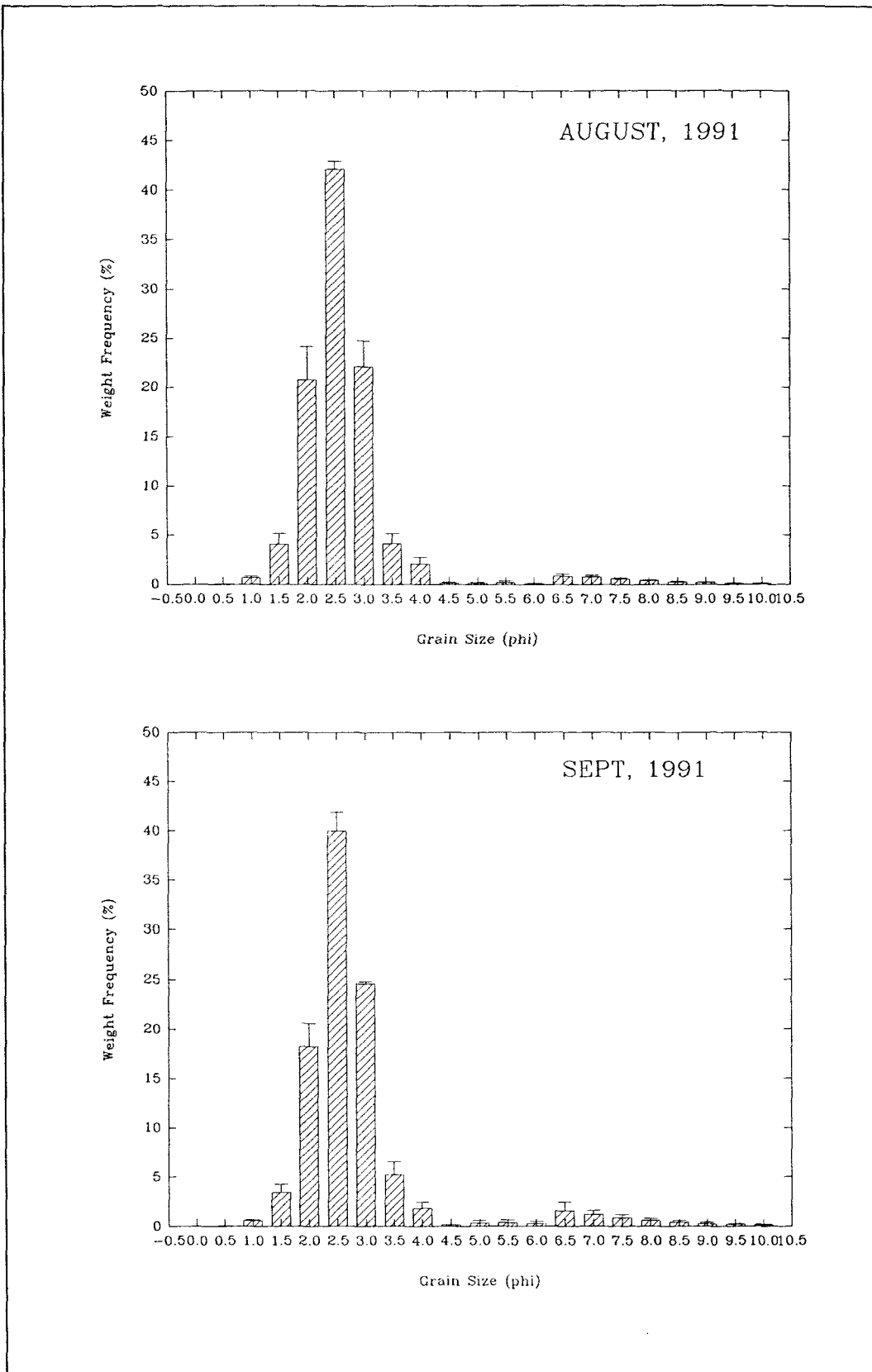


Figure 7.2(b). Grain size distributions of surficial sediment samples, as histograms, August 1991 and September 1991 (Y error bars represent standard errors)

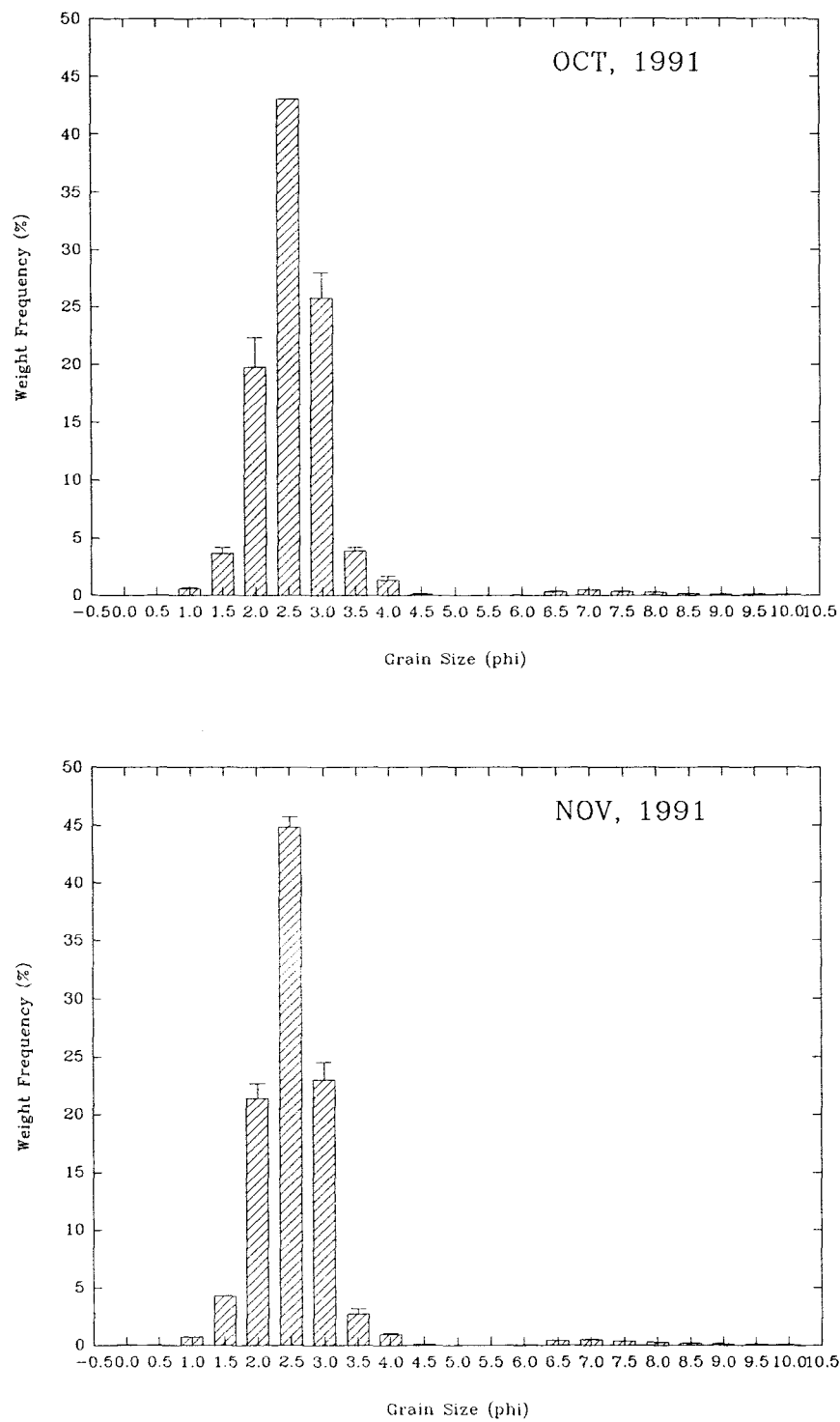


Figure 7.2(c). Grain size distributions of surficial sediment samples, as histograms, October 1991 and November 1991 (Y error bars represent standard errors)

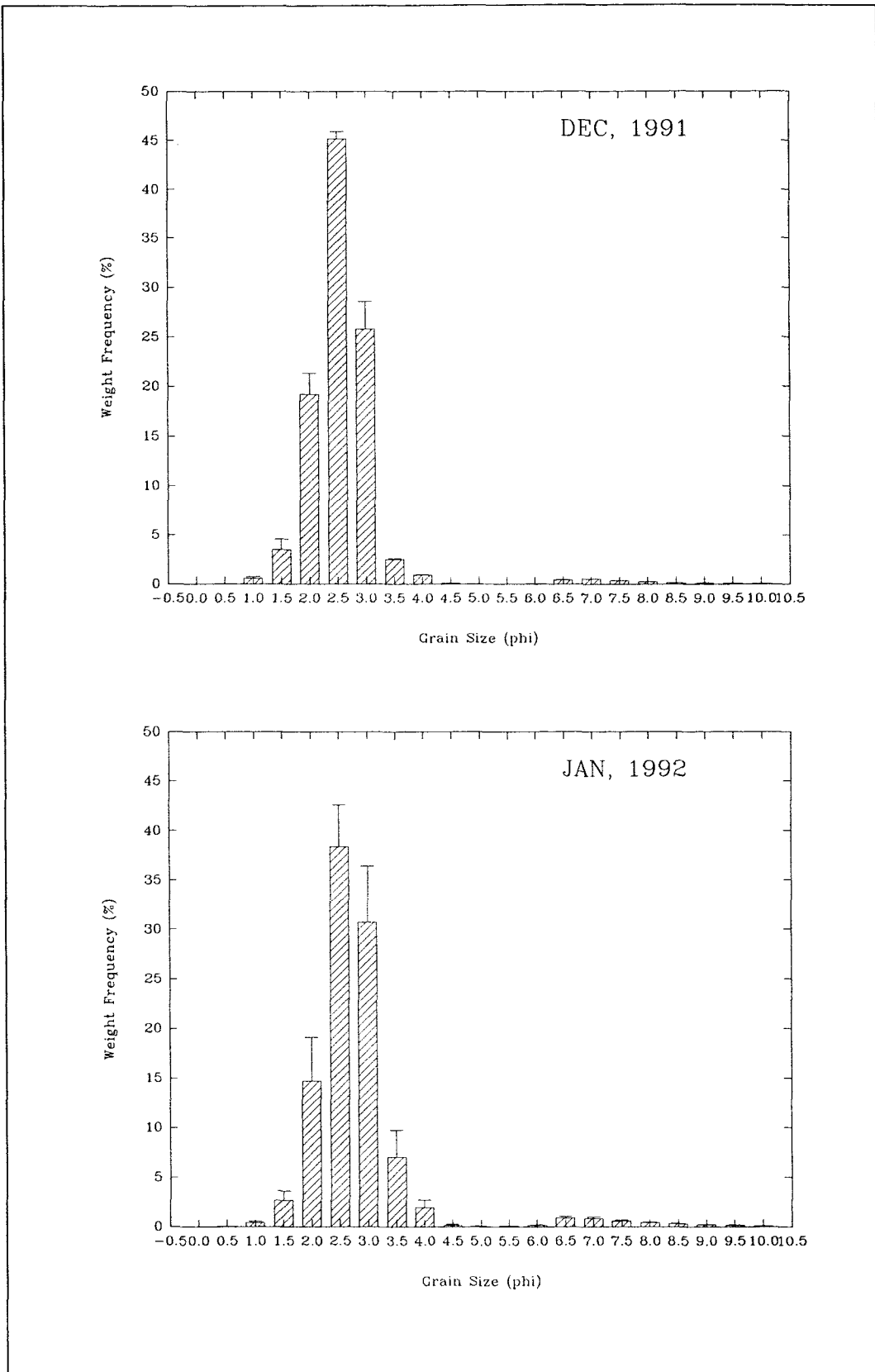


Figure 7.2(d). Grain size distributions of surficial sediment samples, as histograms, December 1991 and January 1992 (Y error bars represent standard errors)

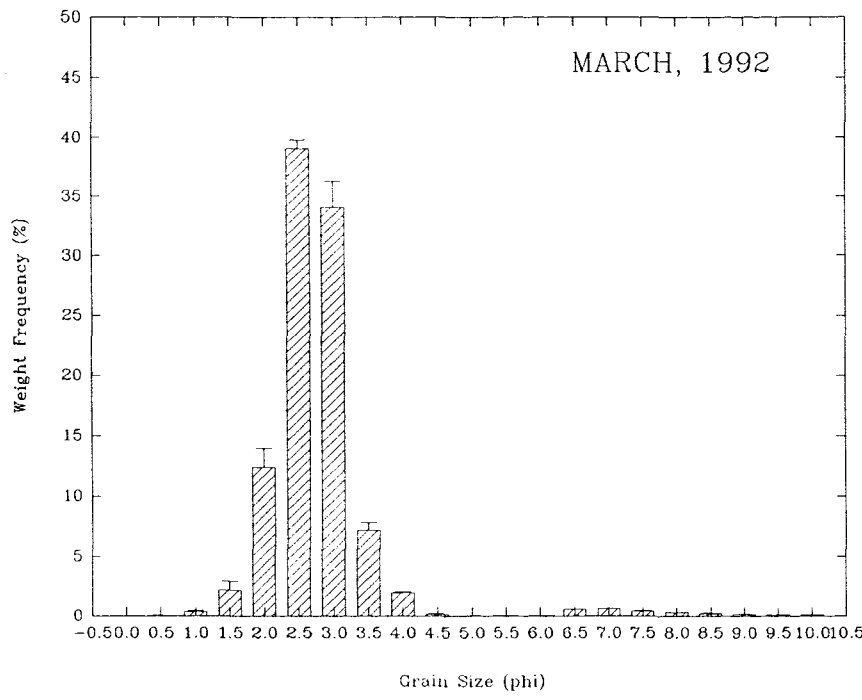
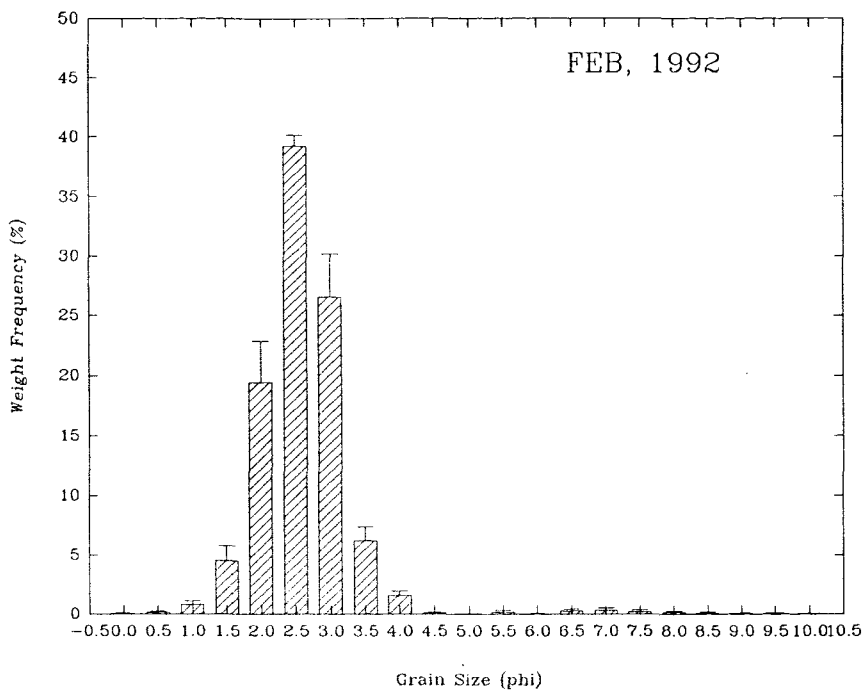


Figure 7.2(e). Grain size distributions of surficial sediment samples, as histograms, February 1992 and March 1992 (Y error bars represent standard errors)

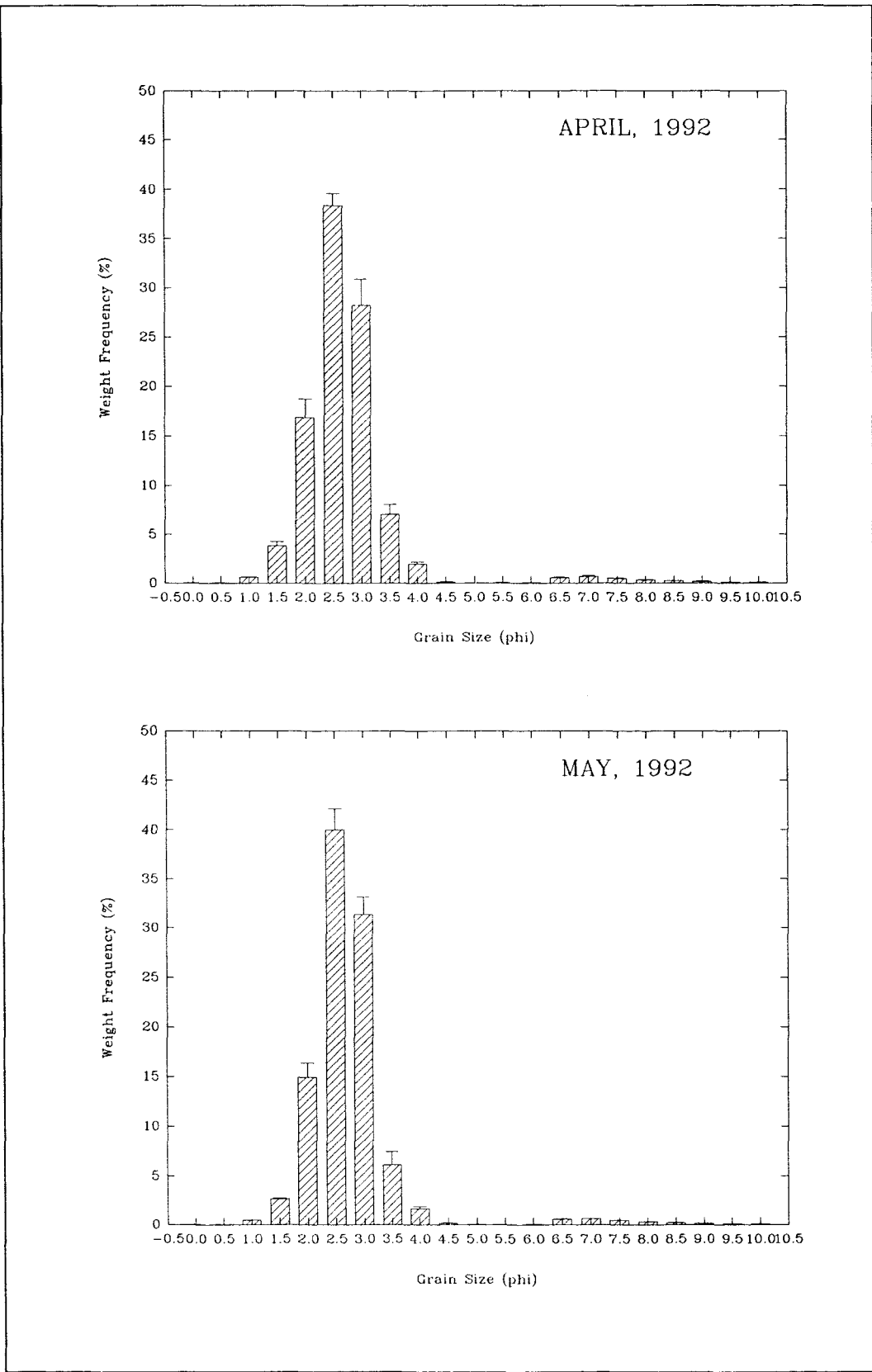


Figure 7.2(f). Grain size distributions of surficial sediment samples, as histograms, April 1992 and May 1992 (Y error bars represent standard errors)

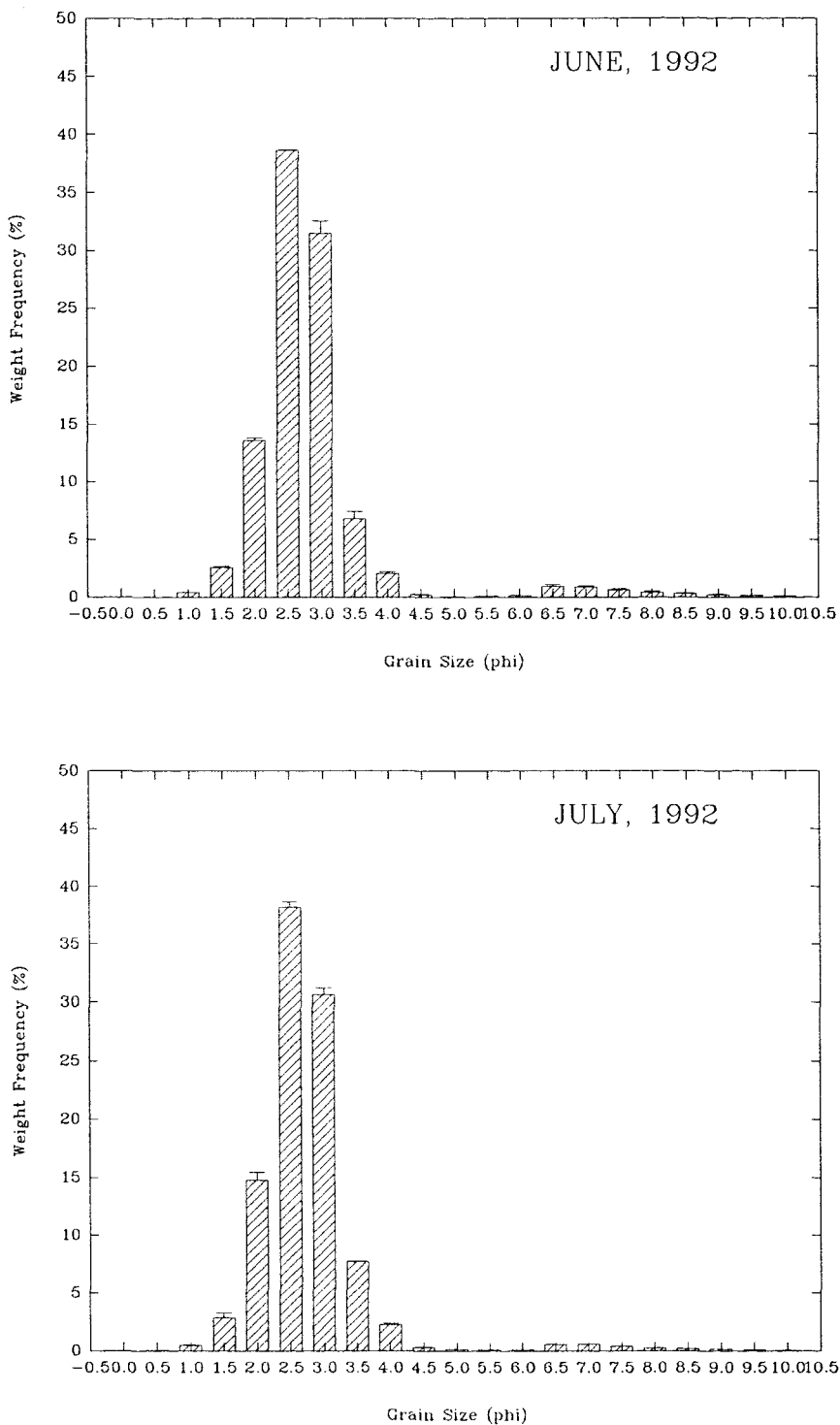


Figure 7.2(g). Grain size distributions of surficial sediment samples, as histograms, June 1992 and July 1992 (Y error bars represent standard errors)

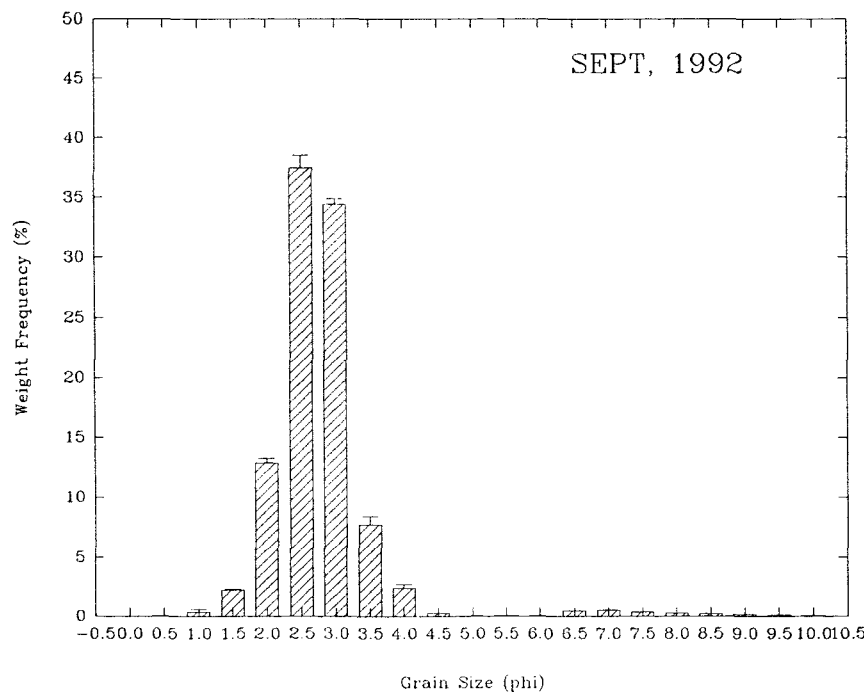
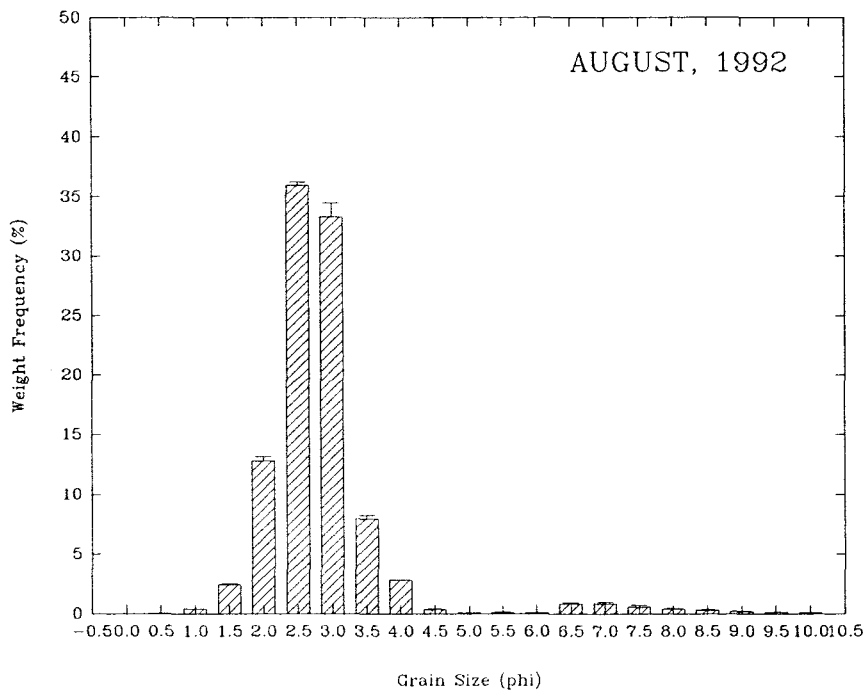


Figure 7.2(h). Grain size distributions of surficial sediment samples, as histograms, August 1992 and September 1992 (Y error bars represent standard errors)

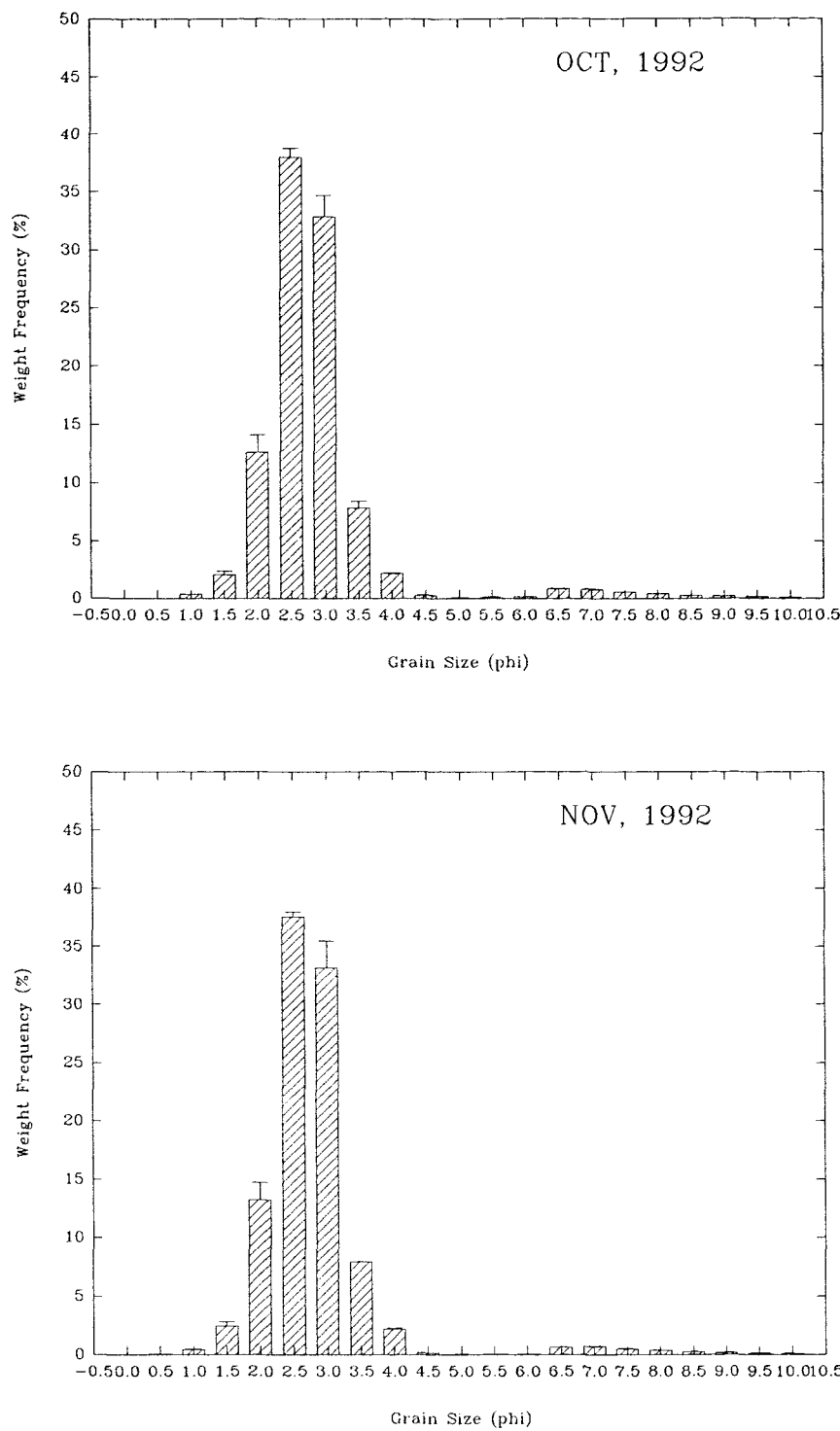


Figure 7.2(i). Grain size distributions of surficial sediment samples, as histograms, October 1992 and November 1992 (Y error bars represent standard errors)

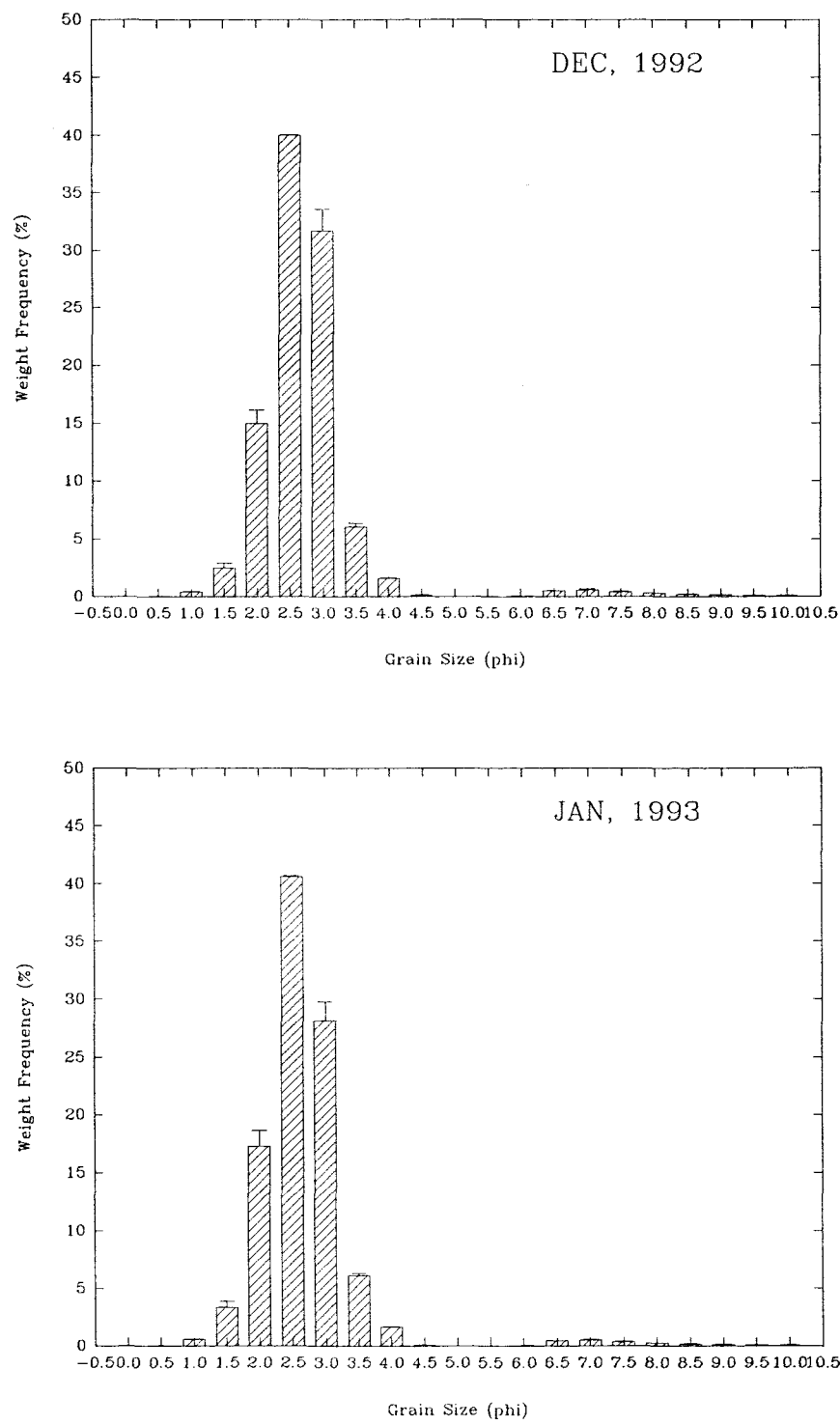


Figure 7.2(j). Grain size distributions of surficial sediment samples, as histograms, December 1992 and January 1993 (Y error bars represent standard errors)

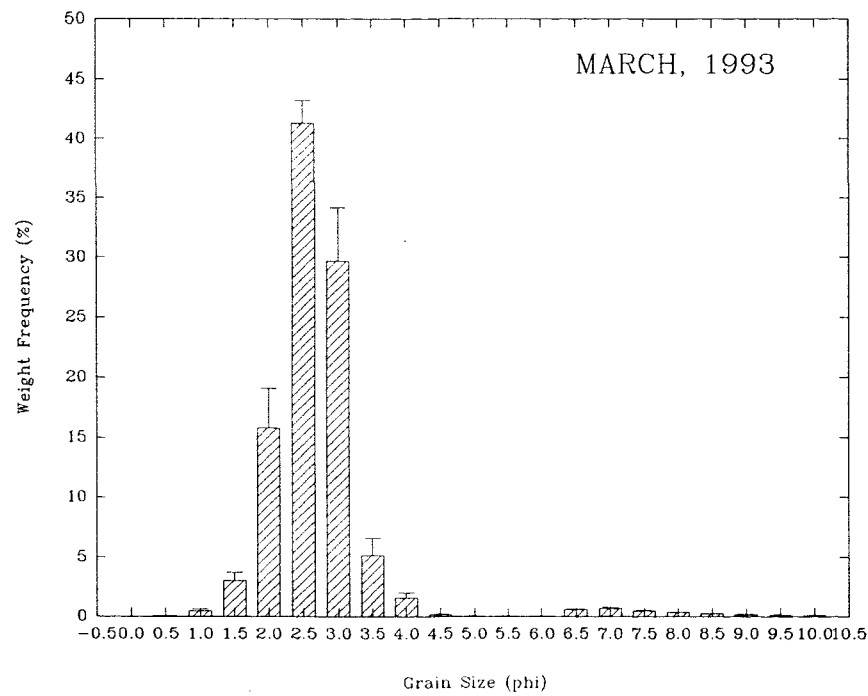
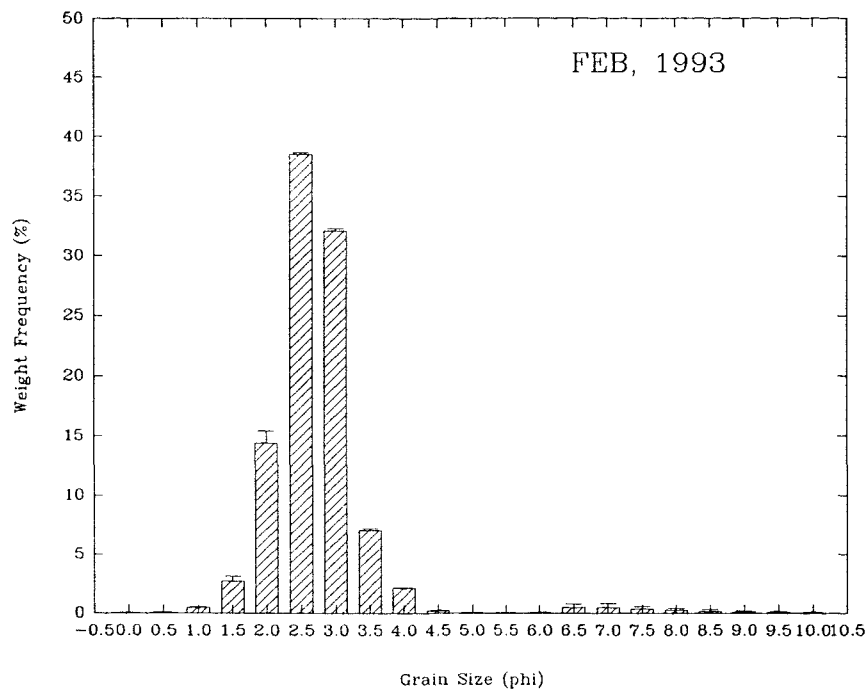


Figure 7.2(k). Grain size distributions of surficial sediment samples, as histograms, February 1993 and March 1993 (Y error bars represent standard errors)

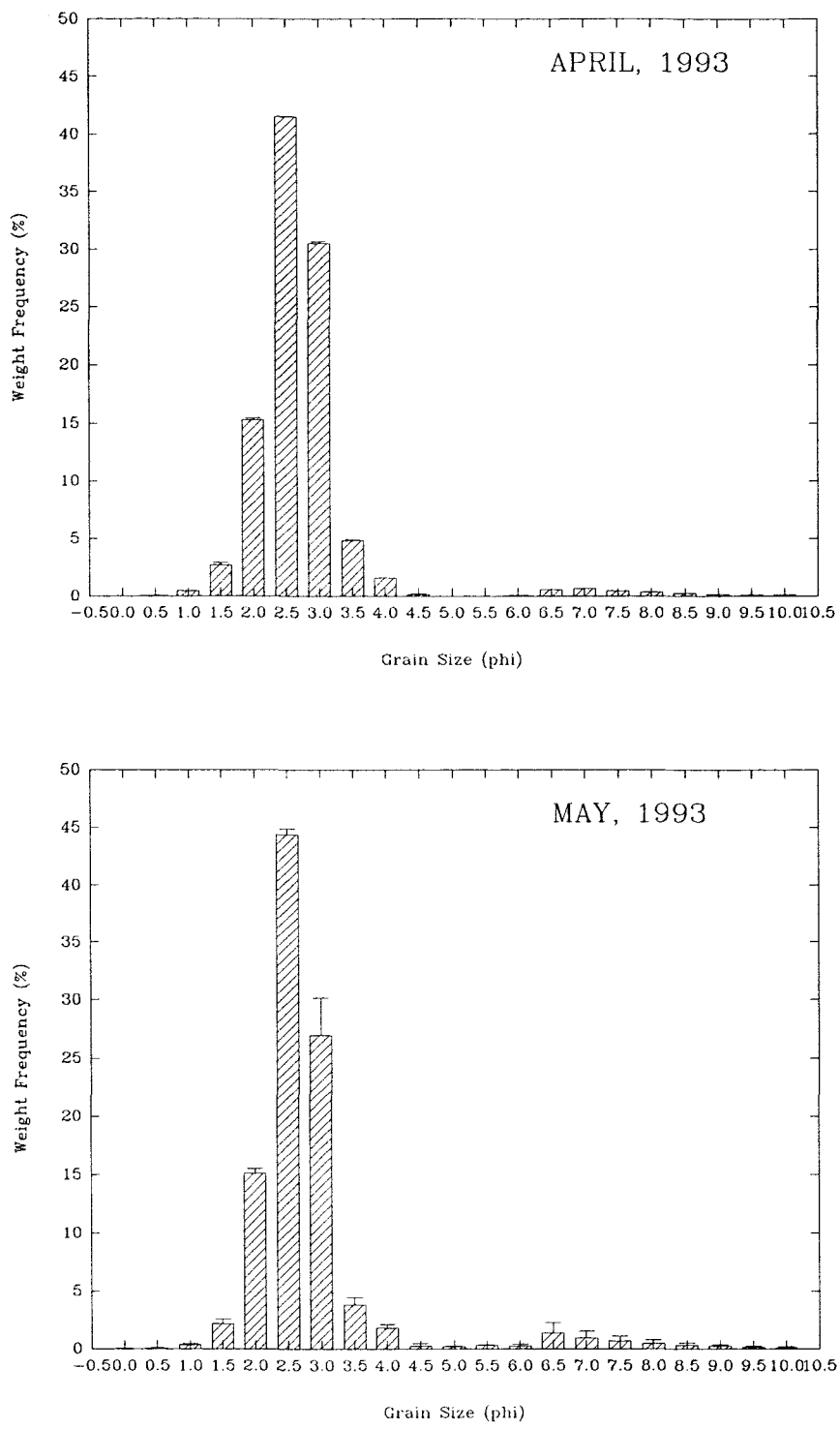


Figure 7.2(l). Grain size distributions of surficial sediment samples, as histograms, April 1993 and May 1993 (Y error bars represent standard errors)

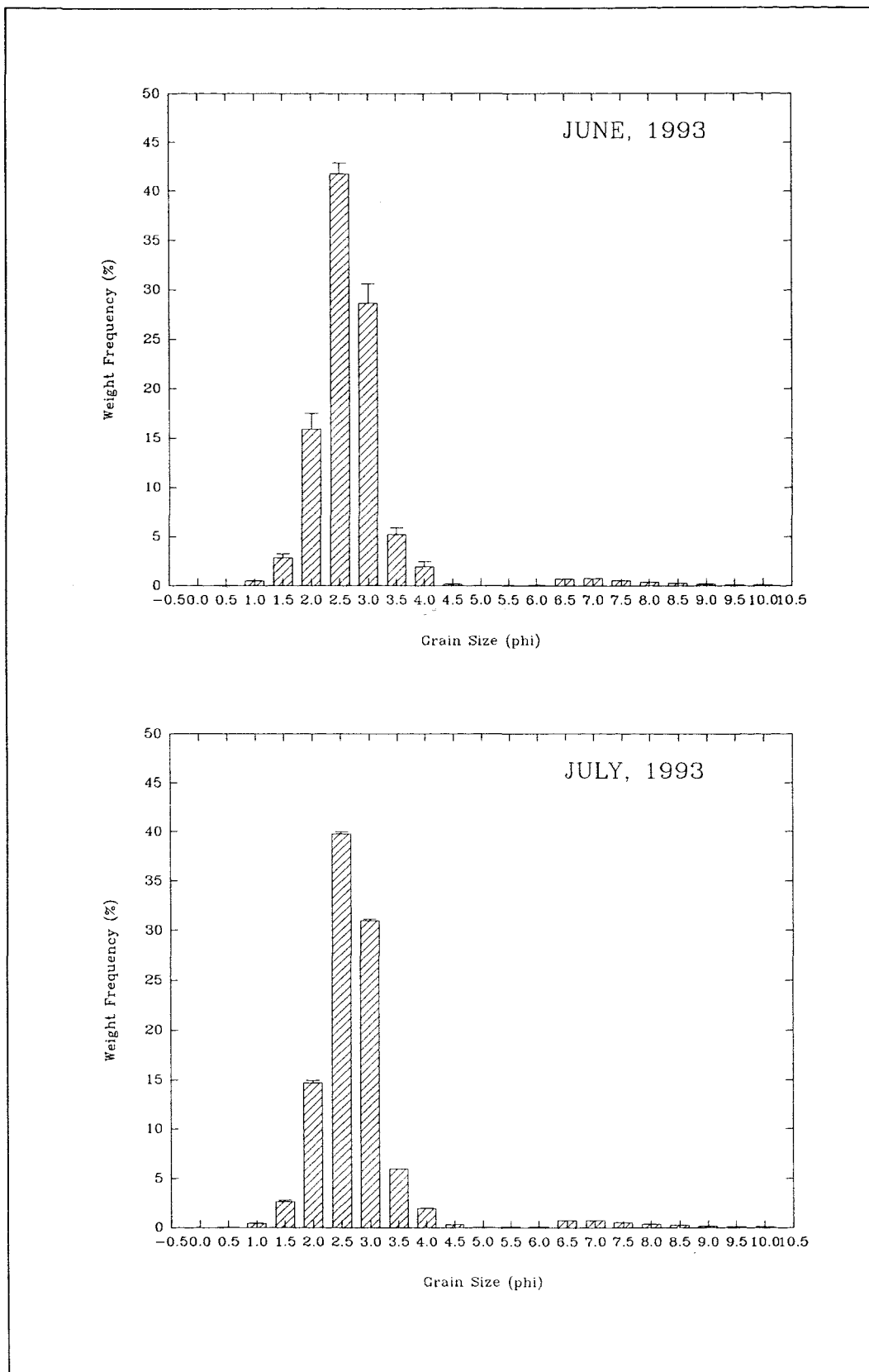


Figure 7.2(m). Grain size distribution of surficial sediment samples, as histograms, June 1993 and July 1993 (Y error bars represent standard errors)

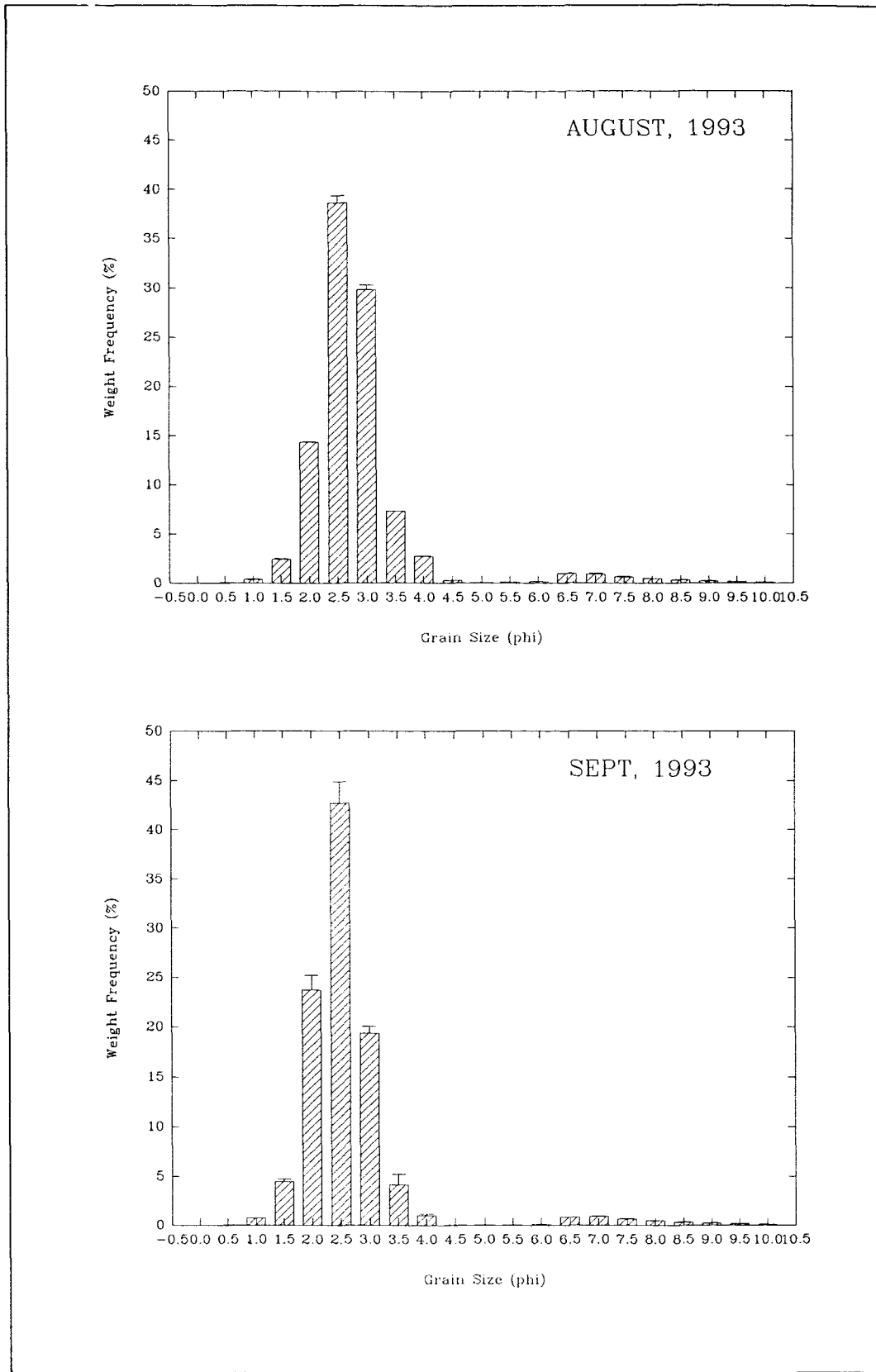


Figure 7.2(n). Grain size distributions of surficial sediment samples, as histograms, August 1993 and September 1993 (Y error bars represent standard errors)

its slope and the nature of any irregularities; these parameters permit the curves to be characterised and compared (McManus, 1988).

Parameters used for characterising grain size curves fall into three principal categories: (a) the average or mean grain size; (b) the spread of sizes about the average (sorting); and (c) the asymmetry of any preferential spread to one side of the average (skewness). The definitions of the parameters used for the definition of grain size in the present study are listed in Table 7.3. Here, sizes are expressed in Φ units, defined as,

$$\Phi = -\log_2 d$$

where d is diameter of grain in mm (Krumbein, 1934). The textural parameters derived for all of the statistical sediment samples from the area under investigation are presented in Table 7.4.

(a) Mean Grain Size

The mean represents the average size of the sediment and is affected by both the source of sediment and the environment of deposition (Folk, 1966). It is, therefore, a function of both the energy of the transporting medium and the size range of the available materials (Glaister and Nelson, 1974).

The mean grain size of the surficial sediment samples, collected on a monthly basis during the present investigation, are shown on Figure 7.3. The mean grain size fluctuates only slightly during the study period, towards the end of the investigation. The smallest mean grain size (3.14 Φ) occurred in August 1992, whilst the largest (2.84 Φ) was in July 1991. Generally, throughout the first year of the investigation, the grain size is coarser than in the second year; this may indicate that rougher hydrodynamic conditions prevailed during the earlier part of the investigation.

Table 7.3. Parameters and descriptive terms applied to various ranges of grain size parameters (from Folk and Ward, 1957)

$$\text{Mean } M_z = \frac{1}{3} (\Phi_{16} + \Phi_{50} + \Phi_{84})$$

$$\text{Sorting } \sigma_1 = \frac{1}{2} \left(\frac{\Phi_{84} - \Phi_{16}}{2} + \frac{\Phi_{95} - \Phi_5}{3.3} \right)$$

$$\text{Skewness } Sk_1 = \left(\frac{\Phi_{16} + \Phi_{84} - 2\Phi_{50}}{2(\Phi_{84} - \Phi_{16})} \right) + \left(\frac{\Phi_5 + \Phi_{95} - 2\Phi_{50}}{2(\Phi_{95} - \Phi_5)} \right)$$

Φx = Φ size of the x th percentile

Sorting (σ_1)	Skewness (Sk_1)
Very well sorted < 0.35	Very positively skewed + 0.3 to + 1
Well sorted $0.35 - 0.50$	Positively skewed + 0.1 to + 0.3
Moderately well sorted $0.50 - 0.70$	Symmetrical + 0.1 to - 0.1
Moderately sorted $0.70 - 1.00$	Negatively skewed - 0.1 to - 0.3
Poorly sorted $1.00 - 2.00$	Very negatively skewed - 0.3 to - 1.0
Very poorly sorted $2.00 - 4.00$	
Extremely poorly sorted > 4.00	

Table 7.4. Textural parameters (in Φ) of statistical sediment samples from Solent Breezes

Month (Year)	Mean	Sorting	Skewness
June (1991)	2.89	0.98	2.76
July	2.84	0.78	1.83
August	2.97	1.09	2.56
September	3.10	1.23	2.31
October	2.89	0.88	2.79
November	2.85	0.90	2.87
December	2.89	0.91	2.95
January (1992)	3.09	1.08	2.55
February	2.88	0.80	1.32
March	3.07	0.95	2.66
April	3.00	1.01	2.48
May	3.02	0.97	2.69
June	3.11	1.10	2.49
July	3.04	0.96	2.41
August	3.14	1.08	2.39
September	3.06	0.92	2.54
October	3.13	1.07	2.52
November	3.08	1.00	2.59
December	3.02	0.96	2.71
January (1993)	2.96	0.92	2.60
February	3.02	0.90	1.92
March	3.01	1.00	2.73
April	3.01	1.00	2.74
May	3.09	1.12	2.3
June	3.02	1.02	2.69
July	3.05	1.03	2.58
August	3.12	1.12	2.45
September	2.92	1.12	2.71

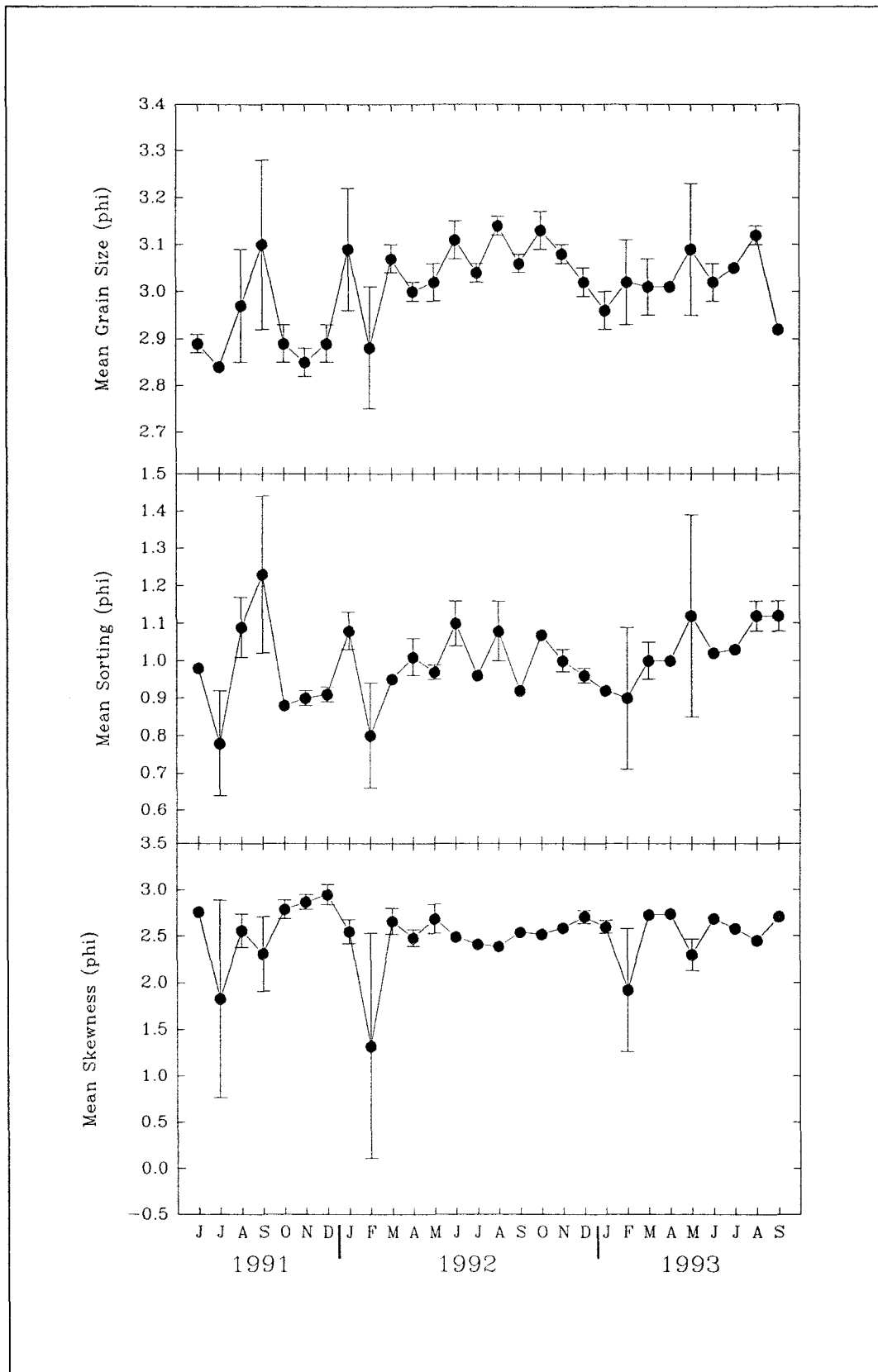


Figure 7.3. Long-term measurements of mean grain size, mean sorting and mean skewness of surficial sediment samples (Y error bars represent standard errors)

(b) Sorting

Sorting depends upon the source of material, the nature of the sedimentary processes (such as wave and current action), and the uniformity and persistence of the energy conditions (Glaister and Nelson, 1974). Sediment which consists of only a single grain size distribution represents the best sorted material, with low sorting values (McManus, 1988). Likewise, sediments become finer-grained and better sorted in the direction of transport as a result of selected reworking. The long-term distribution of sorting values recorded during the present study are illustrated on Figure 7.3. The sorting ranges from 0.78 (in July 1991) to 1.23 (in September 1991). Overall, the sorting of the sediments at Solent Breezes ranges from moderately to poorly sorted. The sorting fluctuates on a monthly basis; it generally worsens throughout the study period, changing gradually from 'moderately sorted' at the beginning to 'poorly sorted' by the end. In general, the sorting is worse during the summer months, than during winter.

(c) Skewness

Skewness is represented by a positive or negative dimensionless number, lying within the range of - 1 to + 1. This value represents the tendency for a distribution to be biased towards one side of, or to deviate, from normality (McManus, 1988). Strongly skewed samples are associated usually with areas of the mixing of sediments from different sedimentary environments (Folk, 1966). For example, skewness reflects the degree of contamination of the sediments by coarse size grades, transported by strong tidal currents (Allen, 1971). The skewness is negative if there is more material contained within the coarse tail (coarse skewed); in contrast, skewness is positive if there is more material contained within the fine tail (fine skewed) (Lindholm, 1987). The long-term distribution of skewness values obtained during the present study are shown on Figure 7.3. In general, the samples are extremely positively skewed. The skewness varies slightly between the various months, from a lowest value of +

1.32 (December 1991) to the highest value of + 2.95 (February 1992).

Generally, if a sediment deposit is eroded, the resultant sediment in transport must be finer, better sorted and more positively skewed than the source; this arises since the probability of moving fine (light) grains is greater than coarse (heavy) grains (McLaren, 1981). The remaining sediment, in contrast, must be coarser, better sorted and more negatively skewed than the original deposit. Any sediment in transport may become finer or coarser, however, depending upon the action of the transporting agent: the finer the sediment, the more negatively skewed the sediment distribution; and the coarser the sediment, the more positively skewed the sediment distribution (McLaren and Little, 1987).

Based upon the above observations, it may be inferred that during the (28 months period of) investigation, the distribution patterns of sediments at Solent Breezes gradually becomes finer, moderately sorted and positively skewed. Some slight fluctuations in this general trend occurs between summer and winter. The overall changes may indicate: a downstream transport direction; and/or changing transport direction or mixing with a material of different source, such as from Calshot Spit (Figure 3.1).

7.5.3. Scatter Plots of the Textural Parameters

Many investigators have used bivariate scatter plots of textural parameters to discern the geological significance of the derived grain size parameters (Folk and Ward, 1957; Miola and Weiser, 1968, Allen, 1971; Glaister and Nelson, 1974). Thus, it has been suggested elsewhere that a plot of skewness against kurtosis is a useful technique to assist in the interpretation of the genesis of sediments. Likewise, plotting mean grain size against sorting and skewness provides information on the original conditions of sedimentation. Sorting is plotted against mean grain size on Figure 7.4. The overall correlation between the two parameters (at 5 % level of significance) suggests that sorting improves as the mean grain size becomes coarser. Generally, tidal currents represent an efficient transport process; they are, however, inefficient sorting mechanisms.

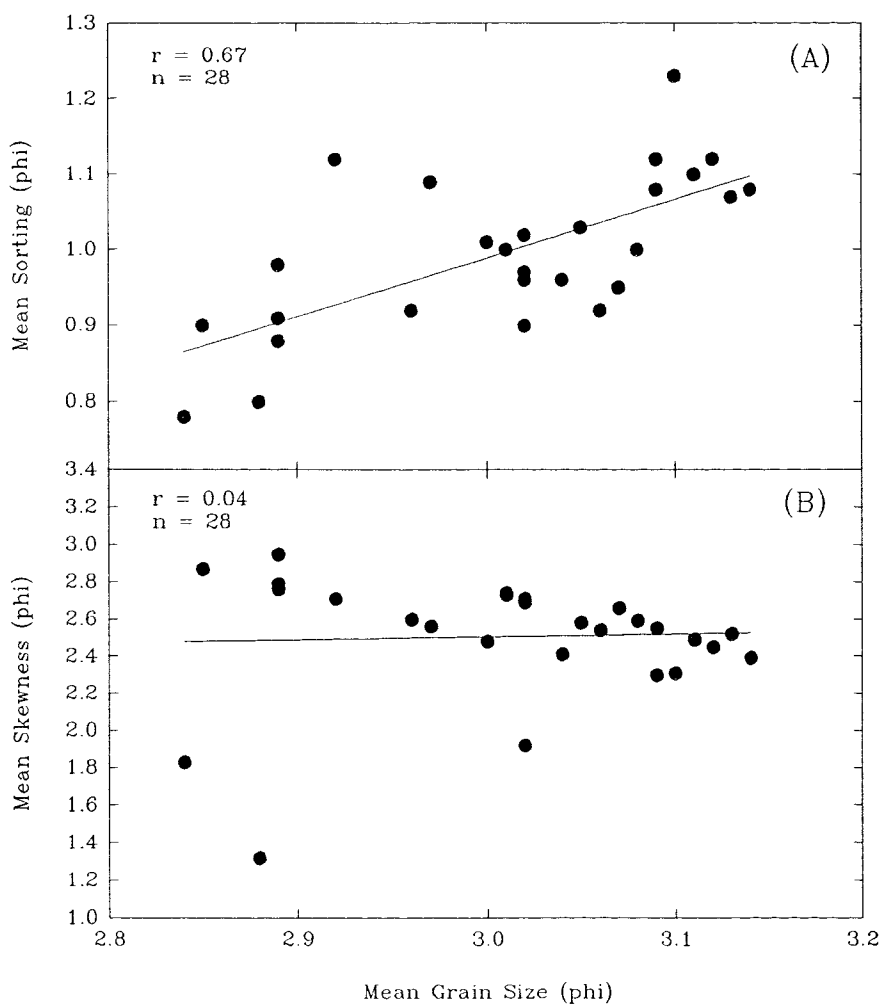


Figure 7.4. Relationships between mean sorting and mean grain size (A), and mean skewness and mean grain size (B)

Sediment in tidally-dominated areas are, therefore, typically coarser grained, less well sorted and negatively skewed (Nordstrom, 1977). On the basis of these observations, the samples from Solent Breezes vary slightly with time; this may suggest that they are influenced by different transport mechanisms.

Skewness is plotted, once again in relation to mean grain size on Figure 7.4. In general, there is no significant association (at 5 % level of significance) between the two parameters. The data are spread around the line of best fit, with a slight increase in skewness as the mean grain size becomes finer. Overall, tidally-dominated areas are characterised by sediments which are less well sorted and negatively skewed than those from other environments (Duane, 1964). The spread of the samples represented on Figure 7.4 may indicate, therefore, slight variation in energy and hydrodynamics conditions occurring within the period of study.

7.6. Moisture Content

The moisture content of the surficial sediment samples, measured throughout the study period, are presented in Table 7.5 and illustrated on Figure 7.5. The data presented show moisture content fluctuates considerably during the period of the investigation. Some interesting inverse relationships appear to exist between the amount of moisture present in the sediments and low water height. On the basis of the above, the moisture content appears to be affected by temperature (cf Figure 7.1); with low moisture contents tending to coincide with high temperatures; this would lead to evaporation of water from the sediment surface. Wind may also influence the sediment moisture content, through an increase in evaporation processes i.e. samples collected on windy days may result, therefore, in lower recorded moisture contents. The lowest moisture content (27.88 %) was recorded in June 1992, with the highest (34.88 %) in September 1991.

Table 7.5. Mean moisture content, low water height and mean organic matter content

Month (Year)	Moisture Content (%)	Low Water Height (m)	Organic Matter Content (%)
June (1991)	30.29	0.8	0.91
July	33.86	0.6	1.09
August	34.16	0.6	1.07
September	34.88	0.8	1.32
October	32.33	0.5	1.05
November	31.84	0.6	1.04
December	29.23	1.1	1.14
January (1992)	33.67	0.3	1.24
February	32.79	0.4	1.65
March	32.95	0.2	1.62
April	32.65	1.0	1.20
May	31.44	0.7	1.32
June	27.88	1.1	1.43
July	30.12	0.7	2.01
August	32.43	1.0	1.31
September	30.95	0.9	1.06
October	29.58	0.9	1.14
November	31.42	0.6	1.15
December	30.15	1.0	1.65
January (1993)	31.39	0.6	1.13
February	31.78	0.8	1.11
March	31.34	0.0	1.19
April	29.84	0.2	1.08
May	31.47	0.9	1.45
June	30.84	0.8	1.22
July	34.02	1.0	1.64
August	33.99	0.7	1.32
September	31.53	0.9	1.93

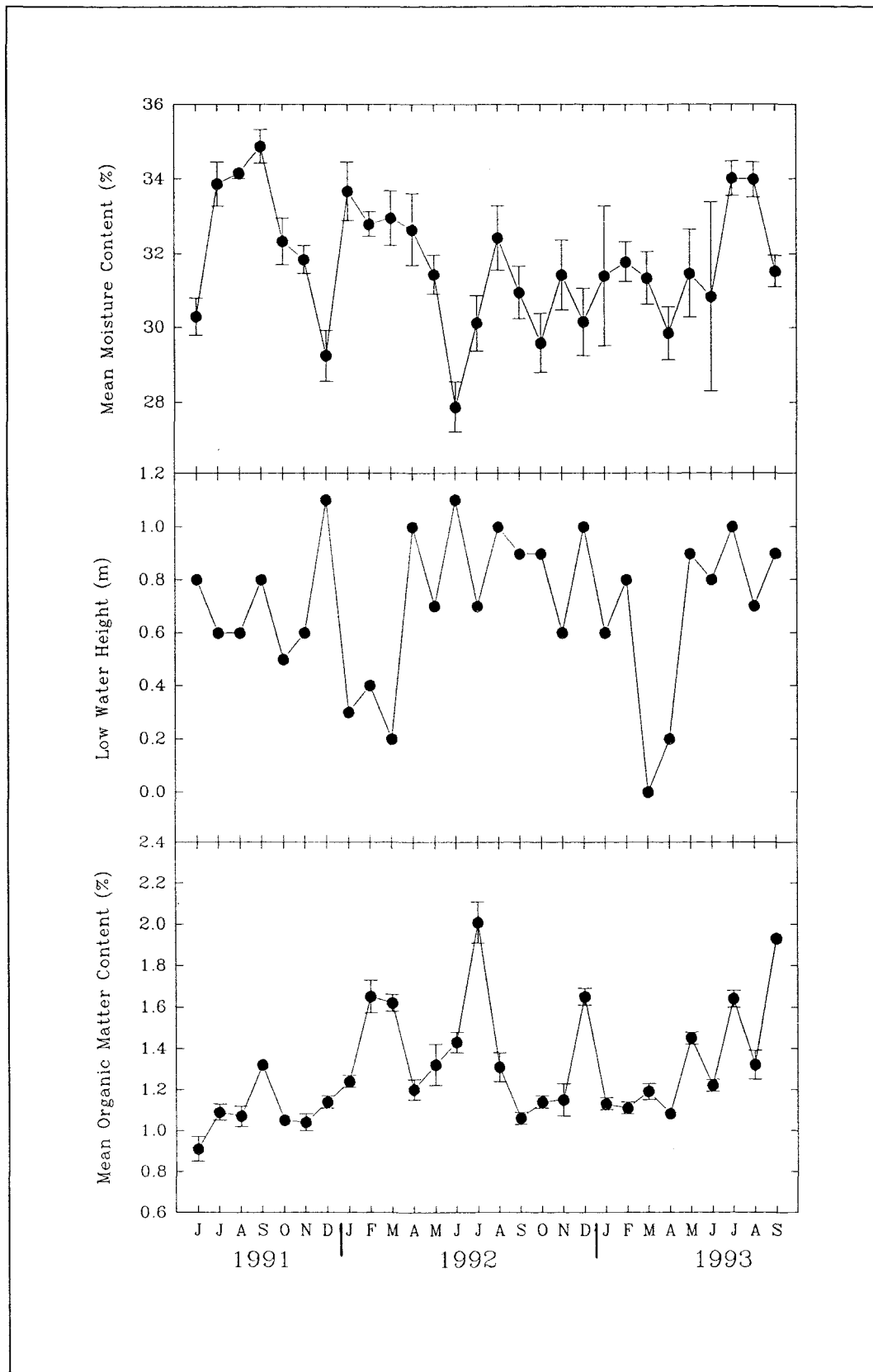


Figure 7.5. Long-term measurements of mean moisture content, low water height (for explanation, see text) and mean organic matter content (Y error bars represent standard errors)

7.7. Low Water Height

Low water heights are presented in Table 7.5 and displayed on Figure 7.5; these are secondary data obtained from the Southampton Tide Tables, supplied by Associated British Ports (ABP) in Southampton. Most of the data collected coincided with very low water heights (i.e. spring tides), with low water heights above datum of less than a metre; this was to allow a longer time for data collection. The lowest low water height is around the datum level (in March 1993), whilst the highest low water height is 1.1 m above datum (December 1991 and June 1992). These levels may serve as indicators of ground water level during each of the sampling occasions. As the ground water level depends upon, and is linearly associated with, sea bed slope and low water level, the lower the low water level then the deeper the ground water level. This condition may affect the moisture content recorded during the present study.

7.8. Organic Matter Content

The long-term variability in total organic matter content is, once again represented in Table 7.5 and on Figure 7.5. The data show that the mean total organic matter content increases gradually from the beginning, towards the end, of the study. This trend is accompanied by some distinctive fluctuations in the organic matter content of surficial sediments. The lowest organic matter content is 0.91 % (June 1991) and the highest is 2.01 % (July 1992). The higher organic matter contents tend to coincide with high silt/clay contents (cf Figure 7.6); this is due to the fact that organic matter can be embedded/associated with the larger surface area of the silt/clay-sized material.

7.9. Silt/Clay Content

The variability in the measured silt/clay contents are presented in Table 7.6 and shown on Figure 7.6, where a seasonal pattern is revealed. The silt/clay content increases during summer months and decreases during winter. Such a pattern may result from the relative calm weather which occurs during summer, compared to the rough weather of the winter. During the summer, wind speeds are generally slightly lower than during the winter (cf Figure 7.7). The lowest silt/clay content was 0.1 % (July 1991), whilst the highest silt/clay content was 0.73 % (September 1991).

7.10. Tube Density

Tube density variability, with time, is presented in Table 7.6 and illustrated on Figure 7.6; these are the measurements associated with the shear strength of the sediment. The tube density decreases gradually from the beginning of the experiment; this is accompanied by some slight fluctuations towards the end of study. Possible reasons for this trend have been discussed in Chapter 6. The lowest density of tube was 4.17 per 100 cm square (March 1993), whilst the highest tube density was 8.67 per 100 cm square (June 1991).

7.11. Meteorological Data

Meteorological observations were obtained from the Meteorological Office; these included daily climatological data which were considered of paramount importance to the present study. The data were categorised (into air temperature, wind speed, rainfall and sunshine) for 28 months, commencing in May 1991 and extending to September 1993. Since a complete set of the necessary meteorological data were not available from a single source, it was

Table 7.6. Mean silt/clay content and mean tube density

Month (Year)	Silt/Clay Content (%)	Tube Density (100 cm ⁻²)
June (1991)	0.14	8.67
July	0.10	8.38
August	0.53	7.93
September	0.73	8.25
October	0.26	5.17
November	0.17	8.33
December	0.15	7.75
January (1992)	0.18	5.42
February	0.14	6.00
March	0.18	6.83
April	0.22	6.92
May	0.20	5.83
June	0.54	5.58
July	0.44	6.13
August	0.50	5.93
September	0.13	4.67
October	0.64	5.62
November	0.13	4.87
December	0.12	5.69
January (1993)	0.12	5.00
February	0.17	6.83
March	0.16	4.17
April	0.27	4.80
May	0.62	5.63
June	0.17	5.80
July	0.13	3.13
August	0.60	4.93
September	0.31	4.75

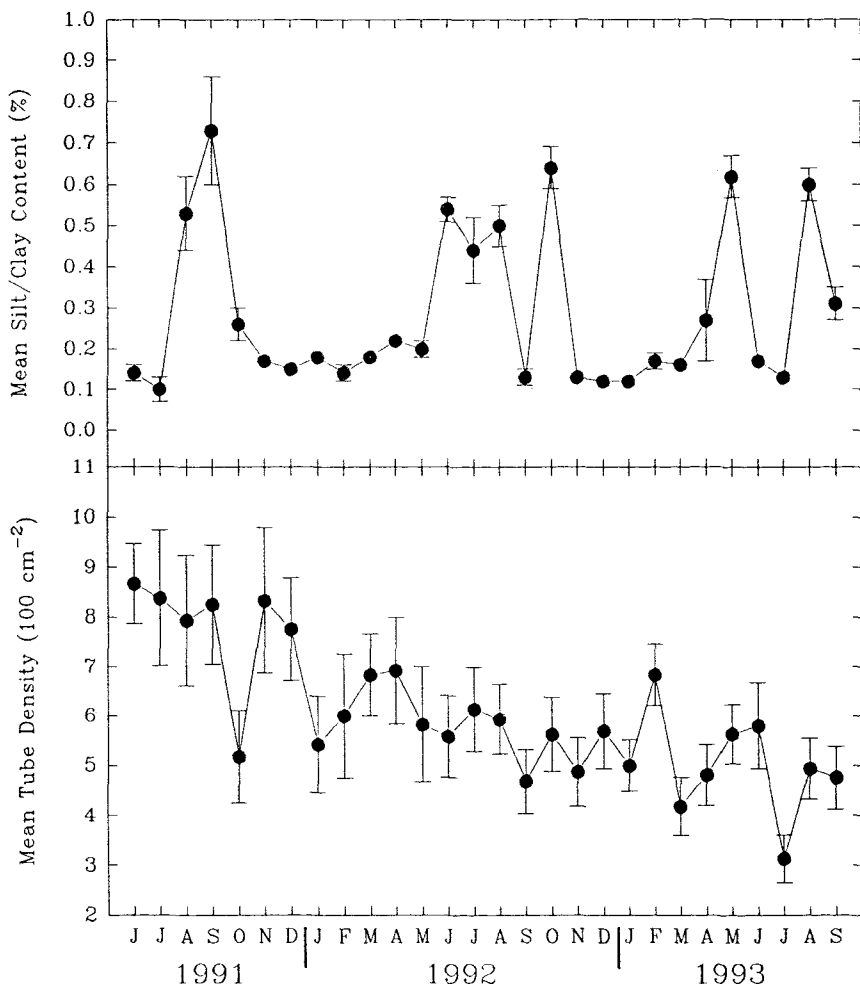


Figure 7.6. Long-term variation in mean silt/clay content and mean tube density (Y error bars represent standard errors)

regarded necessary to utilise data recordings from two meteorological stations closest to the area of the present investigation. In this way, the recordings from both stations would constitute a complete data set. The relevant stations were: (i) Solent MRSC, located at 50°48' N and 01°13' W, which provided temperature and wind speed data; and (ii) Southampton Mayflower Park, located at 50°54' N and 01°24' W, which provided rainfall and sunshine data. Since the sampling dates did not always coincide with the middle of the month, the existing data had to be reworked and analysed in order to form a data base for inter-sampling periods i.e. instead of monthly data. Mean values of the revised data set were then derived separately.

The meteorological results (inter-sampling data) are displayed in Table 7.7 and on Figure 7.7. It can be seen from the Figure that the mean daily air temperature exhibits a seasonal pattern, where the high temperatures occur during the summer months and the low temperatures occur during the winter. The lowest recorded daily air temperature was 4.95 °C (January 1992) and the highest daily air temperature was 18.32 °C (August 1991). In contrast, the mean daily wind speed fluctuates considerably, without any distinct pattern throughout the period of study. In general, the mean daily wind speed is slightly higher in winter months than in summer months. The lowest mean daily wind speed was 7.64 knots (3.93 m s⁻¹) (February 1993) and the highest mean daily wind speed was 17.77 knots (9.14 m s⁻¹) (January 1993). The mean daily rainfall also fluctuated slightly during the 28 months period of study; it does not show any clear seasonal pattern. The lowest mean daily rainfall was 0.2 mm (May, 1992) and the highest was 5.83 mm (November 1992). These levels represent a relatively-low rainfall. Sunshine data are available only until October 1992, this was due to the breakdown of the equipment. The mean daily sunshine shows a pattern of seasonality which is similar to that shown by the mean daily air temperature. Thus, as might be expected, mean daily air temperature is heavily dependent upon mean daily sunshine. The lowest mean daily sunshine was 1.46 hours (December 1991) and the highest mean daily sunshine was 9.68 (May 1992).

Table 7.7. Mean daily air temperature, mean daily wind speed, mean daily rainfall and mean daily sunshine

Month (Year)	Air Temperature (°C)	Wind Speed (knots)	Rainfall (mm)	Sunshine (hours)
June (1991)	13.37	13.04	2.95	4.42
July	17.45	11.58	2.36	7.03
August	18.32	9.53	0.40	7.88
September	17.24	9.74	0.48	6.14
October	12.58	10.27	2.80	3.36
November	9.16	12.70	2.91	1.80
December	7.04	10.90	0.92	1.46
January (1992)	4.95	8.71	0.54	1.86
February	6.20	11.36	1.53	2.05
March	7.93	13.36	1.57	2.51
April	10.05	12.63	2.27	5.86
May	15.41	10.41	0.20	9.68
June	16.26	7.70	0.79	7.50
July	17.57	10.77	2.44	5.22
August	16.95	15.00	3.13	4.57
September	14.87	11.49	1.58	3.89
October	9.33	11.38	2.03	4.17
November	9.11	16.58	5.83	
December	5.37	10.07	2.30	
January (1993)	7.36	17.77	3.51	
February	6.14	7.64	0.36	
March	6.23	10.66	0.46	
April	8.73	12.12	3.54	
May	12.52	12.10	1.60	
June	15.66	11.50	2.84	
July	16.39	10.90	1.53	
August	16.53	12.58	1.17	
September	14.03	9.72	3.47	

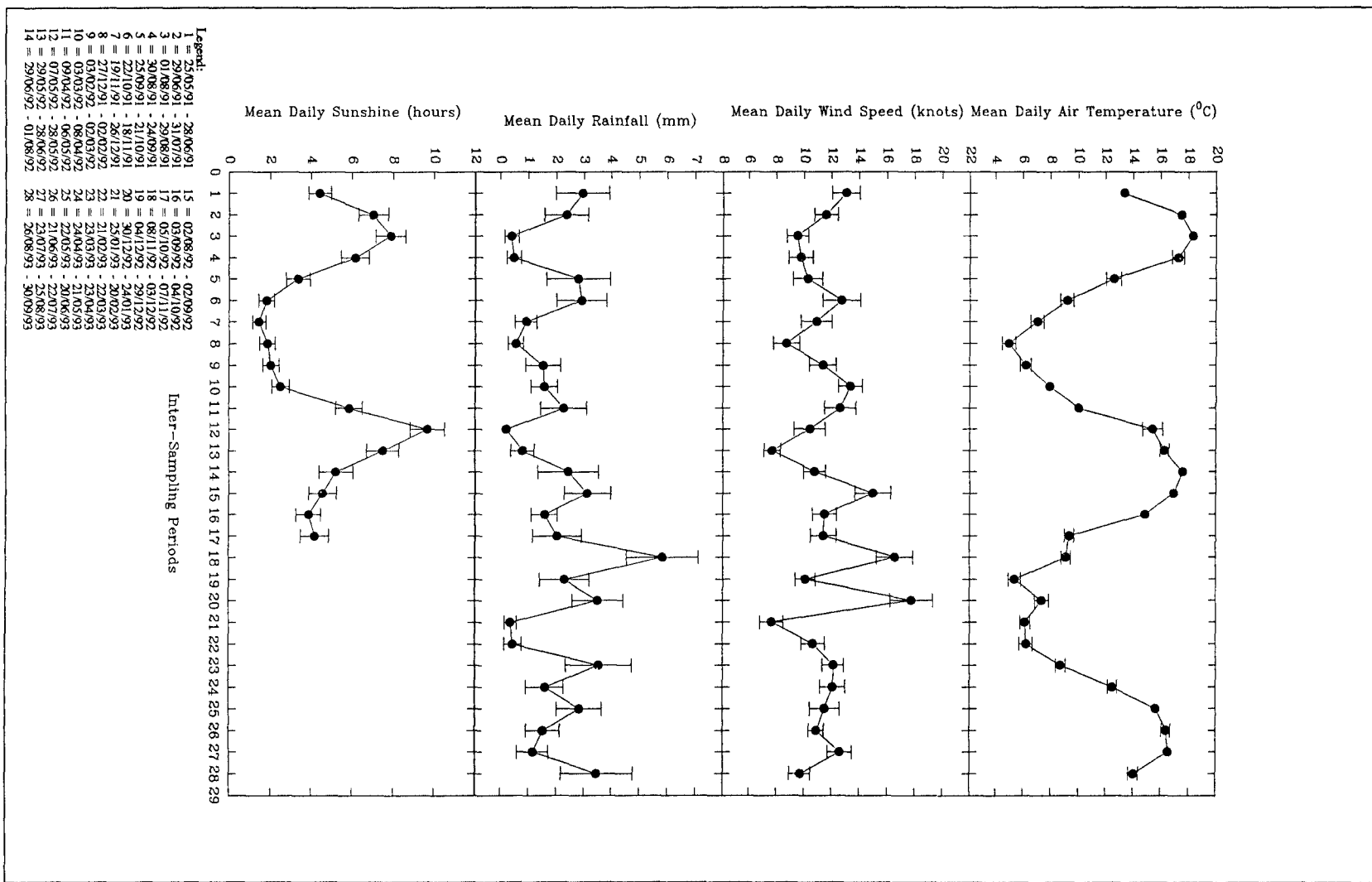


Figure 7.7. Long-term variation in mean daily air temperature, mean daily wind speed, mean daily rainfall and mean daily sunshine (Y error bars represent standard errors)

7.12. Laboratory Experiment

The results of the laboratory experiments undertaken into the effect of temperature on shear strength are represented in Table 7.8 and on Figure 7.8. There is a high and significant (at 5 % level of significance) negative correlation between the shear strength and temperature i.e. with $r = 0.99$. An increase in water temperature within the surficial sediments leads to a decrease in the sediment shear strength. This relationship may be due to the fact that an increase in temperature leads to the decrease in inter-particle bonds between grains which, in turn, reduces the cohesiveness of the sediment (Ariathurai and Arulanandan, 1978; Kelly and Gularce, 1981).

Following the results described above, experiments were undertaken into the effect of straw density on shear strength, at temperatures of 4 °C and 17 °C. These results are presented in Table 7.9 and shown also on Figure 7.8. There is a highly significant positive correlation (at 5 % level of significance) between shear strength and straw density i.e. with $r = 0.99$. An increase in straw density results in an increase in the shear strength of the sediments. This finding appears to be logical, as the straws act together to bind the sediment. The sediment grains more densely packed, therefore, leading to an increase in the shear strength of the sediment sample.

Table 7.8. Water temperature and shear strength of sediment

Water Temperature (°C)	Shear Strength (KPa)
4.0	1.97
5.5	1.90
6.0	1.88
15.0	1.65
16.0	1.63
17.0	1.60
17.5	1.55
18.0	1.53

Table 7.9. Straw density, temperature at 4°C and 17°C

Straw Density (100 cm ⁻²)	Shear Strength (KPa) at Water Temperature of 4°C	Shear Strength (KPa) at Water Temperature of 17°C
0	1.80	1.67
2	1.88	1.77
5	2.03	1.90
7	2.13	2.00
9	2.23	2.09
12	2.30	2.20
14	2.37	2.23
16	2.50	2.33
19	2.56	2.40

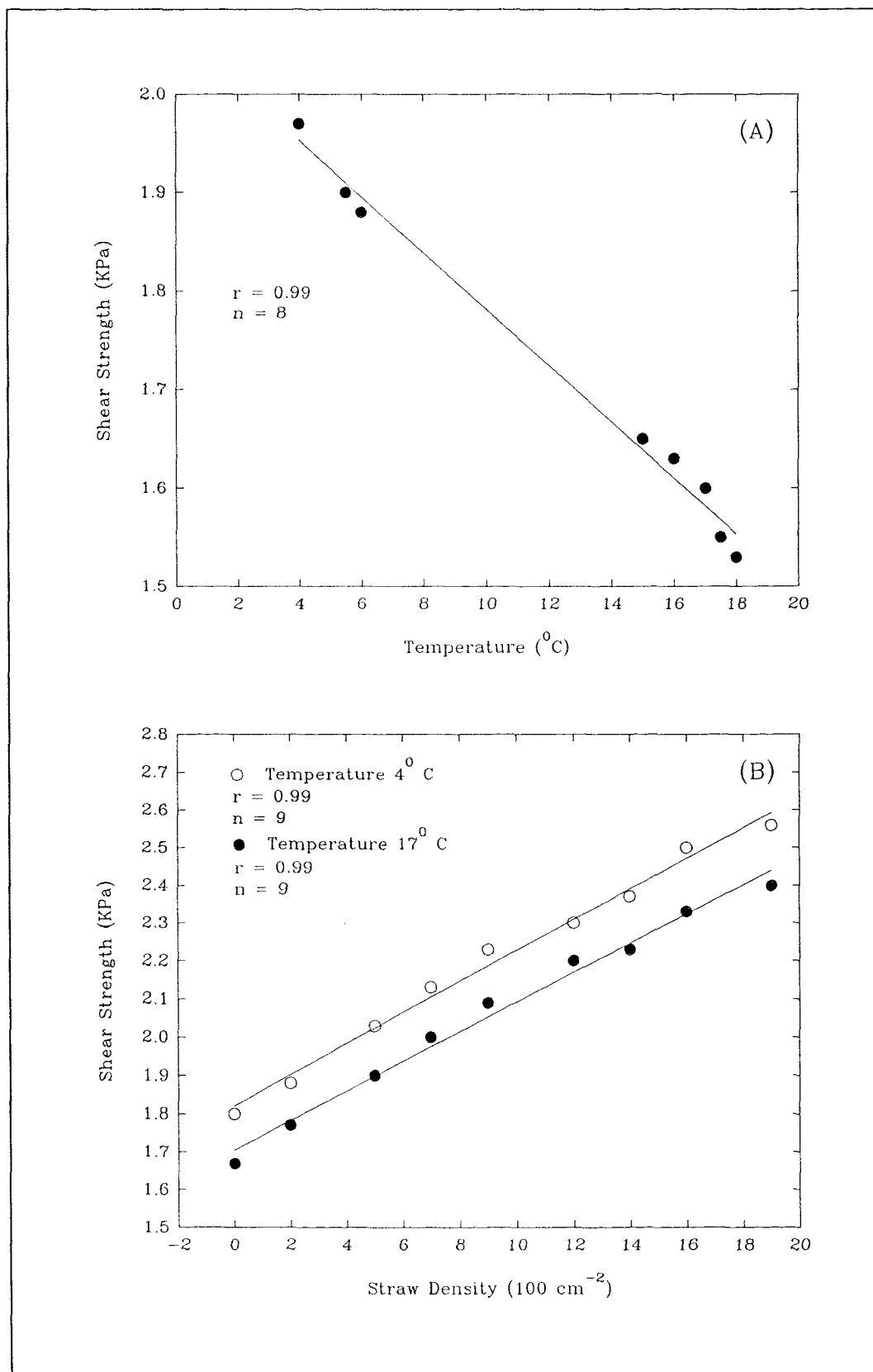


Figure 7.8. Correlations between shear strength and temperature (A), and shear strength and straw density, at different temperatures (B)

CHAPTER 8

DISCUSSION

8.1. Introduction

In this chapter, the results which have been described, interpreted and discussed in Chapters 5, 6 and 7, are examined further within a broader environmental context. The *in situ* measurements of shear strength data are used to predict shear stress, using the relationship presented elsewhere by Dunn (1959). The shear stresses obtained are used then to predict sediment stability, throughout the period of the present investigation, at Solent Breezes (Southampton Water). A statistical model is established on the basis of the parameters studied in an attempt to predict the shear strength (or stress) of intertidal flat sediments. Finally, the results are compared with those obtained from the previous studies elsewhere.

8.2. Shear Stress and Strength

Most studies on intertidal flat sediment dynamics use generally shear stress to predict sediment stability. However, there are no recently published papers which attempt to relate shear strength with shear stress. Following a review of the previous literature, only a few experimenters have investigated such a relationship (Dunn, 1959; Flaxman, 1963; Graf, 1971). Dunn (1959) performed *in situ* shear tests with a vane-shear apparatus mounted on a tripod base. The testing took place underwater, in canals, to furnish values of bed shear strength. Proper calibration of the vane-shear apparatus used in the field investigation enabled the calculation of tractive force (shear stress) for the particular soil (sediment) on the bed. On the basis of the fact that the results of Dunn (1959) were encouraging, Flaxman (1963) advanced the concept that the

erosion resistance of cohesive soils could be determined in relation to the unconfined compressive strength tests of saturated undisturbed soil (sediment) samples. This concept was proved following a series of laboratory and field investigations of 13 streams, in the 16 western states of the United States. Unconfined compressive strength data were obtained in the laboratory, whilst the tractive power data were obtained from field measurements. It was shown, using multiple regression analysis, that the unconfined compressive strength was dependent upon the plasticity index, the dry density of the soil, and the percentage of material finer than $5 \mu\text{m}$. The tractive power relating to sediment in the streams was calculated from the product of bed slope, hydraulic radius, specific weight of water and average velocity. These results showed a relationship between the tractive power (shear stress) and the unconfined compressive strength (shear strength), which was to serve as a useful tool for design engineers and scientists.

Based upon the results of Dunn (1959), a linear regression equation has been derived, showing the relationship between shear stress and strength. The derived graph is shown on Figure 8.1 and the equation is as follows,

$$\tau_c = 2.29824 + 1.6 \times 10^{-4} \tau \quad (8.1)$$

where τ_c is the shear stress in N m^{-2} and τ is the shear strength in N m^{-2} .

Using this equation, the (critical) shear stress (τ_1) and the (critical) friction velocity (U_{*1}) values of the present investigation can be calculated, as the monthly shear strengths were measured directly *in situ*. The results are presented in Table 8.1 and illustrated on Figure 8.2. Elsewhere, Miller *et al.*, (1977) used carefully selected data on the threshold of sediment movement, to re-examine the various empirical curves which are used commonly to predict threshold. Amongst their results, they constructed a graph to predict critical friction velocity (U_*) from a knowledge of grain diameter. To investigate the sediment stability within the present study area, the grain size data are used now to obtain critical friction velocities (U_{*2}). In the calculations, the pore-water density was predicted by plotting the temperature and salinity data of the present study on a standard diagram, showing the variation of sea-water density as a function of temperature

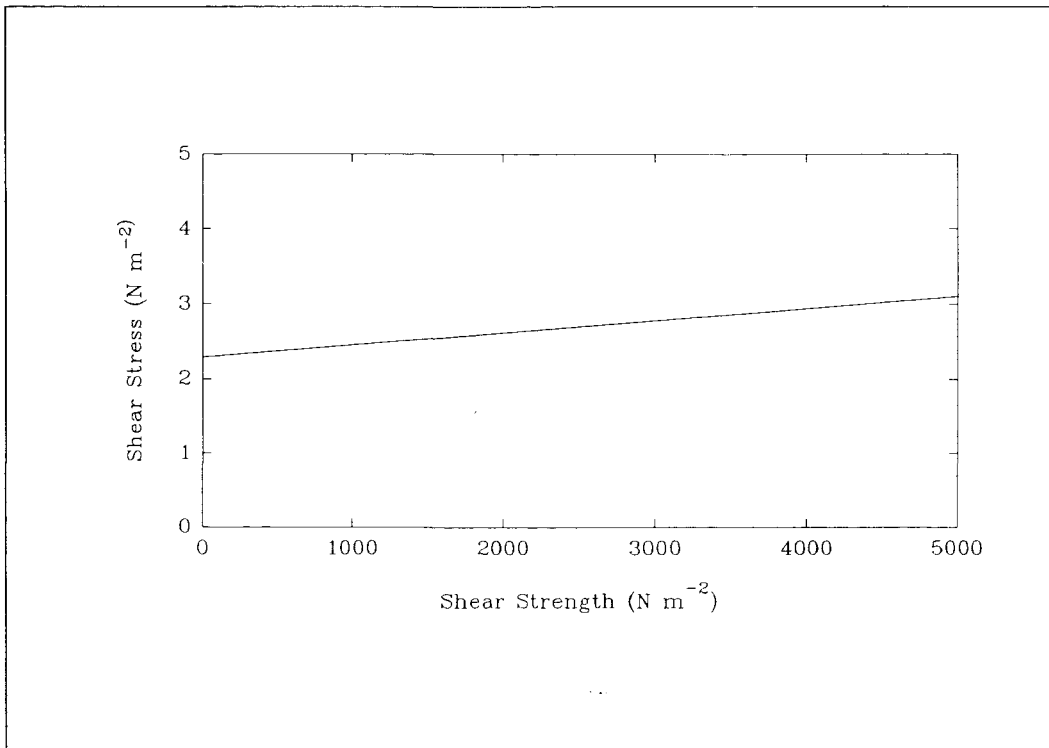


Figure 8.1. Relationship between shear stress and shear strength (derived from Dunn, 1959)

and salinity (Pinet, 1992). With a knowledge of pore-water density, the critical shear stress (τ_c) was calculated using the following equation

$$\tau_c = U_*^2 \rho \quad (8.2)$$

where τ_c is the critical shear stress in N m^{-2} , U_*^2 is the critical friction velocity in cm s^{-2} and ρ is the pore-water density. The critical shear stresses and friction velocities calculated using this equation are also presented in Table 8.1 and illustrated on Figure 8.2. Comparison of the two sets of results demonstrates that both the critical shear stress and friction velocity predicted from the *in situ* shear strength measurements are much higher than those predicted by applying the grain size data to the curve of Miller *et al.*, (1977). The lowest values of critical shear stress and critical friction velocity predicted from the *in situ* shear strength are 2.64 N m^{-2} and 5.07 cm s^{-1} , whilst the highest are 2.95 N m^{-2} and 5.36 cm s^{-1} , consecutively. For the critical shear stress and critical friction velocity

Table 8.1. Derived critical shear stresses and friction velocities (1 - represents *in situ* measurements; 2 - represent measurements based on grain size)

Month (Year)	τ_1 (N m ⁻²)	U_{*1} (cm s ⁻²)	τ_2 (N m ⁻²)	U_{*2} (cm s ⁻²)
June (1991)	2.70	5.12	0.15	1.19
July	2.73	5.17	0.15	1.21
August	2.65	5.08	0.14	1.19
September	2.70	5.13	0.14	1.15
October	2.76	5.18	0.15	1.19
November	2.95	5.36	0.15	1.20
December	2.91	5.32	0.15	1.19
January (1992)	2.64	5.07	0.14	1.15
February	2.82	5.24	0.15	1.20
March	2.77	5.19	0.14	1.16
April	2.80	5.23	0.14	1.18
May	2.80	5.22	0.14	1.17
June	2.73	5.16	0.13	1.14
July	2.70	5.13	0.14	1.16
August	2.71	5.14	0.13	1.12
September	2.68	5.11	0.14	1.16
October	2.71	5.14	0.13	1.11
November	2.70	5.13	0.14	1.15
December	2.68	5.12	0.14	1.17
January (1993)	2.73	5.16	0.14	1.19
February	2.68	5.11	0.14	1.17
March	2.69	5.12	0.14	1.18
April	2.70	5.13	0.14	1.18
May	2.71	5.14	0.14	1.15
June	2.71	5.14	0.14	1.17
July	2.72	5.15	0.14	1.16
August	2.76	5.18	0.13	1.12
September	2.77	5.20	0.15	1.19

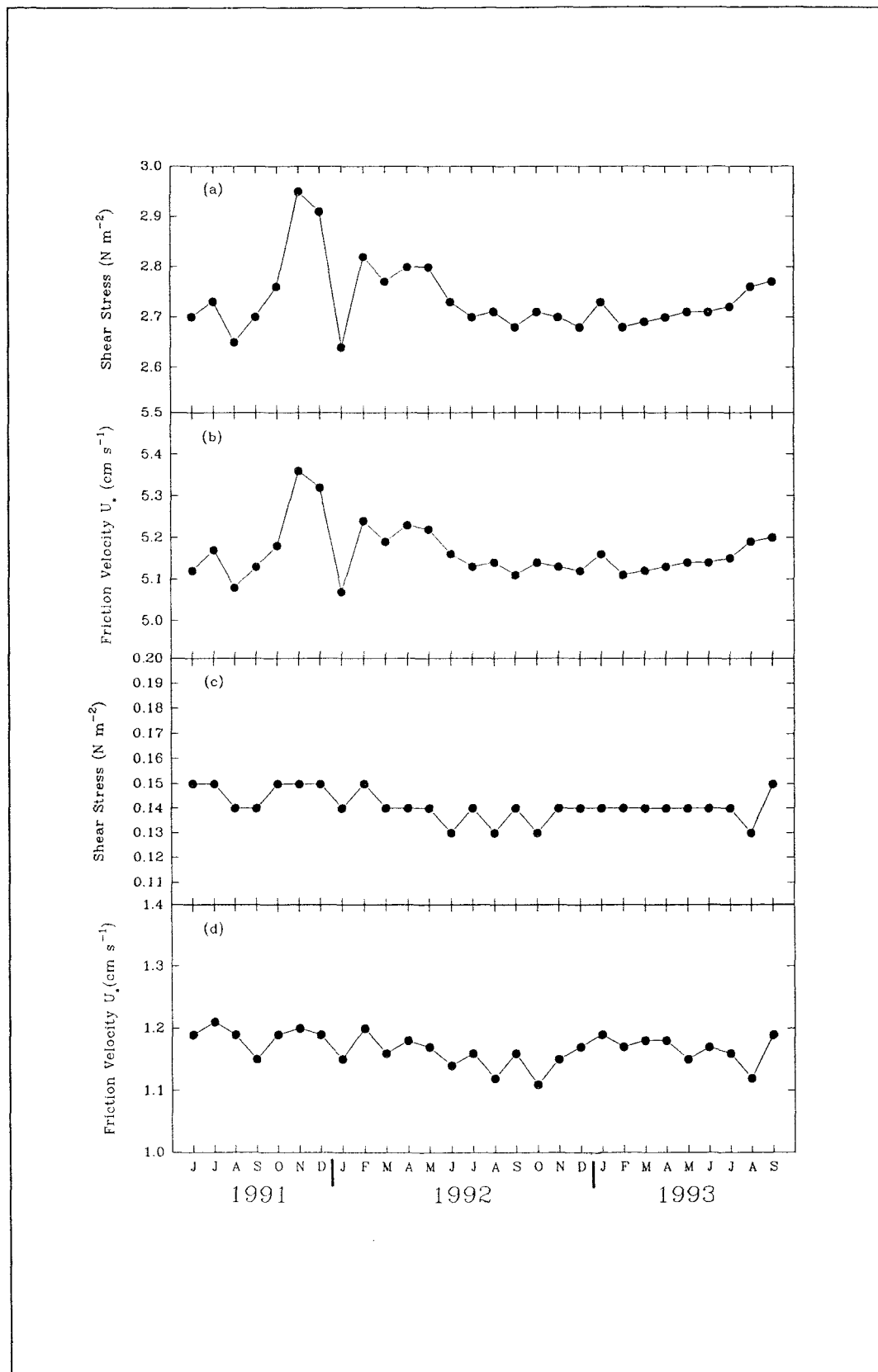


Figure 8.2. Long-term variation in critical shear stresses and friction velocities: based upon *in situ* shear strength (a and b); and based upon mean grain size (c and d)

obtained by applying grain size data to the Shields' curve modified by Miller *et al.*, (1977), their lowest values are 0.13 N m^{-2} and 1.11 cm s^{-1} , whilst the highest are 0.15 N m^{-2} and 1.21 cm s^{-1} , successively. The above findings may be attributable to the stabilising effect caused by *Lanice* tubes and other biotic and abiotic factors. For a comparison, earlier field results established by Fager (1964) showed that the tube-building polychaete *Owenia fusiformis* can stabilise a sand surface against movement by wave surge. Subsequently, Fonseca (1989) revealed that the seagrass *Halophila decipiens* increases the threshold velocity for sediment motion considerably, in comparison to that associated with bare sand. Likewise, Meadows and Hariri (1991) have reported that the construction of tubes by *Pygospio elegans* and *Fabricia sabella* increases the stability of sediments under laboratory conditions; this may increase their resistance to erosion. Based upon the results of the present investigation and the findings presented elsewhere, therefore, it may be inferred that the area under investigation remained stable throughout the period of study.

8.3. The Effects of Temperature on Shear Strength

Laboratory experiments undertaken as part of the present investigation (Section 7.12) have shown that there is a significant (at 5 % level of significance) negative correlation between shear strength and (pore) water temperature. These experiments were followed further by measurements of the effects of straw density on shear strength, at temperatures of 4°C and 17°C . The latter results supported the original findings; they reveal also that there is a highly significant (at 5 % level of significance) positive correlation between shear strength and straw density.

Based upon regression analysis undertaken on the data from the experiments carried out at 4°C and 17°C , at a straw density of 10 per 100 cm^2 , the following equation is obtained

$$Y = 2.26 - 0.01 X \quad (8.3)$$

where Y is shear strength of the sediment (KPa) and X is the (pore) water temperature ($^{\circ}\text{C}$). By applying this equation to the *in situ* temperatures measured in the field, an estimate of the monthly shear strength of the sediment can be obtained (Table 8.2 and Figure 8.3(b)). In order to compare these results with the measured *in situ* shear strength (Section 7.2), monthly shear strength and tube density data have been examined using least square regression. The shear strengths, at a tube density of 10 per 100 cm², predicted from these equations, are presented in Table 8.2 and displayed on Figure 8.3(a). The information presented on the Figure reveal that the predicted shear strength is lower than the measured *in situ* shear strength. Such a discrepancy suggests that temperature is not the only environmental parameter affecting shear strength. Indeed, the shear strength of the sediment deposits may be influenced by biogenous processes such as mucopolysaccharides produced by benthic organisms and diatoms. Such an interpretation is consistent with other findings: (i) that the diatom matrix may influence sediment stability (Paterson, 1988); and (ii) that sediment stability may increase when the mucopolysaccharides matrix within the surface sediments becomes dehydrated when dewatering of the sediment occurs (Paterson *et al.*, 1990).

8.4. Statistical Model

In order to advance the understanding of sediment stability further in intertidal waters, in general, the data of the present investigation are used to construct a model for the prediction of shear strength; thus, in turn, can be used to calculate the shear stress. This process involves several stages of involving statistical testing and analysis, such as: standardisation of the data matrix; establishing the correlation matrix; performing a cluster analysis; and undertaking principal component and multiple regression analyses. Such a detailed procedure was adopted, in order to ensure that the derived model will provide reliable predictions of shear strength using new data in the future.

Table 8.2. *In situ* shear strength measurement at tube density of 10 per 100 cm² and shear strength predicted based on *in situ* temperature

Month (Year)	<i>In Situ</i> Shear Strength (KPa)	Predicted Shear Strength (KPa)
June (1991)	2.56	2.11
July	3.10	2.04
August	2.47	2.05
September	2.84	2.10
October	4.35	2.05
November	4.41	2.18
December	4.39	2.18
January (1992)	2.85	2.20
February	4.22	2.18
March	3.67	2.16
April	3.71	2.15
May	3.89	2.09
June	3.40	2.04
July	3.15	2.08
August	3.38	2.08
September	3.29	2.11
October	3.20	2.13
November	3.09	2.13
December	3.15	2.17
January (1993)	4.09	2.19
February	3.22	2.18
March	3.49	2.20
April	3.41	2.14
May	3.09	2.12
June	3.19	2.04
July	4.23	2.08
August	3.85	2.09
September	4.14	2.10

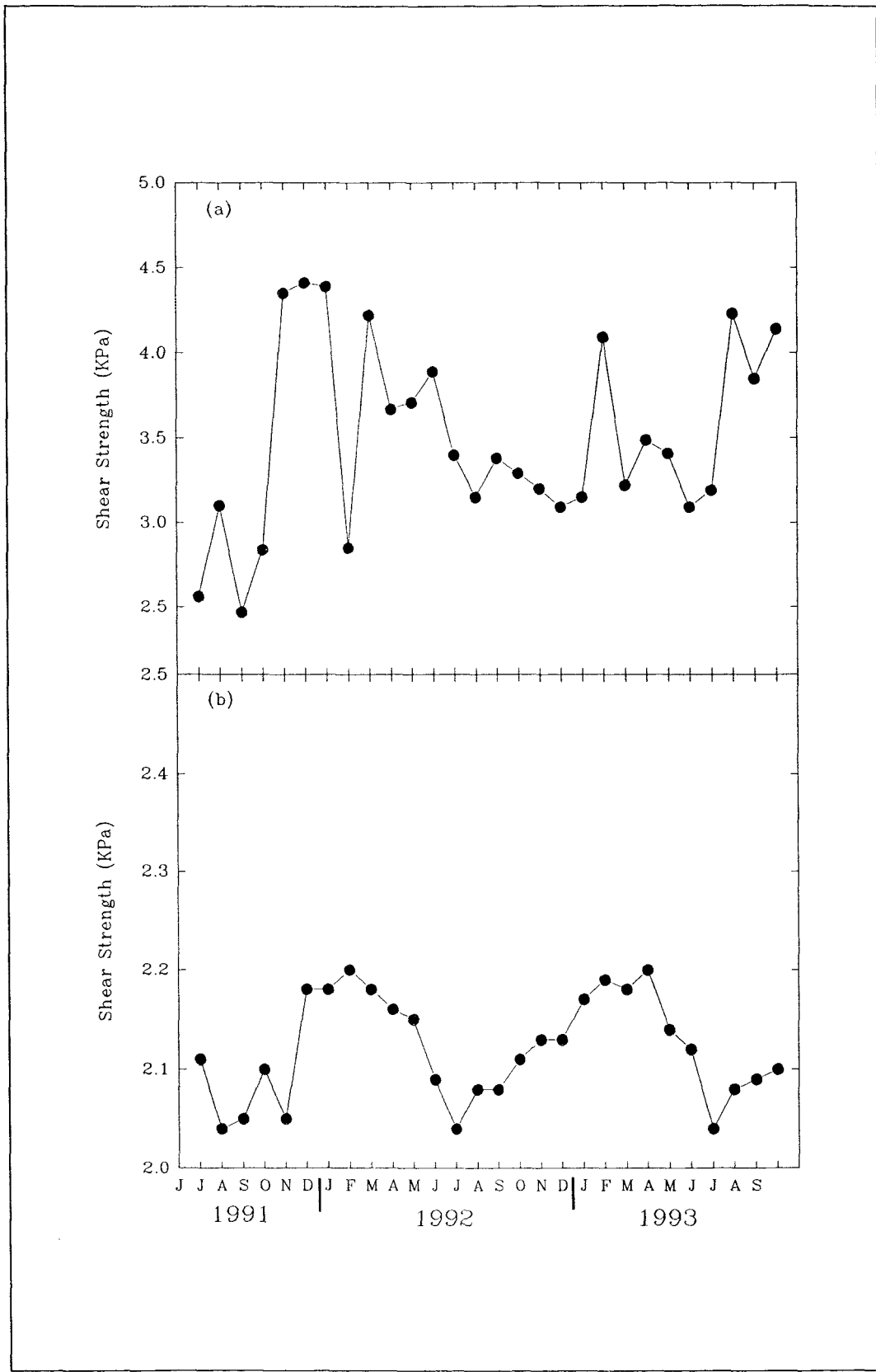


Figure 8.3. (a) *In situ* shear strength measurements at a tube density of 10 per 100 cm², (b) Predicted shear strength from *in situ* (pore) water temperature measurements

8.4.1. Data Matrix

The data matrix consist of 18 parameters, measured either directly or indirectly during the (28 month) sampling period, from June 1991 to September 1993. These data are presented in Table 8.3. Since the parameters were measured in different units, the data have to be standardised or converted to a dimensionless form prior to the statistical testing and analyses. The data standardisation was performed by subtracting the mean of the data set from each observation, then dividing by the standard deviation (Davis, 1973). Consequently, the newly standardised variables will have a mean of zero and a variance of unity. This method enables the data representing each of the variables to be comparable.

8.4.2. Correlation Matrix

On the basis of the fact that there is more than one independent variable, the collection of all the zero-order correlation coefficients (r 's) between all possible pairs of variables can be represented most compactly in terms of a correlation matrix (Kleinbaum *et al.*, 1988). Each of the correlations may be examined separately, in terms of the level of the linear relationship between the two variables involved. Such a representation provides an initial insight into the inter-relationships between variables. The correlation matrix between all the parameters have been analysed and the results are presented in Table 8.4. In the Table, correlation coefficients which are significant (at 5 % level of significance) are highlighted; whilst those which are not significant are lightly printed.

The t -test is used here to assess the significance of each of the relationships between the parameters, at 5 % level of significance. Since the data matrix contains 18 parameters, it has 17 degrees of freedom. This provides a critical value of t equal to 2.11. This t value is then converted to r using the following relationship,

Table 8.3. Data matrix for the present investigation

Month (Year)	Shear Strength (kPa)	Shear Stress (N m ⁻²)	Water Temperature (°C)	Water Salinity (‰)	Grain Size (Φ)	Sorting (Φ)
June (1991)	2.48	2.70	14.8	34.0	2.89	0.98
July	2.72	2.73	22.5	36.0	2.84	0.78
August	2.19	2.65	21.5	38.0	2.97	1.09
September	2.54	2.71	16.0	36.0	3.10	1.23
October	2.87	2.76	21.5	38.0	2.89	0.88
November	4.08	2.95	8.5	36.0	2.85	0.90
December	3.80	2.91	8.0	34.0	2.89	0.91
January (1992)	2.11	2.64	6.0	33.0	3.09	1.08
February	3.25	2.82	8.0	33.0	2.88	0.80
March	2.94	2.77	10.0	34.0	3.07	0.95
April	3.15	2.80	11.5	32.0	3.00	1.01
May	3.13	2.80	17.0	34.0	3.02	0.97
June	2.68	2.73	22.5	35.0	3.11	1.10
July	2.52	2.70	18.5	35.0	3.04	0.96
August	2.55	2.71	18.5	34.0	3.14	1.08
September	2.40	2.68	15.5	34.0	3.06	0.92
October	2.55	2.71	13.0	33.0	3.13	1.07
November	2.48	2.70	13.0	32.0	3.08	1.00
December	2.40	2.68	9.5	29.0	3.02	0.96
January (1993)	2.68	2.73	7.5	29.0	2.96	0.92
February	2.40	2.68	8.0	32.0	3.02	0.90
March	2.44	2.69	6.5	34.0	3.01	1.00
April	2.52	2.70	12.0	34.0	3.01	1.00
May	2.57	2.71	14.5	34.0	3.09	1.12
June	2.58	2.71	22.0	34.0	3.02	1.02
July	2.65	2.72	18.0	34.0	3.05	1.03
August	2.87	2.76	17.0	34.0	3.12	1.12
September	2.97	2.77	16.5	34.0	2.92	1.12

Table 8.3. (Continued)

Month (Year)	Skewness (Φ)	Moisture Content (%)	Low Water Height (m)	Organic Matter Content (%)	Protein (mg g ⁻¹ ds)	Bacterial Protein $\times 10^4$ (mg g ⁻¹ ds)
June (1991)	2.76	30.29	0.8	0.91	1.27	29.51
July	1.83	33.86	0.6	1.09	1.31	29.53
August	2.56	34.16	0.6	1.07	1.61	29.27
September	2.31	34.88	0.8	1.32	1.27	15.60
October	2.79	32.33	0.5	1.05	0.98	11.51
November	2.87	31.84	0.6	1.04	0.78	6.72
December	2.95	29.23	1.1	1.14	1.08	14.28
January (1992)	2.55	33.67	0.3	1.24	1.02	5.31
February	1.32	32.79	0.4	1.65	1.24	9.28
March	2.66	32.95	0.2	1.62	1.30	14.40
April	2.48	32.65	1.0	1.20	1.22	23.92
May	2.69	31.44	0.7	1.32	2.10	29.42
June	2.49	27.88	1.1	1.43	1.99	46.38
July	2.41	30.12	0.7	2.01	2.42	54.45
August	2.39	32.43	1.0	1.31	1.97	35.83
September	2.54	30.95	0.9	1.06	1.02	12.53
October	2.52	29.58	0.9	1.14	1.06	12.50
November	2.59	31.42	0.6	1.15	0.86	7.43
December	2.71	30.15	1.0	1.65	1.57	20.67
January (1993)	2.60	31.39	0.6	1.13	0.93	4.84
February	1.92	31.78	0.8	1.11	0.83	6.24
March	2.73	31.34	0.0	1.19	0.95	10.58
April	2.74	29.84	0.2	1.08	1.10	21.53
May	2.30	31.47	0.9	1.45	2.31	32.32
June	2.69	30.84	0.8	1.22	1.70	39.57
July	2.58	34.02	1.0	1.64	1.97	44.43
August	2.45	33.99	0.7	1.32	1.98	36.11
September	2.71	31.53	0.9	1.93	1.85	22.81

Table 8.3. (Continued)

Month (Year)	Bacterial Abundance $\times 10^9$ (g ⁻¹ ds)	Silt/Clay Content (%)	Tube Density (100 cm ⁻²)	Air Temperature (°C)	Wind Speed (knots)	Rainfall (mm)
June (1991)	0.84	0.14	8.67	13.37	13.04	2.95
July	0.84	0.10	8.38	17.45	11.58	2.36
August	0.84	0.53	7.93	18.32	9.53	0.40
September	0.45	0.73	8.25	17.24	9.74	0.48
October	0.33	0.26	5.17	12.58	10.27	2.80
November	0.19	0.17	8.33	9.16	12.70	2.91
December	0.41	0.15	7.75	7.04	10.90	0.92
January (1992)	0.15	0.18	5.42	4.95	8.71	0.54
February	0.27	0.14	6.00	6.20	11.36	1.53
March	0.41	0.18	6.83	7.93	13.36	1.57
April	0.68	0.22	6.92	10.05	12.63	2.27
May	0.84	0.20	5.83	15.41	10.41	0.20
June	1.33	0.54	5.58	16.26	7.70	0.79
July	1.56	0.44	6.13	17.57	10.77	2.44
August	1.02	0.50	5.93	16.95	15.00	3.13
September	0.36	0.13	4.67	14.87	11.49	1.58
October	0.36	0.64	5.62	9.33	11.38	2.03
November	0.21	0.13	4.87	9.11	16.58	5.83
December	0.59	0.12	5.69	5.37	10.07	2.30
January (1993)	0.14	0.12	5.00	7.36	17.77	3.51
February	0.18	0.17	6.83	6.14	7.64	0.36
March	0.30	0.16	4.17	6.23	10.66	0.46
April	0.62	0.27	4.80	8.73	12.12	3.54
May	0.92	0.62	5.63	12.52	12.10	1.60
June	1.13	0.17	5.80	15.66	11.50	2.84
July	1.27	0.13	3.13	16.39	10.90	1.53
August	1.03	0.60	4.93	16.53	12.58	1.17
September	0.65	0.31	4.75	14.03	9.72	3.47

Table 8.4. Correlation Matrix between the Various (Normalised) Parameters Measured as Part of the Present Investigation

Parameter	Shear Strength	Shear Stress	Water Temperature	Salinity	Grain Size	Sorting	Skewness	Moisture Content	Low Water Height	Organic Matter Content	Protein	Bacterial Protein	Bacterial Abundance	Silt/Clay Content	Tube Density	Air Temperature	Wind Speed	Rainfall
Shear Strength	1.00																	
Shear Stress	1.00	1.00																
Water Temperature	-0.20	-0.20	1.00															
Salinity	0.12	0.12	0.59	1.00														
Grain Size	-0.52	-0.52	0.08	-0.21	1.00													
Sorting	-0.36	-0.36	0.22	0.10	0.67	1.00												
Skewness	0.12	0.12	-0.01	0.04	0.04	0.27	1.00											
Moisture Content	-0.09	-0.09	0.08	0.27	-0.01	0.12	-0.34	1.00										
Low Water Height	0.12	0.12	0.34	-0.13	0.16	0.25	0.05	-0.26	1.00									
Organic Matter Content	0.02	0.02	0.07	-0.14	0.19	0.17	-0.19	0.01	0.13	1.00								
Protein	-0.12	-0.12	0.57	0.15	0.34	0.41	-0.06	-0.02	0.39	0.64	1.00							
Bacterial Protein	-0.15	-0.15	0.72	0.27	0.24	0.30	0.01	-0.11	0.41	0.42	0.88	1.00						
Bacterial Abundance	-0.15	-0.15	0.72	0.27	0.24	0.30	0.01	-0.11	0.41	0.42	0.88	1.00	1.00					
Silt/Clay Content	-0.20	-0.20	0.39	0.35	0.55	0.74	-0.08	0.08	0.26	0.15	0.46	0.36	0.36	1.00				
Tube Density	0.29	0.29	0.03	0.32	-0.42	-0.16	-0.13	0.13	0.10	-0.31	-0.18	-0.07	-0.07	0.08	1.00			
Air Temperature	-0.15	-0.15	0.91	0.59	0.15	0.35	-0.03	0.22	0.37	0.12	0.64	0.75	0.75	0.48	0.10	1.00		
Wind Speed	0.13	0.13	-0.16	-0.35	-0.06	-0.15	0.12	0.04	-0.11	-0.20	-0.17	-0.16	-0.16	-0.18	-0.07	-0.09	1.00	
Rainfall	0.05	0.05	0.06	-0.23	-0.17	-0.16	0.19	-0.21	0.01	-0.04	-0.16	-0.06	-0.06	-0.24	-0.15	-0.05	0.69	1.00

$$t = \frac{r}{\sqrt{\frac{(1 - r^2)}{(n - 1)}}} \quad (8.4)$$

where $n - 1$ is the degrees of freedom. The calculated r based on this equation gives a value of 0.456 which is used as a barometer for significance in the correlation matrix.

From the results presented in Table 8.4, there are 20 significant (at 5 % level of significance) correlations between the various parameters. Salinity and water temperature show a positive correlation (0.59), with a temperature increase related to an increase in salinity. Grain size (Φ) and shear strength/shear stress are represented by negative correlations (-0.52), indicating that a decrease in grain size leads to an increase in shear strength/shear stress. Sediment sorting and grain size reveal a positive correlation (0.67), indicating that grain size increase results in decrease in sorting.

Protein (0.57), bacterial protein (0.72) and bacterial abundance (0.72) are all positively correlated with pore-water temperature; this appears to be acceptable, as the warmer temperatures lead to higher activities of the microorganisms. The silt/clay content shows positive correlation with grain size (0.55) and sorting (0.74). Thus, the smaller the grain size, the more surficial area; this provides more space for silt/clay materials. Air temperature positively correlated with both pore-water temperature (0.91) and salinity (0.59). This relationship means that pore-water temperature and salinity increases in accordance with an increase in air temperature. Correlation between protein and organic matter content is represented positively (0.64), suggesting that protein increases with an increase in organic matter content (this may be explained in terms of the protein in this study being calculated from the organic matter content). A similar pattern is representative of bacterial protein and bacterial abundance, which were derived from protein content. Thus, these two parameters have positive correlation with protein (0.88). Air temperature and the silt/clay content reveal a positive correlation (0.48). Such an inter-relationship may be indirect, because the high air temperatures in summer tend to coincide with relatively calm weather conditions. Such conditions are conducive for the

enhanced deposition of silt/clay. Finally, rainfall and wind conditions are represented by a positive correlation (0.69), indicating that rainy days tend to be accompanied by stronger wind speeds.

The correlation patterns summarised above provides mainly an initial insight into the inter-relationships between the parameters within the data matrix. Subsequently, statistical tests and analyses have been undertaken to delimit the parameters of importance in controlling sediment stability on intertidal flats. Such approaches are described in the succeeding text.

8.4.3. Cluster Analysis (see also Section 4.5.3)

Cluster analysis is a classification technique to place objects into more or less homogenous groups, in such a way that it will reveal the relationship between the groups (Davis, 1973). This method is used by taxonomists, in an attempt to deduce the lineage of living creatures from their characteristics and similarities. In later developments, it has been used in other branches of scientific investigations.

There are four different types of cluster analysis (Sneath and Sokal, 1973), including 'hierarchical cluster analysis' which is adopted in the present study. The hierarchical cluster analysis operates by joining the most similar observations, then connecting the next most similar observations to the first cluster. Assuming that there are m parameters with n measurements, the data set will form $m \times n$ matrix. Measurements of resemblance, or similarity coefficients, must then be calculated between every pair of parameters; this is termed a standardised m -space Euclidian distance, d_{ij} . The distance coefficient is calculated by,

$$d_{ij} = \sqrt{\frac{\sum_{k=1}^m (X_{ik} - X_{jk})^2}{m}} \quad (8.5)$$

where X_{ik} represents the k th variable measured on object i and X_{jk} represent the k th variable measured on object j .

Firstly, the most similar observations are joined; this is followed then by joining the next similar observations to the first cluster or group (see above). This procedure is performed by averaging the similarities in the combined

observations, then joining them with their closest similarity. This process continues until the similarity matrix is reduced to 2×2 . The level of similarity amongst the observations are used then to construct a dendrogram.

The present data consist of 18 parameters with 28 observations, leading to an 18×28 matrix. Applying these data to hierarchical cluster analysis results in a dendrogram, which is represented as Figure 8.4. The dendrogram reveals that the present data may be categorised into four main clusters. The first cluster consists of shear strength, shear stress and tube density. The second cluster consists of wind speed, rainfall and skewness. The third cluster consists of pore-water temperature, air temperature, bacterial protein, bacterial abundance, protein, salinity, low water height, sorting, silt/clay content, grain size and organic matter content. The fourth cluster consists only of moisture content. Within the first cluster, tube density is related closely to shear strength, with a Euclidian distance of approximately 6. This is followed by the second cluster, which is separated from the first cluster at an Euclidian distance of approximately 7. The third and fourth cluster are the farthest, in terms of their relationship to shear strength; they are separated from the first and second cluster at Euclidian distance of approximately 7.5. Overall, that cluster analysis provides only the distance of similarity between the variables; therefore, further statistical analysis needs to be performed to identify the main controlling variables.

8.4.4. Principal Components Analysis (PCA)

Principal Components are merely the eigenvectors of a variance-covariance matrix, where the eigenvectors are the vectors that define the arbitrary axis of an m dimensional ellipsoid (Davis, 1973). The method used in this analysis is to find the combination of m original variables to form a new set of m variables which are uncorrelated (Manly, 1986). Any lack of correlation is a useful property, because it means that the new variables are measuring different dimensions in the data. This method has been described more fully in Section 4.5.2.

The data from the present study are analysed here using the PCA

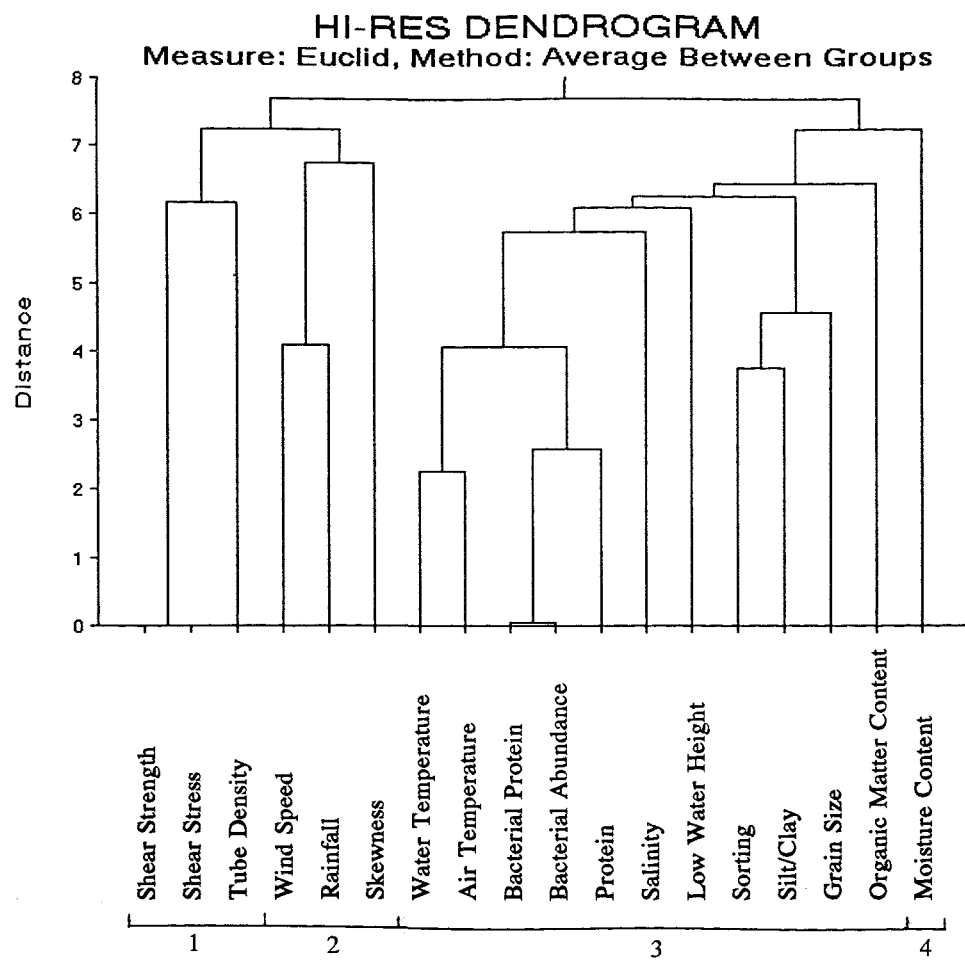


Figure 8.4. Dendrogram showing classification of parameters, using Hierarchical Cluster Analysis

technique, in order to determine the parameters which cause major variation in the data. The percentage variances of each Principal Components are presented in Table 8.5. The results reveal that the first five components have cumulative percentage variance of more than 75 % (75.7 %). Since there are only 5 components causing the majority of variation in the data, the factor loadings of these 5 factors have been taken for further interpretation. The factor loadings of these five factors are presented in Table 8.6 and are shown diagrammatically on Figures 8.5(a) and 8.5(b).

Factor loadings describe the correlations between the factors emerging from a factor analysis and the original variables (Kleinbaum *et al.*, 1988). A loading is the correlation of a variable with a factor; hence, it can be used to identify those variables which are highly correlated (i.e. high loading) with a given factor. On this basis, the factor can be interpreted conceptually.

It may be seen from Table 8.6 that the most important variables in Factor 1 are: bacterial abundance, bacterial protein, protein, air temperature and water temperature. The first three parameters (bacterial abundance, bacterial protein, protein) can be considered as a single biological factor, as they are predicted from organic matter content. The last two parameters (air temperature and water temperature) can be considered as interrelated physical controls, whereby water temperature depends upon air temperature.

The most dominant variables in Factor 2 are: shear strength, shear stress, grain size and tube density. Shear strength and shear stress can be considered as one factor, because they are linked with each other. In terms of dominance, shear strength and shear stress are the most dominant variables; these are followed

successively by grain size and tube density.

In Factor 3, the most dominant variables are: rainfall, moisture content and salinity. These parameters can also be considered as one physical factor, because rainfall influences moisture content and salinity. Likewise, moisture content also influences salinity. Factor 4 is represented by rainfall, organic matter content and wind speed. Factor 5 is represented by skewness, sorting and silt/clay content. These latter three parameters can be considered as one

Table 8.5. Percentage variance represented by each of the Principal Components

Component	Percent Variance	Cumulative Percent Variance
1	30.69	30.69
2	15.43	46.11
3	12.05	58.16
4	9.21	67.38
5	8.33	75.70
6	6.58	82.28
7	5.66	87.94
8	3.21	91.15
9	2.98	94.13
10	2.64	96.76
11	1.02	97.79
12	0.84	98.63
13	0.46	99.09
14	0.41	99.51
15	0.33	99.84
16	0.16	100.0

sedimentological factor, because skewness and sorting are statistical parameters representing grain size. In turn, grain size will influence the silt/clay content.

In terms of the parameters which cause major variation in the data, it can be deduced that bacterial abundance, bacterial protein, protein, temperature, shear strength, shear stress, grain size, tube density, rainfall and silt/clay content are the most dominant parameters. Hence, the principal components analysis has isolated the most important of the variables measured during the present investigation. The final step on the analysis is to understand how these variables influence the shear strength of intertidal flat sediments.

Table 8.6. Factor loadings of the five Factors explaining the majority of the variation in the data set

Parameter	Factor 1	Factor 2	Factor 3	Factor 4	Factor 5
Shear Strength	-0.35	0.75	0.25	-0.27	0.24
Shear Stress	-0.35	0.75	0.25	-0.27	0.24
Water Temperature	0.78	0.32	-0.05	0.40	-0.13
Water Salinity	0.37	0.54	-0.54	0.26	0.10
Grain Size	0.49	-0.70	0.03	-0.08	0.26
Sorting	0.60	-0.41	-0.11	0.01	0.53
Skewness	-0.03	-0.01	0.34	0.27	0.63
Moisture Content	0.05	0.02	-0.58	0.12	-0.31
Low Water Height	0.44	0.20	0.36	-0.16	0.30
Organic Matter Content	0.41	-0.06	0.33	-0.57	-0.34
Protein	0.86	0.09	0.26	-0.24	-0.15
Bacterial Protein	0.88	0.21	0.26	-0.01	-0.17
Bacterial Abundance	0.88	0.21	0.26	-0.01	-0.17
Silt/Clay	0.66	-0.12	-0.26	-0.03	0.42
Tube Density	-0.12	0.57	-0.38	0.08	0.18
Air Temperature	0.83	0.33	-0.10	0.33	-0.07
Wind Speed	-0.30	-0.07	0.49	0.55	-0.07
Rainfall	-0.20	-0.01	0.62	0.60	-0.13

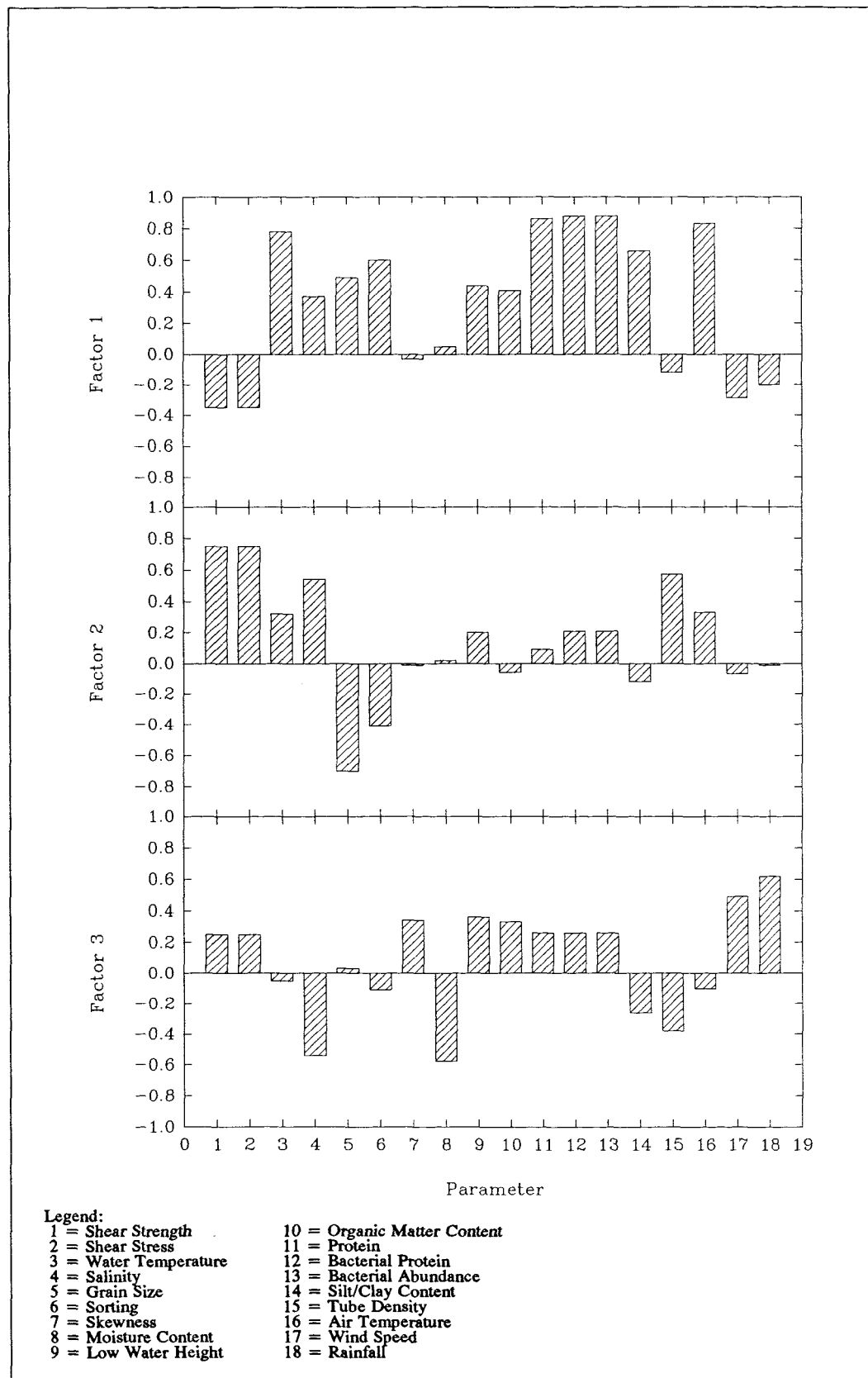
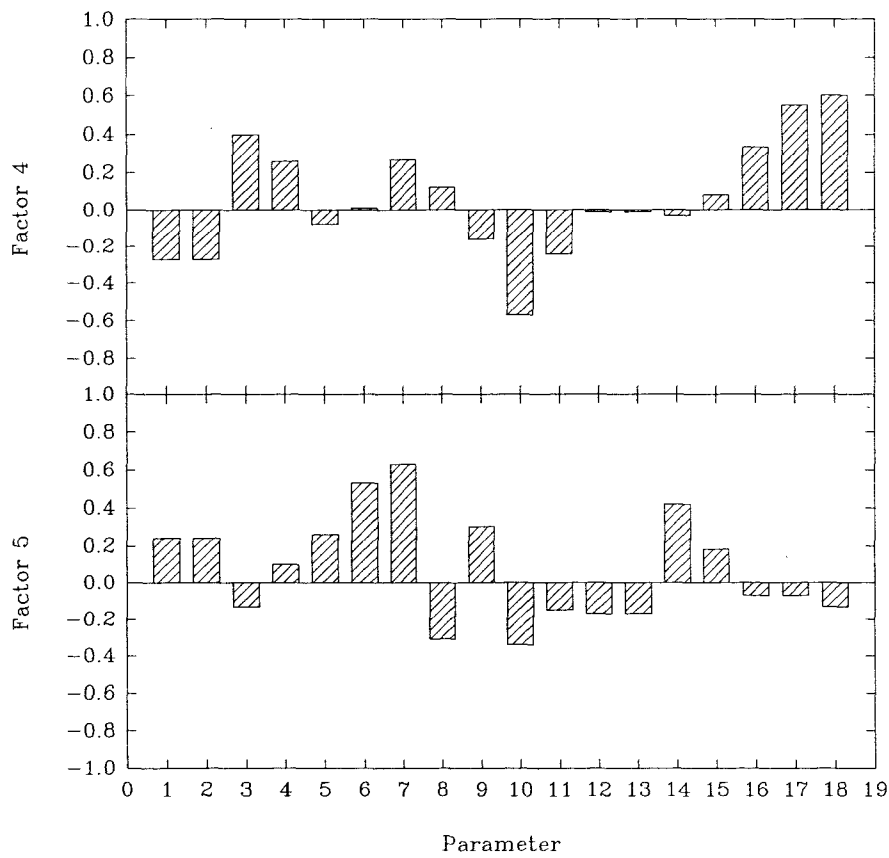


Figure 8.5(a). Factor loadings of Factors 1, 2 and 3



Legend:

1 = Shear Strength	10 = Organic Matter Content
2 = Shear Stress	11 = Protein
3 = Water Temperature	12 = Bacterial Protein
4 = Salinity	13 = Bacterial Abundance
5 = Grain Size	14 = Silt/Clay Content
6 = Sorting	15 = Tube Density
7 = Skewness	16 = Air Temperature
8 = Moisture Content	17 = Wind Speed
9 = Low Water Height	18 = Rainfall

Figure 8.5(b). Factor loadings of Factors 4 and 5

8.4.5. Multiple Linear Regression (see also Section 4.5.3)

Multiple linear regression can be considered as an extension of linear regression analysis (which involves only one independent variable) to the situation when there is more than one independent variable to be considered (Kleinbaum *et al.*, 1988). An example of a multiple regression model is given by any second or higher order polynomial. The addition of high order terms such as an X^2 or X^3 , to the model, is equivalent to the addition of new variables.

Renaming X as X_1 and X^2 as X_2 for the second order model,

$$Y = \beta_0 + \beta_1 X + \beta_2 X^2 + E \quad (8.6)$$

This equation can be rewritten as,

$$Y = \beta_0 + \beta_1 X_1 + \beta_2 X_2 + E \quad (8.7)$$

In polynomial regression, there is only one basic independent variable; the others are relatively simple mathematical functions of this basic variable. In more general multiple linear regression analyses, however, there can be more than one basic independent variable. The general form for a regression model with k independent variables is given by,

$$Y = \beta_0 + \beta_1 X_1 + \beta_2 X_2 + \dots + \beta_k X_k + E \quad (8.8)$$

where $\beta_0, \beta_1, \beta_2, \dots, \beta_k$ are the regression coefficients to be estimated; X_1, X_2, \dots, X_k may all be separate variables, or some function of a few basic variables.

The ability of a multiple regression analysis to quantify the relative importance of several possible independent variables makes it a useful approach to understanding complicated problems (Glantz and Slinker, 1990). As the purpose of this analysis is to quantify the relative importance of several independent variables against the dependent variable, multiple regression is adopted for the present analysis. Multiple regression is applied to the present data set, with shear strength as the dependent variable and the other 16 parameters as independent variables. Shear stress is removed from this analysis, since it is considered another form of expressing shear strength. Generally, certain

independent variables will prove to be greater predictors of the dependent variable than others.

In the first stage of the analysis, multiple regression is undertaken using all 28 months data (using Sigmastat Statistical Package). The regression equation obtained was

$$\tau = 9.531 - 0.014WT - 2.259GS + 0.033TD \quad (8.9)$$

where τ is the shear strength (KPa), WT is the pore-water temperature ($^{\circ}$ C), GS is grain size (Φ) and TD is tube density (100 cm^{-2}). The value of $r = 0.553$ and $p = 0.03$. With 27 degrees of freedom, four variables and 5 percent level of significance, the critical value of $r = 0.498$. The computed r exceeds the critical r ; therefore, the null hypothesis that there is no association between the variables is rejected at the given level of significance (Kennedy and Neville, 1986). This interpretation suggests that there is a significant correlation between the variables and that the derived equation can be used to predict shear strength from a new data set.

Despite the fact that the above equation is statistically significant, it would appear that seasonal variation in the data may lead to a low computed value r (from the regression between dependent and independent variables). Consequently, the data have been divided on seasonal basis, representing summer and winter. This division is based upon pore-water temperature measurements, which appear to represent the most distinct seasonal pattern (compared to other parameters under study (see Figure 7.1)). Summer months are represented by data collected from May to October, whilst winter months include November to April. This method leads to the division of the present data into three summer and two winter seasonal data sets. The data are then merged, resulting in 16 summer months and 12 winter months. Each group of data has been analysed independently using multiple regression analysis.

The regression equation obtained for the summer months is as follows,

$$\tau = 5.758 - 0.004WT - 0.863GS - 0.073TD \quad (8.10)$$

This regression expression has $r = 0.483$ and $p = 0.346$. With 15 degrees of

freedom, 4 variables and at the 5 percent level of significance, the critical value of $r = 0.630$. The computed value is less than the critical r , suggesting that the regression equation is not significant at the given level of significance.

The regression equation obtained for the winter months only data is as follows,

$$\tau = 15.633 + 0.051WT - 4.868GS + 0.217TD \quad (8.11)$$

This regression gives a value of $r = 0.947$ and a value of $p = 0.001$. With 11 degrees of freedom, 4 variables and 5 percent level of significant, the critical value of $r = 0.703$. Hence, the computed r exceeds the critical r ; this suggests that the regression equation is significant, at the given level of significance.

Overall, there are only two regression equations which are statistically significant; those obtained using all the data and for the equation using winter months only. The equation representing all the data indicates that shear strength is affected negatively by both pore-water temperature and grain size; it is affected positively by tube density. The equation demonstrates also that grain size is the dominant parameter affecting the shear strength; this is followed by tube density and pore-water temperature.

The equation obtained using the data obtained during the summer months alone indicates that there is an inverse relationship between tube density and shear strength. This finding appears to contradict the established notion that tube-building polychaetes will increase sediment stability. However, a possible argument for the present discrepancy may be that benthic organisms tend to be more active, increasing the level of bioturbation, during the summer months; this would lead to disturbance of the surficial sediments of the intertidal flats.

Another possible cause is that bait digging and mussel collection over the study area may increase during summer months; this may cause disturbance to the surface sediments. These effects may reverse the contribution of tube density to shear strength, from a positive to a negative effect.

The equation obtained for the winter data indicates only a positive effect of pore-water temperature on shear strength. Once again, this does not appear to be in agreement with the previous findings i.e. that the relationship between

temperature and shear strength is negative. Since the range between the lowest and the highest winter temperature during this investigation is relatively small (6°C to 13°C); it may be that the usual inverse relationship cannot be measured. This condition may have been enhanced by the effects of tube density and the presence of other organisms, leading to the present positive correlation.

Having selected a model which best represents a particular data set, it has to be investigated if such a model can be applied reliably to other samples. Such a model can only be said to be reliable if it can predict successfully for subsequent samples, from the population of interest (Kleinbaum *et al.*, 1988). The three models obtained in this study (see above), have to be tested, therefore, for their reliability in predicting new samples. For this purpose, the PRESS statistics are used as an overall measure of how well the candidate regression model predicts new data (Glantz and Slinker, 1990). PRESS (the Predicted Residual Error Sum of Squares) is calculated by summing the squares of the prediction errors (the differences between the predicted and observed values) for each observation, with that point deleted from the computation of the regression equation. The test operates by comparing the PRESS statistical values of several different candidate regression models. The model associated with the lowest value could then be judged the most appropriate in terms of its predictive ability. The PRESS statistics values for the three models described above are: 5.187 for all data (equation 8.9); 0.938 for the summer data only (equation 8.10); and 0.836 for the winter data only (equation 8.11). Thus, equation 8.11 is shown to be the most reliable for the prediction of new data on shear strength.

8.5. Comparison with Previous Studies

8.5.1. The Shields' Diagram

Various empirical relationships have been proposed to define the threshold conditions of sediment movement (Miller *et al.*, 1977). These relationships are in the form of a critical velocity (u_c) or a critical shear stress (τ_c), which are related

to sediment parameters; they adopt the form of equations or graphs (Miller *et al.*, op. cit.). Although some of the equations appear to successfully relate to threshold over certain limits of the parameters, none has been shown to be a general relationship for all combinations of grain size, densities and flow conditions. Amongst these approaches, the most frequently used graphs are those presented by Hjulström (1935, 1939) and Shields (1936).

The Shields' diagram provides a major advance in the determination of threshold (Shields, 1936). In those early experiments, physical arguments were used to combine the parameters of interest into several non-dimensional relationships. The parameters considered included: density of the sediment (ρ_s); the grain diameter (D); fluid density (ρ); kinematic fluid viscosity (ν); the shear stress of the fluid flow (τ); and the acceleration due to gravity (g). The dimensionless relationships derived for these combined parameters are

$$\theta = \frac{\tau}{(\rho_s - \rho) g D} = \frac{\rho U_*^2}{(\rho_s - \rho) g D} = f\left(\frac{U_* D}{\nu}\right) = f\left(\frac{D}{\delta}\right) \quad (8.12)$$

where θ is the 'Shields entrainment function' representing the non-dimensional relative shear stress, δ is the thickness of the viscous sublayer and U_* is the friction velocity.

The thickness of the viscous sublayer can be obtained using the following equation (Kline *et al.*, 1967),

$$\delta = \frac{1.0 \nu}{U_*} \quad (8.13)$$

The friction velocity can be calculated as follows,

$$U_* = \sqrt{\frac{\tau}{\rho}} \quad (8.14)$$

The friction velocity is a measure of shear stress but, with units of velocity. A combination of friction velocity, grain diameter and kinematic fluid viscosity describes the dimensionless grain Reynolds number, which is generally denoted,

$$Re_* = \frac{U_* D}{\nu} \quad (8.15)$$

When the 'Shields entrainment function' represents threshold conditions

for sediment motion, it is usually denoted by θ_t and is called the Shields criterion (Miller *et al.*, 1977). It may be considered also as a form of grain Froude number, since it can be shown to represent the relative magnitudes of the inertial force and gravitational force on a grain acted upon a fluid flow. Similarly, this function can be viewed as a drag coefficient, which is the ratio of the applied tangential force to the resisting force.

The Shields diagram of θ_t versus Re proposed originally (Shields, 1936) was modified by Miller *et al.*, (1977) using additional and selected data. For the comparison with previous studies, the modified Shields curve is used here. Using equations 8.12 and 8.15, the 'Shields entrainment function' and the grain Reynolds number are calculated for the data obtained during the present investigation; these are presented in Table 8.7. The values obtained have been plotted on the Shields diagram, together with data from other investigators on Figure 8.6. All the data points lie well above the modified Shields curve, suggesting that natural parameters have an overall stabilising effect on surficial sediments in intertidal waters. However, both the original and modified Shields curves were derived using unimodal abiotic sediments. Elsewhere, it has been suggested that without the presence of large macrofaunal organisms, sediment cohesion is a function of microbially-induced binding (Black, 1991). Such conditions can result in a 40 % increase in critical shear stress, compared to the abiotic state.

It has to be taken into account, however, that numerous criteria have been used by investigators elsewhere to define the 'initiation of motion' of sediment grains. Generally, the criterion which has been adopted has been the number of particles in motion, per unit area and per unit time. This method results in different locations of the Shields curve (see Lavelle and Mofjeld, 1987); the more particles in motion, the higher the θ_t (Shields Criterion). The modified Shields curve as used by Miller *et al.*, (1977) appears to relate to the lowest number of particles in motion (approx 1 to 10). Despite the fact that the results of the present study lie well above the modified Shields curve (Figure 8.6), the application of the conclusions obtained (i.e. that biological factors, particularly tube density of *Lanice conchilega* increase the shear strength of surficial

Table 8.7. Shields' Entrainment Function and Grain Reynolds Number for the data obtained during the present investigation

Month (Year)	θ_t	Re.
June (1991)	1.25	6.92
July	1.23	7.24
August	1.30	6.50
September	1.45	6.00
October	1.28	6.99
November	1.33	7.44
December	1.35	7.18
January (1992)	1.41	5.93
February	1.30	7.13
March	1.46	6.18
April	1.41	6.54
May	1.43	6.43
June	1.47	5.98
July	1.39	6.26
August	1.48	5.91
September	1.40	6.14
October	1.49	5.86
November	1.43	6.05
December	1.37	6.30
January (1993)	1.32	6.66
February	1.37	6.29
March	1.36	6.34
April	1.37	6.36
May	1.45	6.01
June	1.38	6.33
July	1.41	6.23
August	1.50	5.96
September	1.32	6.86

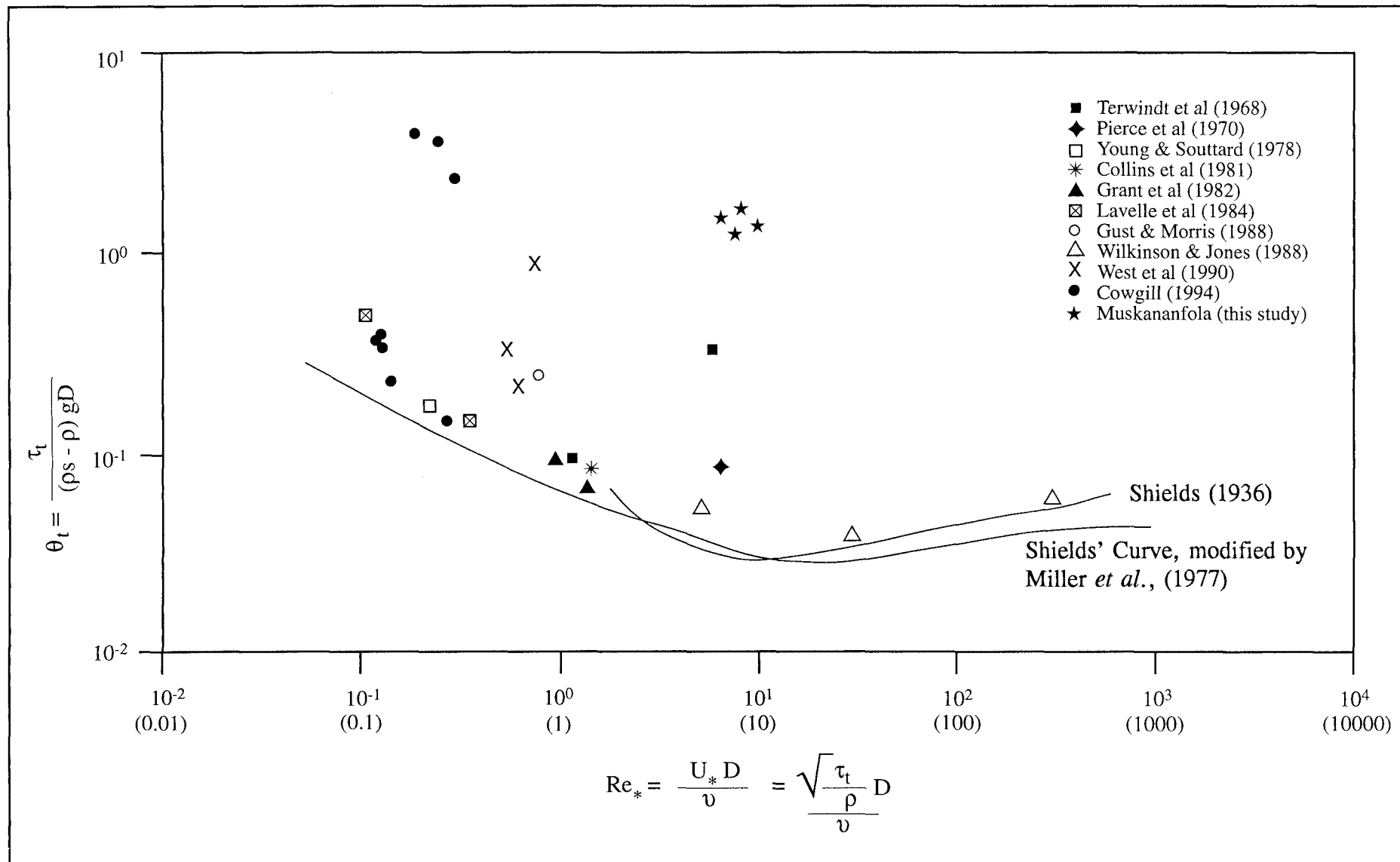


Figure 8.6. The Shields' Curve, with the addition of data from previous studies and the present investigation

sediments) may be somewhat limited. Such an observation results from the fact that different initial motion criteria will provide different results. Further, the results and critical conditions defined originally by Dunn (1959) are not valid for shear strength of less than 2873.4 N m^{-2} .

Overall, however, the present data (on the Shields entrainment function and the Grain Reynolds Number) can be used to predict and obtain an insight into the general conditions of sediment stability over intertidal flats, in particular, or within the marine environment generally. This conclusion is supported by statistical tests undertaken on the data of the present investigation, which reveal that (at least, to a certain extent) the tube densities of *Lanice conchilega* contribute to an increase of shear strength of surficial sediments.

8.5.2. Intertidal Sediment Stability

The earliest experiment undertaken into *in situ* sediment stability was performed by Scoffin (1968), using a seaflume in the Bimini Lagoon (Bahamas). The results revealed that filamentous algae play a major role in controlling sediment stability. Later, Scoffin (1970) reported for the same area that mangrove and microscopic algae stabilise the sediment on which they grow. It was found that sediment overgrown by vegetation was two orders of magnitude more resistant to erosion, in relation to: (i) the fact that part of the plants above the sediment-water interface acts as a baffle to the currents, reducing their velocity; and (ii) that the root system or holdfast of the plants binds the sediment grains together.

Another flume experiment was conducted in the Haringvliet Estuary, the Netherlands (Terwindt *et al.*, 1968). The results of this investigation indicated a critical bed shear stress of 1.1 N m^{-2} , for a grain diameter of $200 \mu\text{m}$. Furthermore, Collins *et al.*, (1981) performed an *in situ* sediment erodibility study in the Wash, Eastern England. These researchers reported values for the critical shear stress and the critical shear velocity of 0.172 N m^{-2} and 1.3 cm s^{-1} , respectively, for a grain size of $180 \mu\text{m}$. In comparison with these results, the present study revealed a range in critical bed shear stresses of 2.64 N m^{-2} to

2.95 N m⁻² and a range of critical shear velocity of 5.07 cm s⁻¹ to 5.36 cm s⁻¹, for a range of grain size of 113 µm to 140 µm (see Table 8.1). The way these results were derived has been explained in Section 8.2. The higher critical shear stresses and velocities obtained during the investigation may be related to the influence of smaller grain size and the high density of *Lanice* tubes.

Studies have been carried out in an attempt to quantify the importance of subaerial exposure on the erodibility of the fine-grained sediment of intertidal flats (Amos *et al.*, 1988). Such results have revealed an increase in vane shear strength, from 4 KPa to 42 KPa, during mid-summer. It was concluded that the shear strength at any particular site was most sensitive to changes in exposure and evaporation; it was least sensitive to organic content and biological activity. However, relationships between vane shear strength, sediment properties and biological activity or abundance were often weak; this was due to spatial and temporal changes in exposure time, evaporation and precipitation. Furthermore, Amos *et al.*, (1992) have demonstrated recently that in areas where the surface biological content has been 'poisoned off', there was a marked decrease in the critical shear stress. Similarly, it has been shown also that diatom mucilage increases the stability of the surface sediments.

A series of experiments using the Cohesive Strength Meter (CSM) have been undertaken to examine the effects of physical and biological controls on the threshold of sediment movement (Paterson, *et al.*, 1990). The results of these investigations have suggested that an increase in (subaerial) exposure led to an increase in sediment stability. Such conditions were enhanced by the presence of epipelagic diatoms. Hence, the greatest increase in sediment stability occurred with prolonged subaerial exposure and when a dense population of epipelagic diatoms cover the surface of the sediments. These findings are in agreement with the notion that the extracellular products of a sufficient quantity of diatom populations increase the stability of intertidal flat sediments. It has been reported that biogenic stabilisation of intertidal flat sediments are 25 % to 77 % higher than their abiotic counterparts (Paterson and Daborn, 1991).

Experiments undertaken on bed shear strength have shown a 3-fold increase in the cohesion of surficial sediments, from less than 40 Pa to more than

120 Pa, during subaerial exposure (Faas *et al.*, 1993). Such an increase was related to the production of soluble mucopolysaccharide, by benthic diatoms. It has been shown also that the elimination of biological processes (by poisoning), resulted in the destabilisation of the surficial sediment and the development of non-cohesive bedforms, in what seemed previously to be cohesive beds. This finding is consistent with the results of the present study, where the predicted shear strength has been shown to be lower than the *in situ* shear strength. Moreover, the measurements used to predict the shear strength for the present investigation were obtained in the laboratory. Such conditions were supposed to contain less biota compared to that associated with *in situ* measurements.

Within a regional context, it has been suggested by Cowgill (1994) that the major factors influencing the erodibility of fine-grained sediments on the Keyhaven Marshes (West Solent) are a combination of subaerial exposure and the biological content of the surficial sediments. Likewise, high levels of biological activity could be related also to high levels of insolation. For the present study, the shear strength of the sediment deposits has been found to be dependent upon grain size, tube density and pore-water temperature. The high contribution made by grain size to shear strength may be attributable to the high angle of internal friction between the coarser grains (Pestrong, 1969). This effect will be enhanced by the presence of *Lanice* tubes, acting as an intricate network of root fibres which effectively bind the sediment. This argument is supported by the earlier investigation of Pestrong (op. cit.), whereby the dense roots of *Salicornia* plants have been shown to increase the shear strength of the sediments. Temperature effects seem to be less dominant in affecting stability, because the coarser sediments are non-cohesive; thus, this effect (insolation) does not increase the cohesiveness between the individual sediment grains. For smaller grain sizes, the effect of temperature on the shear strength of a sediment deposit may be distinctive i.e. the smaller grains have a larger surface area per unit mass, which may adhere together when exposed to insolation.

Since the sediment deposits of the present investigation consisted of less cohesive materials, the main factor responsible for shear strength was the size and weight (gravity) of the grains. This effect will be enhanced by the presence

of *Lanice* tubes. The tubes bind the sediment grains together (see below), leading to an increase in shear strength. As the field study area of the investigation was relatively flat, with no significant spatial difference in shear strength, it can be inferred that (at least, to a certain extent) tube density increases the shear strength of the surficial sediments - in addition to grain size and temperature.

The effect of the tubes on shear strength (sediment stability) is due to 'compactness' effect exerted on the sediment grains. As the tubes become larger and/or increase in density, the grains contained within the sediment deposit become more compact; this leads to an increase in shear strength. This effect is enhanced also by gravity and frictional effects between the sediment grains. The tube density increases also the shear stress of the sediments, since high tube densities and their associated tentacles covering the surface of sediment protect the bed from the high energy of the current flow. For a comparison, Burke (1989) has undertaken a flume experiment on the biological effects on shear stress, using *in situ* sediment samples covered with an algal mat. The results revealed that the critical shear stress (at threshold) increased in response to an increase in shear strength. It was revealed also by Burke (op. cit.) that critical shear stress increases linearly in response to increase in algal cover over the surface of the sediments (Figure 8.7). Early investigators elsewhere have also established a linear relationships between shear strength and shear stress (cf Dunn, 1959; Flaxman, 1963; Graf, 1971). Furthermore, in previous flume experiments, Muskananfola (1990) has shown that an increase of *Lanice* tubes density leads to an increase in the flow velocities and energy required to move sediment (sand) grains. All the above results, together with the findings of the present study, suggest strongly that biological factors (in particular, the density of *Lanice conchilega* tubes) influence sediment stability. The presence of individual tubes, however, may cause localised erosion (scour) of the surficial sediment (Eckman and Nowell, 1984) and resuspension of sediment particles (Carey, 1983). Hence, biological factors can either 'stabilise' or 'destabilise' a sediment surface depending upon the nature and density of their influence.

The 'stabilising effect' of biological factors on a sediment surface can be due to: (i) a 'binding or compactness' effect (i.e. *Lanice* tubes, microalgae); (ii)

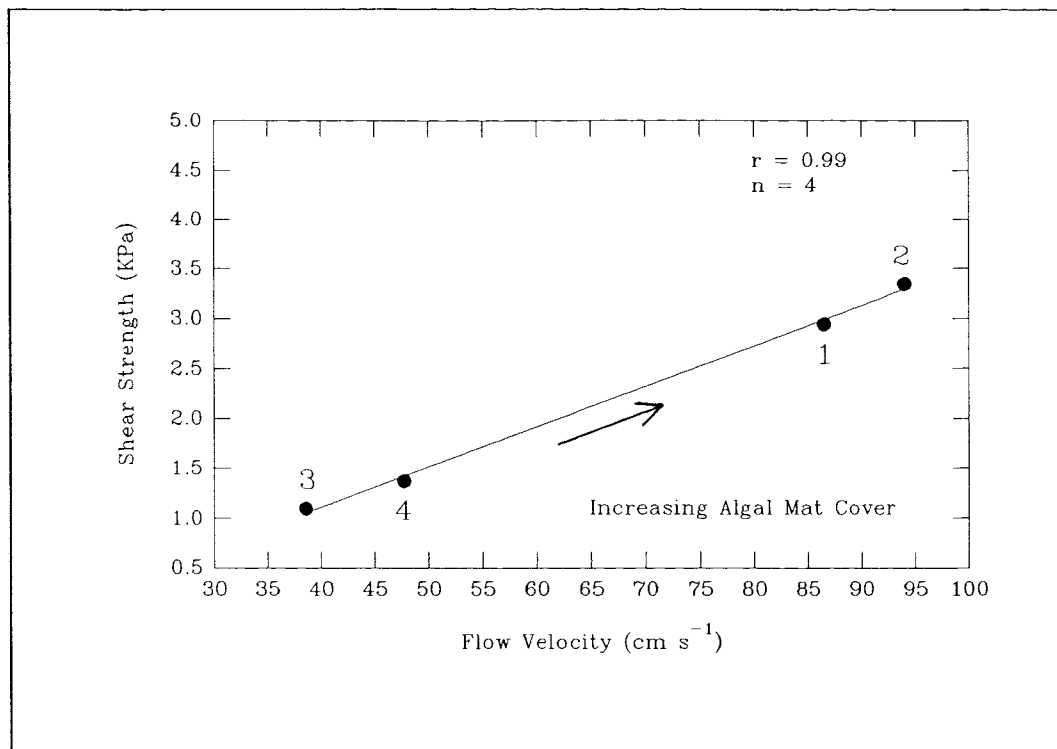


Figure 8.7. Relationship between shear strength and flow velocity required to erode *in situ* sediment samples placed in a flume (data from Burke, 1989)

a 'cover' effect (i.e. macroalgae mat); and (iii) a combination of (i) and (ii) (i.e. *Spartina* and *Salicornia*). The effect of binding can influence both the shear strength of the deposits and the critical stress required to move the surficial deposits. The effect of cover influences only shear stress. Finally, a combination of binding and cover effects influence both the shear strength and stress associated with the surficial sediment deposits. In the present study, the tube density of *Lanice conchilega* was considered to be influenced by recruitment failure or species interactions (juvenile predation by other macrofauna) (Section 6.2). It may be assumed, therefore, that other factors (biological, sedimentological and physical) which have been found to be less important in this study affect sediment stability indirectly.

The 'destabilising effect' can be due to: (i) individual tubes, which cause localised scouring of the sediments; and (ii) bioturbation of fauna, which leads to a decrease in the critical velocity (stress) required to move the sediments.

Scouring of sediment around individual tubes occurs because, being isolated, they do not create any baffle effect necessary to protect the surface sediments from the energy of the flow. An individual tube increases the net boundary skin friction locally, tending to promote sediment entrainment near its base (Eckman and Nowell, 1984). Suspended particles transported by the flow may be deposited immediately downstream of an individual tube. Deposition and/or scouring caused by any individual tube will depend both upon the tube height and on the boundary shear stress exerted by the external flow (Eckman and Nowell, op. cit.). In comparison, bioturbation by benthic organisms results in less compact sediment grains; these are, therefore, more easily eroded or resuspended by bottom currents.

CHAPTER 9

CONCLUSIONS AND FUTURE RESEARCH

9.1. Introduction

The present study is concerned mainly with coastal sediment stability, using shear strength as an indicator of prevailing conditions. The effects of biological, physical and sedimentological parameters have been investigated in an estuarine environment, over 28 months of field data collection; this was followed by a series of laboratory studies. Experiments into the effects of (pore-water) temperature and straw density, on shear strength, were also undertaken. In addition to primary data, secondary data on daily climatological parameters covering the study area were obtained from The Meteorological Office (in Bracknell). Overall, some 21 parameters were investigated as part of the present investigation: shear strength; shear stress; pore-water temperature; pore-water salinity; mean grain size; sediment sorting; sediment skewness; moisture content; low water height; organic matter content; protein; bacterial protein; bacterial abundance; silt/clay content; tube density of the polychaete *Lanice conchilega*; total numbers of species of macrobenthic organisms; total numbers of individuals within the benthic macrofauna; air temperature; wind speed; and rainfall and sunshine. The results have been described, interpreted and discussed (Chapters 5, 6 and 7); this was followed by further analysis and discussions (Chapter 8). In the present Chapter, all the main conclusions are summarised.

9.2. Regional Setting

The area under investigation (Solent Breezes, Southampton Water), has been found to be a relatively stable marine environment during the period of study, with an absence of any significant accretion and erosion. Water depths are

around 4.5 m on Mean High Water Springs (MHWS). The bed of the intertidal flats is covered with fine-grained sands within the upper 5 - 10 cm; below this, the deposits consist of muds. At the high water mark, the area is covered extensively with gravels and shingles. The study area is comparatively flat, with vertical topographic variations only of the order of 0.5 cm in every 1 m increase in horizontal distance.

There is no evidence of heavy bioturbation having occurred within the surface sediments, although the density of the upper 5 cm reveals a slight variation between samples. Such variation may be due to variability in the natural composition of the sediment deposits, or to human activities. In the former case, sandy materials usually have a higher density than the silt/clay materials; in the latter, people usually dig for mussels and live bait around the area during low tide. However, overall, these differences in sediment density do not contribute significantly to changes in the shear strength. Throughout the study, the mean density of the upper 5 cm of the surface sediments varied from 2.32 g cm^{-3} to 2.65 g cm^{-3} .

Velocities measured during a spring tidal cycle have revealed that most of the profiles are logarithmic in characters; this indicates that velocity profiles over the intertidal flats follow generally the Von Karman-Prandtl equation. Current speeds recorded varied from 2.2 cm s^{-1} to 43.5 cm s^{-1} , at the bottom and surface of the water column, respectively. The critical shear stress varied from 0.01 N m^{-2} to 4.45 N m^{-2} , whilst the critical shear velocity ranged from 0.25 cm s^{-1} to 5.71 cm s^{-1} . Bed roughness length varied from 0.02 cm to 14.3 cm. The highest bed roughness length occurred during the ebb phase of the tide.

9.3. Biological Investigations

The study area is populated densely by the tubes of a polychaete *Lanice conchilega*. The tube density over the study area decreased gradually, from the beginning to the end of the investigation period. Such a pattern may have been caused by the failure of recruitment of new-born larvae into the population, or

predation of newly-settled larvae (by several dominant species of macrobenthic organisms).

Twenty nine species of macrobenthic organisms were identified during the study. The benthic macrofauna are composed mainly of a few species which existed in relatively large numbers; they showed constant seasonal fluctuation, with some rarer species occurring sporadically. The total number of species fluctuated seasonally, with a slight increase towards the end of study. The total number of individuals of benthic macrofauna showed a similar pattern to that of the total number of species i.e. fluctuating seasonally, then increasing towards the end of the investigation.

The dominant species identified refer to those which contribute more than 3 % to the total individuals of macrobenthic organisms, consisting of: *Euclymene oerstedii* (25.6 %), *Exogone hebes* (19.3 %), *Aricidea minuta* (11.2 %), *Pygospio elegans* (8.5 %), *Scoloplos armiger* (7.2 %), *Nephrys hombergii* (6.0 %), *Tanaissus lilljeborgi* (3.6 %) and *Syllis sp* which contributes 3.2 % to the total individuals of benthic macrofauna.

The diversity index of macrobenthic organisms was relatively high, varying from 1.27 to 2.38 during the period of study. The 'diversity index' was lower during the winter months and higher in the summer. This change may represent the degree of disturbance of the surface sediments, with less disturbance in summer and more in winter. In intertidal waters, the associated fauna is subjected to environmental factors which fluctuate considerably; therefore, many species are not able to tolerate such fluctuations. The factors most influencing the diversity indices is the seasonal pattern of recruitment and mortality - in addition to disturbance.

The principal components analysis reveals that the main parameters which affect the distribution of benthic macrofauna may be summarised as: (i) bioavailability of organic matter (protein, bacterial protein, organic matter content, grain size characteristics); (ii) factors influencing sediment strength (shear strength of the sediment, tube density of *Lanice conchilega*); and (iii) physical factors (temperature, salinity, moisture content). Any dependency of benthic macrofauna on bioavailability of organic matter seems to be appropriate,

since food available in this form (rather than total organic matter) can be utilised directly by the organisms. The presence of *Lanice conchilega*, could affect other macrofauna in one of the following manners: (a) act as protection from predators; (b) alter hydrodynamic conditions near the bed; (c) lead to the deposition of more organic matter (which, presumably, contains more food); and (d) adult *Lanice* may predate upon newly-settled macrofauna larvae.

9.4. Sedimentological Investigations

The shear strength of the surface sediments fluctuated from 2.11 KPa to 4.08 KPa. The low and high shear strength values coincided with low and high tube densities; this suggests that an increase in tube density is responsible for the increase in strength. Under such circumstances, the tubes act as intricate root fibres, which bind the sediment together and increase the shear strength.

Pore-water temperature showed a seasonal pattern of variation, with high temperatures in summer and low temperatures in winter. Such a pattern was not reflected in the pore-water salinity, indicating that temperature is not the only factor influencing salinity. Other factors include, for example: rainfall; freshwater input from the rivers; and, particularly, the prevailing wind speed.

The (moisture) water content within the upper sediment deposits fluctuated considerably, varying from 27.9 % to 34.9 %. Organic matter content increased from the beginning, towards the end of the study. The organic matter content varied from 0.91 % to 2.01 %. At the same time, the silt/clay content revealed a seasonal pattern; it increased during the summer and decreased during winter. The lowest silt/clay content was 0.1 %, whilst the highest was 0.73 %.

Sediments deposited over the study area are represented by fine sands, with their mean grain size varying from 3.14Φ to 2.84Φ (or 113 μm to 140 μm). The seasonal distribution of mean grain size remained relatively stable and uniform; there were some fluctuations and a slight decrease in mean size towards the end of the investigation. The sorting of the sediments ranged from moderately sorted to poorly sorted (0.78 to 1.23); this tended to worsen during

the summer months. The sediment samples were extremely positively skewed, varying from + 1.32 to + 2.95.

The various experiments undertaken elsewhere into the stability of the intertidal flat sediments resulted in similar conclusions, that the main factors affecting erodibility were: the presence of seagrasses; the mean grain size of the deposits; subaerial exposure; and the microbial activity of the benthic organisms. Statistical tests on the present data reveals that shear strength of the intertidal flat deposits is affected mainly by: grain size; the tube density of *Lanice conchilega*; and pore-water temperature. It appears that the effect of these three parameters are seasonally dependent.

Only two of the regression equations obtained are statistically significant; those obtained using all the data and for the equation using winter months only. The equation representing all the data indicates that shear strength is affected negatively by both pore-water temperature and grain size; it is effected positively by tube density. The equation reveals also that grain size is the dominant parameter affecting the shear strength; this is followed by tube density and pore-water temperature. The equation obtained for the winter data indicates only a positive effect of pore-water temperature on shear strength. This result contradicts previous findings, including other results obtained during the present study (Section 7.12) where the relationship between temperature and shear strength is negative. This effect may be due to relatively small differences in the *in situ* temperature measurements, the effect of tube density and other organisms, leading to the observed positive correlation.

Biological factors can influence the stability of sediments, in terms of stabilisation or destabilisation. Stabilisation can be caused by: (i) binding or compaction effects, caused by *Lanice* tubes and microalgae which produce mucus; (ii) the effect of cover caused by a macroalgae mat; and (iii) a combination of (i) and (ii), e.g. as caused by *Spartina* and *Salicornia*. Destabilisation can be caused by: (i) individual tubes causing scouring of the sediments around the tube; and (ii) bioturbation of fauna, which would cause a reduction in the critical velocity of sediment.

9.5. Future Research

The present study was undertaken over a 28 month period, examining the various factors which may affect shear strength (or sediment stability) of intertidal flat sediments i.e. biological, physical and sedimentological controls. The factors responsible for the existing patterns of *Lanice conchilega* and benthic macrofauna have also been investigated.

Since the study has concentrated upon *in situ* data collection, it is recommended that future studies should undertake field or controlled laboratory experiments on flow pattern around the tubes. Such patterns may influence larval recruitment which, in turn, influence juvenile tubes and sediment stability. Such investigations, together with studies undertaken on other parameters (biological, sedimentological and physical) may enhance our understanding of sediment stability.

The biological data described as part of the present investigation (such as protein, bacterial protein and bacterial abundance) were not measured *in situ*, or directly from the sediment samples. It would appear, however, that these factors may contribute to stabilisation of the intertidal flat sediments. It may be advisable in the future studies, therefore, that such parameters should be considered and measured *in situ*. Likewise, it is necessary to measure the shear strength and shear stress associated with the same samples, to establish any direct relationship between the variables. The latter can be undertaken by collecting *in situ* sediment samples (using glass containers) and transporting them into the laboratory. The samples are placed into a flume (fitted into a special box which can accommodate the sample containers) and velocities required to move sediment grains measured using a laser beam. Subsequently, the shear strength of similar samples are measured. The obtained data are then correlated to establish any relationship between shear stress and shear strength. In order to obtain a reliable relationship, the experiment should be performed also on sediment samples from different places with different grain size characteristics.

REFERENCES

Admiraal, W. 1984. The ecology of estuarine sediment-inhabiting diatoms. In *Progress in Phycological Research* (Round, F.E. and Chapman, D.J., eds.). Biopress, Bristol, pp. 269 - 322.

Alexander, D.W. 1969. *A Study of the Biology of Animals Living on and in Littoral Sponges with Special Reference to Halichondria panicea*. Unpublished Ph.D. Thesis. University of London.

Allen, G.P. 1971. Relationship between grain size parameter distribution and current patterns in the Gironde Estuary (France). *J. Sedim. Petrol.*, **41**: 74 - 88.

Allersma, A. 1982. Mud in estuaries and along coasts. *Delft Hydraulics Laboratory Publication no. 270*. Waterloopkundig Laboratorium, pp. 663 - 667.

Amos, C.L. and Mosher, D.C. 1985. Erosion and deposition of fine-grained sediments from the Bay of Fundy. *Sedimentology*, **32**: 815 - 832.

Amos, C.L., Daborn, G.R., Christian, H.A., Atkinson, A. and Robertson, A. 1992. In situ erosion measurements on fined-grained sediments from the Bay of Fundy. *Marine Geology*, **108**: 175 - 196.

Amos, C.L., Van Wagoner, N.A. and Daborn, G.R. 1988. The influence of subaerial exposure on the bulk properties of fine-grained intertidal sediment from Minas Basin, Bay of Fundy. *Estuarine, Coastal and Shelf Science*, **27**: 1 - 13.

Anderson, F.E. 1983. The northern muddy intertidal: a seasonally changing source of suspended sediment to estuarine waters - a review. *Canadian Journal of Fisheries and Aquatic Science*, **40**: 143 - 159.

Anderson, F.E. and Howell, B.A. 1984. Dewatering of an unvegetated muddy tidal flat during exposure-desiccation or drainage? *Estuaries*, **7**: 225 - 232.

Anderson, J.G. and Meadows, P.S. 1978. Microenvironments in marine sediments. *Proc. R. Soc. Edinb.*, **76B**: 1 - 16.

Ariathurai, R. and Arulanandan, K. 1978. Erosion rates of cohesive soils. *American Society of Civil Engineers, Journal of Hydraulics Division*, 104: 279 - 282.

Bailey-Brock, J.H. 1979. Sediment trapping by chaetopterid polychaetes on a Hawaiian fringing reef. *J. Mar. Res.*, 37: 643 - 656.

Barnes, R.S.K. 1973. The intertidal lamellibranchs of Southampton Water with particular reference to *Cerastoderma edule* and *C. glaucum*. *Proc. Malac. Soc. Lond.*, 40: 413 - 433.

Barnes, R.S.K., Coughlan, J. and Holmes, N.J. 1973. A preliminary survey of the macroscopic bottom fauna of the Solent, with particular reference to *Crepidula fornicata* and *Ostrea edulis*. *Proc. Malac. Soc. Lond.*, 40: 253 - 275.

Beukema, J.J. 1976. Biomass and species richness of the macro-benthic animals living on the tidal flats of the Dutch Wadden Sea. *Neth. J. Sea Res.*, 10: 236 - 261.

Bielakoff, J., Damas, D. and Vovelle, J. 1975. Histology and biochemistry of the glandular formations involved in the building of the tube of *Lanice conchilega*. *Arch. Zool. Exp. Gen.*, 116: 499 - 520.

Black, K. 1991. *The Erosion Characteristics of Cohesive Estuarine Sediments: Some In Situ Experiments and Observations*. Unpublished Ph.D. Thesis. University College of North Wales, Bangor, U.K., 313 pp.

Blain, W.R. 1980. *Tidal hydraulics of the West Solent*. Unpublished Ph.D. Thesis. University of Southampton, 326 pp.

Blegvad, H. 1914. Food and conditions of nourishment among the communities of invertebrate animals found on or in the sea bottom in Danish Waters. *Rep. Dan Biol. Stn.*, 22: 43 - 78

Bloom, S.A., Simon, J.L. and Hunter, V.D. 1972. Animal-sediment relations and community analysis of a Florida estuary. *Mar. Biol.*, 13: 43 - 56.

Bone, M.G. 1973. *The Factors Influencing the Distribution and Growth of Mya arenaria on the South coast of Britain*. Unpublished M.Sc. Thesis. University of London.

British Geological Survey, 1988. *Marine Aggregate Survey: A study undertaken by the BGS on behalf of the Crown Estate*. Phase 2, South Coast, Scale 1 : 250,000. Map 1, Bathymetry.

Bruno, S.F., Staker, R.d. and Sharma, G.M. 1980. Dynamics of phytoplankton productivity in the Peconic Bay estuary, Long Island. *Estuar. Coast. Shelf Sci.*, **10**: 247 - 263.

Bryan, J.R. 1980. *The production and decomposition of organic material in an estuary - Southampton Water*. Unpublished Ph.D. Thesis. University of Southampton, 198 pp.

BS 1377. 1975. *Methods of Test for Soils for Civil Engineering Purposes*. British Standards Institution, London, 143 pp.

Buhr, K.-J. 1976. Suspension feeding and assimilation efficiency in *Lanice conchilega* (Polychaeta). *Marine Biology* **38**: 373 - 383.

Buhr, K.-J. 1979. Eine massensiedlung von *Lanice conchilega* (Polychaeta: Terebellidae) in Weser-Astuar. *Veröff. Inst. Meeresforsch. Bremerh.*, **17**: 101 - 149.

Buhr, K.-J. and Winter, J.E. 1977. Distribution and maintenance of a *Lanice conchilega* association in the Weser Estuary (FRG) with special reference to the suspension-feeding behaviour of *Lanice conchilega*. In *Biology of Benthic Organisms* (Keegan, B.F., O'Ceidigh, P.O. and Boaden, P.J.S., eds.), 11th European Symp. on Marine Biology, Galway, Oct. 1976. Pergamon Press, Oxford. pp. 101 - 113.

Buller, A.T. and McManus, J. 1979. Sediment sampling and analysis. In *Estuarine Hydrography and Sedimentation* (Dyer, K.R., ed.), pp. 87 - 130. Cambridge University Press.

Burd, B.J., Nemec, A. and Brinkhurst, R.O. 1990. The development and application of analytical methods in benthic marine infaunal studies. *Advances in Marine Biology*, **26**: 169 - 247.

Burke, K. 1989. *The Erodibility of Cohesive Sediments - A Study of the Intertidal Saltmarshes at Keyhaven, Hampshire*. Unpublished M.Sc. Thesis. University of Southampton, 105 pp.

Busch, W.H. and Keller, G.H. 1983. Analysis of sediment stability on the Peru-Chile continental slope. *Marine Geotechnology*, **5**: 181 - 211.

Cadée, G.C. 1976. Sediment reworking by *Arenicola marina* on tidal flats in the Dutch Wadden Sea. *Neth. J. Sea Res.* **10**: 440 - 460.

Carey, D.A. 1983. Particle resuspension in the benthic boundary layer induced by flow around polychaete tubes. *Can. J. Fish. Aquat. Sci.*, **40** (suppl. 1): 301 - 308.

Carr, J.F., de Turville, C.M., Jarman, R.T. and Spencer, J.F. 1980. Water temperatures in the Solent estuarine system. In *The Solent Estuarine System*. The Natural Environment Research Council Publications Series C No. 22 November 1980, pp. 36 - 43.

Carrigy, M.A. 1970. Experiments on the angles of repose of granular materials. *Sedimentology*, **14**: 147 - 158.

Channon, R.D. and Hamilton, D. 1971. Sea bottom velocity profiles on the continental shelf southwest of England. *Nature*, **231**: 383 - 385.

Charnock, H. 1959. Tidal friction from currents near the seabed. *Geophysical Journal of the Royal Astronomical Society*, **2**: 215 - 221.

Chepil, W.S. 1961. The use of spheres to measure lift and drag on wind-eroded soil grains. *Proc. Soil Sci. Soc. Am.*, **25**: 343 - 345.

Coles, S.M. 1979. Benthic microalgal populations on intertidal sediments and their role as precursors to salt marsh development. In *Ecological Processes in Coastal Environments* (Jeffries, R.L. and Davy, A.J., eds.). Blackwell, Oxford, pp. 25 - 42.

Collins, M.B., Amos, C.L. and Evans, G. 1981. Observations of some sediment transport processes over intertidal flats, the Wash, U.K. *Special Publications of the International Association of Sedimentologists*, **5**: 81 - 98.

Connel, J.H. 1978. Tropical rain forests and coral reefs as open non-equilibrium systems. In *Population Dynamics* (Anderson, R.M., Taylor, B.D. and Taylor, L.R., eds.). Blackwell, London, pp. 141 - 163.

Costerton, J.W., Geesey, G.G. and Cheng, K.J. 1978. How bacteria stick. *Scientific American*, **238**: 86 - 95.

Cowgill, C.M. 1994. *In Situ Determination of Fine-grained Sediment Erodibility*. Unpublished Ph.D. Thesis. Department of Oceanography, University of Southampton.

Crisp, D.J. and Southward, A.J. 1958. The distribution of intertidal organisms along the coast of the English Channel. *J. Mar. Biol. Ass. U.K.*, **37**: 157 - 208.

Cullen, D.J. 1973. Bioturbation of superficial marine sediments by interstitial meiobenthos. *Nature*, **242**: 323 - 324.

Cuvier, G. 1836. *Le Règne Animal distribué d'après son organisation pour servir de base à l'Histoire naturelle des animaux et d'introduction à l'anatomie comparée*, Annelides, Paris, 54 pp.

Davis, J.C. 1973. *Statistics and Data Analysis in Geology*. John Wiley & Sons, Inc., New York, 550 pp.

de Boer, P.L. 1981. Mechanical effects of micro-organisms on intertidal bedform migration. *Sedimentology*, **28**: 129 - 132.

de Souza Lima, H. and Williams, P.J.L. 1978. Oxygen consumption by the planktonic population of an estuary - Southampton Water. *Est. and Coast. Mar. Sci.*, **6**: 515 - 521.

Doodson, A.T. and Warburg, H.D. 1941. *Admiralty Manual of Tides*. H.M.S.O. 223 - 226.

Duane, D.B. 1964. Significance of skewness of recent sediments, Western Pamlico Sound, North Carolina. *J. Sedim. Petrol.*, **34**: 864 - 874.

Dunn, I.S. 1959. Tractive resistance of cohesive channels. *American Society of Civil Engineers, Journal of Soil Mechanics and Foundation*, **85**: 1 - 24.

Dyer, K.R. 1969. *Some Aspects of Coastal and Estuarine sedimentation*. Unpublished Ph.D. Thesis. University of Southampton.

Dyer, K.R. 1970. Current velocity profiles in a tidal channel. *Geophysical Journal of the Royal Astronomical Society*, **22**: 153 - 161.

Dyer, K.R. 1971. The distribution and movement of sediment in the Solent, S. England. *Mar. Geol.*, **11**: 175 - 187.

Dyer, K.R. 1972a. *Recent sedimentation in the Solent area*. Memoir 79, BRGM Paris, pp. 271 - 280.

Dyer, K.R. 1972b. Bed shear stresses and sedimentation of sandy-gravels. *Mar. Geol.*, **13**: 31 - 36.

Dyer, K.R. 1980. Velocity profiles over a rippled bed and the threshold of movement of sand. *Estuarine and Coastal Marine Science*, **10**: 181 - 199.

Dyer, K.R. and King, H.L. 1975. The residual water flow through the Solent, South England. *Geophys. J.R. Astr. Soc.*, **42**: 97 - 106.

Eagle, R.A. 1975. Natural fluctuations in a soft bottom benthic community. *J. Mar. Biol. Ass. U.K.*, **55**: 865 - 878.

Eckman, J.E. 1983. Hydrodynamic processes affecting benthic recruitment. *Limnol. Oceanogr.*, **28**: 241 - 257.

Eckman, J.E. and Nowell, A.R.M. 1984. Boundary skin friction and sediment transport about an animal-tube mimic. *Sedimentology*, **31**: 851 - 862.

Eckman, J.E., Nowell, A.R.M. and Jumars, P.A. 1981. Sediment destabilization by animal tubes. *J. Mar. Res.*, **39**: 361 - 374.

Edgar, L.A. and Pickett-Heaps, J.D. 1984. Diatom Locomotion. In *Progress in Phycological Research 3* (Round, F.E. and Chapman, D.J., eds.). Biopress, Bristol, pp. 47 - 88.

Eleftheriou, A. and Nicholson, M.D. 1975. The effects of exposure on beach fauna. *Cah. Biol. Mar.*, **16**: 695 - 710.

Esser, J.R. 1972. *Polychaete Distribution in Southampton Water and the Solent*. Unpublished M.Sc. Dissertation. University of Southampton.

Evans, G. and Collins, M.B. 1975. The transport and deposition of suspended sediment over the intertidal flats of the Wash. In *Nearshore Sediment Dynamics and Sedimentation* (Hails, J. and Carr, A., eds.). John Wiley, London, pp 237 - 306.

Faas, R.W., Christian, H.A., Daborn, G.R. and Brylinsky, M. 1993. Biological control of mass properties of surficial sediments: an example from Starr's Point tidal flat, Minas Basin, Bay of Fundy. In *Nearshore and Estuarine Cohesive Sediment Transport* (Mehta, A.J., ed.). Springer-Verlag.

Fager, E.W. 1964. Marine sediments: effects of a tube-building polychaete. *Science* **143**: 356 -359.

Fauchald, K. and Jumars, P.A. 1979. The diet of worms: a study of polychaete feeding guilds. *Oceanogr. Mar. Biol. Ann. Rev.*, 17: 193 - 284.

Fazio, S.A., Uhlinger, D.J., Parker, J.H. and White, D.C. 1982. Estimations of uronic acids as quantitative measures of extracellular and cell wall polysaccharide polymers from environmental samples. *Applied and Environmental Microbiology*, 43: 1151 - 1159.

Field, J.G., Clarke, K.R. and Warwick, R.M. 1982. A practical strategy for analysing multispecies distribution patterns. *Marine Ecology Progress Series*, 8: 37 - 52.

Findlay, S. and Tenore, K.R. 1982. Effect of a free-living marine nematode (*Diplopaimella chitwoodi*) on detrital carbon mineralization. *Mar. Ecol. Prog. Ser.*, 8: 161 - 166.

Fish, J.D. and Fish, S. 1989. A student 's guide to the seashore. Unwin Hyman Ltd., London.

Fischer-Piette, E. 1936. Etudes sur la biogeographie intercotidale des deux rives de la manche. *J. Linn. Soc. (Zool.)*, 40: 181 - 272.

Flaxman, E.M. 1963. Channel stability in undisturbed cohesive soils. *Journal of the Hydraulics Division, Proceedings of the American Society of Civil Engineers*, HY 2: 87 -96.

Flood, R.D. 1981. Distribution, morphology, and origin of sedimentary furrows in cohesive sediments, Southampton Water. *Sedimentology*, 28: 511 - 529.

Folk, R.L. 1966. A review of grain size parameters. *Sedimentology*, 6: 73 - 93.

Folk, R.L. and Ward, W.C. 1957. Brazos River bar: a study in the significance of grain size parameters. *J. Sedim. Petrol.*, 27: 3 - 26.

Fonseca, M.S. 1989. Sediment stabilization by *Halophila decipiens* in comparison to other seagrasses. *Estuarine, Coastal and Shelf Science*, 29: 501 - 507.

Fonseca, M.S. and Fisher, J.S. 1986. A comparison of canopy friction and sediment movement between four species of seagrass with reference to their ecology and restoration. *Marine Ecology Progress Series*, 29: 15 - 22.

Frankel, L. and Mead, D.J. 1973. Mucilaginous matrix of some estuarine sands in Connecticut. *J. Sed. Petrol.*, 43: 1090 - 1095.

Gerlach, S.A. 1978. Food-chain relationships in subtidal silty sand marine sediments and the role of meiofauna in stimulating bacterial productivity. *Oecologia (Berl.)*, 33: 55 - 69.

Glaister, R.P. and Nelson, H.W. 1974. Grain size distribution an aid in facies identification. *Bull. Can. Petroleum. Geology*, 22: 203 - 240.

Glantz, S.A. 1992. *Primer of Biostatistics*. Third edition. McGraw-Hill, Inc., New York, 440 pp.

Glantz, S.A. and Slinker, B.K. 1990. *Primer of Applied Regression and Analysis of Variance*. McGraw-Hill, Inc., New York, 777 pp.

Graf, W.H. 1971. *Hydraulics of Sediment Transport*. McGraw-Hill Book Company, New York, 513 pp.

Grant, W.D., Boyer, L.F. and Sanford, L.P. 1982. The effects of bioturbation on the initiation of motion of intertidal sands. *J. Mar. Res.*, 40: 659 - 677.

Grant, J. and Gust, G. 1987. Prediction of coastal sediment stability from photopigment content of mats of purple sulphur bacteria. *Nature*, 330: 244 - 246.

Gray, J.S. 1971. Factors controlling population localizations in polychaete worms. *Vie Milieu.*, 2: 707 - 722.

Gray, J.S. 1974. Animal-sediment relationships. *Ann. Rev. Oceanogr. Mar. Biol.*, 12: 223 - 261.

Gray, J.S. 1981. *The Ecology of Marine Sediments*. Cambridge University Press, Cambridge, 185 pp.

Gust, G. and Morris, M.J. 1988. Erosion thresholds and entrainment rates of undisturbed *in situ* sediments. *Journal of Coastal Research, Special Issue No. 5*, 30 pp.

Head, P.C. 1969. *Studies on the distribution and behaviour of iron and molybdenum in sea water, with particular reference to an estuarine environment*. Unpublished Ph.D. Thesis. University of Southampton.

Henderson, G. and Webber, N.R. 1977. Storm surge in the U.K. South coast.
Dock and Harbour Authority, **58**: 21 - 22.

Hjulström, F. 1935. Studies in the morphological activity of rivers as illustrated by the River Fyris. *Geol. Inst. Univ. Upsala, Bull.*, **25**: 221 - 528.

Hjulström, F. 1939. Transportation of detritus by moving water. In *Recent Marine Sediments* (Trask, P.D., ed.). American Association of Petroleum Geology, pp. 5 - 31.

Holland, A.F. and Polgar, T.T. 1976. Seasonal changes in the structure of an intertidal community. *Mar. Biol.*, **37**: 341 - 348.

Holland, A.F., Zingmark, R.G. and Dean, J.M. 1974. Quantitative evidence concerning the stabilization of sediments by marine benthic diatoms. *Marine Biology*, **27**: 191 - 196.

Holmes, N.J. 1971. The acidian fauna of Southampton Water. *Central Electricity Res. Lab. Note No. RD/L/N 187/71*

Howells, W.R. 1964. The macrofauna of the intertidal soils of the Towy Estuary, Carmarthenshire. *Ann. Mag. Nat. Hist.*, (13)**7**: 577 - 607.

Huston, M. 1979. A general hypothesis of species diversity. *Am. Nat.*, **113**: 81 - 101.

Hydrographer of the Navy. 1974. *The Solent and Adjacent Waters - Pocket Tidal Stream Atlas*. Hydrographer of the Navy.

Hylleberg, J. 1975. Selective feeding by *Arenicola pacifica* with notes on *Abarenicola vagabunda* and a concept of gardening in lugworms. *Ophelia* **14**: 113 - 137.

Inman, D.L. 1963. Sediments: Physical properties and mechanics of sedimentation. In *Submarine Geology*, second edition (Shepard, F.L.). Harper and Row, New York, Chapter 5: 101 - 147.

Jarman, R.T. and de Turville, C.M. 1974. Dispersion of heat in Southampton Water. *Proc. Inst. Civ. Engrs.*, **57**: 129 - 142.

Johnson, R.G. 1970. Variations in diversity within benthic marine communities. *Am. Natur.*, **104**: 285 - 300.

Jones, N.S. 1950. Marine bottom communities. *Biol. Rev.*, **25**: 283 - 313.

Juario, J.V. 1975. Nematode species composition and seasonal fluctuation of a sublittoral meiofauna community in the German Bight. *Veroff. Inst. Meeresforsch. Bremerh.*, 15: 283 - 337.

Jumars, P.A. 1975. Target species of deep-sea studies in ecology, genetics and physiology. *Zool. J. Linnean Soc.* 57: 341 - 348.

Jumars, P.A. and Nowell, A.R.M. 1984. Effects of benthos on sediment transport: Problems with functional grouping. *Cont. Shelf Res.*, 3: 115 - 130.

Juniper, A.J. 1963. *A Survey of the Intertidal Fauna of the Portsmouth Area*. Unpublished M.Sc. Thesis. University of Durham.

Kamphius, J.W. and Hall, R. 1983. Cohesive material erosion by unidirectional current. *American Society of Civil Engineers, Journal of Hydraulics Engineering*, 109: 49 - 61.

Kelly, W.E. and Gularce, R.c. 1981. Erosion resistance of cohesive soils. *American Society of Civil Engineers, Journal of Hydraulics Division*, 107: 1211 - 1224.

Kennedy, J.B. and Neville, A.M. 1986. *Basic Statistical Methods for Engineers and Scientists*. Third edition. Harper & Row, Publishers, Inc., New York, 613 pp.

Kessler, M. 1963. Die entwicklung von *Lanice conchilega* (Pallas) mit besonderer beruchsichtigung der lebensweise. *Helgoländer Wiss. Meeresunters.* 8: 425 - 476.

Kifle, D. 1992. *Seasonal and Spatial Variation in Species Composition, Abundance, Biomass and Primary Production of Phytoplankton in Southampton Water, U.K.* Unpublished Ph.D. Thesis. Department of Oceanography, University of Southampton, 306 pp.

Kirby, R. and Parker, W.R. 1983. Distribution and behaviour of fine sediment in the Severn Estuary and inner Bristol Channel, U.K. *Canadian Journal of Fisheries and Aquatic Sciences*, 40: 83 - 95.

Kleinbaum, D.G., Kupper, L.L. and Muller, K.E. 1988. *Applied Regression Analysis and Other Multivariable Methods*. Second edition. PWS-KENT Publishing Company, Belmont, California, 718 pp.

Kline, S.J., Reynolds, W.C., Schraub, F.A. and Runstadler, P.W. 1967. The structure of turbulent boundary layers. *J. Fluid Mech.*, **30**: 741 - 773.

Kraeuter, J.N. and Wetzel, R.L. 1986. Surface sediment stabilization-destabilization and suspended sediment cycles on an intertidal mudflat. In *Estuarine Variability* (Wolfe, D.A., ed.). Academic Press, Orlando, FL, pp. 203 - 223.

Krugermeier, L. and Grunwald, M. 1978. The influence of sea waves on the wind profile. *Boundary-Layer Meteorology*, **10**: 403 - 414.

Krumbein, W.C. 1934. Size-frequency distributions of sediments. *Journal of Sedimentary Petrology*, **4**: 65 - 77.

Kühl, H. 1972. Hydrography and biology of the Elbe estuary. *Oceanogr. Mar. Biol. Ann. Rev.*, **10**: 225 - 309.

Lambshead, P.J.D. 1986. Sub-catastrophic sewage and industrial waste contamination as revealed by marine nematode faunal analysis. *Mar. Ecol. Prog. Ser.*, **29**: 247 - 260.

Lavelle, J.W., Mofjeld, H.O. and Baker, E.T. 1984. An *in situ* erosion rate for a fine-grained marine sediment. *Journal of Geophysical Research*, **89**: 6543 - 6552.

Lettau, H. 1969. Note on aerodynamic roughness parameter estimation on the basis of roughness element description. *J. Applied Meteorology*, **8**: 828 - 832.

Lindholm, R.C. 1987. *A Practical Approach to Sedimentology*. Allen & Unwin Inc., 276 pp.

Lonsdale, B.J. 1970. *A Sedimentary Study of the Eastern Solent*. Unpublished M.Sc. Dissertation. University of Southampton.

Luckenbach, M.W. 1986. Sediment stability around animal tubes: The roles of hydrodynamic processes and biotic activity. *Limnol. Oceanogr.*, **31**: 779 - 789.

Malvern Instruments Particle Sizer Reference Manual, 1987. Manual version 6.0.

Manly, B.F.J. 1986. *Multivariate Statistical Methods, A Primer*. Chapman & Hall, London.

Margalef, R. 1958. Temporal succession and spatial heterogeneity in phytoplankton. In *Perceptives in Marine Biology* (Buzzati-Traverso, A.A., ed.). University of California Press, Berkeley, pp. 323 - 349.

Martin, R.T. 1962. Discussion on experiments on the scour resistance of cohesive sediments by W.L. Moore and F.D. Masch. *J. Geophys. Res.*, **67**: 1447 - 1449.

Mattin, V.J. 1992. *The Seasonal Variation in Bioavailable Sedimentary Organics at Solent Breezes, Southampton Water*. Unpublished B.Sc. Thesis. Department of Oceanography, Southampton University, 116 pp.

May, V.J. 1964. *A Study of Recent Coastal Changes in S.E. England*. Unpublished M.Sc. Thesis. University of Southampton.

Mayer, L.M., Schick, L.L. and Setchell, F.W. 1986. Measurement of protein in nearshore marine sediments. *Mar. Ecol. Prog. Ser.*, **30**: 159 - 165.

McIntyre, A.D. 1958. The ecology of Scottish inshore fishing grounds. I. The bottom fauna of East coast ground. *Marine Research* **1**: 3 - 24.

McIntyre, A.D. and Eleftheriou, A. 1968. The bottom fauna of a flatfish nursery ground. *J. Mar. Biol. Ass. U.K.*, **48**: 113 - 142.

McLaren, P. 1981. An interpretation of trends in grain size measures. *J. Sedim. Petrol.*, **51**: 611 - 624.

McLaren, P. and Little, D.I. 1987. The effects of sediment transport on contaminant dispersal: an example from Milford Haven. *Mar. Pollut. Bull.*, **18**: 586 - 594.

McManus, J. 1988. Grain size determination and interpretation. In *Techniques in Sedimentology* (Tucker, M., ed.). Blackwell Scientific Publications, Oxford, pp. 63 - 85.

Meadows, P.S. 1964. Substrate selection by *Corophium* species: the particle size of substrates. *J. Anim. Ecol.*, **33**: 387 - 394.

Meadows, P.S. and Hariri, M.S.B. 1991. Effects of two infaunal polychaetes on sediment shear strength and permeability: an experimental approach. *Symposium of the Zoological Society of London*, **63**: 319 - 321.

Meadows, P.S. and Tait, J. 1989. Modification of sediment permeability and shear strength by two burrowing invertebrates. *Marine Biology*, 101: 75 - 82.

Meadows, P.S. and Tufail, A. 1986. Bioturbation, microbial activity and sediment properties in an estuarine ecosystem. *Proceedings of the Royal Society of Edinburgh*, 90B: 129 - 142.

Mehta, A.J. 1986. Characterization of cohesive sediment properties and transport processes in estuaries. In *Estuarine Cohesive Sediment Dynamics* (Mehta, A.J., ed.). Springer-Verlag, Berlin, pp. 290 - 325.

Mehta, A.J., Parachure, T.M., Dixit, J.A. and Ariathurai, R. 1982. Resuspension of deposited cohesive sediment beds. In *Estuarine Comparisons* (Kennedy, V.S., ed.), Academic Press, pp. 591 - 609.

Middleton, G.V. and Southard, J.B. 1984. *Mechanics of Sediment Movement*. Second edition. Lecture notes for short course no. 3, sponsored by the Eastern Section of the Society of Economic Paleontologists and Mineralogists, Tulsa, Oklahoma, 401 pp.

Miller, R.L. and Byrne, R.J. 1966. The angle of repose for a single grain on a fixed rough bed. *Sedimentology*, 6: 303 - 314.

Miller, M.C., McCave, I.N. and Komar, P.D. 1977. Threshold of sediment motion under unidirectional currents. *Sedimentology*, 24: 507 - 527.

Mills, E.L. 1967. The biology of an ampeliscid amphipod crustacean sibling species pair. *J. Fish. Res. Bd. Canada*. 24: 305 -355.

Miola, R.J. and Weiser, D. 1968. Textural parameters an evaluation. *J. Sedim. Petrol.*, 38: 45 - 53.

Moore, C.G. and Pearson, T.H. 1986. Response of marine benthic copepode assemblage to organic enrichment. In *Proceedings of the Second International Conference on Copepoda*, Ottawa, Canada, 13 - 17 August, 1984 (Schriever, G., Schminke, H.K. and Shih, C.-t, eds.). Ottawa: National Museums of Canada, pp. 369 - 373.

Morris, H.M. 1955. A new concept of flow in rough conduits. *Trans. Amer. Soc. Civil Engr.* 120: 373 - 398.

Muskananfola, M.R. 1990. *The Effects of Biogenous Processes on the Transport of Marine Sediments*. Unpublished M.Sc. Thesis. Department of Oceanography, University of Southampton, 80 pp.

Neumann, A.C., Gebelein, C.D. and Scoffin, T.P. 1970. The composition, structure and erodibility of subtidal mats, Abaco, Bahamas. *J. Sed. Petrol.*, **40**: 274 - 297.

Niedoroda, A.W., Dalton, C. and Bea, R.J. 1981. The descriptive physics of scour. *13th Annual Offshore Technology Conference*. Houston, Texas, May 4 - 7, 1981, OTC 4145, pp. 297 - 301.

Nordstrom, K.F. 1977. The use of grain size statistics to distinguish between high and moderate-energy beach environments. *J. Sedim. Petrol.*, **47**: 1287 - 1294.

Nowell, A.R.M. and Church, M. 1979. Turbulent flow in a depth-limited boundary layer. *J. Geophys. Res.*, **84**: 4816 - 4824.

Nowell, A.R.M., Jumars, P.A. and Eckman, J.E. 1981. Effects of biological activity on the entrainment of marine sediments. *Mar. Geol.*, **42**: 133 - 153.

Ollivier, M.-T. 1969. Études des peuplements de *Zostères*, *Lanice* et *Sabelles* de la région Dinardaise. *Tethys* **1**: 1097 - 1138.

Owen, M.W. 1977. *Erosion of Avonmouth mud*. Hydraulics Research Station, Wallingford, England. Report No. INT 150 September 1975, Second Impression November, 1977.

Parthenaides, E. and Paaswell, R.E. 1970. Erodibility of channels with cohesive boundaries. *American Society of Civil Engineers, Journal of Hydraulics Division*, **96**: 755 - 769.

Paterson, D.M. 1988. The influence of epipelagic diatoms on the erodibility of an artificial sediment. *Proceedings of the 10th International Symposium on Living and Fossil Diatoms*, pp. 345 - 351.

Paterson, D.M. 1989. Short-term changes in the erodibility of intertidal cohesive sediments related to the migratory behaviour of epipelagic diatoms. *Limnology and Oceanography*, **34**: 223 - 234.

Paterson, D.M., Crawford, R.M. and Little, C. 1990. Subaerial exposure and changes in the stability of intertidal estuarine sediments. *Estuarine, Coastal and Shelf Science*, 30: 541 - 556.

Paterson, D.M. and Daborn, G.R. 1991. Sediment stabilisation by biological action: significance for coastal engineering. *Developments in Coastal Engineering*, University of Bristol, March 1991, pp. 111 - 119.

Pearson, T.H. 1971. The benthic ecology of Loch Linnhe and Loch Eil, a sea-loch system on the west coast of Scotland. III. The effect on the benthic fauna of the introduction of pulp mill effluent. *J. Exp. Mar. Biol. Ecol.*, 6: 211 - 233.

Pearson, T.H., Gray, J.S. and Johannessen, P.J. 1983. Objective selection of selective species indicative of pollution-induced change in benthic communities. 2. Data analyses. *Mar. Ecol. Prog. Ser.*, 12: 237 - 255.

Perkins, E.J. 1974. *The Biology of Estuaries and Coastal Waters*. Academic Press, London.

Pestrong, R. 1969. The shear strength of tidal marsh sediments. *Journal of Sedimentary Petrology*, 39: 322 - 326.

Petersen, C.G.J. 1913. Valuation of the sea. II. The animal communities of the sea bottom and their importance for marine zoogeography. *Rep. Dan. Biol. Stn.*, 21: 1 - 44.

Pielou, E.C. 1966. The measurement of diversity in different types of biological collections. *J. Theoret. Biol.*, 13: 131 - 144.

Pierce, T.J., Jarman, R.T. and De Turville, C.M. 1970. An experimental study of silt scouring. *Proceedings of the Institute of Civil Engineers*, 45: 231 - 243.

Pinet, P.R. 1992. *Oceanography, An Introduction to the Planet Oceanus*. West Publishing Company, St. Paul, M.N., 571 pp.

Postma, H. 1967. Sediment transport and sedimentation in the estuarine environment. In *Estuaries* (Lauff, G.M., ed.). Washington, pp. 158 - 179.

Raymont, J.E.G. 1964. The marine fauna of Southampton Water. In *A survey of Southampton and its region* (Monkhouse, F.J., ed.), for Brit. Ass. Adv. Sci. Southampton, pp. 118 - 120.

Raymont, J.E.G. and Carrie, B.G.A. 1964. The production of zooplankton in Southampton Water. *Int. Revue ges. Hydrobiol.*, **49**: 185 - 232.

Reineck, H.-E., Dörjes, J., Gadow, S. and Hertweck, G. 1968. Sedimentologie, Faunenzonierung und faziesabfolge vor der ostküste der inneren Deutschen Bucht. *Senckenbergiana Lethaia* **49**: 261 - 309.

Rhoads, D.C. 1967. Biogenic reworking of intertidal and subtidal sediments in Barnstable Harbor and Buzzards Bay, Massachusetts. *Journal of Geology.*, **75**: 461 - 476.

Rhoads, D.C. 1974. Organisms-sediment relations on the muddy sea floor. *Oceanogr. Mar. Biol. Annu. Rev.* **12**: 263 - 300.

Rhoads, D.C. and Young, D.K. 1970. The influence of deposit-feeding organisms on sediment stability and community trophic structure. *J. Mar. Res.* **28**: 150 - 178.

Rhoads, D.C., Yingst, J.Y. and Ullman, W. 1978. Seafloor stability in central Long Island Sound. Part I. Temporal changes in erodibility of fine-grained sediment. In: *Estuarine Interactions* (Wiley, M.L., ed.), pp. 221 - 224, Academic Press, New York.

Robert, J.M. and Gouleau, D. 1977. Experimental confirmation of the role of benthic diatom, *Navicula ramosissima* (Agardh) Cleve in the secretion of mucoidal materials which stabilize muddy marine littoral flats. *Comptes Rendus*, **284**: 1915 - 1918.

Ronan, T.E. Jr. 1977. Formation and paleontologic recognition of structures caused by marine annelids. *Paleobiology* **3**: 389 - 403.

Rowe, G.T. 1974. The effects of the benthic fauna on the physical properties of deep-sea sediments. In: *Deep-Sea Sediments: Physical and Mechanical Properties* (Inderbitzen, A.L., ed.), Plenum Press, New York, 497 pp.

Ruillier. 1959. Etude bionomique de l'aber de Roscoff. *Trav. Stat. Biol. Roscoff* **10**: 5 - 350.

Russell, B.J. 1974. Wave height observations of IHU Slip 1968 - 71 and 1972 - 74. *Interservice Hovercraft Unit Tech. Notes Nos. 71/1, 74/4.*

Ryther, J.H. 1969. Photosynthesis and fish production in the sea. *Science*, **166**: 72 - 76.

Sanders, H.L. 1958. Benthic studies in Buzzards Bay. I. Animal-sediment relationships. *Limnol. Oceanogr.*, **3**: 245 - 258.

Sanders, H.L. 1960. Benthic studies in Buzzards Bay. III. The structure of the soft-bottom community. *Limnol. Oceanogr.*, **5**: 138 - 153.

Sanders, H.L. 1968. Marine benthic diversity: a comparative study. *American Naturalist*, **102**: 243 - 282.

Sanders, H.L., Goutsmith, E.M., Mills, E.L. and Hampson, G.E. 1962. A study of the intertidal fauna of Barnstable Harbor, Massachusetts. *Limnol. Oceanogr.* **7**: 63 - 79.

Schäfer, W. 1972. *Ecology and Palaeoecology of Marine Environments*. Craig, G. Y. (ed.). Oliver & Boyd, Edinburgh.

Scoffin, T.P. 1968. An underwater flume. *J. Sedimentary Petrology*, **38**: 244 - 247.

Scoffin, T.P. 1970. The trapping and binding of subtidal carbonate sediment sediments by marine vegetation in Bimini Lagoon, Bahamas. *J. Sed. Petrol.* **40**: 249 - 273.

Seilacher, A. 1951. Der Röhrenbau von *Lanice conchilega* (Polychaeta) ein Beitrag zur deutung fossiler Lebensspuren. *Senckenbergiana Lethaea.*, **32**: 267 - 280.

Seilacher, A. 1953. Studien zur Palichnologie. *Neues Jahrb. Geol. Palaeontol. Abhandlungen.*, **96**: 421 - 452.

Serota, S. and Jangle, A. 1972. A direct-reading pocket shear vane. *Civil Engineering - ASCE*, January 1972

Shannon, C.E. and Weaver, W. 1963. *The Mathematical Theory of Communication*. University of Illinois Press, Urbana, 125 pp.

Shields, A. 1936. Application of similarity principles and turbulence research to bed-load movement. *Mitteilungen der Preussischen Versuchsanstalt für Wasserbau und Schiffbau*, Berlin. In: Ott, W.P. & van Uchelen, J.C. (translators), California Inst. Tech., W.M. Keck Lab. of Hydraulics and Water Resources, Rept. No. 167.

Simberloff, D. 1979. Nearest neighbor assessments of spatial configurations of circles rather than points. *Ecology* 60: 679 - 685.

Skjoldal, H.R. 1982. Vertical and small-scale horizontal distribution of chlorophyll-A and ATP in subtropical beach sand. *Sarsia*, 67: 79 - 84.

Smerdon, R.T. and Beasley, R.P. 1959. *The Tractive Force Theory Applied to Stability of Open Channels in Cohesive Soils*. Research Bulletin, Montana Agricultural Experimental Station No. 715.

Smith, J.D. 1969. *Investigations of Turbulent Boundary Layers and Sediment Transport Phenomena as Related to Shallow Marine Environments*. Part 2. Studies of non-uniform boundary layer flows. Report A69-7. Department of Oceanography, University of Washington.

Smith, J.D. and McLean, S.R. 1977. Spatially averaged flow over a wavy surface. *Journal of Geophysical Research*, 82: 1735 - 1746.

Sneath, P.H.A. and Sokal, R.R. 1973. *Numerical Taxonomy*. W.H. Freeman & Co., San Francisco, 573 pp.

Southard, J.B. 1974. Erodibility of fine abyssal sediment; deep sea sediments; physical and mechanical properties; relationships between physical, mechanical and geologic properties. *Marine Science*, 2: 367 - 379.

Spooner, G.M. and Moore, H.B. 1940. The ecology of the Tamar estuary. VI. An account of the intertidal muds. *J. Mar. Biol. Ass. U.K.*, 24: 283 - 330.

Statham, I. 1977. *Earth Surface Sediment Transport*. Clarendon Press, Oxford, 184 p.

Sternberg, R.W. 1966. Boundary layer observations in a tidal current. *J. Geophys. Res.*, 71: 2175 - 2178.

Stockner, J.G., Cliff, D.D. and Shortreed, K.R. 1979. Phytoplankton ecology of the Strait of Georgia, British Columbia. *J. Fish. Res. Bd. Can.*, **36**: 657 - 666.

Strathmann, R. 1974. The spread of sibling larvae of sedentary marine invertebrates. *Am. Nat.*, **108**: 29 - 44.

Stripp, K. 1969. Die assoziationen des benthos in der Helgoländer Bucht. *Veröff. Inst. Meeresforsch. Bremerh.*, **12**: 95 - 142.

Sutcliffe, W.H. 1973. Correlation between seasonal river discharge and local landings of American lobster (*Homarus glossus*) in the Gulf of Saint Lawrence. *J. Fish. Res. Bd. Can.*, **30**: 856 - 859.

Taghon, G.L., Self, R.F.L. and Jumars, P.A. 1978. Predicting particle selection by deposit feeders: a model and its implications. *Limnol. Oceanogr.*, **23**: 752 - 759.

Taylor, P.A., Gent, P.R. and Keen, J.M. 1976. Some numerical solutions for turbulent boundary-layer flow above fixed, rough, wavy surfaces. *Geophysical Journal of the Royal Astronomical Society*, **44**: 177 - 201.

Tenore, K.R. 1972. Macrofauna of the Pamlico River estuary, North Carolina. *Ecol. Mongr.*, **42**: 51 - 69.

Terwindt, J.H.S., Breusers, H.N.C. and Svasek, J.N. 1968. Experimental investigation on the erosion-sensitivity of a sand-clay lamination. *Sedimentology*, **11**: 105 - 114.

Terzaghi, K. and Peck, R.B. 1967. *Soil Mechanics in Engineering Practice*. Second Edition. John Wiley & Sons, Inc., New York, 729 pp.

Thorn, M.F.C. and Parsons, J.G. 1980. *Erosion of Cohesive Sediments in Estuaries*: an engineering guide. Third International Symposium on Dredging Technology, March, 1980, pp. 349 - 358.

Thorp, C.H. 1980. The benthos of the Solent. In *The Solent Estuarine System*. The Natural Environment Research Council Publications Series C No. 22 November 1980, pp. 76 - 85.

Thorpe, J. 1977. *Ecological Genetics and Some Speciation Problems in Bryozoa*. Unpublished Ph.D. Thesis. University of Wales, 280 pp.

Thorson, G. 1946. Reproduction and larval development of Danish marine bottom invertebrates. *Meddelel. Komm. Danmarks Fisk-Havundersog.*, 4: 1 - 523.

Tiberi, J. and Vovelle, J. 1975. Données histochimiques sur la nature et la formation du tube larvaire chez *Lanice conchilega* Pallas, Polychète Terebellidae. *Arch. Zool. Exp. Gén.*, 116: 303 - 318.

Tubbs, C.R. 1980. Bird populations in the Solent, 1951 - 77. In *The Solent Estuarine System*. The Natural Environment Research Council Publications Series C No. 22 November 1980, pp. 92 - 100.

Turk, T.R., Risk, M.J., Hirtle, R.W.M. and Yeo, R.K. 1980. Sedimentological and biological changes in the Winsor mudflat, an area of induced siltation. *Can. J. Fish. Aquat. Sci.*, 37: 1387 - 1397.

van Smirren, J.R. 1982. *Hydrodynamic and Sedimentary Characteristics of a Predominantly Sandy Intertidal Zones: The Wash, Eastern England*. Unpublished M.Sc. Thesis. University of Wales, 144 pp.

Vos, P.C., de Boer, P.L. and Misdorp, R. 1988. Sediment stabilization by benthic diatoms in intertidal sandy shoals: qualitative and quantitative observations. In *Tide-influenced Sedimentary Environments and Facies* (de Boer, P.L., van Gelder, A. and Nio, S.D., eds.). Reidel, Dordrecht, pp. 511 - 526.

Watkins, E.E. 1942. The macrofauna of the intertidal sands of Kames Bay, Milport, Buteshire. *Trans. R. Soc. Edinburgh* 60: 543 - 561.

Watling, L. 1975. Analysis of structural variations in a shallow water estuarine deposit-feeding community. *J. Exp. Mar. Biol. Ecol.*, 19: 275 - 313.

Watson, A.T. 1890. The tube-building habits of *Terebella littoralis*. *J. R. Microsc. Soc., Ser. 2*, 10: 685 - 689.

Watson, A.T. 1901. Structure and habits of Ammocharidae. *J. R. Microsc. Soc.*, 21: 532 - 533.

Watson, A.T. 1916. A case of apparent intelligence exhibited by a marine tube-building worm, *Terebella conchilega*. *J. R. Microsc. Soc.*, 1916: 253 - 256

Webb, J.E. 1969. Biologically significant properties of submerged marine sands. *Pro. R. Soc. B.*, 174: 355 - 402.

Webber, N.B. 1980. Hydrography and water circulation in the Solent. In *The Solent Estuarine System*. The Natural Environment Research Council Publications Series C No. 22 November 1980, pp. 25 - 35.

West, I.M. 1980. Geology of the Solent Estuarine System. In *The Solent Estuarine System*. The Natural Environment Research Council Publications Series C No. 22 November 1980, pp. 6 - 18.

West, J.R., Oduyemi, O.K., Bale, A.J. and Morris, A.W. 1990. The field measurement of sediment transport parameters in estuaries. *Estuarine, Coastal and Shelf Science*, 30: 167 - 183.

Whitlatch, R.B. 1977. Seasonal Changes in the community structure of the macrobenthos inhabiting the intertidal sand and mudflats of Barnstable Harbor, Massachusetts. *Biol. Bull.*, 152: 275 - 294.

Wieser, W. 1959. The effect of grain size on the distribution of small invertebrates inhabiting the beaches of Puget Sound. *Limnol. Oceanogr.*, 4: 181 - 194.

Wildish, D.J. 1977. Factors controlling marine and estuarine sublittoral macrofauna. *Helgolander Wiss. Meeresunters.*, 30: 445 - 454.

Wilkinson, D.L. and Jones, I.S.F. 1988. Developments towards a marine sediment probe. *Report 10, Ocean Sciences Institute of Technology at the University of Sidney*, 30 pp.

Willetts, B.B. and Murray, C.G. 1981. Lift exerted on stationary spheres in turbulent flow. *J. Fluid Mech.*, 105: 487 - 505.

Williams, P.J.L. 1980. Phytoplankton in Southampton Water. In *The Solent Estuarine System*. The Natural Environment Research Council Publications Series C No. 22 November 1980, pp. 73 - 75.

Wilson, W.H., Jr. 1979. Community structure and species diversity on the sedimentary reefs constructed by *Petaloprocus socialis* (Polychaete: Maldanidae). *J. Mar. Res.* 37: 623 - 641.

Wolff, W.J. 1973. The estuary as a habitat, an analysis of data on the soft-bottom macrofauna of the estuarine area of the rivers Rhine, Meuse and Scheldt. *Zoologische Verhandlingen, Leiden*, **126**: 1 - 242.

Wooding, R.A. 1973. Drag due to regular arrays of roughness elements geometry. *Boundary Layer Meteorol.* **5**: 285 - 308.

Wunderlich, F. 1970. Korngrößenverschiebung durch *Lanice conchilega* (Pallas). *Senckenbergiana Marit.*, **2**: 119 - 125.

Yingst, J.Y. and Rhoads, D.C. 1978. Seafloor stability in central Long Island Sound: Part II. Biological interactions and their potential importance for seafloor erodibility. In *Estuarine Interactions* (Wiley, M.L., ed.). Academic Press, New York, pp. 245 - 260.

Young, R.A. 1977. Seaflume: A device for in situ studies of threshold erosion velocity and erosion behavior of undisturbed marine beds. *Mar. Geol.*, **23**: pp. M11 - M18.

Young, D.K. and Rhoads, D.C. 1971. Animal-sediment relation in Cape Cod Bay, Massachusetts. I. A transect study. *Mar. Biol.* **11**: 242 - 254.

Young, R.N. and Southard, J.B. 1978. Erosion of fine-grained marine sediments: sea-floor and laboratory experiments. *Geol. Sci. Amer. Bull.* **85**: 663 - 67.

Zeman, A.J. 1983. Erosion of cohesive sediments bibliography and annotated abstracts. *National Water Research Institute Study 354*. Burlington, Ontario: National Water Research Institute.

Ziegelmeier, E. 1952. Beobachtungen über den Röhrenbau von *Lanice conchilega* (Pallas) im experiment und am natürlichen Standort. *Helgoländer Wiss. Meeresunters.*, **4**: 107 - 129.

Ziegelmeier, E. 1963. Das makrobenthos in Ostteil der Deutschen Buch nach qualitativen und quantitativen Bodengreiferuntersuchungen in der zeit von 1949 - 1960. *Veröff. Inst. Meeforsch. Bremherh.*, **23**: 101 -114.

Ziegelmeier, E. (1969). Neue untersuchungen über die Wohnröhren-Bauweise von *Lanice conchilega* (Polychaeta, Sedentaria). *Helgoländer Wiss. Meeresunters.*, **19**: 216 - 229.

APPENDICES

Appendices comprise of data which are not necessary for inclusion in the main thesis. These data consist of monthly measurements of the parameters under investigation.

Appendix A. Shear strength (in KPa) data from June 1991 to December 1991

Sample	June 1991	July 1991	August 1991	Sept 1991	Oct 1991	Nov 1991	Dec 1991
1	3.33	3.17	1.17	1.83	2.17	4.97	3.83
2	2.33	1.58	2.80	2.63	2.83	4.73	2.17
3	3.00	4.17	2.33	2.20	4.33	3.33	2.58
4	1.97	2.17	3.67	1.33	3.00	4.67	4.67
5	2.73	3.67	2.23	3.90	1.13	2.67	3.17
6	2.72	1.37	2.90	1.63	4.33	5.30	4.17
7	2.83	3.67	1.97	2.37	2.50	2.80	3.80
8	1.80	3.83	1.57	3.07	2.17	3.83	3.73
9	2.82	2.17	1.30	1.73	2.80	4.07	4.17
10	2.50	1.10	2.07	2.07	1.63	3.67	2.67
11	1.90	3.42	3.00	3.67	3.00	2.50	5.67
12	1.98	3.17	2.63	3.47	4.50	6.40	5.00
13	2.47	3.57	2.30	1.80			
14	2.13	4.07	1.13	1.90			
15	1.93	1.02	1.77	3.33			
16	2.40	1.33		3.67			
17	3.00						
18	2.80						

Appendix A. Continued, from January 1992 to July 1992

Sample	Jan 1992	Feb 1992	March 1992	April 1992	May 1992	June 1992	July 1992
1	0.07	4.00	4.00	2.33	5.00	3.07	3.50
2	1.67	4.30	3.50	2.90	3.33	1.73	2.30
3	2.00	1.83	1.40	3.50	2.97	3.13	3.40
4	2.07	3.83	3.50	2.17	3.00	2.63	2.73
5	0.67	1.83	2.23	4.73	2.83	2.07	1.67
6	2.67	2.67	2.83	3.40	2.83	3.57	2.90
7	1.50	2.23	2.67	3.50	2.83	2.67	3.57
8	3.17	4.00	3.90	2.50	2.20	2.83	2.50
9	1.83	4.00	2.90	2.83	2.23	3.07	2.17
10	2.67	5.17	3.00	3.83	2.33	3.00	2.50
11	2.83	2.33	2.33	2.83	3.80	2.17	2.40
12	2.17	2.80	3.17	3.30	4.17	2.17	1.50
13							1.80
14							2.70
15							2.67
16							2.00
17							
18							

Appendix A. Continued, from August 1992 to February 1993

Sample	August 1992	Sept 1992	Oct 1992	Nov 1992	Dec 1992	Jan 1993	Feb 1993
1	2.90	2.30	2.33	2.77	2.37	2.17	1.07
2	1.67	2.67	3.17	2.23	1.10	3.23	2.10
3	3.00	3.00	3.07	1.73	2.73	1.73	2.47
4	2.50	2.50	1.73	2.17	2.50	3.00	2.00
5	3.00	1.30	2.87	3.33	2.10	2.60	2.00
6	3.50	2.67	2.03	2.17	2.83	2.47	2.17
7	2.80	2.50	2.30	2.43	2.40	2.93	3.33
8	2.33	2.50	3.00	2.27	1.87	3.43	2.50
9	2.63	3.33	2.57	2.73	2.07	2.00	3.00
10	2.70	1.67	1.87	2.83	2.53	2.23	2.17
11	2.80	2.23	2.57	3.07	1.93	2.50	2.37
12	2.60	2.40	3.00	2.43	2.67	3.17	3.57
13	1.57	2.90	2.70	2.17	2.33	3.50	
14	1.67	2.00		2.30	2.00	3.33	
15		2.00		2.53	3.60	1.97	
16					3.30		
17							
18							

Appendix A. Continued, from March 1993 to September 1993

Sample	March 1993	April 1993	May 1993	June 1993	July 1993	August 1993	Sept 1993
1	2.83	2.50	2.43	2.30	2.67	2.10	2.53
2	3.17	2.73	2.97	1.97	2.80	2.77	3.03
3	2.00	2.60	2.57	2.43	2.87	2.50	3.83
4	2.03	1.83	1.87	3.30	2.13	2.70	3.37
5	2.50	3.57	2.60	2.07	2.13	3.17	2.80
6	2.50	3.33	2.83	3.70	2.23	3.63	3.00
7	2.87	2.50	2.63	2.27	2.33	2.63	2.03
8	2.77	2.70	2.37	1.80	2.60	2.43	3.80
9	2.40	2.47	3.53	2.03	2.47	3.50	2.73
10	2.07	2.20	2.10	2.57	2.00	3.20	3.70
11	1.90	2.47	2.60	2.40	3.67	3.27	3.03
12	2.23	1.83	2.40	2.97	3.40	2.97	1.67
13		2.53	2.30	3.43	2.87	3.33	2.93
14		2.27	2.87	2.43	2.47	2.07	2.63
15		2.33	2.60	3.00	3.07	2.77	3.10
16			2.43				3.30
17							
18							

Appendix B. Moisture content (in %) data from June 1991 to December 1991

Sample	June 1991	July 1991	August 1991	Sept 1991	Oct 1991	Nov 1991	Dec 1991
1	29.13	35.00	33.79	33.93	30.34	30.15	28.55
2	31.02	34.70	34.33	34.71	31.64	33.73	26.73
3	30.48	34.00	34.20	34.44	32.94	31.19	28.86
4	31.63	33.98	34.63	36.57	34.02	31.97	27.60
5	29.18	31.62	33.83	34.77	32.71	32.92	30.91
6						31.11	34.27
7						30.48	28.97
8						31.97	30.32
9						31.60	28.08
10						33.32	27.97

Appendix B. Continued, from January 1992 to July 1992

Sample	Jan 1992	Feb 1992	March 1992	April 1992	May 1992	June 1992	July 1992
1	36.65	34.03	35.82	34.67	34.21	26.20	30.85
2	36.62	32.80	33.06	34.23	29.26	25.60	31.25
3	30.40	33.26	35.97	34.50	32.05	27.13	30.58
4	29.20	33.70	34.92	30.96	31.82	28.54	30.19
5	32.85	31.81	31.76	34.77	30.32	24.94	25.20
6	34.60	31.59	30.32	35.52	29.34	28.10	29.48
7	32.54	32.20	34.99	35.37	32.91	28.08	34.71
8	34.83	33.33	30.25	27.79	32.91	27.77	30.77
9	35.63	34.03	30.85	30.16	29.88	31.41	29.19
10	33.39	31.11	31.57	28.33	31.67	31.02	28.96

Appendix B. Continued, from August 1992 to February 1992

Sample	August 1992	Sept 1992	Oct 1992	Nov 1992	Dec 1992	Jan 1993	Feb 1993
1	29.80	29.52	26.26	27.23	29.26	29.28	31.33
2	32.03	32.07	27.04	34.61	26.31	19.47	32.22
3	34.54	31.79	29.72	28.65	33.20	43.04	32.84
4	26.55	26.21	26.11	27.58	24.91	26.88	28.32
5	33.64	31.08	30.59	31.31	29.34	33.45	30.52
6	36.27	32.57	32.74	29.88	31.28	32.06	31.85
7	34.44	29.97	28.98	31.57	31.05	32.03	32.09
8	32.43	34.54	29.61	34.46	32.78	34.90	33.30
9	32.26	32.16	32.15	33.99	33.70	30.28	34.55
10	32.33	29.57	32.64	34.88	29.71	32.51	30.81

Appendix B. Continued, from March 1993 to September 1993

Sample	March 1993	April 1993	May 1993	June 1993	July 1993	August 1993	Sept 1993
1	31.85	25.72	27.44	30.51	34.19	34.13	28.30
2	30.56	28.99	29.26	32.74	32.22	31.00	32.00
3	29.05	27.47	35.16	32.79	35.19	35.64	31.91
4	26.99	30.39	26.42	11.64	33.72	34.41	31.78
5	29.51	30.69	28.20	31.07	36.25	34.94	30.28
6	33.62	32.26	33.40	30.85	34.80	33.65	33.06
7	34.22	29.48	32.30	27.91	33.83	32.90	31.54
8	33.35	28.72	29.62	35.39	30.97	36.28	32.44
9	32.07	31.11	36.34	31.20	34.43	33.19	32.36
10	32.13	33.57	36.55	44.32	34.58	33.79	31.59

Appendix C. Organic matter content (in %) data from June 1991 to December 1991

Sample	June 1991	July 1991	August 1991	Sept 1991	Oct 1991	Nov 1991	Dec 1991
1	1.12	1.02	0.97	1.27	1.02	0.91	1.24
2	0.89	0.97	1.08	1.32	0.97	0.95	1.18
3	0.91	1.07	0.95	1.29	1.06	0.91	1.01
4	0.85	1.16	1.18	1.33	1.06	1.10	1.17
5	0.76	1.21	1.16	1.37	1.12	0.95	1.06
6						1.08	1.19
7						1.32	1.09
8						1.15	1.31
9						0.96	1.09
10						1.05	1.04

Appendix C. Continued, from January 1992 to July 1992

Sample	Jan 1992	Feb 1992	March 1992	April 1992	May 1992	June 1992	July 1992
1	1.21	1.50	1.78	1.26	1.68	1.25	2.46
2	1.18	1.64	1.60	1.20	1.46	1.23	1.85
3	1.35	1.56	1.75	1.26	1.18	1.41	2.10
4	1.10	1.75	1.67	1.03	1.39	1.35	1.88
5	1.16	1.54	1.42	1.36	1.46	1.54	1.72
6	1.36	1.50	1.68	1.34	1.53	1.40	1.89
7	1.20	1.69	1.62	1.37	0.53	1.51	2.64
8	1.42	2.31	1.45	1.14	1.28	1.37	1.84
9	1.22	1.43	1.62	1.05	1.27	1.55	1.77
10	1.18	1.61	1.64	0.98	1.40	1.69	1.93

Appendix C. Continued, from August 1992 to February 1993

Sample	August 1992	Sept 1992	Oct 1992	Nov 1992	Dec 1992	Jan 1993	Feb 1993
1	1.18	1.03	1.24	1.11	1.66	1.11	0.91
2	1.38	1.12	1.27	1.21	1.64	1.12	1.17
3	1.39	1.06	1.13	1.00	1.82	1.18	1.16
4	1.13	1.05	1.15	1.05	1.67	1.08	1.02
5	1.14	1.14	1.28	0.57	1.60	1.16	1.11
6	1.84	1.01	1.07	1.28	1.81	1.17	1.09
7	1.44	0.86	0.99	1.18	1.65	1.17	1.13
8	1.18	1.13	1.20	1.31	1.74	1.25	1.13
9	1.21	1.01	1.04	1.41	1.49	0.95	1.13
10	1.23	1.14	1.02	1.33	1.42	1.09	1.15

Appendix C. Continued, from March 1993 to September 1993

Sample	March 1993	April 1993	May 1993	June 1993	July 1993	August 1993	Sept 1993
1	1.22	1.03	1.43	1.11	1.74	1.13	1.84
2	1.13	1.10	1.55	1.19	1.49	1.10	1.97
3	1.01	1.13	1.53	1.14	1.43	1.26	2.00
4	1.15	1.08	1.35	1.23	1.65	1.85	1.96
5	1.42	1.09	1.38	1.23	1.74	1.47	1.88
6	1.09	1.15	1.35	1.15	1.76	1.52	1.98
7	1.21	0.98	1.41	1.17	1.57	1.19	1.87
8	1.15	1.06	1.44	1.37	1.63	1.24	1.98
9	1.15	0.98	1.50	1.17	1.70	1.11	1.98
10	1.36	1.22	1.59	1.44	1.69	1.32	1.83

Appendix D. Silt/clay content (in %) data from June 1991 to December 1991

Sample	June 1991	July 1991	August 1991	Sept 1991	Oct 1991	Nov 1991	Dec 1991
1	0.10	0.18	0.20	0.76	0.25	0.14	0.15
2	0.10	0.05	0.58	0.44	0.20	0.16	0.12
3	0.17	0.03	0.58	0.57	0.40	0.17	0.16
4	0.12	0.15	0.72	1.19	0.19	0.15	0.13
5	0.20	0.10	0.58	0.67	0.24	0.16	0.20
6						0.19	0.12
7						0.23	0.16
8						0.16	0.16
9						0.18	0.13
10						0.11	0.15

Appendix D. Continued, from January 1992 to July 1992

Sample	Jan 1992	Feb 1992	March 1992	April 1992	May 1992	June 1992	July 1992
1	0.18	0.22	0.16	0.21	0.26	0.70	1.07
2	0.23	0.13	0.22	0.25	0.23	0.43	0.45
3	0.17	0.12	0.13	0.32	0.18	0.45	0.40
4	0.21	0.13	0.24	0.19	0.24	0.45	0.33
5	0.15	0.08	0.12	0.23	0.12	0.47	0.29
6		0.14	0.18	0.20	0.17	0.61	0.42
7	0.23		0.16	0.22	0.13	0.51	0.57
8	0.17		0.19	0.15	0.15	0.51	0.44
9	0.10		0.22	0.19	0.12	0.68	0.19
10	0.19	0.17	0.13	0.20	0.35	0.58	0.21

Appendix D. Continued, from August 1992 to February 1993

Sample	August 1992	Sept 1992	Oct 1992	Nov 1992	Dec 1992	Jan 1993	Feb 1993
1	0.85	0.15	0.70	0.12	0.13	0.16	0.10
2	0.37	0.18	0.95	0.16	0.11	0.11	0.14
3	0.36	0.17	0.64	0.11	0.15	0.11	0.16
4	0.40	0.21	0.58	0.12	0.14	0.13	0.12
5	0.71	0.09	0.76	0.15	0.13	0.14	0.11
6	0.56	0.08	0.52	0.13	0.12	0.14	0.24
7	0.46	0.14	0.40	0.12	0.15	0.12	0.11
8	0.35	0.01	0.57	0.12	0.13	0.12	0.21
9	0.42	0.12	0.64	0.13	0.10	0.10	0.32
10	0.51	0.13	0.59	0.13	0.08	0.10	0.23

Appendix D. Continued, from March 1993 to September 1993

Sample	March 1993	April 1993	May 1993	June 1993	July 1993	August 1993	Sept 1993
1	0.16	0.23	0.76	0.19	0.10	0.52	0.40
2	0.15	0.25	0.72	0.14	0.19	0.56	0.29
3	0.16	0.19	0.78	0.13	0.15	0.67	0.54
4	0.23	0.19	0.34	0.24	0.13	0.51	0.42
5	0.14	0.20	0.64	0.15	0.07	0.62	0.24
6	0.13	0.26	0.43	0.09	0.17	0.71	0.32
7	0.13	0.15	0.55	0.23	0.11	0.41	0.22
8	0.15	0.12	0.67	0.18	0.16	0.58	0.18
9	0.09	0.05	0.77	0.16	0.15	0.67	0.19
10	0.23	0.06	0.54	0.14	0.10	0.79	0.26

Appendix E. Tube density (100 cm⁻²) data for shear strength from June 1991 to December 1991

Sample	June 1991	July 1991	August 1991	Sept 1991	Oct 1991	Nov 1991	Dec 1991
1	11	9	0	4	1	13	9
2	8	3	11	10	5	8	2
3	9	13	8	5	8	6	4
4	3	6	17	0	7	13	12
5	14	15	8	15	0	2	7
6	11	3	12	3	8	15	10
7	13	12	7	8	5	1	9
8	3	15	3	12	3	4	7
9	8	6	2	2	6	10	8
10	11	2	6	9	2	7	2
11	5	13	15	14	6	5	13
12	9	11	13	12	11	16	10
13	13	12	10	6			
14	5	14	2	5			
15	5	0	5	14			
16	9	0		13			
17	11						
18	8						

Appendix E. Continued, from January 1992 to July 1992

Sample	Jan 1992	Feb 1992	March 1992	April 1992	May 1992	June 1992	July 1992
1	10	7	9	1	15	7	11
2	2	10	9	5	5	2	3
3	6	1	1	12	7	8	10
4	6	11	8	2	5	5	9
5	0	0	3	13	4	2	1
6	10	5	7	7	7	9	10
7	2	2	6	8	3	5	11
8	10	8	9	3	2	6	7
9	3	11	8	6	1	8	3
10	5	12	7	8	2	10	6
11	7	2	4	8	10	2	6
12	4	3	11	10	9	3	2
13							2
14							7
15							6
16							4
17							
18							

Appendix E. Continued, from August 1992 to February 1993

Sample	August 1992	Sept 1992	Oct 1992	Nov 1992	Dec 1992	Jan 1993	Feb 1993
1	7	4	4	8	4	3	2
2	2	5	10	6	0	7	7
3	7	5	7	1	8	1	7
4	5	6	1	2	7	6	4
5	8	0	6	12	5	5	6
6	10	4	2	3	8	4	8
7	6	5	4	4	6	6	9
8	5	5	10	3	4	8	7
9	8	9	4	6	4	4	8
10	6	3	5	3	6	4	6
11	8	3	6	6	2	5	8
12	8	6	7	5	7	6	10
13	2	10	7	4	4	7	
14	1	3		5	4	7	
15		2		5	13	2	
16					9		
17							
18							

Appendix E. Continued, from March 1993 to September 1993

Sample	March 1993	April 1993	May 1993	June 1993	July 1993	August 1993	Sept 1993
1	5	3	8	6	3	2	3
2	8	7	6	5	4	3	5
3	3	6	7	5	3	5	9
4	4	3	1	11	2	3	6
5	4	9	7	3	1	7	3
6	6	8	9	4	1	8	5
7	6	5	5	11	4	4	1
8	5	8	6	2	3	2	9
9	4	5	9	2	2	7	4
10	2	4	2	5	1	6	7
11	1	4	7	4	7	8	3
12	2	1	5	6	5	5	1
13		4	3	13	5	8	5
14		3	7	3	1	1	2
15		2	5	7	5	5	7
16			3				6
17							
18							

Appendix F. Tube density (100 cm^{-2}) data for biology from October 1991 to March 1992

Sample	Oct 1991	Nov 1991	Dec 1991	Jan 1992	Feb 1992	March 1992
1	1	2	1	2	0	5
2	2	6	2	0	2	3
3	1	4	2	3	4	4
4	0	6	3	2	5	2
5	0	4	2	2	3	3
6	1	6	3	8	1	3
7	0	6	5	5	2	4
8	2	2	3	5	4	0
9	1	6	2	5	3	3
10	0	2	3	4	3	3
11	7	7	9	9	6	6
12	9	10	7	11	10	7
13	9	8	8	12	7	8
14	7	9	7	11	8	6
15	8	10	10	8	8	5
16	9	9	7		9	6
17	6	8	9		5	5
18	9	9	6		8	6
19	9	10	5		8	6
20	10	10	10		10	6
21	11	10	10		11	9
22	10	14	12		14	9
23	17	12	15		11	9
24	13	15	10		13	11
25	15	11	11		14	12
26	13	11	13		12	12
27	14	16	12		12	9
28	12	11	12		15	10
29	11	16	11		15	9
30	15	14	10		12	10

Appendix F. Continued, from April 1992 to September 1992

Sample	April 1992	May 1992	June 1992	July 1992	August 1992	Sept 1992
1	2	2	1	1	3	3
2	5	3	4	4	1	1
3	0	2	2	3	2	3
4	4	4	2	4	2	2
5	1	4	2	3	3	1
6	2	4	4	4	1	2
7	5	1	6	6	3	3
8	5	3	5	8	3	2
9	4	2	3	7	3	4
10	3	4	5	7	3	2
11	5	8	5	5	4	5
12	8	8	6	5	6	4
13	8	9	7	6	5	5
14	9	6	7	8	6	5
15	8	7	7	10	6	4
16	7	9	8	11	5	4
17	6	8	6	13	4	3
18	6	7	5	10	4	4
19	8	5	6	12	4	3
20	6	7	7	11	4	5
21	12	13	8	14	7	9
22	11	10	11	9	9	7
23	10	9	13	12	13	7
24	12	11	8		8	5
25	11	11	10		11	6
26	5	7	7		8	6
27	7	11	13		13	6
28	8	9	9		15	6
29	9	12	9		11	6
30	9	10	9		9	5

Appendix F. Continued, from October 1992 to March 1993

Sample	Oct 1992	Nov 1992	Dec 1992	Jan 1993	Feb 1993	Mar 1993
1	2	3	1	1	3	1
2	1	0	3	1	1	3
3	3	1	3	3	2	2
4	0	3	2	3	2	2
5	2	1	2	4	3	1
6	2	3	3	3	2	6
7	3	3	4	7	3	3
8	3	5	4	6	5	5
9	2	4	4	6	6	4
10	1	4	5	6	5	3
11	4	4	6		5	4
12	5	4	6		5	5
13	5	4	5		5	6
14	5	5	9		6	6
15	5	5	6		4	8
16	5	5	8		9	6
17	6	7	8		7	
18	5	10			7	
19	6	11			8	
20	5	9			8	
21	7	9			7	
22	9					
23	7					
24	8					
25	8					
26	9					
27	9					
28	8					
29	8					
30	7					

Appendix F. Continued, from April 1993 to September 1993

Sample	April 1993	May 1993	June 1993	July 1993	August 1993	Sept 1993
1	2	2	2	1	1	3
2	3	3	2	3	2	2
3	3	1	3	2	3	1
4	3	3	2	1	2	1
5	1	2	1	2	2	3
6	3	3	1	2	3	6
7	1	2	4	3	2	4
8	2	4	6	3	4	4
9	2	5	4	4	5	5
10	3	5	4	3	4	5
11	4	3	4	3	5	6
12	6	5	7	5	3	4
13	6	4	8	4	4	5
14	6	4	7	6	4	4
15	5	5	10	5	6	4
16	4	6			7	8
17	4	6			8	7
18	4	7			8	7
19	5	8			8	9
20	4	7			9	9
21	8	7			7	
22	8	7			7	
23	9	3				
24	10	8				
25	7	8				
26	6					
27	8					
28	8					
29	9					
30	7					

Appendix G. Principal Components of eight most dominant Components
of macrobenthic organisms, PC1 to PC4

Month (Year)	PC1	PC2	PC3	PC4
Oct (1991)	4.7852	0.0684	-1.5153	0.2936
Nov	0.9370	-5.1969	-2.2584	-2.1080
Dec	2.3057	-1.1329	-1.2826	0.0725
Jan (1992)	4.3666	1.5075	2.3191	0.9561
Feb	4.1842	-0.4926	2.3772	0.0841
March	-0.9801	-0.4017	1.8654	-0.7192
April	-2.9039	-4.1126	5.0161	0.0891
May	-0.4666	-0.8205	0.1176	0.7511
June	-0.3232	-1.1148	0.0839	-1.1938
July	-0.3400	0.9516	-1.6707	-1.6106
August	-0.5774	-2.2301	-2.4374	-1.5320
Sept	1.5312	0.2800	-0.8193	0.0239
Oct	1.0106	1.4139	-0.8114	0.1362
Nov	0.2533	0.3208	0.4941	0.6364
Dec	-0.4978	-0.3939	-1.4181	1.2179
Jan (1993)	3.1000	0.9266	1.2582	0.6189
Feb	-0.3312	1.1726	1.0575	1.4043
March	-2.8959	1.0825	-1.4583	1.1768
April	-4.4429	-0.0704	-0.6286	2.5097
May	-4.1712	-0.2426	-0.1742	1.7276
June	0.5121	0.7228	-0.9080	2.8115
July	-0.8299	2.4687	0.8754	-3.8568
August	-3.0207	2.9418	1.2140	-3.1386
Sept	-1.2051	2.4888	-1.2961	-0.3508

Appendix G. Continued, PC5 to PC8

Month (Year)	PC5	PC6	PC7	PC8
Oct (1991)	0.6503	-0.1621	0.6046	0.5357
Nov	-2.7786	-1.7997	-0.4602	-0.1441
Dec	-1.6128	2.6429	0.8635	-0.0702
Jan (1992)	-0.6116	0.1770	-1.5084	0.2392
Feb	-0.4557	-2.1756	1.3693	-1.4647
March	1.5181	0.1149	1.2793	-2.4048
April	1.0370	0.7118	0.2963	2.1920
May	1.7564	1.4704	0.0104	-1.2000
June	-1.1851	3.2631	-0.4967	-2.3830
July	1.3551	2.3625	-0.4439	1.4668
August	3.2811	-1.6663	0.1249	0.2152
Sept	1.9112	-0.7545	0.5786	0.5714
Oct	1.2784	0.8257	0.1410	1.0630
Nov	0.1373	-0.0868	-1.6593	-0.4061
Dec	-0.2192	-0.6058	-2.1925	0.9061
Jan (1993)	-0.2721	-0.3619	-0.4631	0.4409
Feb	-0.1910	-0.9928	-1.4737	0.0570
March	-0.8777	-0.5373	0.0557	-0.2584
April	0.1577	-0.7662	-1.9794	-1.7560
May	-1.7024	0.0032	1.8848	1.5558
June	-1.2993	0.1927	2.3187	0.8268
July	-1.3879	-0.1767	-1.5025	1.1738
August	-0.8142	-1.1452	1.3637	-0.2603
Sept	0.3251	-0.5334	1.2892	-0.8959

Appendix H. Velocity profiles measured in situ using a Velocity Rig with five current meters during a spring tidal cycle late September 1992

Time (hour)	Water Depth (m)	Meter 1 Velocity (cm s ⁻¹)	Meter 2 Velocity (cm s ⁻¹)	Meter 3 Velocity (cm s ⁻¹)	Meter 4 Velocity (cm s ⁻¹)	Meter 5 Velocity (cm s ⁻¹)
09.00	0.40			22.2	7.1	6.6
09.15	0.60			5.7	4.9	4.7
09.30	0.70			3.9	3.2	3.0
09.45	0.70			3.2	2.2	3.2
10.15	0.80			5.7	5.2	2.2
10.30	0.80			7.1	4.2	4.9
10.45	0.85		12.8	9.0	7.9	6.9
11.00	1.05		17.4	13.8	14.9	10.3
11.15	1.25		26.0	23.6	20.3	14.4
11.30	1.50		30.6	24.1	10.9	7.4
11.45	1.60	37.6	20.6	18.7	16.8	
12.00	2.05	41.9	30.8	19.0	19.0	
12.15	2.30	43.5	30.3	21.9	18.2	
12.30	2.60	40.8	26.5	20.1	15.2	
12.45	3.00	25.9	14.4	11.1	7.6	
13.00	3.60	17.3	7.6	5.4	7.4	
13.30	3.60	6.6	6.9	2.5	3.2	
13.45	3.50	14.9	10.9	7.6	6.9	
14.00	3.40	10.9	6.9	4.4	3.9	
14.30	3.55	5.6	7.9	6.4	6.4	5.2
14.45	3.55	12.0	11.1	6.9	5.9	3.9
15.00	3.40	13.6	10.3	6.9	5.7	3.4
15.15	3.20	9.6	6.6	5.4	3.9	
15.30	3.00	5.6	14.1	3.7	3.7	2.5
16.15	2.90	11.7	10.6	8.4	8.2	
16.30	2.60	22.4	18.7	15.7	13.6	7.4
16.45	2.35	32.5	27.6	24.4	21.4	12.2
17.00	2.00	39.5	35.7	25.7	28.7	21.7
17.15	1.40		33.8	22.8	24.9	5.4
17.30	1.20		32.2	19.0	22.5	